

**High-resolution seismo-acoustic studies  
of alongslope and downslope sediment transport processes  
shaping depositional patterns at continental margins**

Dissertation  
zur Erlangung des Doktorgrades der Naturwissenschaften  
am Fachbereich Geowissenschaften  
der Universität Bremen

vorgelegt von  
Benedict Preu  
Bremen, Dezember 2011

Gutachter:  
Prof. Dr. Volkhard Spieß  
Prof. Dr. Dierk Hebbeln

## Table of contents

	<b>Page</b>
<b>Abstract</b>	<b>1</b>
<b>Kurzfassung</b>	<b>3</b>
<b>Chapter 1 Introduction</b>	<b>6</b>
1.1 The ocean as archive for climate changes	6
1.2 Sedimentation under influence of bottom currents	7
1.3 Motivation and objectives	11
1.4 Regional setting of the northern Argentine margin	13
1.5 Methods	17
1.6 Thesis outline	22
1.7 Additional contributions to articles	23
<b>Chapter 2 Sedimentary growth pattern on the northern Argentine slope: the impact of North Atlantic Deep Water on southern hemisphere slope architecture</b>	<b>25</b>
<b>Chapter 3 Morpho-sedimentary characteristics of the northern Argentine margin: the interplay between erosive, depositional and gravitational processes</b>	<b>45</b>
<b>Chapter 4 Interaction of along-slope and down-slope processes: The Mar del Plata Canyon and its effects on contourite deposition</b>	<b>75</b>
<b>Chapter 5 The impact of lee eddies on sediment dynamics: Acoustic Imaging of Nepheloid layers within the Agulhas Current</b>	<b>90</b>
<b>Chapter 6 Conclusions and future perspectives</b>	<b>98</b>
<b>References</b>	<b>100</b>
<b>Abbreviations</b>	<b>112</b>
<b>Appendix 1</b>	<b>113</b>
<b>Appendix 2</b>	<b>123</b>
<b>Acknowledgements</b>	<b>125</b>

## **Abstract**

Downslope and alongslope sediment transport are the dominant processes during the evolution of continental margins. While downslope transport is driven by gravity, slope parallel transport is mainly controlled by the thermohaline circulation and associated bottom currents. Although several studies focused on either one of these processes, knowledge on bottom current induced sediment transport and its interplay with downslope oriented processes is still limited. The major goal of this thesis is to reveal the impact of both alongslope and downslope oriented sediment transport on slope architecture in highly dynamic oceanographic settings and to assess their interaction.

The main investigation area covers the continental slope in the border region of Uruguay and Argentina, where a major contourite depositional system (CDS) is located beneath the Brazil-Malvinas Confluence, which represents a key location within the deep and intermediate water loop of the global conveyor belt. The CDS encompasses well defined depositional and erosive features, the most prominent represented by contourite terraces and the Mar del Plata submarine canyon.

By means of high resolution multichannel seismic data, three major seismic units were identified in the subsurface of the middle slope, which allow reconstruction of former oceanographic settings based on changes in their reflection stacking pattern. In agreement with earlier studies, first current controlled sedimentation can be observed around the Eocene/Oligocene boundary coeval with the opening of the Drake Passage. During the Middle Miocene the formation of large plastered drift sequences marks the onset of Northern Sourced Deep Water (NSDW) production, which resulted in a major vertical shift of water mass interfaces off northern Argentina. Finally, the modern oceanographic regime was established with the closure of the Central American Seaway in the Late Pliocene, which due to the strengthening of NSDW resulted in the formation of another plastered drift. Consequently, it can be shown that alongslope sedimentary processes dominated the evolution of the northern Argentine slope architecture. Furthermore, highlighting the impact of the NSDW on slope architecture, it is likely that since the Middle Miocene deep water production in the northern hemisphere plays a significant role in shaping continental slopes in the western South Atlantic.

To study the recent sedimentary system, the morpho-sedimentary features of the northern Argentine margin were mapped in great detail based on seismo- and hydro-acoustic data sets including conventional and high-resolution seismics, parametric echosounder and single and swath bathymetry. Erosive and depositional features of the CDS were described in detail with special emphasis on spatial variations north and south of the Mar del Plata Canyon. Joint interpretation with regional hydrographic data sets revealed that most of the morpho-sedimentary features are the result of bottom current driven sediment transport. In particular, the evolution of large-scale contourite terraces including their associated depositional and erosive features can be explained by alongslope processes, which are controlled by the interplay of water mass interfaces, helicoidal flow patterns and topography.

However, spatial analysis of sedimentary features revealed a major deficit in sediment budget on the northern flank of the Mar del Plata Canyon. This area of non-deposition reveals the effect of the

canyon on bottom current flow pattern, which is a flow disturbance over this seafloor irregularity by a loss in topographic constraint. This major disturbance decreases not only flow velocity, but also the sediment transport capacity of the bottom current. Therefore, particles transported alongslope are released into the canyon, from where the suspension flows down the canyon floor. Tracing this distinct sedimentary signature on geological time scales, slope architecture analysis by means of high-resolution multichannel seismic data indicated that the Mar del Plata Canyon interacts at least since the Late Miocene with the northern Argentine oceanographic regime.

To justify such an interpretation, which suggests sediment pirating of a submarine canyon from bottom currents, a modern analog study from SE Africa showing the huge transport capacity of bottom currents in the water column has been carried out for comparison. By means of 18 kHz parametric echosounder and Acoustic Doppler Current Profiler (ADCP) data several smaller-scale lee eddies have been identified within the Agulhas Current offshore Mozambique, which erode, resuspend and transport vast amounts of sediments by forming nepheloid layers. With this approach for the first time the impact of high energetic eddies on sediment dynamics could be visualized. This analysis confirms that indeed massive sediment transport occurs due to the interplay between dynamic bottom currents and the topographic framework.

Overall, this thesis makes a comprehensive attempt to decipher the impact of both alongslope and downslope sediment transport processes. Based on slope architecture analysis it becomes obvious that the overall margin shape and its associate sedimentary stacking pattern represent paleoclimatic archives, which provide insight into former oceanographic settings. In particular, the existence of contourite terraces might be used to not only determine distinct water masses but also to trace their interface in space and time. Furthermore, in this study, the interaction of alongslope and downslope oriented sediment transport processes and its margin shaping character within the framework of a highly dynamic oceanographic setting could be shown. The mechanism, which suggests a feeding of submarine canyons by bottom currents, might present a possible material source of canyons, which are not connected to major river systems or shelf edges at all. Thus, the results of this thesis improve the understanding on alongslope and downslope oriented sediment transport and their interaction.

## **Kurzfassung**

Hangabwärts gerichteter und hangparalleler Sedimenttransport stellen die bedeutendsten Prozesse während der Evolution eines Kontinentalrandes dar. Während hangabwärts gerichteter Transport von der Schwerkraft angetrieben ist, wird der hangparallele Transport hauptsächlich durch die thermohaline Zirkulation und den damit verbundenen Bodenwasserströmungen kontrolliert. Obwohl sich bereits mehrere Studien gezielt mit einem der beiden genannten Prozesse auseinandergesetzt haben, ist das Wissen über durch Bodenwasserströmung hervorgerufenen Sedimenttransport und dessen Interaktion mit Schwerkraft getriebenen Prozessen weiterhin begrenzt. Das Hauptziel dieser Dissertation ist daher, den Einfluss des sowohl hangabwärts gerichteten als auch des hangparallelen Sedimenttransports auf die Hangarchitektur in einem hoch dynamischen Strömungsregime aufzuzeigen und deren mögliche Interaktion zu bestimmen.

Das Hauptuntersuchungsgebiet dieser Studie umschließt den Kontinentalhang der Grenzregion zwischen Uruguay und Argentinien, an dem sich ein größerer kontouritischer Ablagerungsraum befindet. Dieser befindet sich im Einflussgebiet der Brazil-Malvinas Konfluenz, die eine Schlüsselposition innerhalb des mittleren und tiefen Wasserkreislaufes des globalen Zirkulationsmusters darstellt. Der kontouritische Ablagerungsraum umfasst gut ausgeprägte Ablagerungs- und Erosionsstrukturen. Die beeindrucktesten Strukturen stellen kontouritische Terrassen und der Mar del Plata Canyon da.

Mittels hochauflösender Mehrkanalseismik-Daten wurden im Untergrund des mittleren Hanges drei größere seismische Einheiten identifiziert, die auf Grund von sich verändernden Reflektionsmustern eine Rekonstruktion von früheren Strömungsregimen ermöglichen. In Übereinstimmung mit früheren Studien kann erste von Strömung kontrollierte Sedimentation in der Nähe der Eozän/Oligozän-Grenze zeitlich mit der Öffnung der Drake Passage beobachtet werden. Während des mittleren Miozäns markiert die Entwicklung mehrerer am Hang liegender konturitischer Sedimentationsabfolgen das Einsetzen des Nordatlantischen Tiefenwassers. Dieses hatte ein vertikales Verschieben der Wassermassengrenzen vor Argentinien zur Folge. Schlussendlich entstand das heutige ozeanographische Regime durch das Schließen des Isthmus von Panama, der durch ein Verstärken des Nordatlantischen Tiefenwassers zur Ablagerung einer weiteren konturitischen Ablagerung führte. Daher kann gezeigt werden, dass hangparallele Sedimentationsprozesse die Evolution des Argentinischen Kontinentalhanges dominiert haben. Zusätzlich die ausschlaggebende Rolle des Nordatlantischen Tiefenwassers berücksichtigend ist es wahrscheinlich, dass seit dem mittleren Miozän die Tiefenwasserproduktion in der nördlichen Hemisphäre eine signifikante Rolle für die Evolution von Kontinentalhängen im westlichen Atlantik spielt.

Um das heutige sedimentäre System zu studieren wurden basierend auf mehreren seismischen und hydroakustischen Datensätzen, die neben konventionellen und hochauflösenden Mehrkanalseismik-Daten auch Messungen mit parametrischen Sedimentlot und sowohl Schiffs- als auch Fächerecholot beinhalteten, morpho-sedimentäre Merkmale vor Nordargentinien kartiert. Erosions- und

Ablagerungsstrukturen des konturritischen Ablagerungsraums wurden beschrieben mit einem speziellen Augenmerk auf räumliche Unterschiede nördlich und südlich des Mar del Plata Canyons. Gemeinsame Interpretation mit regionalen hydrographischen Daten zeigte, daß die meisten morpho-sedimentären Merkmale durch Bodenwasserströmungen und daher durch hangparallelen Sedimenttransport entstanden sind. Ins besonders die Entstehung von großflächigen konturritischen Terrassen eingeschlossen ihrer Ablagerungs- und Erosionsstrukturen kann auf Hang parallele Prozesse zurückgeführt werden, die durch die Wechselwirkung von Wassermassengrenzen, helicoidalen Strömungsmustern und der Topographie kontrolliert werden.

Die Analyse jener sedimentären Merkmale zeigte ebenfalls auf der nördlichen Flanke des Mar del Plata Canyons ein größeres Gebiet, das durch einen Mangel an Sedimentation gekennzeichnet ist. Dieser Mangel an Sedimentation ist das Ergebnis des Canyons, der ein größeres Strömungshindernis darstellt. Über den Canyon fließende Strömungen verlieren ihre topographische Begrenzung und daher auch an Geschwindigkeit. Einhergehend mit dem Verlust an Geschwindigkeit sinkt auch die Fähigkeit Sedimente zu transportieren. Daher fallen durch Strömung transportierte Sedimente in den Canyon. Das Verfolgen des depositionslosen Gebietes auf geologischen Zeiträumen mit Hilfe von hochauflösenden Mehrkanalseismik-Daten deutet an, dass der Canyon mindestens seit dem späten Miozän mit dem Nordargentinischen Strömungssystem interagierte.

Um eine solche Interpretation zu rechtfertigen, die auf dem Sedimenttransport von Bodenwasserströmungen beruht, wurde eine neuartige Studie vor Südafrika durchgeführt, die das gewaltige Transportvermögen von Bodenwasserströmungen verdeutlicht. Mittels von Datensätzen, die mit einem 18 kHz parametrischen Echolot und einem 75 kHz ADCP (Acoustic Doppler Current Profiler) gesammelt wurden, wurden mehrere kleine Stromwirbel innerhalb des Agulhasstroms vor Mozambique identifiziert, die große Mengen an Sediment erodieren, resuspendieren und in Form von Nepheloidlagen transportieren. Mit diesem Ansatz konnte zum ersten Mal der Einfluss von Stromwirbeln auf die Sedimentdynamik visualisiert werden. Diese Analyse bestätigte, daß tatsächlich gewaltige Mengen von Sediment durch die Wechselwirkung von dynamischen Bodenwasserströmungen und Topografie transportiert werden können.

Diese Dissertation macht einen umfassenden Versuch den Einfluss von sowohl hangabwärts gerichtetem als auch hangparallelen Sedimenttransport zu entschlüsseln. Auf Grund der oben dargelegten Analyse der Hangarchitektur ist es eindeutig, dass die Hangmorphologie und die damit verbunden sedimentären Strukturen paleoklimatische Archive darstellen, die einen Einblick in frühere Ozeanregime ermöglichen. Ins besondere die Existenz von konturritische Terrassen kann dazu benutzt werden, spezifische Wassermassengrenzen zu bestimmen und diese über geologische Zeiträume zu rekonstruieren. Darüber hinaus konnte in dieser Studie die Interaktion zwischen hangparallelem und hangabwärts gerichtetem Sedimenttransportprozessen in einem hoch dynamischen Strömungsregime gezeigt werden. Der dargestellte Mechanismus, der das Befördern von Sedimenten zum Mar del Plata Canyon durch Bodenwasserströmungen beinhaltet, könnte eine mögliche Sedimentquelle für Canyons

darstellen, die nicht mit größeren Flusssystemen oder der Schelfkante verbunden sind. Daher haben die Ergebnisse dieser Arbeit zu einem besseren Verständnis von hangabwärtsgerichteten und hangparallelen Sedimentationsprozessen und deren möglicher Interaktion beigetragen.

## 1. Introduction

### 1.1 The ocean as archive for climate changes

Marine sediments are representing the major climatic archive on Earth. Although short-term climate variations can be analyzed utilizing other archives like tree rings, ice cores and corals, marine sediments, in particular those which were eroded, transported and deposited by water, provide an insight into over 99% of Earth's geological history (Ruddiman, 2001). Traditional paleoclimatic and paleoceanographic studies are based on the analysis of marine sediment components using mineral composition, grain size distribution, microfossils or isotopic composition as climate proxies and were restricted to undisturbed hemipelagic/pelagic sedimentation (Fig. 1.1). Other approaches incorporate structural analysis of small-scale and large-scale sedimentary features which were deposited by non-vertical sediment transport processes and are often linked to atmospheric variability, sea level fluctuations or the thermohaline circulation. Consequently, sediment structures derived from transport processes can also carry a climatic fingerprint and can be used as additional source of information for paleoclimatic and paleoceanographic reconstructions.

Sediment transport can be distinguished through transport direction into either downslope or alongslope transport (Fig. 1.1). Downslope processes are driven by gravity and occur mostly episodically or in single events, which range from slides to turbidity currents (Shanmugam, 2003,

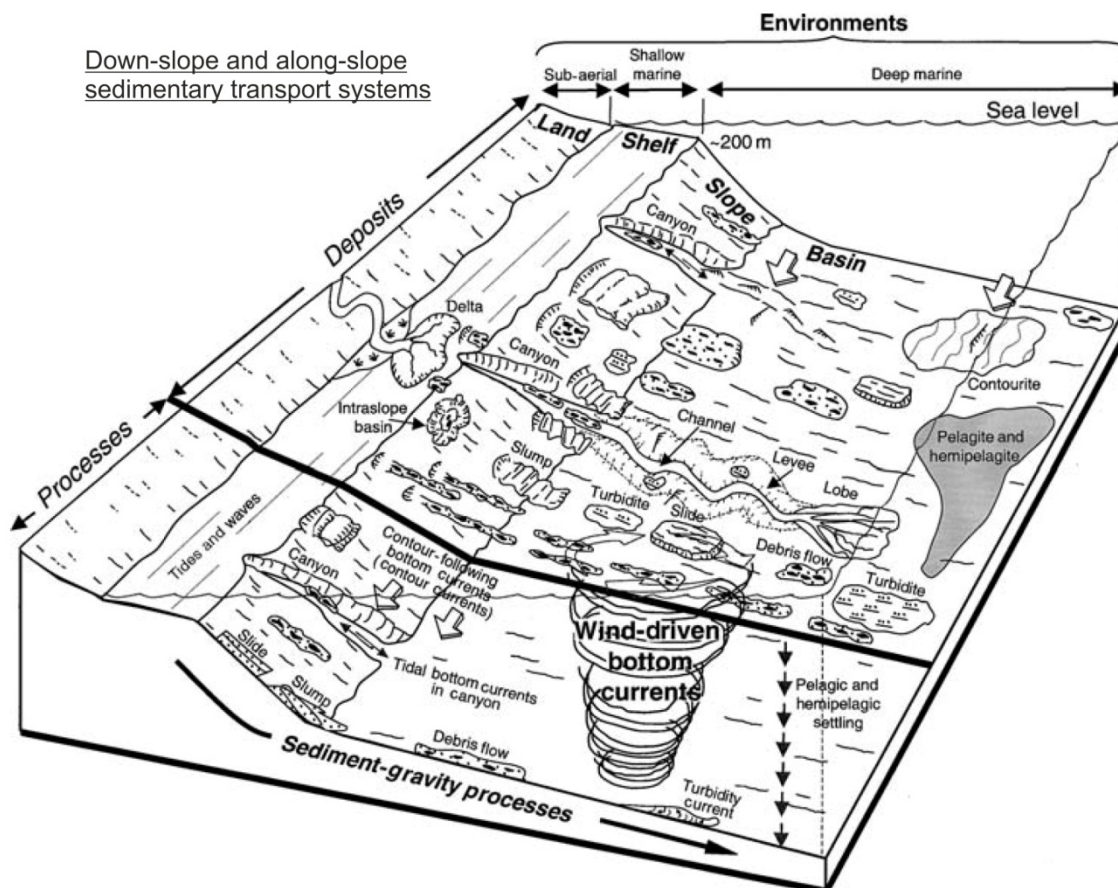


**Figure 1.1:** Schematic diagram showing complex deep-marine sedimentary environments occurring at water depths greater than 200 m. In general, shallow marine environments are characterized by tides and waves, whereas deep-marine (slope and basin) environments are characterized by mass movements, bottom currents and pelagic/hemipelagic sedimentation. Modified from Shanmugam (2003, 2008); with permission from Elsevier.



2008). Depending on the specific transporting process they result in a large variety of deposits. Successive failure of sediments over a extended time periods will shape continental slope morphology and might result in the evolution of channel-levee systems or submarine canyons (Fig. 1.1). While downslope processes were extensively studied not the least due to their importance for hydrocarbon reservoirs and their geohazard potential, alongslope processes gained an increasing scientific awareness during the last decades for similar reasons. Alongslope sediment transport is driven by bottom currents, which follow the contours of the bathymetric framework as part of the thermohaline circulation or are related to rings, meanders and eddies carried within surface as well as deep waters (Fig. 1.1). Persisting for long time periods, bottom currents are steered by the marginal framework, which in turn is continuously altered by depositional and erosive processes associated with alongslope processes (Rebesco and Camerlenghi, 2008).

## **1.2 Sedimentation under influence of bottom currents**

The capacity of ocean currents to transport and redistribute sediments in the deep ocean was first described in the 1930's (Wust, 1936). Nevertheless, the scientific attention was finally drawn to bottom current related sediment transport in the 1960's (Dzulynski and Walton, 1965; Heezen, 1959; Heezen et al., 1955; Wust, 1955, 1958). Inspired by these findings, during the next decades sediment waves and drift deposits were identified in all kinds of marine environments including the shallow marine realm and several formation processes were introduced (Faugeres et al., 1999; Gao et al., 1998; Lovell and Stow, 1981; Okada and Ohta, 1993; Rebesco, 2005; Rebesco and Camerlenghi, 2008; Stow and Mayall, 2000; Stow et al., 2002; Viana et al., 2007). Today, the idea is widely accepted that bottom (contour) currents are capable to significantly shape continental margins (Stow et al., 2009) by eroding, transporting and depositing sediments at the sea floor (Rebesco and Camerlenghi, 2008). These currents, although mostly flowing alongslope, can be extremely variable in space and time, in particular in areas influenced by through-passing eddies or close to gateways connecting ocean basins (Brackenridge et al., 2011; Nowell et al., 1985; Rebesco and Camerlenghi, 2008). Furthermore, bottom currents can be related to a uniform flowing water mass, or encompass several water masses, which might even flow in opposite direction and therefore result in complex flow pattern (Laberg et al., 2005; Viana et al., 2002a; Viana et al., 2002b). However, all deposits formed mainly under the control of geostrophic and thermohaline circulation patterns or substantially reworked by bottom currents are classified as 'contourites' (Faugères and Mulder, 2011; Rebesco and Camerlenghi, 2008). The identification of drift deposits based only on sedimentological evidence is a hard task to accomplish. In the early stages of contourite research scientists were only aware of deposits without a distinct mounded shape (e.g. Heezen and Hollister, 1964; Heezen et al., 1966 and therefore, only samples from current controlled deposits intercalated with turbidites and pelagic sediments were available. This fact prohibited the definition of conclusive sedimentological criteria regarding contourite drift identification. Based on the tremendous amount of samples collected in the following

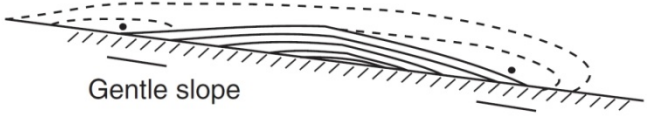
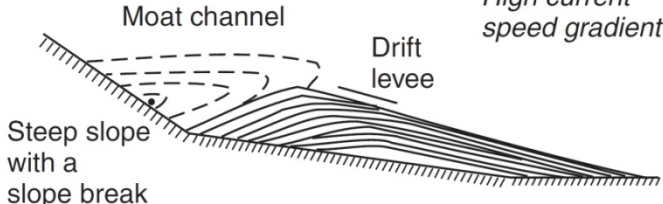
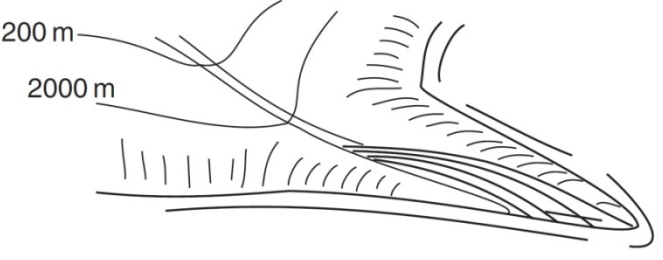
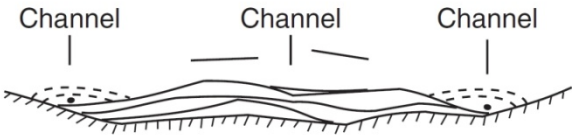
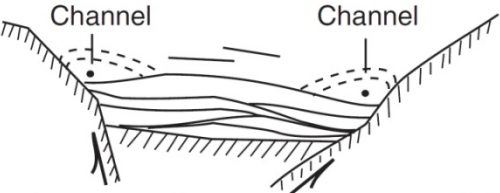
decades, especially during the High Energetic Benthic Boundary Layer Experiment (HEBBLE, McCave and Hollister, 1985; Nowell et al., 1985), a contourite facies model was suggested for both sandy and muddy contourites (Stow, 1982; Stow and Lovell, 1979), which was recently summarized and refined by Stow and Faugères (2008). Although this facies model was already established 30 years ago, it is still debated by the scientific community, in particular by Shanmugam (2003, 2007, 2008) and Shanmugam et al. (1995).

Besides sedimentological evidence, seismic and acoustic imaging of seafloor and subsurface structures can provide detailed information regarding drift identification (Fig. 1.2). Furthermore, by spatial imaging of sedimentary structures the evolution of contourite features can be reconstructed in time and space. Based on the development of both the large-scale shape and the internal seismic facies of drift deposits the paleo-environment factors, which have been constrained deposition, can be deciphered as shown e.g. in the Gulf of Cadíz (Llave et al., 2001), at the Cantabrian Margin (Van Rooij et al., 2010), off SE Africa (Preu et al., 2011) and off South and Central Argentina (Hernández-Molina et al. 2009, 2010).

The shape of contourite deposition is controlled by four main factors: Bottom current velocity and variability, the topographic framework, sediment supply and the time period available for drift formation (Faugères et al. 1999). Based on these variables, different types of contourites are deposited, which were summarized and classified by Faugères et al. (1993, 1999), Faugères and Stow (2008) and Rebesco (2005). In principle, drift deposits are subdivided into sheeted and mounded drifts.

Sheeted drifts cover extensive areas with thicknesses up to hundreds of meters. As the name 'sheeted drift' implies, sediment thickness shows little variations along the drift and only a slight decrease in thickness can be observed across the drift's center to its borders (Faugères et al. 1999). By means of seismo-acoustic facies analysis, sheeted drifts are quite similar to turbidite sheets due to their low-amplitude character, which mostly reveals discontinuous reflections. In some parts these low amplitudes fade into acoustic transparency (Faugères et al. 1999). Overall, sheeted drifts are formed on top of a gentle relief with a smooth topography, which favors non focused, tabular bottom currents. Smaller turbulence in the bottom currents may lead to the formation of sediment waves, which might be comprised within their sedimentary record or are recently formed (Faugères and Stow, 2008). Typical examples of sheeted drifts include those within the Mozambique Basin (Ben-Avraham et al., 1994), the North Rockall Trough (Howe et al., 1994; Richards et al., 1987; Stoker, 1995) and the Argentine Basin (Flood and Shor, 1988).

Mounded drifts differ from sheeted drift by their distinctly mounded and elongated shape. With length/width ratios varying from 2:1 to 10:1 they can extend from several tens of kilometers to over 1000 km (Faugères et al. 1999). Location, orientation and drift migration depend strongly on the interplay between the contours of the continental margin, the slope gradient, the local current regime and the Coriolis force (Fig. 1.2, Faugères and Stow, 2008). They were already classified by McCave and Tucholke (1986) into plastered, separated and detached drifts (Fig. 1.2) depending on their margin

<b>Mounded drifts:</b>		migration and aggradation any type of reflections, except horizontal/parallel reflections
<b>Giant elongated drifts</b>	<p><b>Plastered drift</b></p> <ul style="list-style-type: none"> <li>- along-slope migration (downstream of the current flow)</li> <li>- down-and up-slope migration</li> </ul> <p>Example: Gardar drift</p>	<p><i>Low current speed gradient</i></p>  <p>Gentle slope</p>
	<p><b>Separated drift</b></p> <ul style="list-style-type: none"> <li>- along-slope migration (downstream of the current flow)</li> <li>- up-slope migration</li> </ul> <p>E.g. Faro drift</p>	<p><i>High current speed gradient</i></p>  <p>Moat channel Drift levee</p> <p>Steep slope with a slope break</p>
	<p><b>Detached drift</b></p> <ul style="list-style-type: none"> <li>- predominant down-slope migration</li> </ul> <p>Example: Eirik drift</p>	 <p>200 m 2000 m</p>
<b>channel-related drifts</b>	<ul style="list-style-type: none"> <li>- predominant down-current migration</li> <li>- random lateral migration</li> </ul> <p>Example: Vema contouritic fan</p>	 <p>Channel Channel Channel</p> <p>Downstream of a deep channel issue</p>
<b>Confined drifts</b>	<ul style="list-style-type: none"> <li>- predominant down-current migration</li> <li>- limited lateral migration</li> </ul> <p>Example: Sumba drift</p>	 <p>Channel Channel</p> <p>In between high tectonic or volcanic reliefs</p>

**Figure 1.2:** Summary of the different types of mounded contourite drifts (see McCave and Tucholke, 1986; Faugères et al. 1993, 1999; Stow et al. 2002) showing the drift general geometry and trend of migration – aggradation as well as inferred bottom-current pathways. From Faugères and Stow (2008); with permission from Elsevier.

setting, current strength and migration direction. Additional subclasses, the channel-related and confined drift, were amended by Faugères et al. (1993; 1999) and recently summarized by Faugères and Stow (2008, Fig. 1.2). Due to their strong dependence on the interplay between topographic framework and bottom current velocity and direction, the spatial analysis of these deposits allows to infer on former oceanographic settings. However, since mounded drifts are mostly located along or in

close vicinity to continental slopes, events of downslope sediment transport might add to or overprint the quasi-continuous, but slowly forming bottom current controlled deposits (Faugères et al. 1999; Faugères and Stow, 2008).

The different contourite drift classifications encompass minor disagreements, which are partly related to non-uniform usage of nomenclature, but point also to residual uncertainties in determining the crucial forcing factor in drift formation on a case to case basis. Therefore, next to the drift deposition modern analysis of contourites takes as well into account erosive features, which are often intimately linked to contourite formation (Fig. 1.3). These extensive erosive features are the result of bottom currents interacting with the bottom relief, leading to a development of local and regional hydrodynamic anomalies as e.g. cores, vortices and helicoidal flows (Fig. 1.3, Hernández-Molina et al. 2008a). Although erosive features are not as well studied as drifts, several types have been described during the last years, including contourite terraces, which represent the most common feature (e.g. García et al., 2009; Hernández-Molina et al., 2003, 2008a; Nelson et al., 1993; Nelson et al., 1999; Stow et al., 2009; Stow et al., 2008; Stow and Mayall, 2000). Nevertheless, no detailed model was yet proposed explaining the evolution of contourite terraces in detail. Analogue to turbidite depositional systems, to pronounce the relation between drifts and their associated erosive features, a conglomerate of these features aligned along a particular continental slope is commonly termed contourite depositional system (CDS; Hernández-Molina et al., 2003; 2008b; Rebesco and Camerlenghi, 2008; Stow et al., 2002).

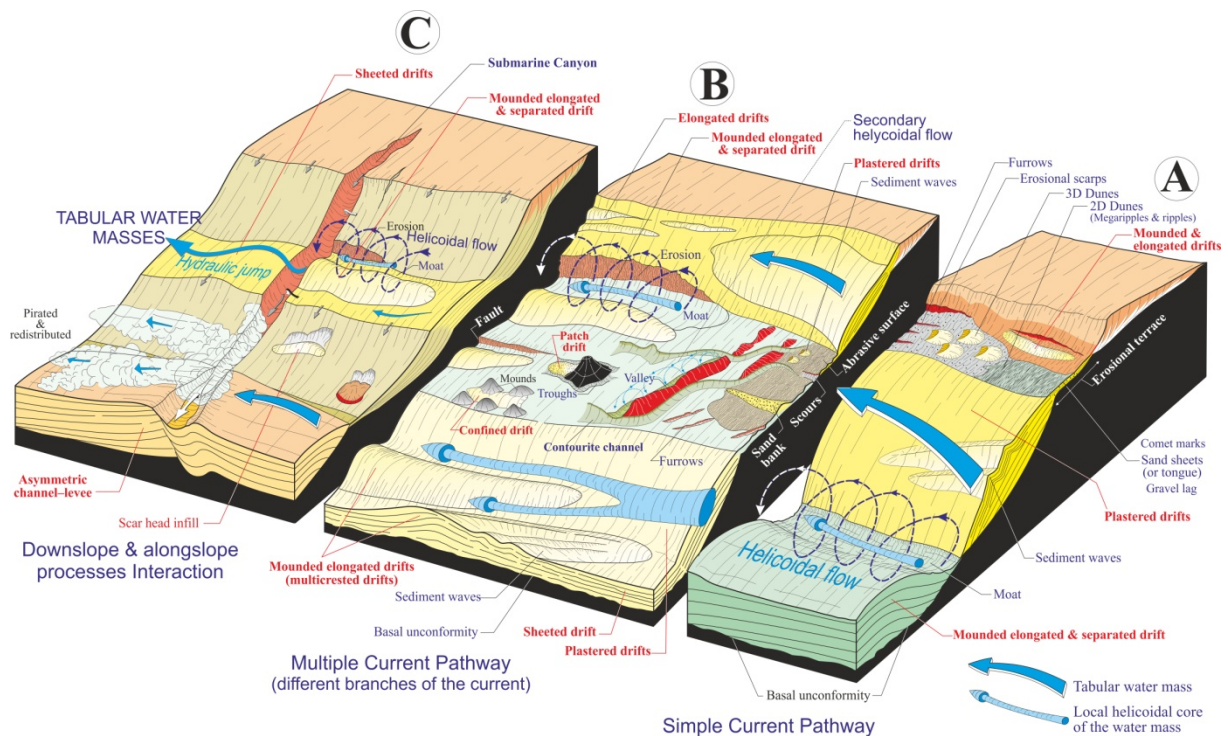


Figure 1.3: 3-D conceptual sketch showing the potential contourite depositional and erosional features on a slope over: (a) margins with different water masses along the slope but with simple current pathways (e.g. the Brazilian slope and the Northern European Margin), (b) margins where recent tectonic activity has produced very complex slope morphology, increasing the possibility of generating multiple-current pathways (e.g. the slopes of the Gulf of Cadiz, western Iberian Margin and some active margins) and (c) interaction between down-slope (submarine canyons and slides). From Hernández-Molina et al. (2008b); with permission from Elsevier.

### 1.3 Motivation and objectives

Along- and downslope sedimentation processes and their interaction have a major impact on the shape of continental slopes. Downslope transport is either caused by mass-wasting events as slumps/slides or occurs in canyons incised into shelf or slope. In contrast, slope parallel sediment transport is mainly controlled by contour-following currents as part of the thermohaline circulation. During the last decades it became evident that contour current controlled deposition and therefore contourites form a significant amount of marginal sediments (Faugères et al. 1993).

At the same time, contouritic sediment deposits became more and more important as paleoceanographic/paleoclimatic archives, as hydrocarbon reservoirs and because of associated slope instabilities and geohazards (Rebesco and Camerlenghi, 2008). Especially due to their high accumulation rates compared to the background sedimentation, studies were carried out focusing on sediment transport processes and paleoceanographic reconstructions (e.g.: Hernández-Molina et al., 2006; Llave et al., 2001; McCave and Tucholke, 1986; Mézerais et al., 1993; Preu et al., 2011; Van Rooij et al., 2010). Nevertheless, the scientific knowledge on contourite drifts, their associated erosive features and their interplay is still limited. In particular, the origin of wide contourite terraces and their linkage to the oceanographic and depositional regime remains unclear.

In contrast to the rapid sediment accumulation associated with contourites, canyons form large incisive, rather erosive features at the seafloor. They strongly influence the sedimentary regime on continental slopes by acting as major conduits for turbidity currents transporting shelf and upper slope material into the deep sea basin. However, canyons are not only interesting from a mass wasting point of view. Reconstruction of activity within canyons and analysis of background sedimentation can provide paleoclimatological and paleoceanographic information (Hanebuth and Henrich, 2009; Henrich et al., in rev.; Henrich et al., 2009; Zühlsdorff et al., 2008). Moreover, canyons strongly influence bottom currents and their resulting drift deposits. This interaction represents a significant and important process for the evolution of continental slopes (Hernández-Molina et al., 2008a; Laberg and Camerlenghi, 2008; Mulder et al., 2008; Mulder et al., 2006). Even though studies focused on the interaction between alongslope processes and canyons (Marchès, 2008; Marchès et al., 2010; Salles et al., 2010), the impact of large-scale incisions on bottom currents and the sediments, which they transport, is not well understood.

In the frame of MARUM Project SD3 'Slope architecture and evolution of sedimentary regimes' the overall goal of this thesis is to assess the impact of both, alongslope and downslope oriented sediment transport, on sedimentary processes and to decipher their interaction. A promising location to study the interplay between gravitational and current-driven sediment transport is the northern Argentine margin, where a huge CDS has formed in the border region between Argentina and Uruguay off the Rio de la Plata in water depths of ~1100-1500 m. This CDS is characterized by drift deposits, by several contourite terraces (Hernández-Molina et al., 2009; Violante et al., 2010) and by the large Mar del Plata submarine canyon (Fig. 1.4, Krastel et al., 2011).

In this context the first objective of this thesis is mapping and analyzing of the sedimentary structures associated with the northern Argentine CDS based on high-resolution multichannel seismic data and multibeam bathymetry data. Mapping depocenter shifts and areas of deposition and non-deposition in time and space within the drift accumulations allow to reconstruct the evolution of the CDS and the oceanographic regime controlling alongslope processes in this area.

The second objective is the spatially inclusive and comprehensive mapping of surface and near-surface sedimentary structures off the Rio de la Plata River. For this purpose sediment echosounder ('Parasound') data collected in 2009 and conventional seismic data provided by the 'Comisión Nacional del Límite Exterior de la Plataforma Continental' (COPLA) are considered to achieve for this purpose sufficient data coverage. Joint interpretation with available hydrographic data sets will allow linking the spatial variations in drift deposition and erosive features with the regional oceanographic setting.

The third objective of this thesis is a morphological and structural analysis of the drifts deposits in close vicinity of the Mar de Plata Canyon, located within the northern Argentine CDS, in time and space based on seismic data. Depocenter shifts in close vicinity to the Mar del Plata Canyon will reveal the history of the Mar del Plata Canyon and its evolving impact on the drift deposition.

At last, the final objective is the spatial analysis of hydro-acoustic water column data recorded using an 18 kHz parametric echosounder. Interpretation of these backscatter signals in relation to Acoustic Doppler Current Profiler data might allow inferring on sediment transport processes within the water column and at the sea floor.

## 1.4 Regional setting of the northern Argentine margin

### 1.4.1 Oceanographic setting

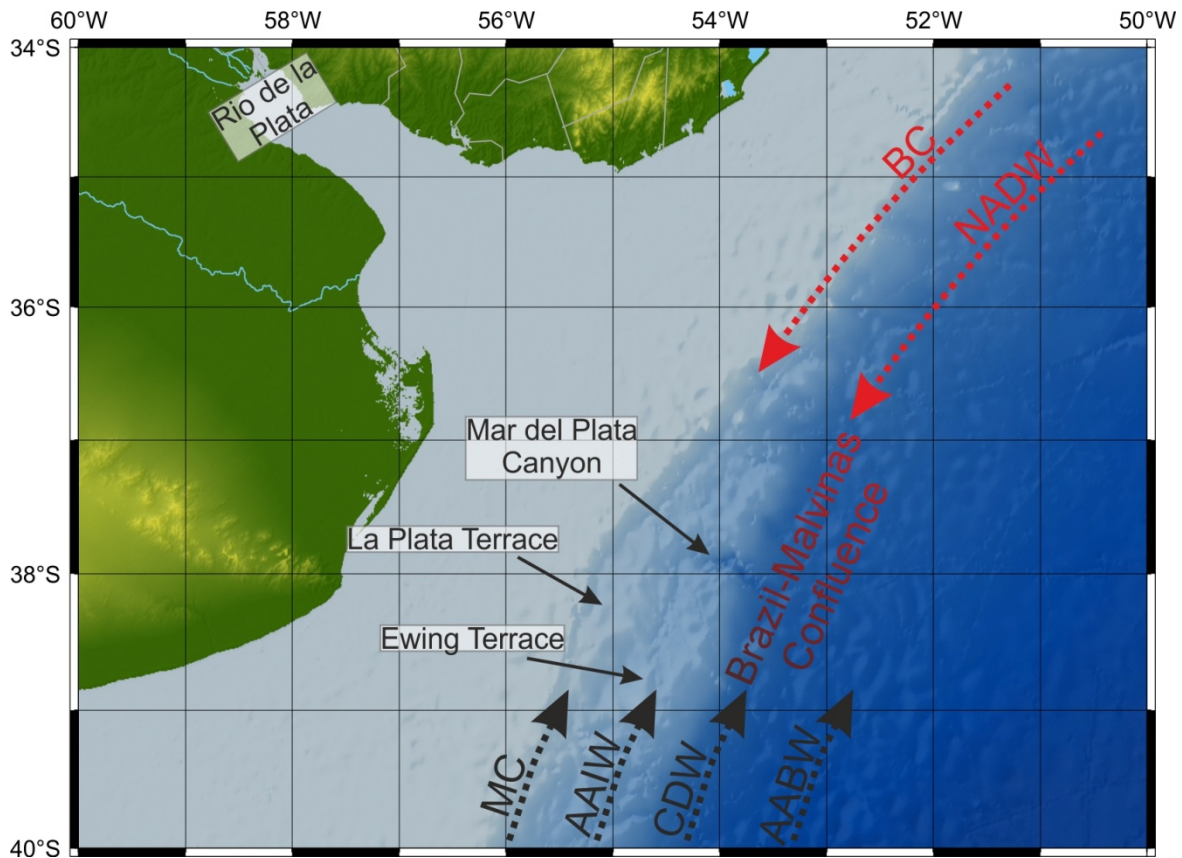


**Figure 1.4:** Map of the boundary region between Uruguay and Argentina indicating besides the main physiographic features, as well the regional oceanographic regime; BC – Brazil Current; MC – Malvinas Current; AAIW – Antarctic Intermediate Water; CDW – Circumpolar Deep Water; NADW – North Atlantic Deep Water; AABW – Antarctic Bottom Water

The northern Argentine margin encompasses one of world's most dynamic oceanographic settings, in which the interaction of ocean currents with the seafloor is ubiquitous (Chelton et al., 1990). Numerous shipboard surveys and satellite image analysis were focused on the identification of water masses and their volume transport, main flow direction and driving forcing (de Souza et al., 2006; Gordon and Greengrove, 1986; Legeckis and Gordon, 1982; Reid, 1989; Reid et al., 1977). The upper circulation pattern is mainly dominated by the northward flowing, subantarctic Malvinas Current (MC), the southward flowing, sub-tropical Brazil Current (BC) and the resulting encounter called the Brazil/Malvinas Confluence (BMC, Figure 1.4, Peterson, 1992; Piola and Matano, 2001).

The 100 km wide MC, as a branch of the Antarctic Circumpolar Current, transports cool, nutrient rich water from the pole equatorward along the Argentine slope (Stramma, 1989). The current originates in the northern portion of the Drake Passage (Tomczak and Godfrey, 2001). In contrast, the BC transports warm, saline and relatively oligotroph water poleward along the shelf of Brazil and Uruguay (Stramma, 1989). As a branch of the South Equatorial Current the BC forms a major surface current in the SW Atlantic, which consists mainly of Tropical Water (TW) and South Atlantic Central Waters (SACW, Fig. 1.5, Piola and Matano, 2001).

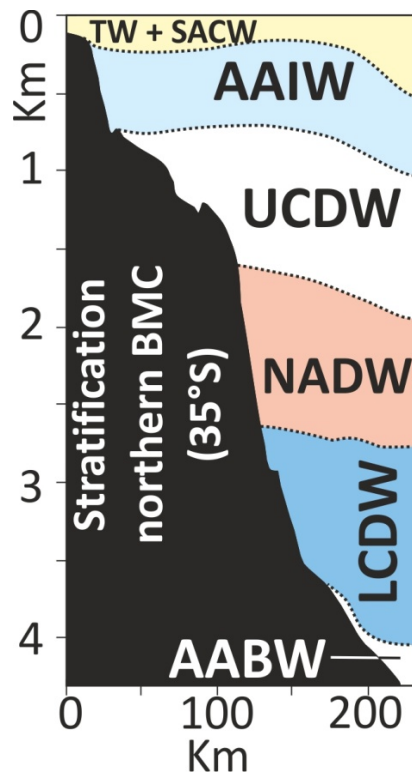


**Figure 1.5.:** Vertical water mass stratification north of the Brazil Malvinas Confluence (BMC); TW – Tropical Water; SACW – South Atlantic Central Water; AAIW – Antarctic Intermediate Water; UCDW – Upper Circumpolar Deep Water; NADW – North Atlantic Deep Water; LCDW – Lower Circumpolar Deep Water; AABW – Antarctic Bottom Water; modified from Hernández-Molina et al., 2009

The confluence zone resulting from the collision of Brazil and Malvinas Current influences an area between 25°S and 45°S depending on the seasonal variability both surface currents. In annual average the axis of this high energetic area is located at 38-39°S (Bisbal, 1995). The confluence zone is hydrographically mainly characterized by intense vertical and horizontal mixing and large variations in temperature and salinity due to the formation of large eddy fields (Piola and Rivas, 1997).

Vortices and eddies are not only associated to the surface waters of the BMC. Eddies originating from the BC are mostly a result of an anomalous poleward migration of the BC (Gordon and Greengrove, 1986; Piola and Matano, 2001). These eddies might strongly influence the underlying water stratification causing a vertical mixing up to 4000 m. Once detached from the BC retroflection these northeastward moving eddies enter the wind-driven sub-tropical South Atlantic anticyclonic gyre (Olson et al., 1988). Cold filaments and shed rings carried within the MC are also driven frequently into this recirculation cell (Piola and Matano, 2001).

However, the BMC is not only characterized by the highly dynamic and complex current setting in surficial waters.

Underlying water mass circulation and stratification along the slope is characterized by the encounter and interaction of northward flowing Antarctic water masses (Antarctic Intermediate Water [AAIW]; Circumpolar Deep Water [CDW] and Antarctic Bottom Water [AABW]) with the southward flowing recirculated AAIW, originating from the BMC itself, and North Atlantic Deep Water (NADW; Figs. 1.4 and 1.5; Carter and Cortese, 2009; Georgi, 1981; Piola and Matano, 2001; Saunders and King, 1995). Interfaces between these water masses are determined by relatively large density gradients, which tend to deepen on a basin scale (Reid et al., 1977) and lead to strong vertical mixing and the shedding of eddies (Arhan et al., 2002, 2003; Piola and Matano, 2001). Intermediate and deep water circulation along the Argentine margin is characterized by the AAIW and the two fractions of the CDW: the Upper Circumpolar Deep Water (UCDW) and the Lower Circumpolar Deep Water (LCDW, Fig. 1.5 (Arhan et al., 2002; 2003; Reid et al., 1977). Within the confluence UCDW and LCDW are vertically separated by the southward flowing NADW (Fig. 1.5), which follows closely the South African slope until the BMC (Fig. 1.4), where it detaches from the margin (Piola and Matano, 2001).



ABWW, partly trapped within the basin, dominates the abyssal circulation pattern in water depth deeper than 3500-4000 m forming a large cyclonic gyre (Arhan et al., 2002, 2003; Piola and Matano, 2001).

### 1.4.2 Geological setting

The tectonic regime of the Argentine margin is controlled by deep located crustal structures established during the break-up of the South Atlantic in the Early Cretaceous or even prior to the continental fragmentation (Franke et al., 2007; Hinz et al., 1999). Structures originating from the rift phase, in particular major seaward dipping reflections are the result of seafloor spreading and extensive volcanic activity during continental drift and ocean-floor spreading in the Early Cretaceous (Ewing and Lonardi, 1971; Franke et al., 2007; Hinz et al., 1999; Keeley and Light, 1993; Light et al., 1993; Ramos, 1999).

Next to complex deep lying crustal structures the south-eastern margin of South America is as well known for its contour current controlled sedimentation regime. Three major sheeted contourite drifts were described in the abyssal plain off Argentina formed under the influence of the AABW: the Ewing Drift, Argyro Drift and Zapiola Drift, which is in particular known for its extensive sedimentary wave field (Ewing and Lonardi, 1971; Hernández-Molina et al., 2008b; Lonardi and Ewing, 1971; von Lom-Keil et al., 2002).

However, not only sedimentary processes in the abyssal plain are influenced by the oceanographic regime, but also several CDSs with well developed depositional and erosive features, forming a contourite depositional system (CDC), are located in mid-slope position off Argentina (Fig. 1.6; Hernández-Molina et al., 2009). The aforementioned Antarctic water masses (see chapter 1.4.1) and their interfaces control sedimentation and shape slope morphology especially in the southern part of Argentina, where contour channels and terraces are carved into the slope sediments. Towards the north the importance of down-slope oriented sediment transport increases resulting in a more complicated sedimentary regime, which is reflected by numerous canyons, scars and mass flow deposits (Fig. 1.6 (Hernández-Molina et al., 2009, 2010, Violante et al., 2010). These down-slope processes are not only related to more than 80 million tons of suspension load per year, which are transported onto Argentine margin from large river systems as the Rio de la Plata representing one of the largest rivers on Earth (Milliman and Meade, 1983), but also to local slope instabilities (Krastel et al., 2011; Violante et al., 2010).

The northernmost drift and shallowest deposits included in the extensive mapping of Hernández Molina et al. (2009) and Violante et al. (2010) is located off the Rio de la Plata mouth in the border region between Uruguay and Argentina (Fig. 1.6). Here, in the northern area of the Ewing Terrace drift deposits were identified in water depths between 1200 and 1400 m north of the Mar del Plata Canyon. The head of this major submarine canyon is located beneath the La Plata Terrace (Urien and Ewing, 1974) in water depth of 1000 m and the canyon exit is located in 4000 m (Krastel et al., 2011).

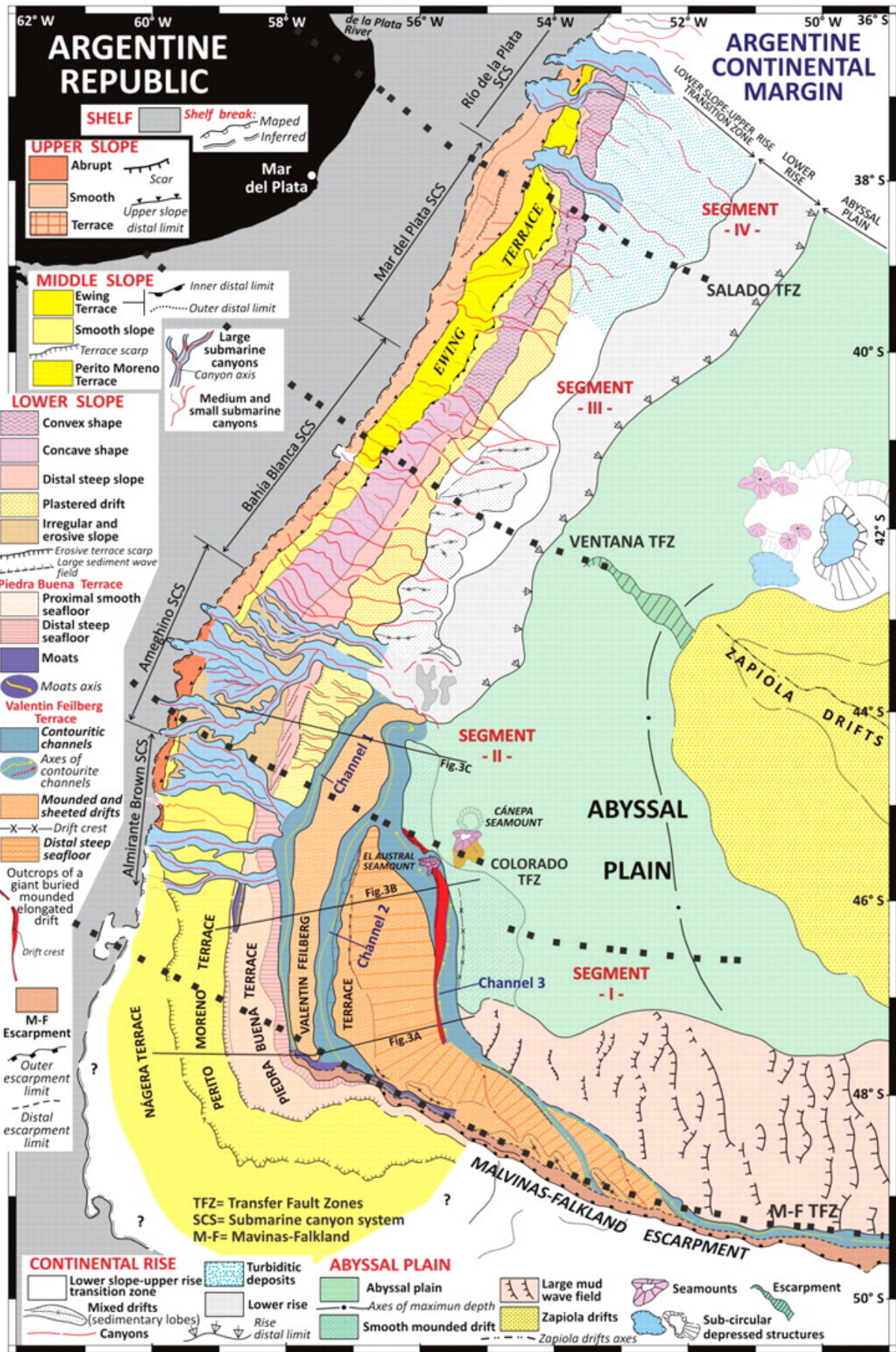
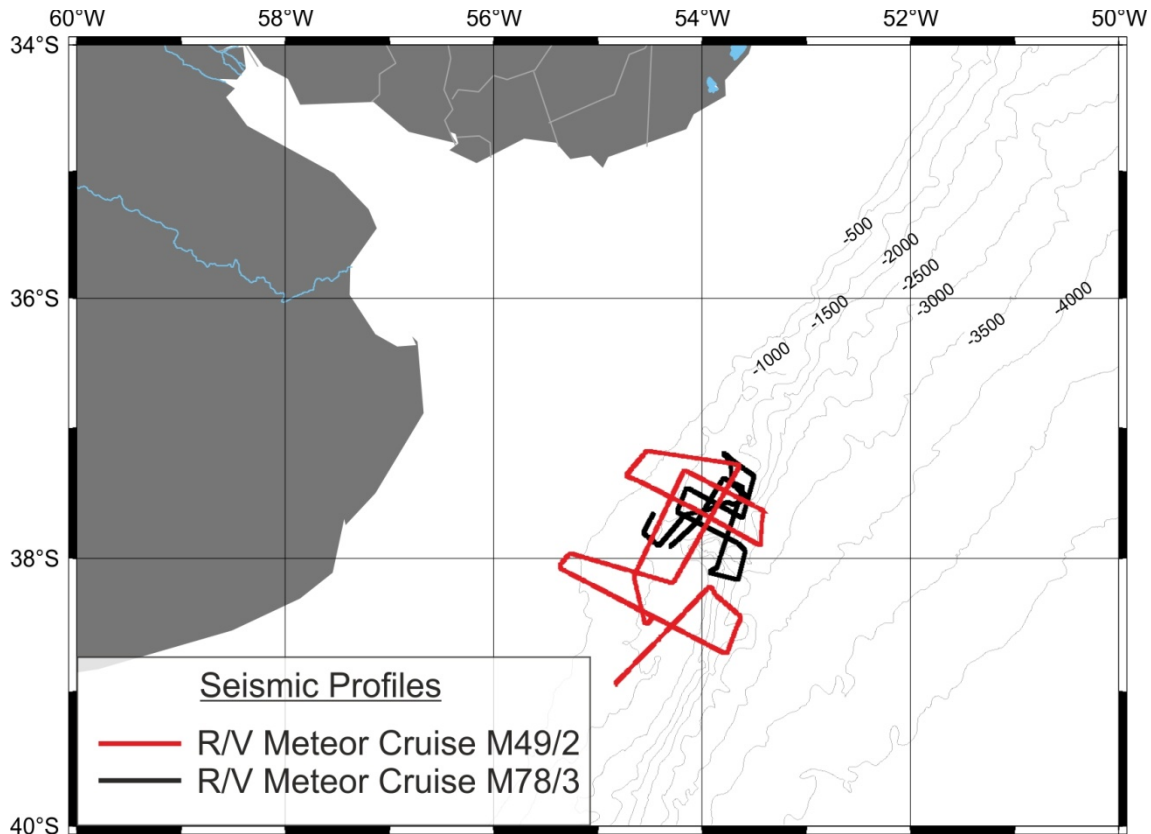


Figure 1.6: Morpho-sedimentary map of the Argentine margin; from Hernández-Molina et al., 2009

In the center part of the Ewing Terrace the canyon extends over 20 km and is incised up to 1500 m into the seafloor. Although the Mar del Plata Canyon is located directly in front of the Rio de la Plata, not only a modern but as well a former connection of both features can be excluded based on subsurface imaging by means of high-resolution multichannel seismic (Krastel et al., 2011).

### 1.5 Methods



**Figure 1.7:** Map of the northern Argentine margin including location of high-resolution multichannel seismic lines recorded during R/V Meteor Cruises M49/2 (2001) and M78/3 (2009)

Spatial and temporal analysis of the northern Argentine slope architecture is mainly based on data sets collected during R/V Meteor Cruise M49/2 (2001) and R/V Meteor Cruise M78/3 (2008). During both cruises integrated seismic and acoustic measurements were carried out, including multichannel seismic using Generator-Injector (GI)-guns (Fig. 1.7), Parasound acoustic profiling and swath bathymetry mapping. However, this thesis focuses mainly on GI gun data, so the following text will only introduce the multichannel systems necessary to acquire GI gun data in greater detail.

While during R/V Meteor Cruise M49/2 the GeoB high-resolution multi-channel seismic system developed by the Department of Geoscience, Bremen was used, during R/V Meteor Cruise M78/3 the seismic equipment of the IFM-GEOMAR was deployed. Both systems are designed to image small scale sedimentary structures and closely spaced layers even in large water depths, which can usually not be imaged with conventional seismic systems. Due to rough weather during the cruises, both systems were temporarily operating under heavy conditions. The resulting technical issues resulted in an increased level of background noise and in several minor data gaps.

In total over 1540 km of multichannel seismic data were processed and analyzed for this study.

### **1.5.1 Data acquisition**

#### **1.5.1.1 R/V Meteor Cruise M49/2**

Two different GI-Guns served as seismic sources during R/V Meteor Cruise M49/2, which were triggered in an alternating mode: The first, a GI-Gun with reduced chamber volume of 2 x 0.41 L (frequency range 100 – 800Hz), and the second, a GI-Gun with an extended chamber volume of 2 x 1.7 L (frequency range ca. 80-400Hz), were both operated in harmonic mode (injector volume does not exceed generator volume) and towed approximately 13 m behind the ship's stern, one on each side of the ship. However, due to the fact, that the GI-Gun with extended chamber volumes ensures deeper penetration of the seismic signal which is still characterized by a reasonable frequency range, only data acquired using the 1.7 L GI-Gun were processed and analyzed in the context of this thesis. The injector was triggered with a delay of 50 ms with respect to the generator signal, which basically eliminated the bubble signal. The gun was triggered at an air pressure of 150 bar in an 18 s time interval, which results by an average ship speed during seismic survey operations of 6 kn in a approximated shot distance of 54 m.

The acoustic signal was received using an analog multichannel seismic streamer, which included a tow-lead, two stretch sections of 50 m and six active sections of 100 m length. Active sections are subdivided in 16 hydrophone groups of 6.25 m length. The streamer was towed in a mean water depth of 3 m, which was controlled by 5 MultiTrak and 5 DigiBird Remote Units (RUs). These RU were attached to the streamer and include a depth and a heading sensor as well as adjustable wings. Via communication coils, nested within the streamer, water depth and heading of each RU was recorded for each shot to ensure a high quality of geometry control for data processing purposes.

Finally, the signal was recorded using a 48 channel JUPITER/ITI/BISON seismograph, providing a sample frequency of 4 kHz at 24 bit resolution over 3 s recording time. The data were demultiplexed and stored in SEG-Y format on a DLT 4000 cartridge tape. Due to the technical limitation of the acquisition unit only every second channel could be recorded for the 1.7 L GI-Gun, which results in a final multichannel seismic data set data set of 48 channels with a 12.5 m spacing recorded during R/V Meteor Cruise M49/2.

#### **1.5.1.2 R/V Meteor Cruise M78/3**

For the seismic data recorded during R/V Meteor Cruise M78/3 a Mini-GI-Gun (2 x 0.2 L) in harmonic GI configuration was used as seismic source, towed 10 m behind the ship's stern. In contrast to the larger source used during the former cruise, the Mini-GI-gun emits higher frequencies (100-800 Hz) resulting in a higher vertical resolution at the expense of lower penetration depth of the acoustic signal. The injector chamber was triggered with a time delay of 20 ms. Overall, the gun was shot with

an air pressure of 150 bar in with water depth varying intervals between 4.5 and 6 s. This results in an shot interval of 11-15 m considering an average ship speed of 5 kn while seismic surveying.

The digital streamer, used to receive the acoustic energy, included a 25 m long stretch section and 16 active sections of 12.5 m length. Towed as well in 3 m water depth, the streamer was steered by three Oyo Geospace Bird RUs, which all include depth sensors, a compass and adjustable wings. Data from these RUs were transmitted by each shot via the streamer to the control unit, which recorded the different parameters.

The data were recorded with acquisition software provided by ‘Geometrics’ with a sampling frequency of 8 kHz and stored as multiplexed SEG-D.

### 1.5.2 Data processing

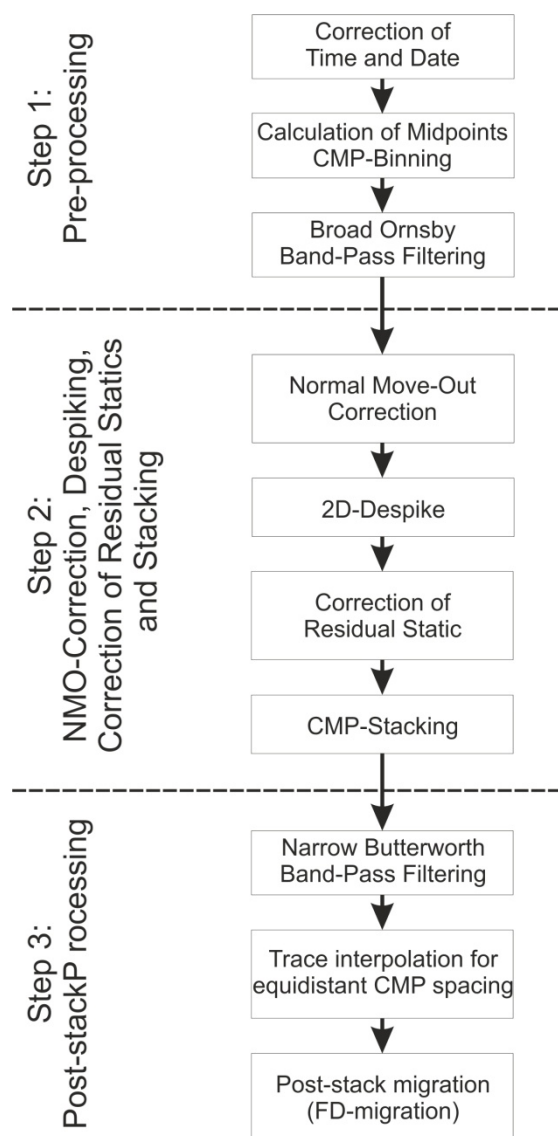


**Figure 1.8:** Schematic processing flow applied to seismic data recorded during R/V Meteor Cruises M49/2 and M78/3

The goal of seismic data processing is to increase the image quality of the geological features in the data set to guarantee a correct and convenient interpretation. To accomplish this goal there are two major tasks: suppress background and electric noise energy inside the data set and migration of the seismic traces to allow correct imaging of dipped surfaces and reflections.

Noise is categorized into coherent noise, which has constant frequency characteristics, and incoherent noise, which distributes its energy randomly over all frequencies. While coherent noise can be treated with trace editing and frequency depended filtering, to suppress incoherent noise is more complicated. To approach this task a common mid-point (CMP) gather stacking can be applied, which is one of the major advantages of multichannel seismic technology. For applying this technique, previously other conventional processing procedures like geometry incorporation, CMP-binning, velocity analysis and normal move-out (NMO) correction have to be carried out. Conditioned by CMP-binning and its implied assumption, that gun-receiver mid-points are the locations of seismic events recorded by corresponding traces, this processing step is susceptible for errors. Because this assumption fails

immediately in areas characterized by dipping layers or diffractive bodies, a migration has to be performed on the stacked data set.

This leads to a general processing sequence schematically summarized in at Fig. 1.8. While the incorporation of acquisition geometry was carried out using the custom software packages GeoApp and WinGeoApp, the applied seismic processing including trace editing, velocity analysis, NMO correction, stacking, filtering and migration was carried out with the commercial software package Vista Seismic Processing. These processing steps will be explained briefly in this chapter based on Yilmaz (1987).

### 1.5.2.1 Pre-processing

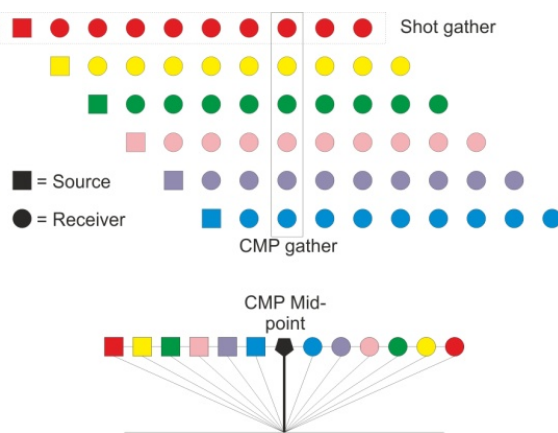


**Figure 1.9:** Geometrical source and receiver relationship in Shot and CMP gather

After trace header information were corrected for time and date mismatches, CMP-binning was carried out based on previously determined source and corresponding receiver positions provided by the custom software packages ‘GeoApp’ (R/V Meteor Cruise M49/2) and ‘WinGeoApp’ (R/V Meteor Cruise M78/3). The resulting CMP gather differs crucially from the shot gather, in which the data was recorded (Fig. 1.9). While a shot gather describes the sorting of traces for each shot with increasing receiver offsets, a CMP gather encompasses all

traces, whose corresponding source-receiver midpoints are located at the same spot on the seafloor.

This processing step is carried out based on the assumption of a horizontal and flat seafloor.

While incorporating acquisition geometry supported by ‘WinGeoApp’ provides full manual control on the binning process, the older ‘GeoApp’ allows correcting the position of the individual receivers for deviations from the standard geometry layout recorded by the RUs. CMP bin size was set to 2 m for data recorded using the Mini-GI-gun. Due to the lower shot rate a CMP bin size of 10 m was chosen for the 1.7 L GI-gun data.

In the first stage of signal processing a broad Ornsby band-pass filter was applied (filter flanks: 10 Hz/25 Hz/ 1000 Hz/ 2000Hz) to suppress low frequent mechanic noise, which partly exceeds the signal, carrying the geological information, by an order of magnitude. Next, damaged or empty channels were selected and deleted. Furthermore, major amplitude anomalies associated to incoherent noise need to be deleted in an interminable process manually. At last the gun delay was corrected.

### 1.5.2.2 Velocity analysis

The main purpose of velocity analysis is to estimate sound velocity and its horizontal and vertical variability utilizing the relationship between two-way travel time of seismic events and shot-receiver

offsets. Since in large water depth and for deep located subsurface structures as well large offsets are required for a precise determination of sound velocity, the configuration of both used streamer systems did not allow for a detailed velocity analysis.

During data processing a constant root-mean-square (RMS) sound velocity of 1500 m/s was assumed.

### **1.5.2.3 Normal move-out (NMO) correction, despiking, correction of residual statics and stacking**

Correcting the time delay caused by the source-receiver offset of every trace is called NMO correction. Afterwards, all seismic events in a CMP gather, should appear at the same two-way time in all traces. This allows suppressing of moderate incoherent noise by applying a 2D-despike algorithm, which operates on the basis of a running average calculation. This algorithm determines the RMS amplitude over all traces within a CMP-gather for a narrow time window and compares the result to the individual amplitudes of each trace. Amplitudes corresponding to a single trace exceeding the RMS amplitude by a factor of 1.3 were reduced to the calculated RMS value. In the next step the window is shifted downward in time with a window overlap of 25%. That way, the algorithm allows suppressing incoherent noise without resulting in abnormal amplitude variations in the final CMP stack.

After despiking minor shifts of seismic events in time between traces in a CMP-gather, called residual static, were corrected. Residual static originates from three dimensional movements of source and receivers during acquisition, which were not yet considered during pre-processing. These shifts are corrected using an auto-correlation algorithm, which was set up to calculate the necessary shift for each trace providing the best stacking result for the seafloor. The correction of residual stacking not only results in a clearer seismic image after CMP-stacking, it also ensures the preservation of high frequent information in this process.

Finally, the seismic data in each CMP-gather were stacked to enhance seismic events and suppress incoherent and random noise, which results in a tremendous increase of the signal to noise (S/N) ratio.

### **1.5.2.4 Post-stack processing**

To reduce the residual noise another band-pass filter was applied. In contrast to the filter applied during pre-processing, a narrow Butterworth band-pass filter was used, which is due to its cosine filter flanks is less susceptible to Gibb's Phenomena at the expense of computing time. The filter was set to 40 Hz /80 Hz/ 600 Hz/ 1200 Hz for the 1.7 L GI-gun data and to 60 Hz/ 120 Hz/ 600 Hz / 1200 Hz for data containing the signals recorded using the Mini-GI-gun. Next, to prepare the data for migration, which requires equidistant trace spacing, missing traces were interpolated, which might have been generated during pre-processing due to the erasing of channels and traces carrying irrelevant seismic signals.

As already mentioned above, the major assumption of processing based on CMP-sorting is, that all traces are located at the mid-point between source and receiver. Since this assumption is not solid for dipped surfaces, in a stacked profile steeply dipping reflectors are displaced and their dipping angle is lowered. At diffractive bodies, hyperbolas would occur on their edges. The process of migration should collapse these diffractions and migrate dipping reflectors to their correct position and angle. Therefore, as a last step in processing a FD time-migration was carried out, which in comparison to other migration algorithms is more tolerate to uncertainties in sound velocity estimations.

## 1.6 Thesis outline

Chapters 2-5 represent stand-alone case studies, written for publication purposes. They focus on individual aspects of onset, evolution and transport processes of CDSs, in particular of the highly dynamic system off northern Argentina. An special case is presented by Chapter 5, which focuses on along-slope processes and transport of suspended particles within the water column off SE Africa. Chapter 6 summarizes the major findings of the four stand-alone articles and evaluates the main results in a greater context regarding the general concept of contourite depositional systems.

In **Chapter 2**, high-resolution reflection seismic data are used to determine the evolution of the northern Argentine continental margin. Derived from spatial and temporal variations in slope architecture for the first time the oceanographic regime can be reconstructed trough time, in particular the history of Antarctic water masses and the North Atlantic Deep Water, in whose transition the contourite drift deposits are formed (Hernández-Molina et al., 2009).

**Chapter 3** concentrates on the mapping and analysis of surface and near-surface sedimentary features. The novel approach here is the use of both, seismo-/hydro-acoustic and hydrographic data sets, to link modern morphological features of the northern Argentine continental margin to the highly dynamic oceanographic regime. This approach provides insights into the origin of contourite terraces and their influence on bottom current flow pattern.

In **Chapter 4** the slope architecture in close proximity of the Mar del Plata Canyon is analyzed. Based on the deeper understanding of the alongslope processes off northern Argentina achieved in chapter 2 and 3, for the first time the influence of the canyon on bottom current controlled sedimentary processes will be evaluated and reconstructed on geological time scales.

The last stand-alone article presented in **Chapter 5**, focuses on spatial analysis of water column backscatter anomalies off SE Africa recorded with a parametric echosounder ('Parasound'). This study was carried with data collected during R/V Meteor Cruise M75/3 (2008). The backscatter anomalies will be interpreted in conjunction with Acoustic Doppler Current Profiler (ADCP) data and results of my master thesis, which were recently published (Preu et al., 2011; Appendix 1), but are not considered as a separate chapter in this thesis. This novel approach of visualizing the distribution of suspended particles within the water column will provide spectacular insights into the interaction of ocean currents, topography and the resultant sediment transport.



## 1.7 Additional contributions to articles

In addition to the four articles presented in this thesis, I contributed to the following complementary studies during my PhD studies:

Title: Sediment dynamics and geohazards off Uruguay and the la Plata River region (northern Argentina and Uruguay)

Authors: Sebastian Krastel, Gerold Wefer, Till J.J. Hanebuth, Andrew A. Antobreh, Tim Freudenthal, **Benedict Preu**, Tilmann Schwenk, Michael Strasser, Roberto Violante, Daniel Winkelmann, M78/3 shipboard party

Journal: Geo-Marine Letters

Status: published 2011 (Appendix 2)

Contribution: paper writing; seismic data processing, conceptual model

Title: Distinct Expressions of the BSR using various various frequencies offshore Uruguay and its correspondence with the gas hydrate stability zone

Authors: Juan Tomasini, **Benedict Preu**, Sebastian Krastel, Tilmann Schwenk, Volkhard Spiess, Héctor de Santa Ana

Book: Proceedings of the 7<sup>th</sup> International Conference on Gas Hydrates (2011)

Status: published

Contribution: paper writing, seismic data processing, data integration

Title: Geotechnical characteristics of submarine slope and mass movement deposits along the Northern Argentine and Uruguayan margin

Authors: Fei Ai, Ina Schulze, Daniel Winkelmann, Sebastian Krastel, **Benedict Preu**, Michael Strasser, Achim Kopf

Journal: Marine Geology

Status: submitted

Contribution: conceptual model; data integration

Title: Las terrazas contorníticas en el Margen Continental Argentino: implicaciones morfosedimentarias y oceanograficas

Authors: F. Javier Hernández-Molina, **Benedict Preu**, Roberto A. Violante, Alberto R. Piola, C. Marcelo Paterlini

Journal: GEOGACETA – Sociedad Geologica de España

Status: submitted

Contribution: seismic data processing, seismostratigraphy, conceptual model

Title: Submarine Slope Failure offshore Uruguay – A Relation to Hydrates?

Authors: Daniel Winkelmann, Michael Strasser, Andrea Anasetti, **Benedict Preu**, Tilmann Schwenk, Sebastian Krastel

Status: in preparation

Contribution: seismic data processing

## **2. Sedimentary growth pattern on the northern Argentine slope: The impact of North Atlantic Deep Water on southern hemisphere slope architecture**

Benedict Preu<sup>(1)</sup>, Tilmann Schwenk<sup>(1)</sup>, F. Javier Hernández-Molina<sup>(2)</sup>, Roberto Violante<sup>(3)</sup>; C. Marcelo Paterlini<sup>(3)</sup>; Juan Tomasini<sup>(4)</sup>; Sebastian Krastel<sup>(5)</sup>, Volkhard Spieß<sup>(1)</sup>

(1) MARUM – Center for Marine Environmental Sciences and Faculty of Geosciences,  
University of Bremen, Bremen, Germany

(2) Facultad de Ciencias del Mar, Universidad de Vigo, Vigo, Spain

(3) Servicio de Hidrografía Naval (SHN), Buenos Aires, Argentina

(4) ANCAP Exploración y Producción, Montevideo, Uruguay

(5) GEOMAR | Helmholtz Centre for Ocean Research Kiel, Germany

To be submitted to 'Marine Geology'

## **Abstract**

Large sedimentary sequences consisting of several major contourite drifts were studied along the middle slope off Northern Argentina to determine the evolutionary stages as well as to identify and assess the possible impact of Northern Source Deep Water (NSDW) on the middle slope architecture. Based on their sedimentary stacking pattern, current controlled sediments deposited beneath the northern extent of the Ewing Terrace allow decoding on the pale-oceanographic setting of the last 32 Ma. By means of high-resolution multichannel seismic data collected during R/V Meteor Cruises M49/2 (2000) and M78/3 (2009) three major seismic units can be identified, which were used to determine growth stages, each representing a different oceanographic setting

Earliest current controlled sedimentation can be observed over the middle slope close to the Eocene/Oligocene boundary within the Complex Unit. The Unit shows an aggradational stacking pattern with a complex and wavy acoustic facies, pointing towards an unstable, turbulent current environment. This facies is in general coeval with the opening of the Drake Passage. Its related global cooling resulted in a strengthening of surface, intermediate and deep ocean currents in the Southern Ocean and allowed the first time sediment deposition at the Argentine slope under current control. During the Middle Miocene the sedimentation regime changes and the Sigmoidal Unit, plastered drift sequences with a sheeted reflection pattern, was deposited. The formation of major plastered drifts indicates weak, non-turbulent current conditions. We conclude that this change in the current regime is the result of the first formation of NSDW during the Mid-Miocene climatic optimum, which led to a major rearrangement of water masses and vertical shifts of water mass boundaries in the study area. Above, the Aggradational Unit shows continuous formation of plastered drift sequences with an aggradational stacking pattern leading to the modern extent of the Ewing Terrace along the middle/lower slope off Argentina. This is the result of the strengthening of NSDW until the final closure of the Central American Seaway (CAS). Today, after the complete closure of the CAS and under the influence of the full force of the NSDW, mounded plastered drift sequences are built upon the Ewing Terrace.

Showing the influence of NSDW on the slope architecture in the study area, we suggest that deep-water production in the northern hemisphere plays a significant key role in shaping the continental slopes in the western South Atlantic since the middle Miocene.

## **2.1 Introduction**

While the large capacity of ocean currents to transport and redistribute sediments in deep ocean basins was first described in the 1930's (Wust, 1936), the scientific interest in bottom current controlled sedimentary deposits grew in the 1960's (e.g.: Dzulynski and Walton, 1965; Heezen, 1959; Heezen et al., 1955; Pettijohn and Potter, 1964; Wust, 1955, 1958). Subsequently, more and more studies identified sediment waves and drift deposits on slopes, in the abyssal plains as well as along continental margins, and several processes shaping the seafloor were introduced (e.g.: Gao et al., 1998;

Rebesco, 2005; Rebesco and Camerlenghi, 2008; Stow et al., 2002; Stow and Mayall, 2000; Viana et al., 2007). Following the definition of Rebesco and Camerlenghi (2008), all such deposits formed mainly under the control of geostrophic and thermohaline driven bottom currents can be classified as contourites.

Erosional features and areas of non-deposition are typically observed in combination and close proximity to contourite drifts, forming in combination a contourite depositional system (CDS, Hernández-Molina et al., 2003, 2008a). Analyzing these large-scale sedimentary patterns in time and space allows studies of former oceanic regimes as shown e.g. off Greenland (Hunter et al., 2007), off Antarctica (Rebesco et al., 2002) and in the Gulf of Cádiz (Habgood et al., 2003; Hernández-Molina et al., 2003; Llave et al., 2007; Mulder et al., 2003, 2006) and off Mozambique (Preu et al., 2011).

Along the Argentine continental margin, a large CDS has developed, which is characterized by large-scale contourite channels, morphological terraces and plastered drift sequences controlled by Antarctic bottom water circulation (Hernández-Molina et al., 2009). Although several studies dealt with the southern part of the Argentine CDS in detail, the continuation of this sedimentary system into the northern area was tentatively described and analyzed in previous studies (Krastel et al., 2011; Violante et al., 2010). However, this part of the margin represents a key location in the global thermohaline ocean circulation due to the convergence of Brazil and Malvinas Current (Brazil-Malvinas Confluence Zone; BMCZ; Fig. 2.1A) two major surficial ocean currents. In addition, the BMCZ marks the

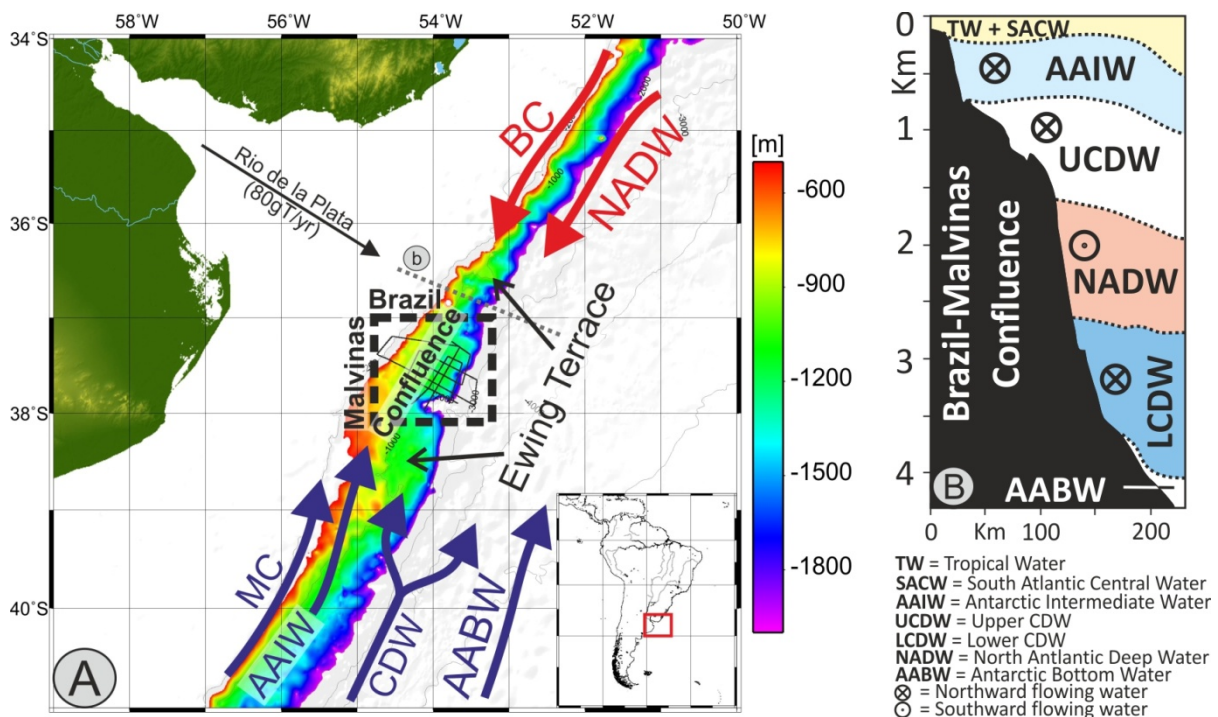


**Figure 2.1:** A) Map of the border region between Argentina and Uruguay (GEBCO, 2008); colors highlight the Ewing Terrace on the middle slope; the black box marks the study area (see Fig. 2); thick arrow mark the flow path of the main currents and water masses: BC (Brazil Current); MC (Malvinas Current); AAIW (Antarctic Intermediate Water); CDW (Circum Polar Deep Water); NADW (North Atlantic Deep Water) and AABW (Antarctic Bottom Water). B) Oceanographic transect crossing the Brazil Malvinas Confluence showing the modern vertical water mass stratification based on Piola and Matano (2001) and Hernandez Molina et al. (2009)

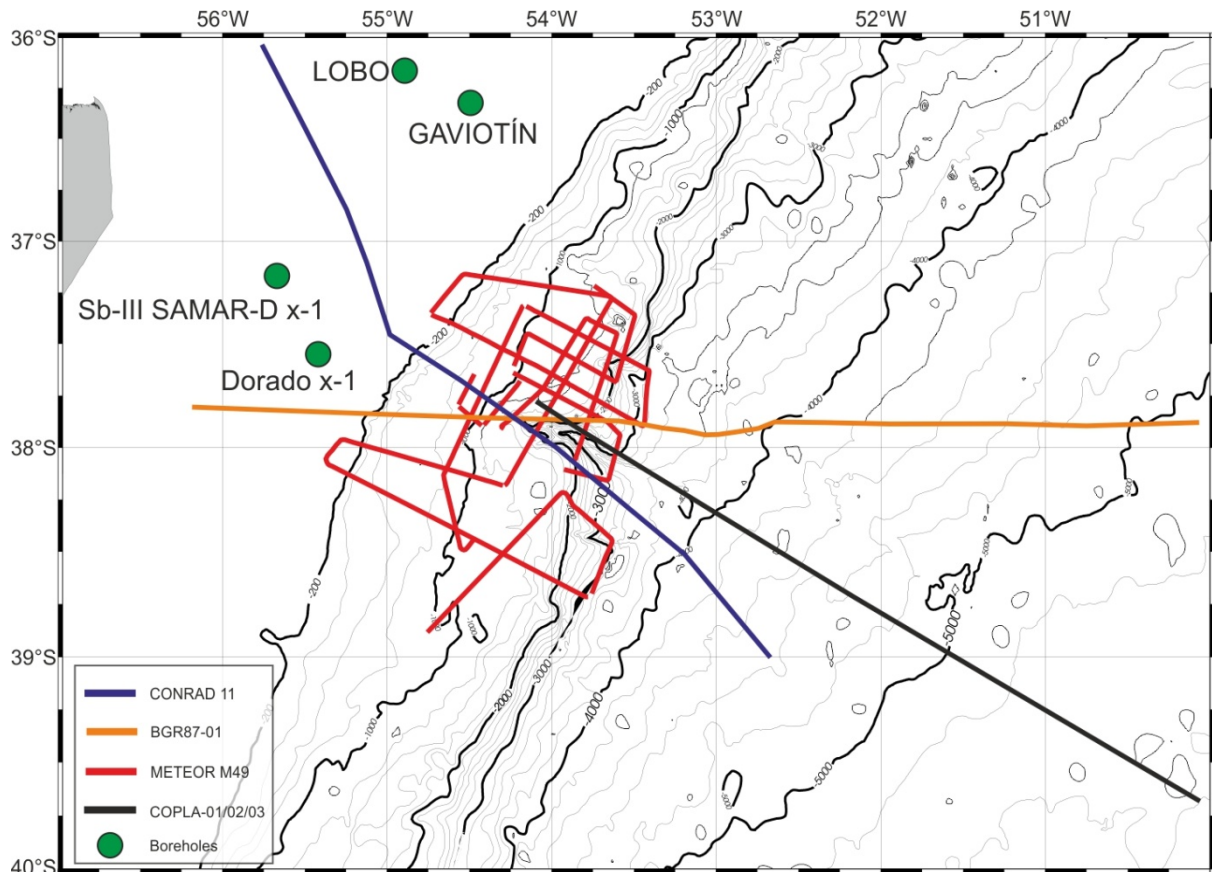


**Figure 2.2:** Map of the northern Argentine and southern Uruguayan continental margin showing the position of seismo-acoustic lines and boreholes used in this study

southernmost extent of Northern Source Deep Water (NSDW) as a bottom current along the western South American margin (Piola and Matano, 2001).

Since NSDW, today known as North Atlantic Deep Water (NADW), acts as a major element within the climatic coupling responsible for glacial/interglacial cycles (Knutz, 2008) and variations in deep water production, transport and depth off Greenland and Norway are considered to strongly influence the thermohaline circulation, pathways of the NSDW in the modern and past ocean all over the globe have been intensely studied using predominantly nano- and microfossils (e.g.: Broecker et al., 1988, 2004; Prell, 1984; Ravelo, 2006; Ravelo et al., 1990; Tiedemann et al., 1994; Zachos et al., 1994).

The main goal of this study is to carry out a seismostratigraphic analysis of the CDS on the north-east Argentina continental margin based on multiple seismo-acoustic data sets (Fig. 2.2) to identify its temporal and spatial variability and to identify major evolutionary stages. This analysis will be used to reveal the evolution of the oceanographic regime controlling the western South Atlantic on geological time scales, and to evaluate the possible impact of North Atlantic Deep Water in margin construction.

## **2.2 Regional setting**

### **2.2.1 Oceanographic framework**

The modern oceanographic regime at the Argentine margin is highly dynamic and variable and became target of several shipboard surveys and satellite image analysis (de Souza et al., 2006; Gordon and Greengrove, 1986; Legeckis and Gordon, 1982; Reid, 1989; Reid et al., 1977). The upper circulation is mainly dominated by the northward flowing, subantarctic Malvinas Current (MC), the southward flowing, sub-tropical Brazil Current (BC) and the resulting Brazil-Malvinas Confluence Zone (Fig. 2.1A; Peterson, 1992).

The MC, as a branch of the Antarctic Circumpolar Current (ACC), transports cool water from the pole equatorward along the Argentine slope (Fig. 2.1A; Matano et al., 2010; Stramma, 1989). The current originates in the northern portion of the Drake Passage (Fig. 2.1A, Tomczak and Godfrey, 2001). In contrast, The BC transports warm and saline water poleward along the shelf of Brazil and Uruguay (Stramma, 1989).

The resulting confluence zone influences an area between 25°S and 45°S depending on the seasonal variability of both surface currents. In annual average the axis of this highly energetic area is located at 38-39°S (Fig. 2.1A; Bisbal, 1995). The confluence zone is hydrographically mainly characterized by intense vertical and horizontal mixing and large variations in temperature and salinity due to the formation of large eddy fields.

The intermediate circulation within this confluence is conditioned by the northward flow of Antarctic Intermediate Water (AAIW), and of the two Circumpolar Deep Water fractions: Upper Circumpolar Deep Water (UCDW) and Lower Circumpolar Deep Water (LCDW; Fig. 2.1B; Arhan et al., 2002, 2003). AAIW is still present below the BC in a depth of 500-1200 m (Fig. 2.1B; Piola, 2006). NADW, originating from northern hemisphere high latitudes, stratifies underneath the BC close to the slope in water depths of 2000-3000 m (Fig. 2.1B). At the southern tip of the BMCZ, the NADW detaches from the slope and flows without morphological constrain further southward (Arhan et al., 2003; Piola and Matano, 2001; Tomczak and Godfrey, 2001).

### **2.2.2 Geological and physiographic framework**

The Argentine margin is characterized by a continental slope of ~1500 km length and 50-300 km width (Ewing and Lonardi, 1971). The underlying crust is constructed by voluminous extrusives due to large scale transient volcanism accompanying the continental break-up and initial seafloor spreading in the Early Cretaceous (Ewing and Lonardi, 1971; Franke et al., 2007; Hinz et al., 1999; Keeley and Light, 1993; Light et al., 1993). Since Late Paleogene times the sedimentation regime is controlled by currents (Hernández-Molina et al., 2009, 2010; Violante et al., 2010). Three major elongated and mounded contourite drifts are known, forming large sediment deposits in the AABW controlled abyssal plain: the Ewing, Argyro and Zapiola Drift (Ewing and Lonardi, 1971; Hernández-Molina et al., 2008b; Lonardi and Ewing, 1971; von Lom-Keil et al., 2002).

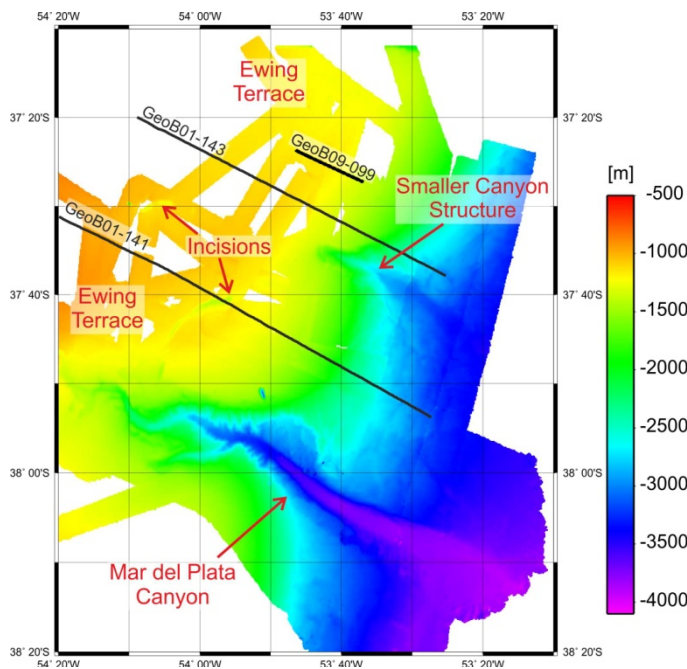


**Figure 2.3:** Bathymetric map of the northernmost slope off Argentina recorded based on multi-beam data recorded during R/V Meteor Cruises M49/2 (2001) and M78/3 (2009) covering water depths of 500-4500m; the map shows the Ewing Terrace with the Mar del Plata Canyon in the south; see position of this frame in Fig. 1A; position of multichannel seismic Lines GeoB01-141, GeoB01-143 and GeoB09-099 are indicated

A major contourite depositional complex has built the mid-slope topography of the Argentine margin controlled by Antarctic water masses and their interfaces. Especially in the southern part of Argentina, large contour channels and terraces are carved into the slope sediments. Toward the north the sedimentation regime becomes more complex due to an increase of down-slope sediment transport processes, which result in numerous canyons, scars and mass flow deposits (Hernández-Molina et al., 2009, 2009; Krastel et al., 2011; Violante et al., 2010). These down-slope processes are related in part to slope sediment instabilities (Krastel et al., 2011; Violante et al., 2010) but also to the more than 80 million tons of suspension load per year

transported onto the Argentine margin from large river system as the Rio de la Plata River, which is one of the largest rivers on earth (Giberto et al., 2004; Milliman and Meade, 1983).

The northernmost and shallowest drift described by Hernández-Molina et al. (2009) and Violante et al. (2010) is located along the mid-slope in the border region between Argentina and Uruguay off the Rio de la Plata River mouth in water depths between 1200 and 1400 m as part of the so-called Ewing Terrace. The terrace, and thereby the drifts, are incised by the Mar del Plata Canyon (Fig. 2.3), which is located between 1000 m and 4000 m water depth (Krastel et al., 2011). In its center the canyon extends over 20 km and the talweg is incised by almost 1500 m into the seafloor (Fig. 2.3).

### 2.3 Methods

High-resolution multichannel seismic (MCS) data were collected off northern Argentina during R/V Meteor Cruises M49/2 (2001) and M78/3 (2009, Fig. 2.2). Data collected during R/V Meteor Cruise M49/2 were acquired using as seismic source a 1.7 L GI-Gun (TM SODERA, France) with main frequencies of 100-500 Hz and an analog MCS streamer of 600 m length hosting 96 channels. During R/V Meteor Cruise M78/3, MCS data were collected with a 0.24 L Mini-GI-Gun (TM SODERA) as seismic source with main frequencies of 100-600 Hz. The seismic signal was received using a 200 m active digital MCS streamer containing 128 channels. Seismic processing was carried out with the commercial seismic processing package Vista (Gedco Co.). Standard seismic processing was applied



including trace editing, normal move-out correction, residual statics correction, geo-referenced common midpoint (CMP) binning and stacking, band-pass filtering and FD time migration. Data recorded during R/V Meteor Cruise M49/2 were processed using 10 m CMP spacing, while for data recorded during R/V Meteor Cruise M78/3 5 m CMP spacing was applied. Interpretation was done using the software the commercial software package The Kingdom Software (SMT).

For bathymetric mapping swath sounder data (HYDROSWEEP DS (M49/2) and EM120 (M78/3) were collected during both cruises.

The seismic data were interpreted in four steps: first, seismostratigraphic analysis was carried out by tracing discontinuities to define major seismic units from the middle through the lower slope to the rise; second, subunits were identified by studying variations in seismic facies to identify changes of the depositional style and to distinguish between down-slope and along-slope sedimentary processes; and last, the ages of seismic units and discontinuities were correlated with borehole data as well as with previous regional seismic-stratigraphic correlations (Fig. 2.2). Correlations of industrial borehole data were provided by Argentine (Instituto Hidrografico Naval, IHN) and Uruguayan (Administración Nacional de Combustibles, Alcohol and Portland, ANCAP) authorities. The seismostratigraphic approaches implemented and discussed in this study (Tab. 2.1) are based on Ewing et al. (1971), Hinz et al. (1999), Franke et al. (2007), Hernández-Molina et al. (2009, 2010), Violante et al. (2010) and Gruetzner et al. (2011).

This study		Ewing and Lonardi (1971)	Hinz et al. (1999)	Hernández Molina et al. (2009+2010)		Violante et al. (2010)	Gruetzner et al. (2011)	Age constrain
Major seismic units and discontinuities	Subunits	Main Reflectors	Major discontinuities	Major Units	Sub Units			
Aggrading Unit	AU5			Upper Unit	a	SD A		Mid-Pleistocene Revolution
	AU4							Quaternary
	AU3							Late Pliocene (~3.2-2.2 Ma)
H1		H1			H1	VF3	Late Pliocene (~3.2 Ma.)	
Aggrading Unit	AU2			Upper Unit	b	SD C		Pliocene
	AU1							c
H2		H2				H2	VF1	Middle - Late Miocene
Sigmoidal Unit				Intermediate Unit		SD D		Middle Miocene
AR5		H3	AR5	AR5		AR5	AR5	Middle Miocene (~16 Ma)
Complex Unit	CU3			Lower Unit	a+b	SD E		upper Miocene
	CU2							
	CU1							
Early Oligocene Upper Slope					c			Oligocene
AR4			AR4	AR4		AR4	AR4	Eocene - Oligocene boundary (~32-33 Ma)

**Table 2.1:** Regional stratigraphic discontinuities and depositional units defined by Ewing and Lonardi (1979), Hinz et al. (1999), Hernández-Molina et al. (2009, 2010), Violante et al. (2010) and Gruetzner et al. (2011).

Nomenclature and classification of erosive and depositional features appearing in a CDS are based on review studies previously published by Faugeres et al. (1999) and Rebesco (2005), which had been summarized and discussed in Rebesco and Camerlenghi (2008).

## 2.4 Results

### 2.4.1 General morphologic characteristic

Bathymetric and multichannel seismic data used for this study show a CDS located on the Ewing Terrace north of the Mar del Plata Canyon in a water depth of ~1200 m (Figs. 2.3-2.6).

This part of the Ewing Terrace covers at least an area of 50 km width by ~90 km length constructed by drift deposits with a maximum thickness of 0.9 s TWT. Landward, the Ewing Terrace is attached to the locally steep upper slope (4-8°). While the proximal part of the terrace in water depths of 1100-1150 m is characterized by very low slope angles (~0.4°), overall the terrace is clearly dipping seaward reaching a slope gradient of 1° in its distal part in water depths of 1300-1350 m. At the

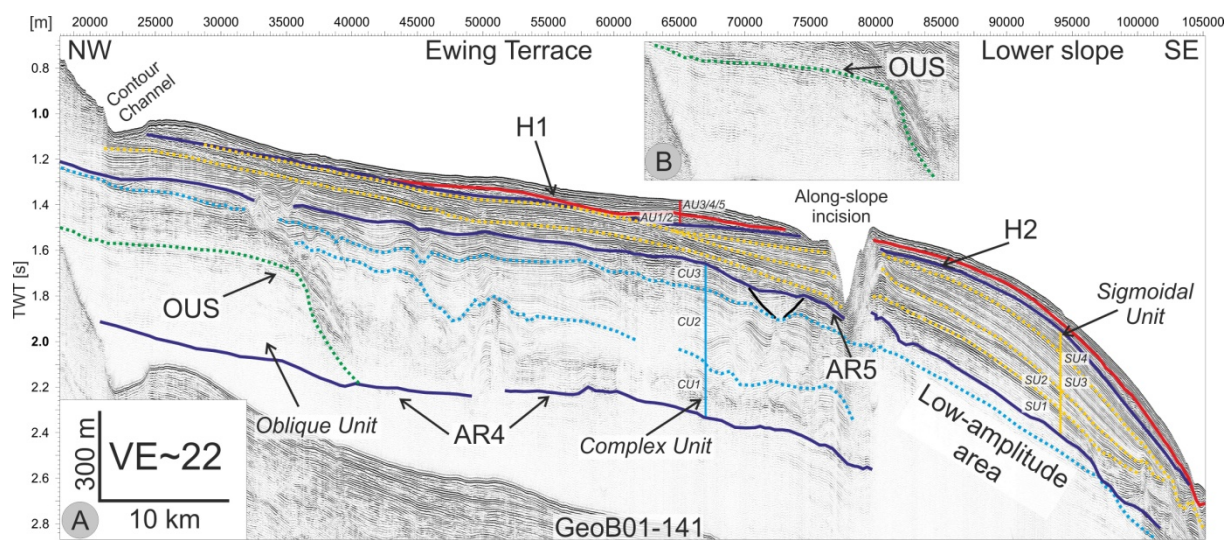


**Figure 2.4:** **A)** Multichannel seismic Line GeoB01-141 as indicated in Fig. 2.3; VE ~20; stratigraphic information was based on Ewing and Lonardi (1978) and Hinz et al. (1999, see Tab. 2.1); **B)** Oblique Unit with imaged with a higher gain for a better illustration of the internal structures

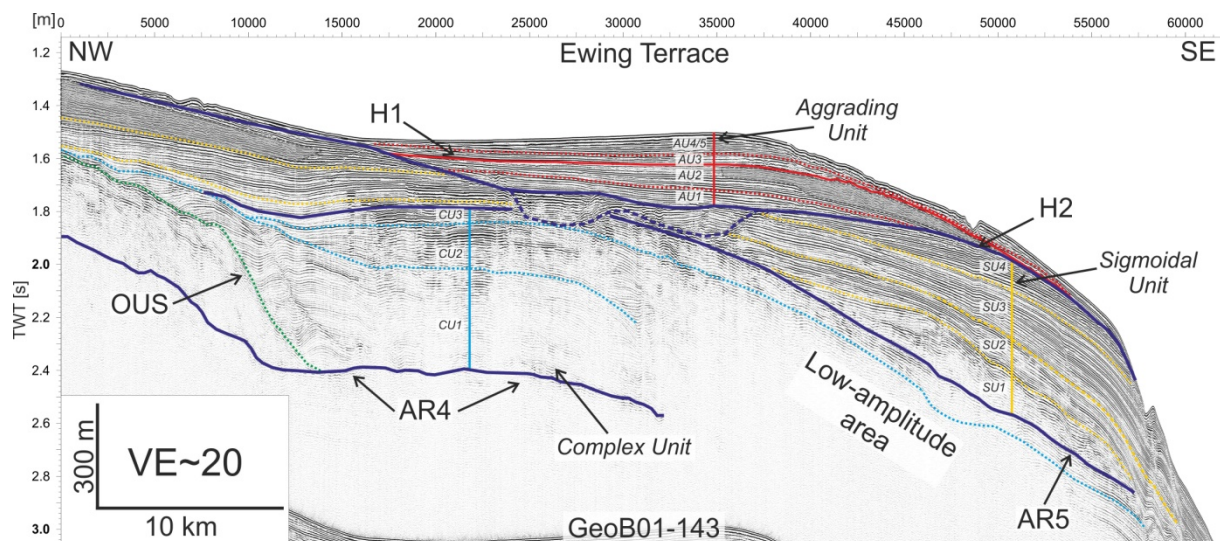


**Figure 2.5:** Multichannel seismic Line GeoB01-143 as indicated in Fig. 2.3; VE ~20; stratigraphic information was based on Ewing and Lonardi (1978) and Hinz et al. (1999, see Tab. 2.1)

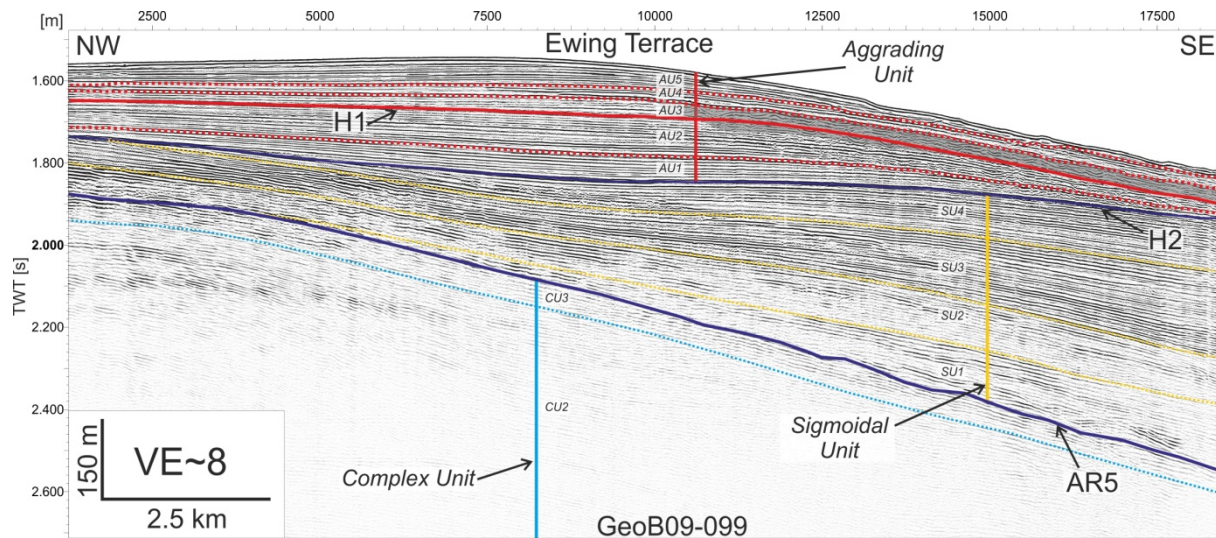


**Figure 2.6:** Multichannel seismic Line GeoB09-099 as indicated in Fig. 2.3; VE ~8; stratigraphic information was based on Ewing and Lonardi (1978) and Hinz et al. (1999, see Tab. 2.1)

seaward limit, the Ewing Terrace descends onto the lower slope, which reveals significantly higher slope angles (3-6°).

In the study area, the terrace is crossed by two submarine canyons: The Mar del Plata Canyon and further north a smaller canyon structure. Additionally, several smaller along- and down-slope oriented incisions cut into the terrace (Fig. 2.3) and were described by Krastel et al. (2011). Despite the incisions, the Ewing Terrace is characterized by a more or less smooth and regular seafloor topography.

## 2.4.2 Seismic analysis

Based on seismostratigraphic analyses, four major regional seismic units were identified in the subsurface of the Ewing Terrace. These units have been named from bottom to top as the Oblique Unit, the Complex Unit, the Sigmoidal Unit and the Aggradational Unit (Figs. 2.4-2.6), which are bounded by the major regional discontinuities AR4, OUS, AR5 and H2 (from bottom to top). Major units are composed by subunits.

### 2.4.2.3 Oblique Unit (OU)

The Oblique Unit represents a seismic unit above the AR4 discontinuity restricted to the proximal part of the present Ewing Terrace. Its upper boundary, the sigmoidal OUS discontinuity, is marked by a high seismic amplitude (Figs. 2.4A and B). The lower boundary represents the AR4 horizon, onto which the reflections of the Oblique Unit onlap. The shape of the 0.3 s TWT thick Oblique Unit has a bank-like morphology, and although its acoustic response is very weak, the oblique-sigmoidal stacking pattern clearly represents a sequence of clinoforms (Fig. 2.4B).

#### 2.4.2.1 Complex Unit (CU)

The Complex Unit represents the seismic unit defined by the regional discontinuities AR4 and OUS, marking its lower boundaries, and AR5, representing the upper boundary. AR4 can be clearly identified under the central area of the modern Ewing Terrace by the change from a parallel to a wavy layered reflection pattern. However, on the landward and seaward termination of the terrace the identification fails due to strong signal attenuation and therefore insufficient penetration of the seismic signal.

The Complex Unit has a region-scale uniform thickness of about 0.6 s TWT and is characterized by low amplitudes and, in contrast to the reflection pattern below, by a wavy, sub-parallel reflection pattern, partly onlapping in the Northwest onto the OUS horizon (Figs. 2.4 and 2.5). It is composed by a complex stacking pattern of the subunits CU1, CU2, and CU3 (from bottom to top). These subunits are deposited in a backstepping configuration or aggrading (Figs. 2.4 and 2.5) on top of the Oblique Unit.

The lowest subunit (CU1, Fig. 2.4) is dominated by a wavy reflection pattern, onlapping landward on the OUS reflection. There, the waviness is highest resulting in an upslope prograding reflection pattern with 0.4 s TWT thickness. Seaward the signature of CU1 is lost in the low amplitude zone. However, the discontinuity marking the upper boundary of CU1 indicates a dipping or a decrease in unit thickness toward the Southeast (Figs. 2.4 and 2.5). The resulting depression is filled by seismic unit CU2 with locally increased thickness, which is indicative of a seaward depocenter shift. Several normal syn-sedimentary faults can be identified within the CU1 (Figs. 2.4 and 2.5). The reflection pattern of CU2 shows a sub-parallel stacking pattern including an onlap onto CU1 landward, and the acoustic facies is generally less wavy compared to CU1 (Fig. 2.5). It is thinner than CU1, with 0.2 s TWT in average. Locally, smaller mounded, prograding sequences can be detected (e.g. 2s TWT at 30 km Fig. 2.5). The youngest and thinnest (0.1 s TWT) subunit (CU3) shows an aggradational stacking pattern with only slight waviness in the Southeast.

#### 2.4.2.2 Sigmoidal Unit (SU)

The Sigmoidal Unit (SU) can be easily identified in all seismic lines in the study area by its boundaries: the base of the unit is marked by the AR5 discontinuity and the top by the H2 horizon, which truncates reflections seaward (Figs. 2.4-2.6).

The formation of the Sigmoidal Unit represents a distinct change in the sedimentary stacking pattern with a wide plastered sedimentary drift development of 0.6 s TWT maximum thickness. The main depocenter of the Sigmoidal Unit is located down-slope compared to the Complex Unit in the transition between middle and lower slope. Small depocenter shifts between the subunits can be determined in the distal area of the Sigmoidal Unit. In contrast, in the proximal area of the terrace the overall stacking pattern of the subunits is aggradational onto the previous Complex Unit. While through time the sigmoidal character of the reflections increases, the overall reflection inclination

decreases toward the H2 horizon, resulting in a widening of the terrace-like morphology shape given by AR5 Horizon (Figs. 2.4 and 2.5).

The Sigmoidal Unit is internally structured by four subunits: SU1, SU2, SU3, and SU4 (from bottom to top, Figs. 2.5 and 2.6) bounded by internal truncations reflections. The deepest subunit (SU1) forms an individual plastered drift with a distinct depocenter down-slope onlapping onto AR 5, which partly builds a mounded morphology (Fig. 2.5). All three above lying subunits (SU2-SU4; Figs. 2.4-2.6) onlap on the unit beneath, which is in turn terminated by a truncation of reflections on their upslope boundary. Each subunit shows seaward a progradational, clinoform-like reflection pattern. All subunits are present in the proximal and distal part of the terrace. However, in the central part of the Ewing Terrace incisions have been identified cutting from the Sigmoidal Unit down to Subunit CU3 (e.g.: between 22500 and 37500 m offset and at ~1.7 TWT in Fig. 2.5).

On the seaward termination of the Sigmoidal Unit it is possible to determine a cyclic change in the seismic facies within the subunits, with more transparent to weak facies at the base and progressively higher amplitudes upward (erosional surfaces, Fig. 2.6). Furthermore, the seismic facies show in some parts disturbance in the proximal area of the Ewing Terrace (grey shaded area in Fig. 2.4 and 2.5) with an irregular and chaotic reflection pattern.

#### **2.4.2.4 Aggradational Unit (AU)**

The Aggradational Unit represents a new important regional change in sedimentary stacking pattern and depositional style of the slope, changing to its present configuration. The aforementioned change is generated by a sharp shift of depocenter landward (Figs. 2.5 and 2.6) with an aggradational configuration over the middle slope. This unit is bounded at its base by the regional discontinuity H2, which truncates the reflections of the previous Sigmoidal Unit, and at its top by the seafloor, which forms a SW-NE-oriented elongated crest.

The Aggradational Unit shows a maximum thickness of 0.3 s TWT (Figs. 2.5 and 2.6), which increases toward the north in the central area of the modern Ewing Terrace. Overall, the seismic facies of this unit shows similar high amplitudes as the upper part (SU3 and SU4) of the Sigmoidal Unit beneath.

Comparable to the underlying seismic units, the Aggradational Unit is composed by several subunits: AU1, AU2, AU3, AU4 and AU5 (from bottom to top, Figs. 2.5 and 2.6). They can be easily distinguished due to the presence of small-scale unconformities, which represent e.g. erosional truncations, or several cycles of onlap upslope and downlap down-slope, which results in minor shifts of the depocenter. Occasionally, local erosional surfaces do not allow identification of all sub-units (Fig. 2.5)

Subunits AU1 and AU2 show more or less undisturbed aggradational sequences. Especially AU1 balances depressions and fills incisions formed by the H2 discontinuity resulting in a terrace-like morphology. Despite the chaotic and wavy areas within Unit AU2 (shaded areas in Figs. 2.5 and 2.6)

at the seaward side of the terrace, which also are noticed in some parts within Subunit AU3, the acoustic facies is characterized by an undisturbed, continuous and high amplitude reflections pattern (Figs. 2.5 and 2.6).

Subunits AU1 and AU2 show a larger thickness (in total 0.15 s TWT in average) than the younger subunits AU3, AU4 and AU5. These two groups of subunits are separated by the H1 discontinuity, which marks a regional stratigraphic surface, marked by a landward prograding reflection stacking pattern. Present sea-bottom morphology was finally established by the deposition of subunits AU3-AU5, which form the modern crest of the drift deposits over the distal part of the Ewing Terrace with an average thickness of 0.15s TWT increasing northward (Fig. 2.6). Whereas the chaotic facies, described for the underlying units, is partly present as well in subunit AU3, AU4 and AU5 show no reflectivity anomalies.

## **2.5 Discussion**

### **2.5.1 Age control**

Based on several seismic studies carried out in the last 40 years along the Argentine margin, a general seismic-stratigraphy for the southwestern Atlantic has been developed. Unfortunately, each study used partly its own nomenclature for basin wide discontinuities and seismic units (see e.g.: Ewing and Lonard, 197; Hernández-Molina et al., 2009, 2010; Gruetzner et al., 2011; Hinz et al., 1999; Violante et al. 2010). A summary and comparison of this nomenclature is given in Table 2.1. Major seismic horizons and the seismic units defined in this study were correlated utilizing their seismic facies and depths with the results of these former studies to establish a stratigraphy in our study area (Tab. 2.1). Following this stratigraphy, AR4 marks the Eocene-Oligocene boundary, AR5 represents Middle Miocene times, H2 is assigned to Late Miocene and H1 is assigned to Late Pliocene.

### **2.5.2 Evolution of the slope**

The seismo-stratigraphic analysis of the MCS data collected on the middle and lower slope revealed four major units. In the following, we reconstruct the evolution of the slope (Fig. 2.7) based on variations within the seismic facies in the framework of changing climate and sea-level in geological

#### **2.5.2.1 Late Oligocene Shelf Break (Oblique Unit)**

As described before, the deepest identified unconformity in our study area is AR4. In general, the margin wide appearance of the AR4 reflector (e.g. Hinz et al., 1999; Franke et al., 2007; Hernández-Molina et al., 2009) reflects the onset of deepwater circulation during the Early Oligocene over the slope, coevally with the initial opening of the Drake Passage and the initiation of the Antarctic Circumpolar Current (e.g.: Barker, 2001; Barker et al., 2007; Katz et al., 2011; Lawver and Gahagan, 2003; Livermore et al., 1994). Whereas in greater depth the newly formed strong bottom currents can be hold responsible for erosional surfaces in the sedimentary record during this time frame

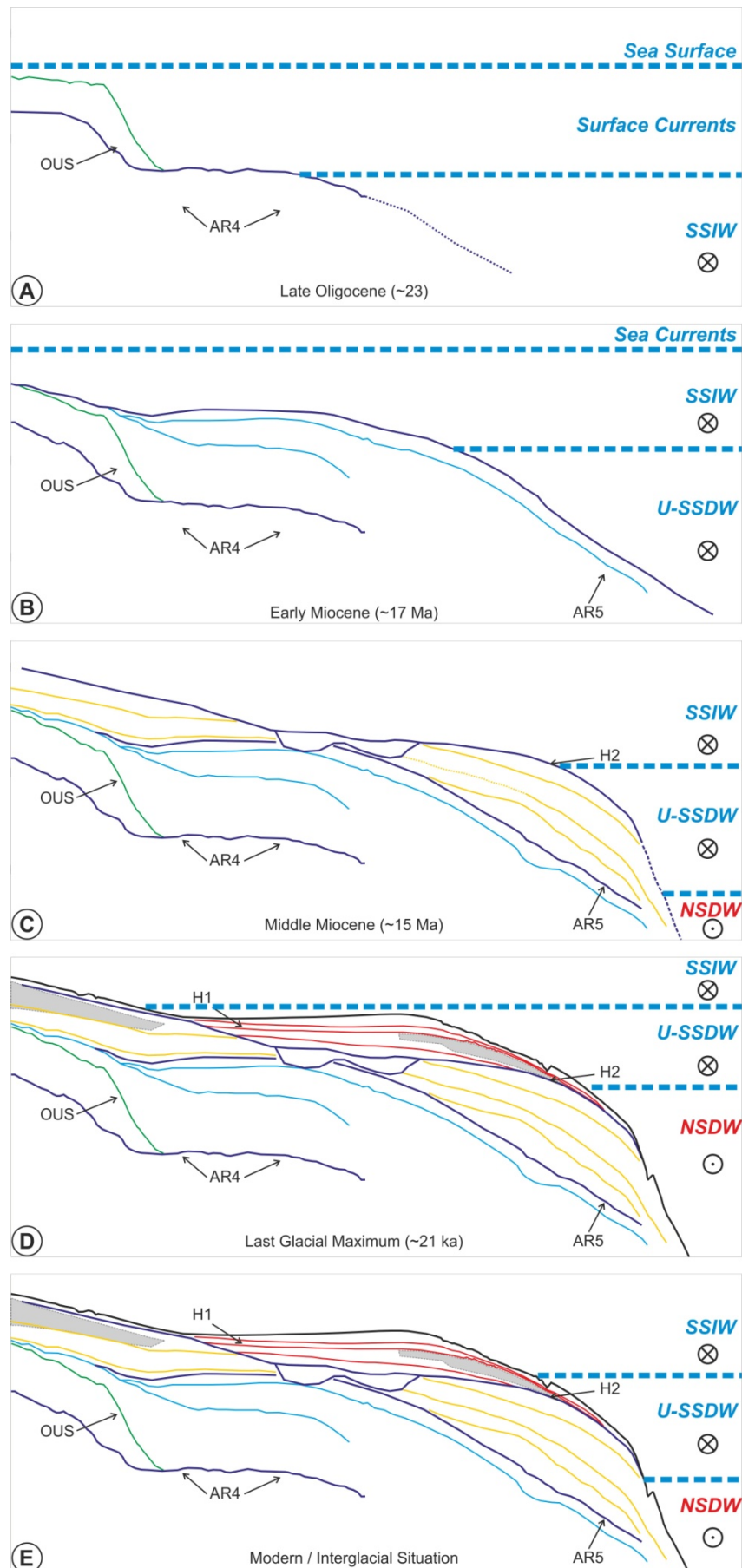


**Figure 2.7:** Line drawing showing evolution of the northern Argentine margin and the related current regime without considering non-uniform subsidence; dotted lines mark missing reflections within the acoustic data

(Hernández-Molina et al., 2009, 2010), the effect of the opening of the Drake Passage on surface currents and intermediate water masses is still intensely discussed (Lagabrielle et al., 2009). However, the opening of the Drake Passage led to the initial build-up of an Antarctic ice-sheet and global cooling, resulting from the thermal isolation of Antarctica (Fig. 2.9; e.g.: Katz et al., 2011; Zachos et al., 2001). This cooling probably led to a strengthening of surface currents in the Southern Ocean, which in turn would enhance the Malvinas Current and its related intermediate and deep water masses. The direct dependence of the MC on the circulation pattern in the Southern Ocean has been shown by conceptual modeling and several oceanographic studies (Gill, 1968; Peterson, 1992; Piola and Gordon, 1989). In general, the resulting bottom currents created for the first time the necessary boundary conditions for contourite drift formation along the Argentine slope (Fig. 2.9; Hernández-Molina et al., 2009, 2010). However, we suggest that not only the opening of the Drake Passage alone, but the climate feedback of this opening is in fact responsible for the margin wide appearance of AR4 in the water depths of our study area.

On top of AR4, the Oblique Unit has been deposited on the upslope part of the margin. Its oblique-sigmoidal stacking pattern forming clinoform-like structures strongly suggests a shallow marine environment comparable to modern shelf breaks or subaqueous delta deposits (e.g.: Palamenghi et al., 2011; Vail et al., 1977; Wolinsky and Pratson, 2005). The stratigraphy indicates that the Oblique Unit has been formed in the Late Oligocene, consequently OUS horizon represents the late Oligocene shelf break and upper slope. Seaward of OUS, no major deposition took place during that period at the slope. In contrast, major sheeted drift deposits were formed on top of the AR4 horizon at the foot of the slope off central and southern Argentina (Hernández-Molina et al., 2009, 2010; Violante et al., 2010). This mismatch could suggest an environment in our study area characterized by high wave energy and fast flowing surface currents prohibiting drift accumulation, which in turn would be consistent with the relative sea level low stand in the late Oligocene (Fig. 2.7A; Haq et al., 1987).

#### **2.5.2.2 Initiation of along-slope sedimentary processes over the middle slope (Complex Unit).**

The Complex Unit has been deposited on top of the regional discontinuity AR4 and landward as well as on top of the OUS discontinuity. The onlap of reflectors building the Complex Unit clearly indicates that this unit has been deposited after the Oblique Unit, namely in the Early Miocene. Three sub-units within the Complex Unit were identified aligned along the mid-slope and dominated by non-uniform waviness and the alternation between a landward prograding stacking pattern and erosional surfaces (Figs. 2.4 and 2.5). It is also noticeable that seismic facies, especially the waviness of reflector packages, change significantly from profile to profile along the slope. This pattern represents a remarkable change in the depositional style at the margin and the onset of contouritic deposition along the slope. This enhanced accumulation is probably related to a significant increase in water depth which supports less vigorous current conditions at the seafloor. In contrast, the absence of large-



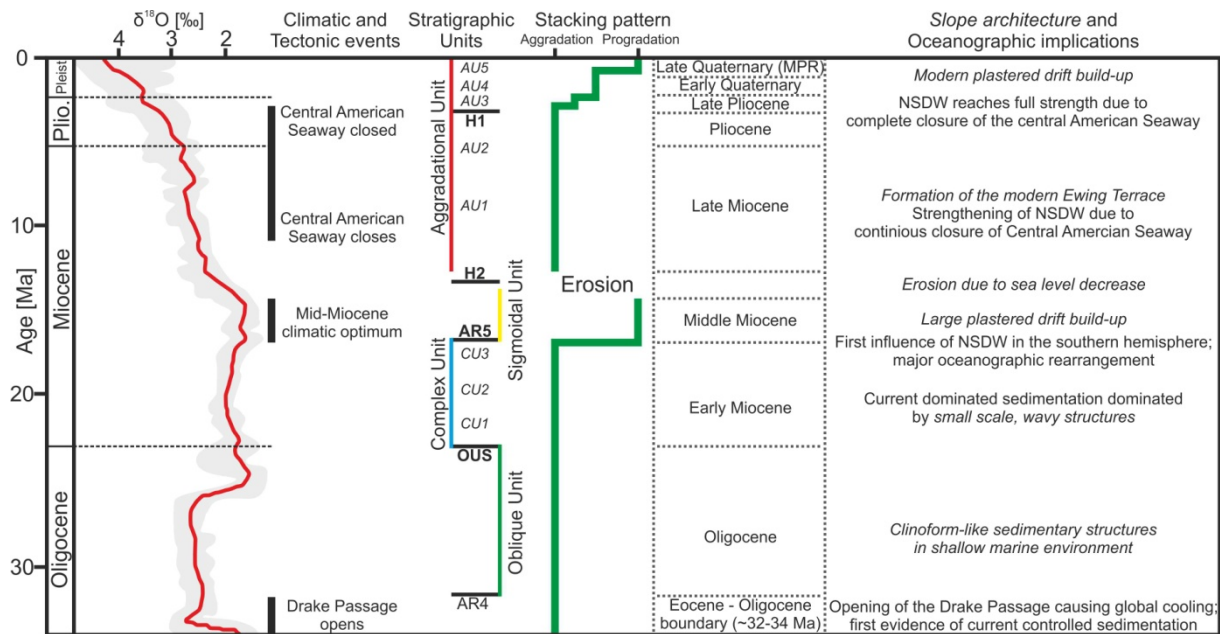


**Figure 2.8:** Discontinuities, seismic units, subunits, sedimentary stacking pattern and their paleoceanographic implication within the Mar del Plata contourite depositional system in correlation with the oxygen isotope record (based on Zachos et al. (2001) and Knutz (2008)); elements of the slope architecture and sedimentary structures are written in italic font

scale sheeted or mounded drifts suggests a variable and unstable currents system (Fig. 2.8), which would prohibit the formation of such large sedimentary bedforms (Fig. 2.7B).

The highly turbulent ocean environment and variable current conditions could be related to the presence of the BMCZ and a margin physiography with many sea-floor irregularities produced by the current environment itself. In accordance to the concept of wind-driven ocean circulation (Munk, 1950) the BMCZ was probably formed simultaneously to the MC with the opening of the Drake Passage 32 Ma ago, though reconstruction of position and strength derived from sedimentary records is even on glacial/interglacial cycles a challenging task (e.g.: Chiessi et al., 2007). Regarding the depth and location as well as the shape of the plastered drifts within the Complex Unit, two potential water masses could have controlled sediment accumulation during this time period: Northward flowing Southern Source Intermediate Water (SSIW), which is comparable to the recent AAIW, and Southern Source Deep Water (SSDW) in Holocene times represented by the CDW. Considering the modern stratification of the water column within of the BMCZ (Fig. 2.1), and considering the complex to chaotic appearance of the CU, we suggest that the Complex Unit was formed by the SSIW or at the interfaces to the Upper-SSDW (Fig. 2.7B).

### 2.5.2.3 Initiation of Northern Source Deep Water (Sigmoidal Unit)

The upper boundary of the Complex Unit (AR5) is not erosional, but instead characterized by onlapping of the reflectors within the upper Sigmoidal Unit. This unit consists mainly of a large plastered drift sequence in the transition between the middle and lower slope, but has also a more sheeted component on the middle slope. In general, the Sigmoidal Unit represents a major depocenter shift on top of AR5. The observed increasing seaward inclination of each subunit within Sigmoidal Unit suggests also differential subsidence which offers additional accumulation space for drift

sedimentation and allowed the Sigmoidal Unit growing to its large extent. Such circumstances are reported for the Middle Miocene, where major regional subsidence occurred in the region (Aceñolaza, 2000; Kennett, 1982; Potter and Szatmari, 2009) and additionally global third order sea-level highstands took place (Haq et al., 1987). These observations together with the stratigraphic definition of AR5 suggest that the SU has been deposited during the Middle Miocene.

The observed shift of depocenter indicates a major rearrangement of the vertical stratification of the water column and therefore a vertical shift in water mass boundaries. Additionally, a transition from a complex wavy, small-scale structure dominated seismic facies of the Complex Unit to a more continuous sheeted, upward convex facies is clearly visible and typical for plastered drifts along middle slopes (Laberg and Vorren, 2004; Pudsey, 2002; Viana and Faugères, 1998). Because plastered drifts are normally formed under weak to moderate but stable current conditions (Faugeres et al., 1999; Stow et al., 2008), Horizon AR5 marks – besides the depocenter shift - the transition from an unstable, turbulent flowing bottom current to a more stratified ocean current setting.

For greater depths, as in our study area, a reduction in bottom water flow and a change to more tabular current conditions in the Middle Miocene was described by Hernández-Molina et al. (2010) for Southern Source Bottom Water (SSBW, today AABW) circulation due to a widening of the Drake Passage. However, the Sigmoidal Unit in our study area is deposited in much shallower water depths than sedimentation controlled by the SSBW and therefore, this reasoning is insufficient to explain changes of the sedimentary regime at the middle slope.

Moreover, a major vertical rearrangement of water masses, which is needed for shifting the depocenter of the Sigmoidal Unit down-slope, can also sufficiently explained by the widening of the Drake Passage. Instead, a strong impact on the stratification can be assigned to the onset of Northern Source Deep Water (NSDW) formation, which correlates today with NADW, and its related influence on the global large-scale circulation pattern (Knutz, 2008). During the middle Miocene – the assumed age of the Sigmoidal Unit - the Faeroe-Iceland-Greenland ridge subsided below sea level, which allowed surface waters to penetrate further north and finally enabled NSDW production (Vogt, 1972). This event marked the onset of NSDW circulation in the southern hemisphere (Kennett, 1982). Comparable to the modern ocean circulation, where NADW is vertically separating UCDW and LCDW (Fig. 2.1B; see also e.g.: Piola and Gordon, 1989; Piola and Matano, 2001), the presence of NSDW probably caused a vertical separation of the SSDW along the Argentine margin, resulting in a major vertical shift of water mass boundaries (Fig. 2.7C). The influence of NSDW would shift the SSIW and Upper-SSDW upward, and therefore also the turbulent zone at their interfaces. This shift translocates the core of the Upper-SSDW also upwards, and thereby the moderate but stable current conditions needed for the build-up of the plastered drift were created at the position where the Sigmoidal Unit was formed (Fig. 2.7C).

Therefore our data suggests that a significant impact of the NSDW on the Argentine Slope in our study area occurred during the Middle Miocene (Fig. 2.8). Since the BMCZ marks the termination of

the NSDW influence at the Argentine margin (Piola and Matano, 2001), the position of the BMCZ must have been located southward of our study area during the Middle Miocene. In other words, similar to its seasonal variability (Bisbal, 1995) the BMCZ was probably shifted southward with respect to its modern position during the Mid-Miocene climatic optimum (Fig. 2.8).

#### **2.5.2.4 Formation of the modern Ewing Terrace (Aggradational Unit)**

The upper boundary of the Sigmoidal Unit is the erosional unconformity H2 (Figs. 2.5 and 2.6) which marked a new terrace similar to the modern one into the slope. The erosion is probably the result of stronger currents, since such terraces are often the result of a local increase in current velocity along steeper slopes and the related erosion leading to a cutting-back (McCave et al., 1982). But modern observations (Hernández-Molina et al., 2009) also reveal that water mass interfaces favor terrace formation and preservation. The stratigraphic position of H2 (Fig. 2.8), also in conjunction with the assumption that stronger currents had developed as a result of rapid global cooling after the termination of the Mid-Miocene climatic optimum, suggests that H2 has been eroded in the Middle Miocene. Consequently, H2 marks the boundary region between the SSIW and the U-SSDW during the Middle Miocene (Fig. 2.7C).

On top of H2, a change in the depositional pattern to the Aggradational Unit with more or less uniform sediment distribution occurred. This can be first explained by the fact that the topography of the terraces enforces a tabular flow pattern, which is required to maintain a steady and uniform sediment thickness increase as identified in the lower two subunits AU1 and AU2. Second, this change in the sedimentary regime could be explained by a continuous upward shifting of the interface of SSIW and U-SSDW caused by a thickening of the NADW due to its gradual strengthening (Newkirk and Martin, 2009). This strengthening was forced by the closure of the Central American Seaway (Fig. 2.8; Hermann, 1990), through which until the Late Pliocene most of the NSDW was flowing into the Pacific Ocean (Nisancioglu et al., 2003).

The AU is vertically subdivided by Horizon H1, which is partly an erosional surface, but also characterized by onlapping of the upper reflectors. H1 marks also a change in the slope architecture by forming a positive relief. Consequently, a new plastered drift sequence is build at the seaward limit of the Ewing Terrace, which is thickening toward the north (compare Fig. 2.5 and 2.6) even in recent geologic times. Therefore, at H1 the modern oceanographic scenario was established and the present morphology started to develop. From stratigraphic correlation, H1 represents Late Pliocene ages, which is in agreement with the modern deep water circulation having evolved as well since the late Pliocene due to the final closure of the Isthmus of Panama (Fig. 2.8; Nisancioglu et al., 2003). By restraining warm surficial Pacific waters from diluting cold and dense waters in the North Atlantic, in the late Pliocene NSDW production increased significantly (Burton et al., 1997; Nisancioglu et al., 2003). This strong influence of NSDW enforces the stratification, shifting the boundary between the

Upper-SSDW and the NSDW further upslope (Figs. 2.7D and E). Therefore, the build-up of the modern plastered drift is controlled by Upper-SSDW, which today is represented by the UCDW.

The sediments on top of H1 are separated by two minor discontinuities into seismic units AU3, AU4 and AU5 (Fig. 2.6). Whereas AU3 has been deposited during the late Pliocene, subsequently AU4 represents probably the early Pleistocene times. With the growth of AU4 the depositional style of the terrace changed and a positive relief was formed on top. Therefore, we suggest that the discontinuity between AU3 and AU4 could mark the onset of the dominant 41 ka glacial/interglacial cycles (Lisiecki and Raymo, 2007), which mainly controlled climate in the early Pliocene. Glacial/interglacial cycles have an impact on the global circulation pattern by leading to a short term weakening of NSDW circulation during glacial times (compare Figs. 2.7D and E; e.g.: Knutz, 2008; McCave et al., 1995; Rasmussen et al., 1996; Venz et al., 1999), which is associated with strong variations in the NSDW flow pattern in the southern hemisphere (Oppo and Fairbanks, 1987). Additionally, the dynamics and position of the BMCZ will probably change within these cycles.

The uppermost Subunit AU5 represents probably the time period after the Mid-Pleistocene Revolution (960 ka, Fig. 2.8), which marks the transition from a glacial/interglacial cycle of 41 ka to the modern 100 ka (e.g.: Mudelsee and Schulz, 1997; Raymo et al., 1997). Overall, this time period is characterized by more extreme climatic conditions within the cycles including four major cycles every 200 ka (Hernández-Molina et al., 2002; Llave et al., 2001). These stronger fluctuations would explain the local increase in sediment thickness compared to AU4 and would be consistent with findings in the Gulf of Cadiz (Llave et al., 2001) and at the Cantabrian Margin (Van Rooij et al., 2010).

### **2.5.3 Downslope mass transports**

As visible in Figs. 2.5 and 2.6, several distinct units are found at different stratigraphic levels which are characterized by a wavy to chaotic reflection pattern (Fig. 2.5 grey boxes). Such pattern is partly visible at the seafloor as well. These units are interpreted as gravity driven, individual downslope mass movements. In general, contourites are sensitive to downslope mass movements due to the horizontally uneven sedimentation, which leads finally to differential pore pressure within the sediment column (Laberg and Camerlenghi, 2008). Large to median sized mass transport deposits have been found all along the Argentine/Uruguayan margin (Hernández-Molina et al., 2009; Krastel et al., 2011). For a distinct mass transport complex offshore Uruguay it has been shown, that an earthquake in 1988 would have been able to trigger this event (Henkel et al., 2011). However, all these described mass transport deposits are characterized by distinct headwalls. As such headwalls are not visible in our bathymetric data, we conclude that the chaotic seismic facies is derived from a slow, non turbulent downslope movement of thin surface sediment packages as creeping probably triggered by exceeding pore pressure, which is a common phenomena within drift deposits (Laberg and Camerlenghi, 2008).

#### **2.5.4 Global oceanographic implications derived from general slope architecture**

The influence of ocean currents on slope architecture was studied all over the world covering depths reaching from shallow to deep sea environments (Hernández-Molina et al., 2008a, 2008b). At least in the southern hemisphere several studies identified comparable growing phases described in this study as in the central Scotia Sea (e.g.: Barker and Thomas, 2006), in the southern Argentine Basin (e.g.: (Hernández-Molina et al., 2009, 2010) and off western South Africa (e.g.: Martin et al., 1982; Preu et al., 2011). However, most of these studies focused on the upper slope, inferring on variations in surface currents, or on the lower slope and the abyssal plains, reconstructing bottom water production rate and velocity. However, only studies dealing with the middle slope allow concrete conclusions on the fast flowing intermediate water masses.

Although former studies already briefly described the middle slope off Argentina (e.g.: Hernández-Molina et al., 2009; Krastel et al., 2011; Violante et al., 2010), the presented data in this study show for the first time the strong impact of NSDW on the large scale slope architecture. The onset and strengthening of NSDW resulted in a change of the sedimentary stacking pattern along the middle slope in the southwestern Atlantic in the Middle Miocene.

Therefore, we infer that the general slope architecture in the western South Atlantic since the Middle Miocene is not only the result of variations in southern hemisphere ocean circulation controlled by the opening of the Drake Passage and the build-up of the Antarctic ice sheet. Instead, Northern Source Deep Water production plays a key role in shaping the Atlantic continental margin of South America.

## **2.6 Conclusions**

Four major sedimentary units could be identified in seismic data collected from the northern extent of the Ewing Terrace offshore Argentina. Based on established regional stratigraphy and by linking the architecture of the units to climate and sea-level changes as well as to regional tectonics, the ages of the different units could be determined. The oldest Oblique Unit represents the Late Oligocene shelf break and upper slope. The following Complex Unit, characterized by a wavy facies with low seismic amplitudes, is build-up by the onset of contouritic deposition in the study area in the early Miocene. This contouritic deposition is mainly driven by the initiation of the Malvinas Current and its related northward flowing Antarctic water masses due to the strengthening of the Antarctic Circum Polar Current as a result of global cooling. The seismic facies of the Complex Unit suggests the establishment of the BMCZ in the study area. The upper boundary of the Complex Unit marks a significant change in the depositional style in the Middle Miocene. The following Sigmoidal Unit shows plastered drift evolution and a downslope depocenter shift. Both findings can be explained by a vertical shift of water masses, which inevitably indicates the first impact of North Atlantic Deep Source Water in the South Atlantic off Argentina. Additionally, the BMCZ must have been located south of the study area during the Middle Miocene. The most recent Aggradational Unit has been deposited since the Late Miocene. The architecture of this unit indicates that deposition is controlled

by an ocean circulation similar to the recent system, reflecting especially the strengthening of the NSDW as a consequence of the closure of the Panama isthmus. In summary, this study reveals a significant impact of NSDW on the slope evolution of the southern hemisphere margins, which might have been underestimated before.

### **Acknowledgements**

The study was funded through through DFG-Research Center / Cluster of Excellence „The Ocean in the Earth System“ and was supported by the Bremen International Graduate School for Marine Sciences (GLOMAR) that is funded by the German Research Foundation (DFG) within the frame of the Excellence Initiative by the German federal and state governments to promote science and research at German universities. The study is related to the CONTOURIBER project (CTM 2008-06399-C04/MAR).

The presented seismic data was interpreted and visualized using the commercial software package ‘The Kingdom Software’ (SMT).

We like to thank Captain Kull, Captain Baschek and the crew of R/V Meteor cruises M49/2 and M78/3 for their excellent work and support.

### **3. Morpho-sedimentary characteristics of the northern Argentine margin: The interplay between erosive, depositional and gravitational processes**

Benedict Preu<sup>(1)</sup>, F. Javier Hernández-Molina<sup>(2)</sup>, Roberto Violante<sup>(3)</sup>, Alberto Piola<sup>(3)</sup>, C. Marcelo Paterlini<sup>(3)</sup>; Tilmann Schwenk<sup>(1)</sup>, Ines Voigt<sup>(1)</sup>, Sebastian Krastel<sup>(4)</sup>, Volkhard Spieß<sup>(1)</sup>

(1) MARUM – Center for Marine Environmental Sciences and Faculty of Geosciences, University of Bremen, Bremen, Germany

(2) Facultad de Ciencias del Mar, Universidad de Vigo, Vigo, Spain

(3) Servicio de Hidrografía Naval (SHN), Buenos Aires, Argentina

(4) GEOMAR | Helmholtz Centre for Ocean Research Kiel, Germany

To be submitted to ‚Deep Sea Research Part I’

## **Abstract**

Bottom currents and their margin-shaping character became a central aspect in the research field of sediment dynamics and paleoceanography during the last decade. They can form large contourite depositional systems (CDS), consisting of both erosive and depositional features.

A major CDS off northern Argentina was studied in front of the Rio de la Plata by means of seismo- and hydro-acoustic methods including conventional and high-resolution seismics, parametric echosounder and single and swath bathymetry. Erosive and depositional features associated with the CDS will be described in this study especially highlighting variations in the sedimentary style south and north of the Mar del Plata Canyon. In addition, mass wasting deposits were identified and described in detail. The overall morpho-sedimentary characteristics are interpreted jointly with hydrographic data sets characterizing the oceanographic framework, which is dominated by the presence of the dynamic and highly variable Brazil-Malvinas Confluence (BMC). We will discuss the location of each sedimentary feature along the margin and its local variability in relation to the regional current system to decipher their origin and evolution through time considering the topographic and tectonic framework.

We focus on three regional terraces identified in the study area, whose locations coincide with water mass interfaces. The shallowest one, the La Plata Terrace (~500 m), is located at the Brazil Current (BC)/Antarctic Intermediate Water (AAIW) interface characterized by its deep and distinct thermocline. In ~1200 m water depth the Ewing Terrace correlates with the AAIW/Upper Circumpolar Deep Water (UCDW) interface. At the foot of the slope in ~3500 m the Necochea Terrace marks the transition between LCDW and Antarctic Bottom Water (AABW) during glacial times.

Based on the correlation of morphology and ocean regime, we propose that the terrace genesis is strongly connected to the turbulent current pattern typical for water mass interfaces. Furthermore, the erosive processes necessary for terrace formation are probably enhanced due to internal waves, which are generated along strong density gradients typical for water mass interfaces. Through time the terraces widen due to locally focused currents along the steep landward slopes and more tabular conditions along the terrace surface.

Considering this new scheme of contourite terrace development, lateral variations of the morpho-sedimentary features off northern Argentina can be used to derive the evolution of the BMC on geological time scales. We propose that the BMC is in modern times located close to its southernmost position in the Quaternary, while during cold periods its center was shifted northward.

## **3.1 Introduction**

Bottom (contour) currents represent a major force shaping ocean margins (Stow et al., 2009) through along-slope oceanographic processes, which are capable of eroding, transporting, and depositing sediments at the seafloor (Rebesco and Camerlenghi, 2008). Depending on the bottom relief, local and regional hydrodynamic features (cores, branches, vortices, helicoidal flows, etc.) might develop, which



dominate sedimentary processes (Hernández-Molina et al., 2008b). A sufficiently strong bottom current acting over an extended time period will profoundly affect the seabed, ranging from winnowing of fine-grained sediments to large-scale erosion and deposition (e. g.: Heezen, 1959; Heezen and Hollister, 1964; Heezen et al., 1966; Kennett, 1982; Pickering et al., 1989; Rebesco and Camerlenghi, 2008; Seibold and Berger, 1993; Shanmugam, 2007; Stow et al., 2009; Stow and Lovell, 1979).

The term ‘contourite’ is now generally accepted for those sediments deposited or substantially reworked by bottom currents and contour currents *sensu stricto* (Faugères and Mulder, 2011; Gonthier et al., 1984; Heezen et al., 1966; Rebesco, 2005; Rebesco and Camerlenghi, 2008; Stow et al., 2002). Major accumulations of contourite deposits are referred to as drifts or contourite drifts, for which several classifications have been proposed based mainly on their morphological, sedimentological, and seismic characteristics (Faugères et al., 1993, 1999; Faugères and Mulder, 2011; McCave and Tucholke, 1986; Rebesco, 2005; Rebesco and Camerlenghi, 2008; Stow et al., 2002).

Where currents are strong enough, a variety of erosive features can develop. Extensive erosion or non-deposition leads to the development of widespread hiatuses in the depositional record. Although erosive features are not as well studied as contourite drifts, several types have been investigated to date (e.g.: García et al., 2009; Hernández-Molina et al., 2003, 2008a, 2009; Nelson et al., 1993, 1999; Stow et al., 2008, 2009; Stow and Mayall, 2000), the most common are represented by contourite terraces. An association of various drifts and related erosive features is commonly termed a Contourite Depositional System (CDS), by analogy with, and of equal importance to, turbidite depositional systems (e.g.: Hernández-Molina et al., 2003, 2008b; Rebesco and Camerlenghi, 2008; Stow et al., 2002).

A huge CDS is located along the Argentine margin (Fig. 3.1) characterized by particularly well developed depositional and erosive features (Hernández-Molina et al., 2009). In regional studies, contourite features were so far mainly identified in the southernmost sector of the margin (Patagonian margin; Cavallotto et al., 2011; Hernández-Molina et al., 2009, 2010; Lastras et al., 2011). However, recently Violante et al. (2010), Bozzano et al. (2011), Preu et al. (chapter 2) and Krastel et al. (2011) have also reported large contourite features along the northern Argentine margin.

Main objective of this work is to identify morpho-sedimentary features along the northern Argentine margin (Fig. 3.1) with special emphasis on contourite terraces, which are present in different depths along the slope. A regional correlation with hydrographic features is presented and a new conceptual model for the onset and evolution of contourite terraces is discussed.

## **3.2 Regional setting**

### **3.2.1 Physiography**

The Argentine continental margin (Fig. 3.1) includes three major physiographic domains: the shelf; the slope and the rise. All three margin segments, which were focused in several regional studies (e.g.:

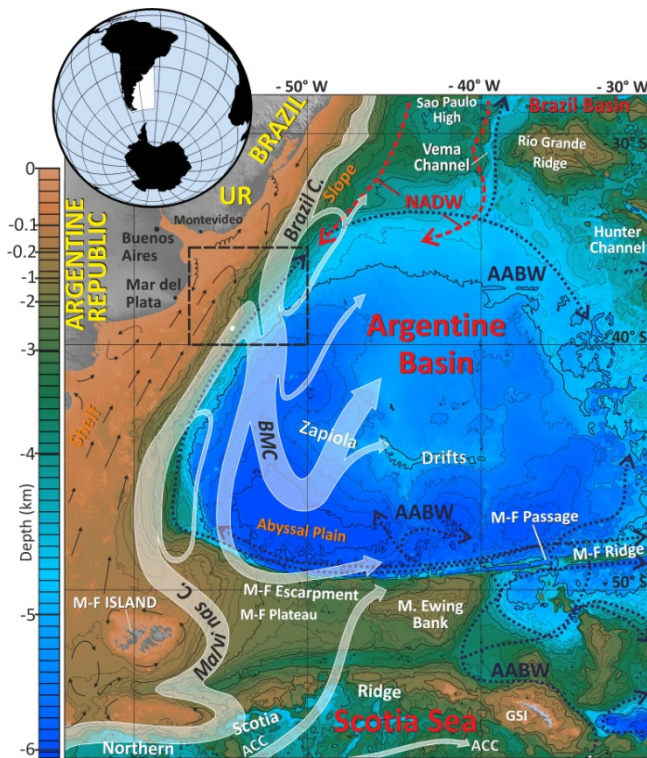


**Figure 3.1:** Regional bathymetric map of the northeastern Argentine margin, including its general ocean circulation pattern; BMC - Brazil-Malvinas Confluence; M/F - Malvinas-Falkland; NADW – North Atlantic Deep Water; AABW – Antarctic Bottom Water; black dashed box marks the study area.

the shelf is close to a straight line, which runs in SSW direction along the 130/150 m isobaths in the study area.

The slope runs almost parallel to the continental shelf with the main SW direction in the study area (Fig. 3.1). In this part of the margin the slope extends over ~180 km in width with a mean slope angle of 2-5°. Located off the Rio de la Plata (Fig. 3.1), two major terraces result in a step-like slope morphology: The La Plata Terrace (Urien and Ewing, 1974) and the Ewing Terrace (Hernández-Molina et al., 2009). Especially, the latter encompasses significant sediment accumulations.

### 3.2.2 Oceanographic context

Interaction of highly active oceanographic processes with the seafloor is an ubiquitous characteristic of the Argentine margin, which is located in one of the most dynamic of the world's ocean basins (Fig. 3.1; e.g.: Chelton et al., 1990). This margin encompasses the Brazil/Malvinas Confluence (BMC), as well as the encounter and interaction of Antarctic water masses (Antarctic Intermediate Water [AAIW], Circumpolar Deep Water [CDW] and Antarctic Bottom Water [AABW]), with the Brazil Current, re-circulated AAIW and North Atlantic Deep Water (NADW; Carter and Cortese, 2009; Georgi, 1981; Piola and Matano, 2001; Saunders and King, 1995) at different depths (Fig. 3.1). The surface circulation around the Argentine margin results from interaction of the northward flowing Malvinas Current with the southward flowing Brazil Current, which form the BMC near 38°S. The BMC strongly controls the sedimentary processes and the margin's morphology (Lonardi and Ewing,

Ewing and Lonardi, 1971; Hernández-Molina et al., 2009; Lonardi and Ewing, 1971; Parker et al., 1997; Parker et al., 1996) include morphological features of minor order, which are relevant indicators for the interaction between ocean dynamics, tectonic processes, sea level fluctuations and other processes (e.g.: Henkel et al., 2011; Hernández-Molina et al., 2009, 2010; Krastel et al., 2011).

The shelf varies drastically in its width (Ewing and Lonardi, 1971; Parker et al., 1997; Parker et al., 1996). The narrowest part of the shelf in the study area is located near Mar del Plata and further south where the shelf is ~180 km wide. North and south of this area the continental shelf width exceeds 200 km. The eastern boundary of the

1971; Piola and Rivas, 1997). The intermediate circulation south of the BMC is conditioned by the circulation toward the north by the Antarctic Intermediate Water (AAIW), and by the two CDW fractions: Upper Circumpolar Deep Water (UCDW) and Lower Circumpolar Deep Water (LCDW; Arhan et al., 2002, 2003; Reid et al., 1977). North of the confluence, apart from the aforementioned water masses, the NADW flows along the margin southward (Fig. 3.1). Interfaces between these water masses are determined by changes in relatively large vertical density gradients, which tend to deepen northward at basin scale (Reid et al., 1977), and are vertically displaced by eddies (Arhan et al., 2002, 2003; Piola and Matano, 2001).

The abyssal circulation is dominated by AABW (Fig. 3.1), which is partially trapped in the basin, generating a large, regionally up to 2000 m thick cyclonic gyre, the influence of which is felt at depths greater than 3500 to 4000 m (Arhan et al., 2002, 2003; Carter and Cortese, 2009; Hernández-Molina et al., 2008b; Piola and Matano, 2001). These circulation patterns may play a significant role in controlling sedimentary processes across the entire ocean basin (Klaus and Ledbetter, 1988; Le Pichon et al., 1971; Reid, 1989), and particularly on the Argentine margin (Arhan et al., 2002, 2003; Flood and Shor, 1988; Hernández-Molina et al., 2009).

### **3.2.3 Geological context**

The northern part of the Argentine margin belongs to the passive volcanic rifted continental margin of South America ranging from southern Brazil to northern Patagonia. The tectonic characteristics of the region are conditioned by deep structures related to the geodynamic evolution prior to the continental fragmentation, as well as by sea-floor spreading, magmatic activity and thermal flux (Ramos, 1999). The margin has been subdivided into four tectonic segments separated each other by transference fracture zones (Franke et al., 2007; Hinz et al., 1999). The study area comprises the northern part of Segment III and the southern part of Segment IV, which are separated by the Salado Transfer Zone (STZ, Fig. 3.2).

Post-Cretaceous sedimentary sequences display six major units separated by conspicuous seismic horizons. These reflectors represent the following times according to the interpretations by Ewing and Lonardi (1971), Urien and Zambrano (1996), Hinz et al. (1999) and Parker et al. (2008), later correlated and synthesized by Hernández Molina et al. (2009) and Violante et al. (2010): AR4 (Eocene-Oligocene boundary), R\* (Oligocene-Miocene boundary), AR5 (Mid Miocene), H2 (Miocene-Pliocene boundary), H1-L (Lower-Mid Miocene) and N (2.4 Ma, base of Quaternary). Sequences between reflectors indicate the different stages of evolution: 1) a first evolutive stage (Early Cenozoic) characterized by a high vertical accretion of the slope; 2) a second evolutive stage (Eocene-Mid Miocene), when the passive margin definitively developed, Antarctic water-masses began to actively influence the region, and prograding-retrograding sedimentary sequences played a significant role in shaping and enlarging the slope with high turbiditic dynamic and formation of submarine canyons; 3) the third evolutive stage (Mid-Late Miocene) comprises the time-span when progradation

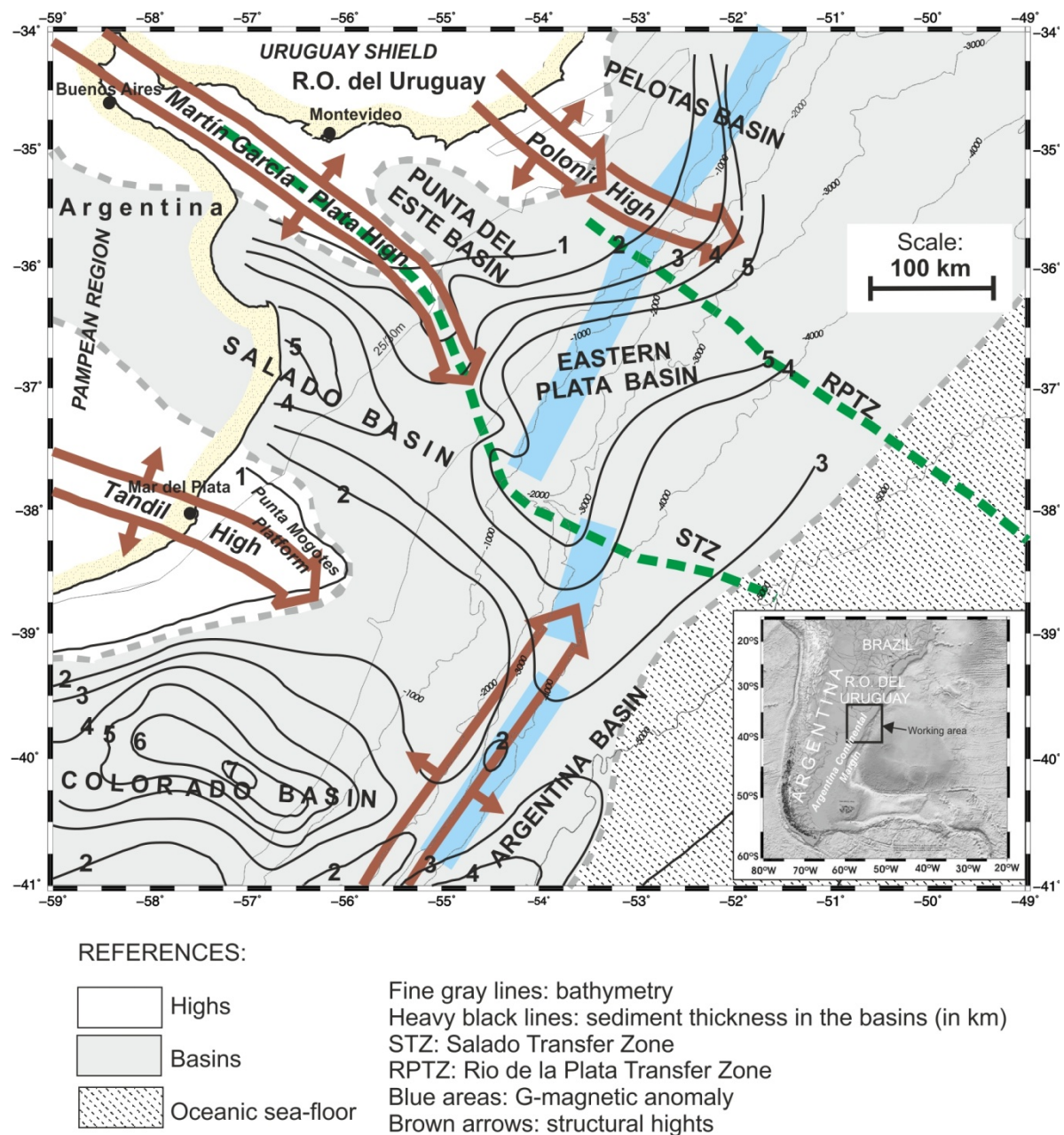


**Figure 3.2:** Schematic map showing the geological and structural features in the study area. The structural and extensional transverse basins contain post-Jurassic-Cretaceous sedimentary sequences up to 8 km thick. The northernmost basin of the Argentine margin is “Salado”. It develops above the metamorphic basement of the Plata Craton (Urien and Zambrano, 1996) between Tandil and Martín García/Plata Highs. The origin of the basin has been attributed to extensional fracturing affecting former weakened zones (Stoakes *et al.*, 1991; Yrigoyen, 1975). The study area is located in the southern flank of the offshore sector of Salado basin in transition to the small Eastern Plata basin, and close to Mogotes Platform, which belongs to the Tandil High (Tavella and Wright, 1996; Urien and Zambrano, 1996); here, the post-Cretaceous sedimentary thickness ranges between 2 and 4 km.

dominated and ocean and sediment dynamics gave rise to contouritic sedimentation with the formation of the Ewing Terrace; 4) finally, the fourth stage (Late Pliocene-Quaternary) represents the definitive morphosedimentary evolution of the slope towards its present characteristics, with intense contouritic and turbiditic activity and the final shaping of the Mar del Plata Submarine Canyon.

### 3.3 Methods

#### 3.3.1 Seismic and hydro-acoustic data sets

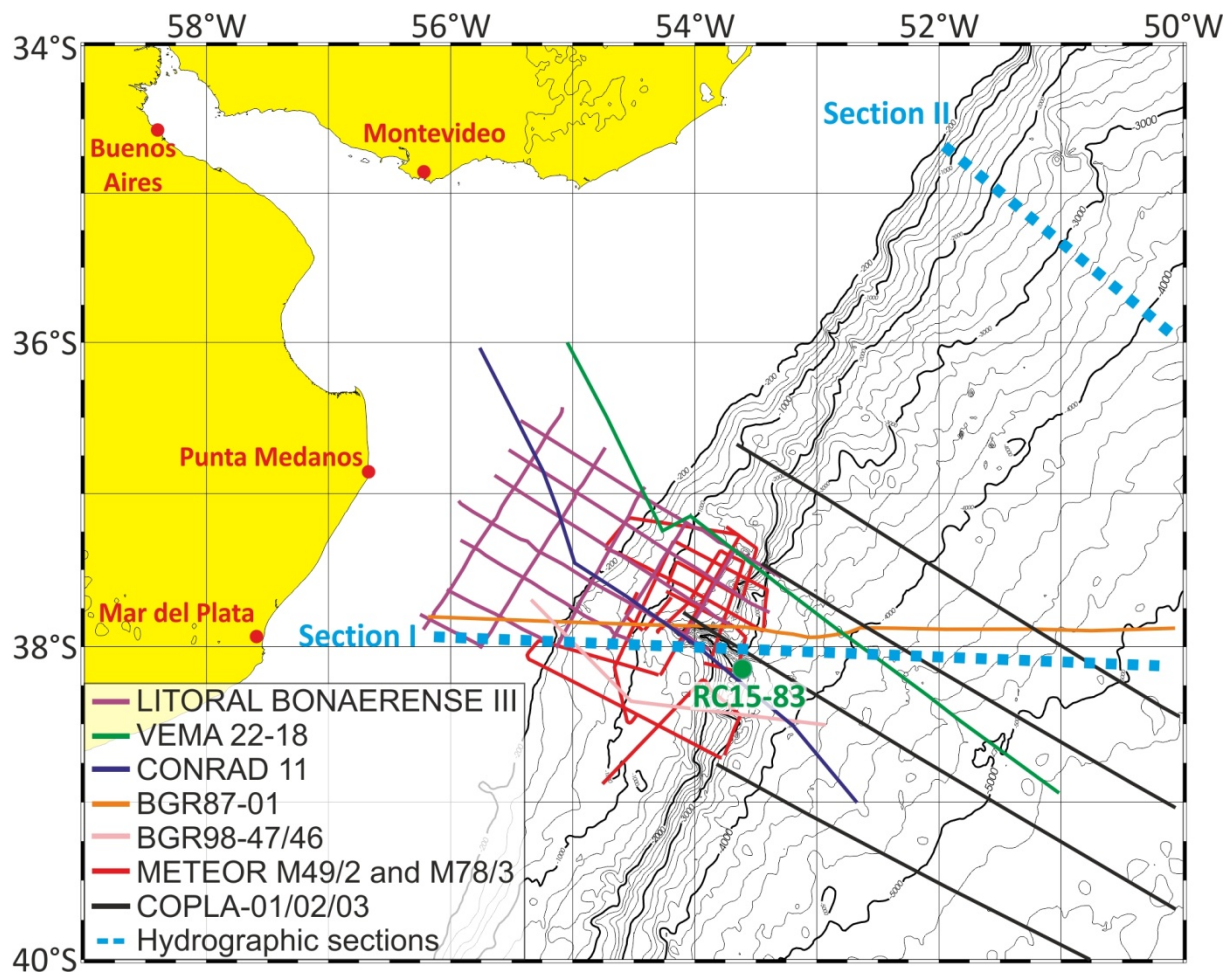


**Figure 3.3:** Map of study area showing the position of the seismic surveys and the water column data including hydrographic sections and turbidity measurements

To allow detailed analysis of small scale variations in morphology and acoustic facies of the shallow subseafloor and to show possible links to the recent oceanographic regime, multiple seismo- and hydroacoustic data sets were used covering a wide range of frequencies. Conventional and high-resolution multi-channel seismic (MCS) profiles, single- and multibeam lines and parametric echosounder data were analyzed and jointly interpreted (Fig. 3.3).

The conventional MCS (10-50 Hz) data were acquired and processed by the ‘Bundesanstalt für Geowissenschaften und Rohstoffe’ (BGR). The shooting interval during all BGR cruises (Fig. 3.3) was 50 m and data were recorded using a 6000 m long streamer system, sampled at a rate of 2 ms. The data were reprocessed on behalf of COPLA (‘Comisión Nacional del Límite Exterior de la Plataforma Continental’) by CGG/VERITAS. These data were used to identify potential structural control on margin physiography and consequently on morpho-sedimentary features.

High-resolution MCS (100-500 Hz) profiles were recorded during R/V Meteor Cruises M49/2 (2001) and M78/3 (2009). During the first cruise data were acquired using the multichannel seismic system of the University of Bremen encompassing a 600 m analog streamer with 96 channels. The sampling frequency was set to 4 kHz. In 2009 data were recorded with the IFM-GEOMAR multichannel seismic

system including its 200 m long digital streamer consisting of 128 channels. Sample frequency during that cruise was constantly 8 kHz. Both data sets were processed with the software package 'VISTA Seismic Processing 2D/3D' (GEDCO) following standard seismic procedures including bandpass filtering, common midpoint (CMP) sorting and binning, CMP stacking, residual static correction and post-stack time migration. CMP bin size varies among profiles between 5 and 10 m depending on data quality and coverage. Based on these data large scale erosive and depositional features were identified and mapped within the study area.

Single beam echosounder data were collected by Argentine authorities on behalf of COPLA during multiple cruises with R/V Puerto Deseado during the last decade. This data set was analyzed in conjunction with a dense multibeam echosounder data set confined to the Mar del Plata Canyon, recorded during R/V Meteor Cruise M78/3, to determine large and small-scale morphological features. Additionally, parametric sediment echosounder data (PARASOUND P70 with a lower parametric frequency of 4kHz) acquired along the multibeam tracks were used for detailed morphological and seismoacoustic analysis of the uppermost tenth of meters.

To discuss the origin, evolution and lateral extent of the morpho-sedimentary features, acoustic data sets were jointly interpreted using the software package 'The Kingdom Software' (SMT) and the software 'GeoMapApp' created at the Lamont-Doherty Earth Observatory (Ryan et al., 2009).

Identification of erosive and depositional features related to CDSs and the related nomenclature are based on previous comprehensive and reviewing studies carried out by Faugeres et al. (1999) and Rebesco (2005). Both publications were recently summarized and discussed by Rebesco and Camerlenghi (2008).

### **3.3.2 Hydrographic data sets**

The detailed distribution of water masses down the northern portion of the Argentine margin is depicted by two full-depth, high-resolution cross-sections of potential temperature, salinity, dissolved oxygen and neutral density (Fig. 3.3). A zonal section referred to as Section I was collected close to 38°S in 1984 as part of the Marathon Expedition (Camp et al., 1985) and a second section occupied further north during the SAVE-5 Expedition, referred to as Section II runs southeastwards down the slope intersecting the 2000 m isobath near 35°S (Fig. 3.3). Note that the cross-slope resolution of Section I is about 30 km, while that of Section II east of the 200 m isobath is quite lower and irregular. Both sections will be used to identify changes in circulation based on distinct variations in water mass distributions over the study area.

As pointed out above, the abyssal Argentine Basin is subject to the influence of the circulation of AABW, however, as bottom depth decreases along the continental margin various water masses interact with the bottom. To understand the role of the circulation and water mass structure on the sediment redistribution over the slope it is necessary to determine where each water mass interacts with the bottom across and along the slope. For this purpose we analyzed the distribution of near-

bottom (within 150 m) water mass properties based on all data available (World Ocean Database 2009) in the Argentine Basin. We adopted water mass property criteria as shown in Table 3.1.

To allow detailed analysis of the interplay between the oceanography and the morpho-sedimentary features, the hydrographic sections and seismic lines were combined into single profiles. These seismic/hydrographic intersections were calculated using the program ‘Ocean Data View 4.0’ (Schlitzer, 2011).

Additionally, sea surface temperature (SST) measurements were used for this study derived from published high-resolution satellite climatology (Casey and Cornillon, 1999). Based on these data, SST gradients were calculated and averaged to southern hemisphere ‘summer’ (October-March) and ‘winter’ (April-September) to visualize the seasonal variability of the BMC.

Water mass		Criteria
SACW	$\theta > 8$	$S > 34.8$
AAIW	$33.90 < S < 34.25$	
AAIW (recirc.)	$O_2 < 5.6 \text{ ml/l}$	
UCDW	$27.75 < \gamma^n < 27.90$	$O_2 < 4.5 \text{ ml/l}$
NADW	$27.90 < \gamma^n < 28.10$	$S > 34.8$
LCDW	$28.06 < \gamma^n < 28.20$	$S < 34.8$
AABW	$\theta < 0^\circ\text{C}$	

**Table 1:** water mass property criteria for figure 10

### 3.4 Results

#### 3.4.1 Physiography of the study area

In the study area the continental slope varies in width between 160 and 200 km. It clearly narrows in the north, in principle at the location of the Mar del Plata submarine canyon (Fig. 3.4), which separates the southern from the northern part of the study area. The continental slope can be subdivided into the upper, middle and lower slope, which include several major terraces (La Plata Terrace, Ewing Terrace, T3 and Necochea Terrace) located in different water depths (Fig. 3.4). The region where the lower slope merges with the continental rise is sometimes hard to identify due to a constant concave shape of the continental slope, however the transition is located close to ~3500 m water depth, where slope angles reach ~0.6°. The continental rise covers an extensive area with an overall width of more than 200 km.

Three major submarine canyons are located in the study area (Fig. 3.4): The most prominent is the aforementioned Mar del Plata Submarine Canyon, which originates at ~1000 m water depth cutting into the middle slope and reaches toward the foot of the lower slope (Krastel et al., 2011). The head of the Mar del Plata Canyon is located in the middle slope, mid-way between the La Plata and the Ewing Terrace (Fig. 3.4).

North of the Mar del Plata Canyon a smaller structure, called Querandi Submarine Canyon, is located, incised into the Ewing Terrace. A much smaller canyon structure originates from the lower slope south of the Mar del Plata Canyon, called Punta Mogotes Submarine Canyon (Fig. 3.4).

### 3.4.2 Morpho-sedimentary features

#### 3.4.2.1 Erosive features

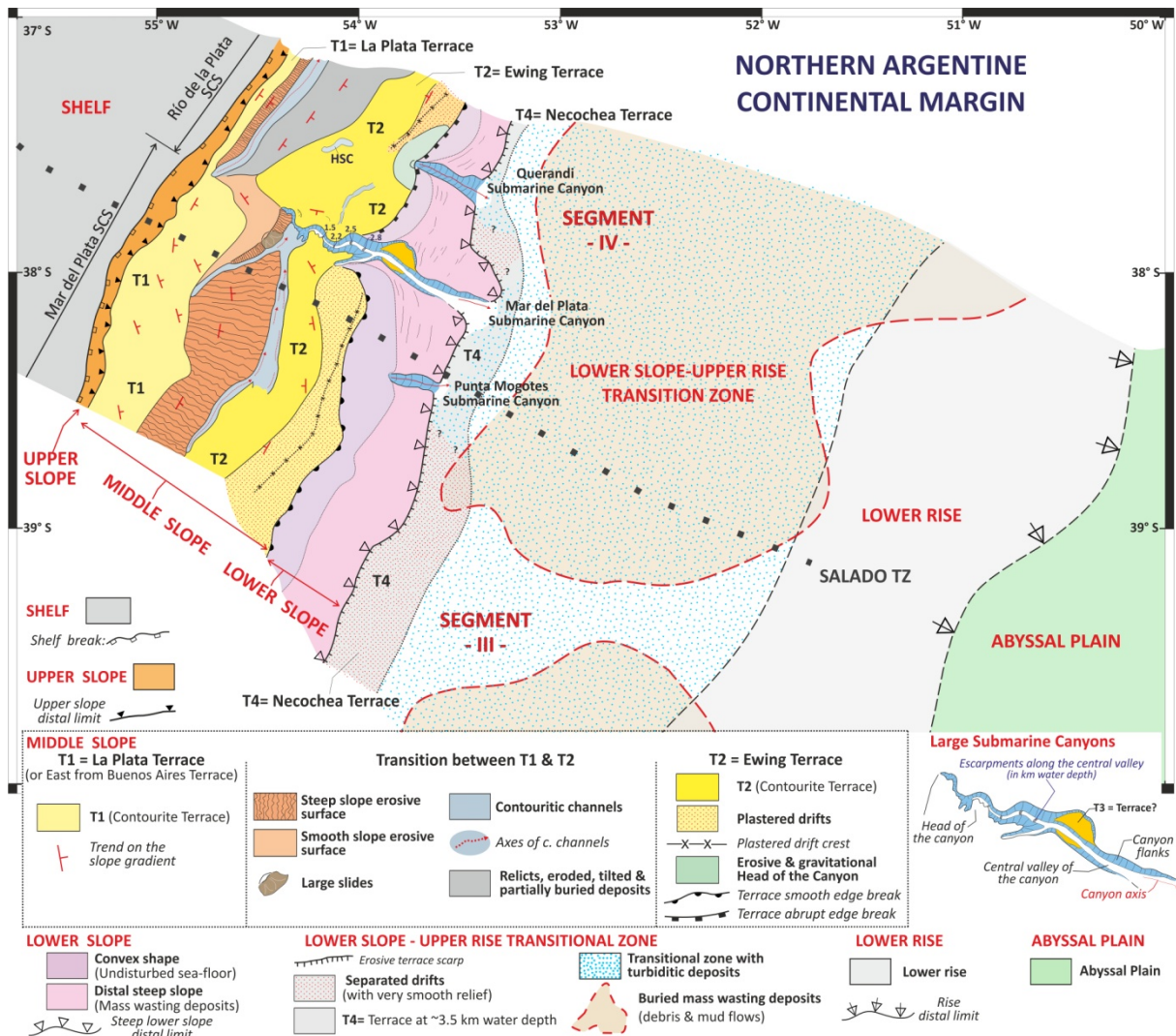


**Figure 3.4:** Morpho-sedimentary map of the NE Argentine margin

Erosive features in the study area encompass steep erosive surfaces, channels and minor slope parallel incisions located at the lower slope. Overall these features are very pronounced in the northern and southern part of the study area (Figs. 3.4-3.8).

#### *Erosive surfaces*

Two major large-scale erosive surfaces were imaged in the northern and southern part of the study area, one represented by the upper slope landward of the La Plata Terrace and the other one located along the middle slope located landward of the Ewing Terrace (Figs. 3.5, 3.6, 3.8a and b).

The upper slope connects the shelf break located close to the 130/150 m isobaths with the La Plata Terrace characterized by a mean slope angle of  $\sim 4-6^\circ$ . Independent of the width of the La Plata Terrace the upper slope has a more or less constant width of  $\sim 5-10$  km reaching its maximum upslope of the Mar del Plata Canyon. The upper slope is hard to characterize based on the available seismic data sets due to technical limitations resulting from the hydrophone group length of the GeoB seismic



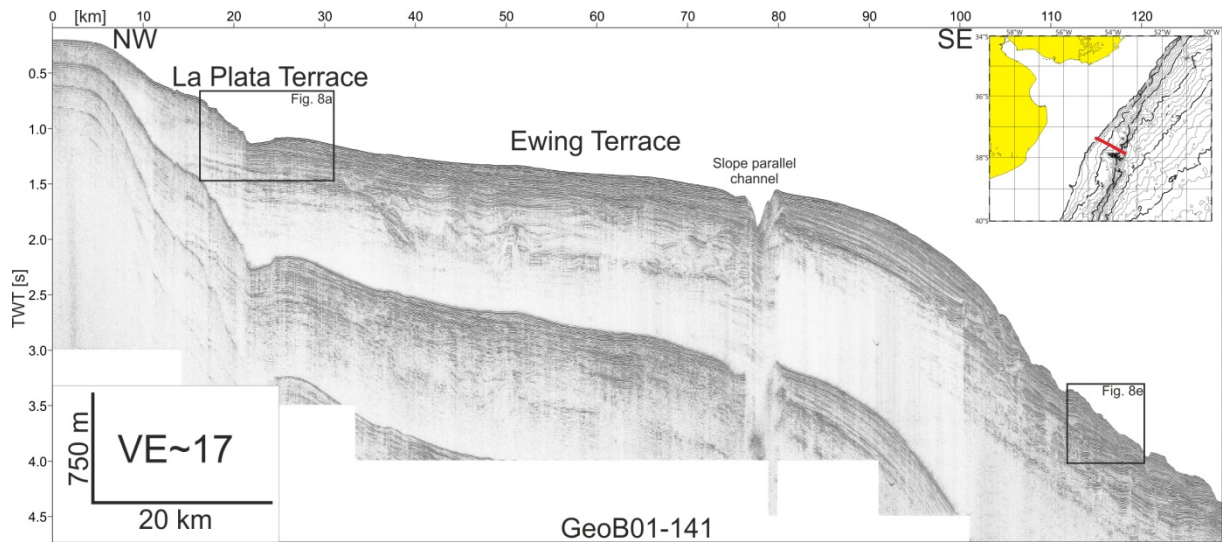


**Figure 3.5:** Multichannel seismic Line GeoB01-141; inlet indicates position of seismic line; black box marks area shown in Fig. 8; VE ~17

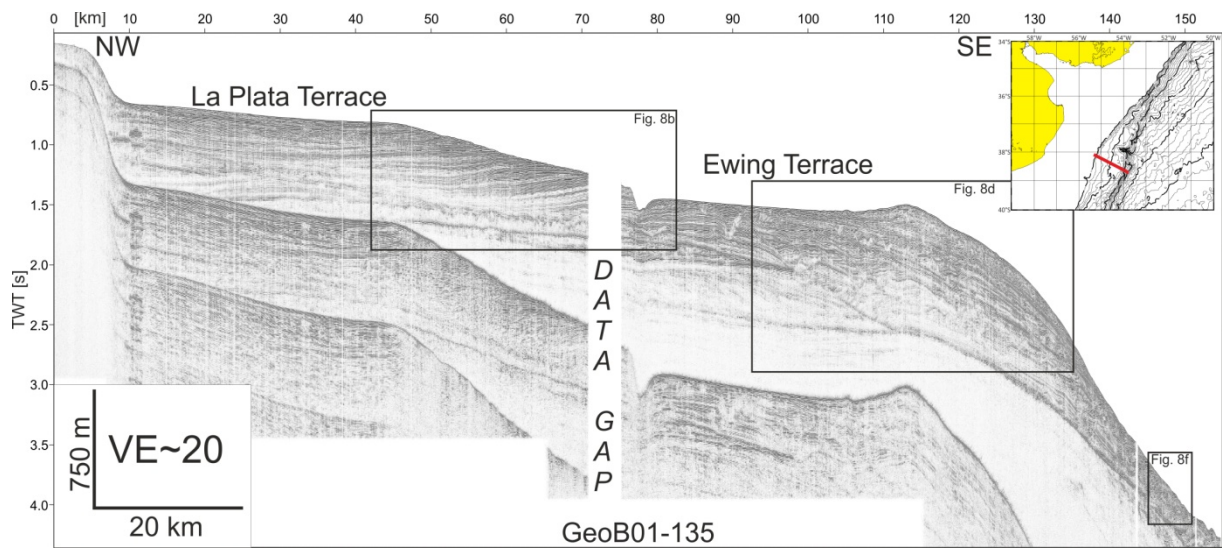


**Figure 3.6:** Multichannel seismic Line GeoB01-135; inlet indicates position of seismic line; black box marks area shown in Fig. 8; VE ~20

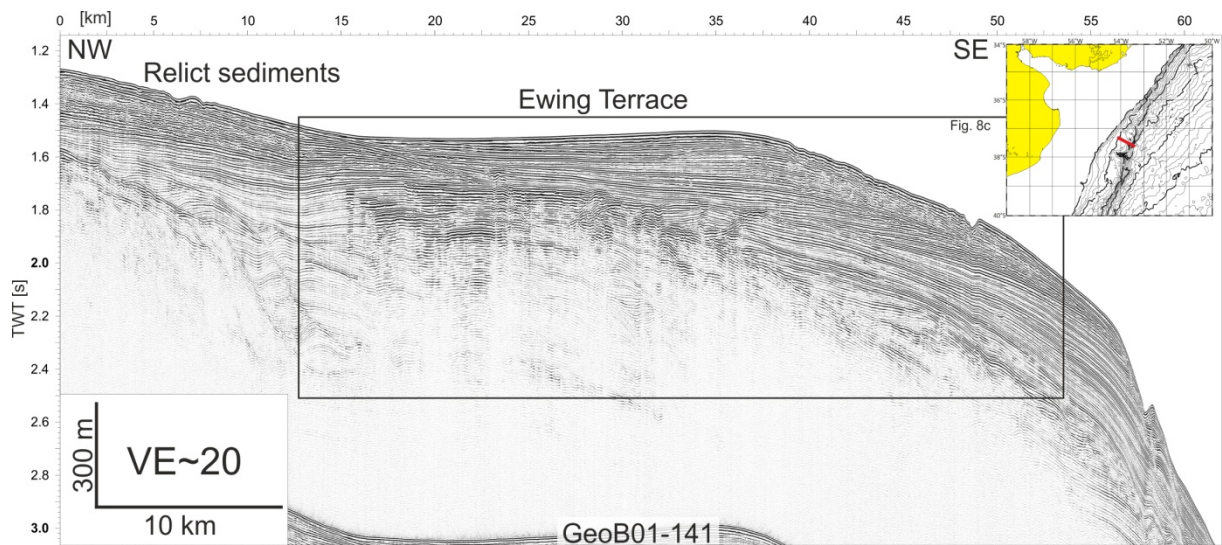


**Figure 3.7:** Multichannel seismic Line GeoB01-143; inlet indicates position of seismic line; black box marks area shown in Fig. 8; VE ~20

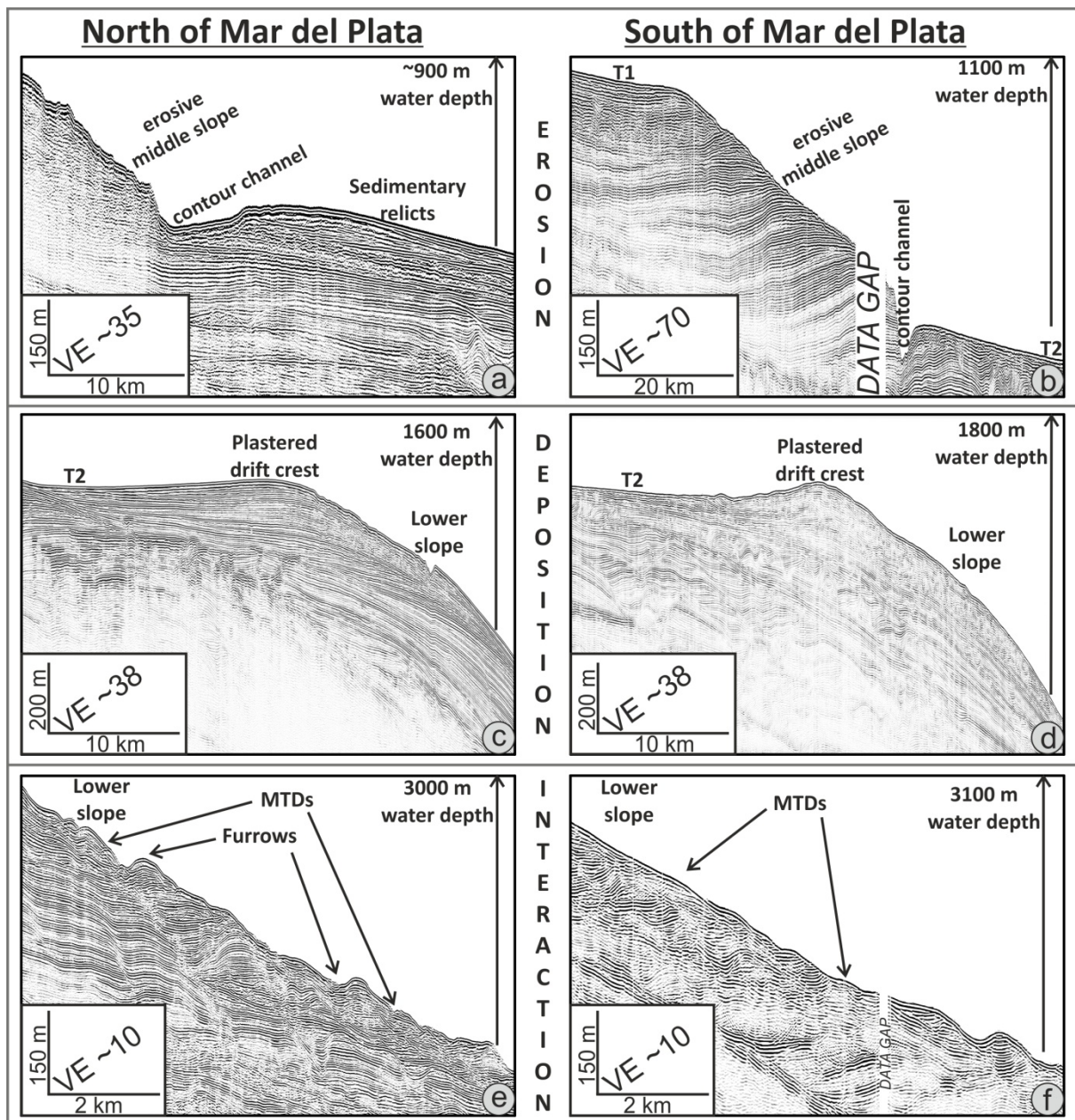


**Figure 3.8:** Examples of morpho-sedimentary features for the northern and southern study area subdivided into erosion, deposition and interaction of along slope and down-slope processes; location of individual examples are marked in Figs. 5-7; T2 – Ewing Terrace

system and high slope angles. However, the acoustic appearance including truncated reflections points at least in the transition between the upper slope and La Plata Terrace to predominantly erosive processes (Figs. 3.5 and 3.6).

In the transition between the La Plata Terrace and the Ewing Terrace a mid-slope erosive surface is located (Fig. 3.4). Its width varies distinctly in accordance with the above described variability of the Ewing Terrace. While south of the canyon the middle slope has a mean width of ~35 km with a slope angle of 3-4°, north of the Mar del Plata Canyon the middle slope narrows to ~4 km with a slope gradient of ~6° (Fig. 3.4). Well-defined truncated reflections dominating the seismofacies (Figs. 3.5, 3.6, 3.8a and b) mark this area of the margin clearly as erosive surface.

### *Channels*

Major slope parallel incisions representing channels could be identified north and south of the Mar del Plata Canyon. The most prominent runs along the Ewing Terrace in transition to the aforementioned erosive surface (Fig. 3.4). It follows the shape of the overall margin and is cut into the terrace building strata. In the southern area, the channel is incised ~90 m into the Ewing Terrace and reaches a width of ~5-15 km (Figs. 3.5, 3.6, 3.8a and b). The channel widens in the central part of the southern area, where a second contour parallel channel emerges from the Ewing Terrace. North of the canyon the channel reaches a more or less constant width of ~5 km slightly widening northward with a mean depth of ~35 m.

Another major channel runs across the margin slope at ~38°S connecting the La Plata Terrace with the major contourite channel described above south of the Mar del Plata Canyon (Fig. 3.4). It is incised 15-20 m into the margin and only 1-2 km wide. At last, directly north of the Mar del Plata Canyon at ~54°W a deep contour parallel incision was imaged, which is ~260 m incised into the Ewing Terrace with maximum width of ~350 m (Figs. 3.4 and 3.5).

### *Minor slope parallel incisions*

In the northern part of the study area and between the Mar del Plata Canyon and the Punta Mogotes Canyon minor slope parallel incisions can be identified along the lower slope in water depths of ~2000-3000 m (Figs. 3.4, 3.5 and 3.8e). The width of the features varies between 200 and 400 m and they are ~90 m incised into the lower slope. While they are in the northern area very common, in the southern area ~30 km SW of the Mar del Plata Canyon they are less abundant and of smaller dimension (Figs. 3.7 and 3.8f).

#### **3.4.2.2 Mixed erosive-depositional features – Contourite terraces**

The most remarkable morphological features in the study area are the wide terraces, incised into the continental slope. There are four major terraces (Fig. 3.4): The La Plata Terrace (T1), the Ewing Terrace (T2), and the Necochea Terrace (T4), located at the foot of the slope (Fig. 3.4). Although another terrace, T3, has been described by Hernández-Molina et al. (submitted), this terrace will not be considered in this study due to its small-scale appearance in the study area.

#### *La Plata Terrace (T1)*

The shallowest terrace is the La Plata Terrace located in 500-600 m water depth with a main NE orientation and a mean slope angle of 0.5-1°. The landward and seaward boundaries are marked by the upper and middle slope characterized by steeper slope angles. The terrace distinctly narrows upslope of the Mar del Plata Canyon from south (~35 km) to north (~7 km). The seismoacoustic characteristics of the T1 strongly depend on the lateral variability of the terrace, as well. While in the southern part of the study area, the terrace shows a clear horizontally layered reflection pattern of high amplitudes

(Figs. 3.5 and 3.6), in the north the seismic facies is hard to determine due to the limited lateral extent of the terrace and only single reflections of low amplitude can be observed.

#### *Ewing Terrace (T2)*

In water depths of 1100-1400 m the Ewing Terrace is located running almost parallel to the La Plata Terrace. Characterized by a mean slope angle of  $\sim 0.5-1.5^\circ$  the Ewing Terrace represents the wide area between the erosive middle slope and the lower slope (Fig. 3.4). Northward this area widens from  $\sim 50$  km to  $\sim 80$  km at the Mar del Plata Canyon, where the middle slope is shifted landward. The Ewing Terrace can be subdivided into three zones from land to sea: The first, erosive zone, is located at upslope boundary of the Ewing Terrace, where truncated reflections indicate erosive processes next to the contour parallel channel described above (Figs. 3.5, 3.6, 3.8a and b). While this zone is quite narrow (100-150 m) in the southern part of the study area, north of the Mar del Plata Canyon this area widens to  $\sim 35$  km and is indicated in Figure 3.4 as sedimentary relicts (grey area; Fig. 3.7).

The central zone of the terrace is characterized by close to horizontal layered reflections, which partly do not allow distinguishing between non-deposition and ultra-low sedimentation (Figs 3.5-3.7). Laterally, this part of the terrace drastically varies in width and shape from south ( $\sim 35$  km) to directly north of the Mar del Plata Canyon ( $\sim 65$  km) with the main break along the Mar del Plata Canyon (Fig. 3.4). Further northward, the width of the central zone decreases.

The last zone, located at the seaward boundary of the terrace, encompasses a major mounded plastered drift in 1200-1400 m water depth (Fig. 3.4). While upslope the drift fades into the central zone, seaward deposition is terminated at the lower slope. In the center of the plastered drift a positive relief associated with a sedimentary crest can be identified (Figs. 3.4-3.7, 3.8c and d). The seismic facies indicates intervals of aggradational and progradational stacking patterns resulting in the crest as well as a seaward migration of the drift (Figs. 3.8c and d).

In the southern part of the study area, the 25-35 km wide elongated plastered drift with its 75 m crest covers close to half of the area corresponding to the Ewing Terrace (Figs. 3.4 and 3.6). While the southern termination of the drift cannot be determined in this study due to lack of data, drift deposition is observed toward the southern flank of the Mar del Plata Canyon. At  $\sim 39.3^\circ\text{S}$  the orientation the crest slightly changes from a NE to a NNE trend following the general trend of the middle slope (Fig. 3.4). In the northern part of the study area, no drift deposition occurs close to the Mar del Plata Canyon. The depositional zone can only be identified north of the Querandi canyon. From there it widens northward toward the Uruguayan margin reaching a width of 30 km in the northern boundary of the study area (Figs. 3.7 and 3.8c), encompassing another plastered drift. The crest of the drift runs parallel to the middle slope and reaches a height of 35-40 m (Fig. 3.4).

#### *Necochea Terrace (T4)*

The deepest identified terrace is the Necochea Terrace in water depths of  $\sim 3500$  m (Fig. 3.4). While

landward it is limited by the lower slope, seaward the limit is hard to identify due to the gradual transition into the continental rise. However, in general the width of the terrace varies from 5 to 35 km from north to south. Since data coverage in this deep part is sparse and only conventional seismic imaged the Necochea Terrace, detailed spatial statements on the seismo-acoustic facies are not possible. However, at least the available data indicates an aggradational stacking pattern, representing another plastered drift. The pure data coverage suggests that this depositional pattern is mostly restricted to the southern part of the study area. Only directly north of the Mar del Plata Canyon seismofacies associated to plastered drifts could be identified in a small, distinct area.

### **3.4.2.3 Gravitational features**

Mass transport deposits (MTDs) in the study area are mainly confined to the lower slope area and the heads and flanks of the submarine canyons (Fig. 3.4). As seen in Figures 3.5, 3.6, 3.8e and f gravitational processes are common on both the northern and southern lower slope in water depths between 2000-3000 m and can be identified by their chaotic seismic facies. In contrast to the southern part of the study area, MTDs and their scars are more abundant and of larger dimension in the north. Moreover, mass wasting deposits are associated to the head of the Querandi Canyon and the Punta Mogotes Canyon (Fig. 3.4)

### **3.4.3 Oceanographic features**

#### **3.4.3.1 Section I – South of Mar del Plata Canyon**

In the southernmost section (Fig. 3.9 top) a vertical wedge of cold ( $< 7^{\circ}\text{C}$ ) and fresh ( $S < 34.2$ ) subantarctic waters is observed in the near-surface region of the upper slope. Satellite derived sea surface temperature data reveal that this latitude marks the mean northernmost penetration of the Malvinas Current (e.g. (Piola and Matano, 2001; Saraceno et al., 2004). Thus, the warm-salty and relatively low oxygen Tropical Waters and South Atlantic Central Waters that characterize the South Atlantic subtropical gyre are displaced offshore and are not in contact with the bottom toward the North. Below the subtropical thermocline the salinity minimum ( $S_{\min}$ ) and oxygen maximum of AAIW are well defined, but near the slope they connect with the slightly warmer and less dense outer shelf waters (Fig. 3.9 top). At this latitude the cores of circumpolar deep waters are split by the southward flowing NADW (Reid et al., 1977). The cores of these water masses against the slope, are well defined in the 1200-4000 m depth range by the low-high-low salinity (34.6,  $> 34.8$ , 34.75) and oxygen ( $< 4.25$ ,  $> 5.25$ ,  $< 5$  ml/l) stratification sequences (Fig. 3.6 top). The core of UCDW ( $\text{O}_2 < 4.25$  ml/l) is observed at 1700 m and against the slope spans the 1500-2000 m depth range. UCDW also creates a relative potential temperature minimum matching the  $\text{O}_2$  minimum. The high salinity core of NADW ( $S > 34.9$ ) is located at 2450 m and appears to be just separating from the slope while the NADW

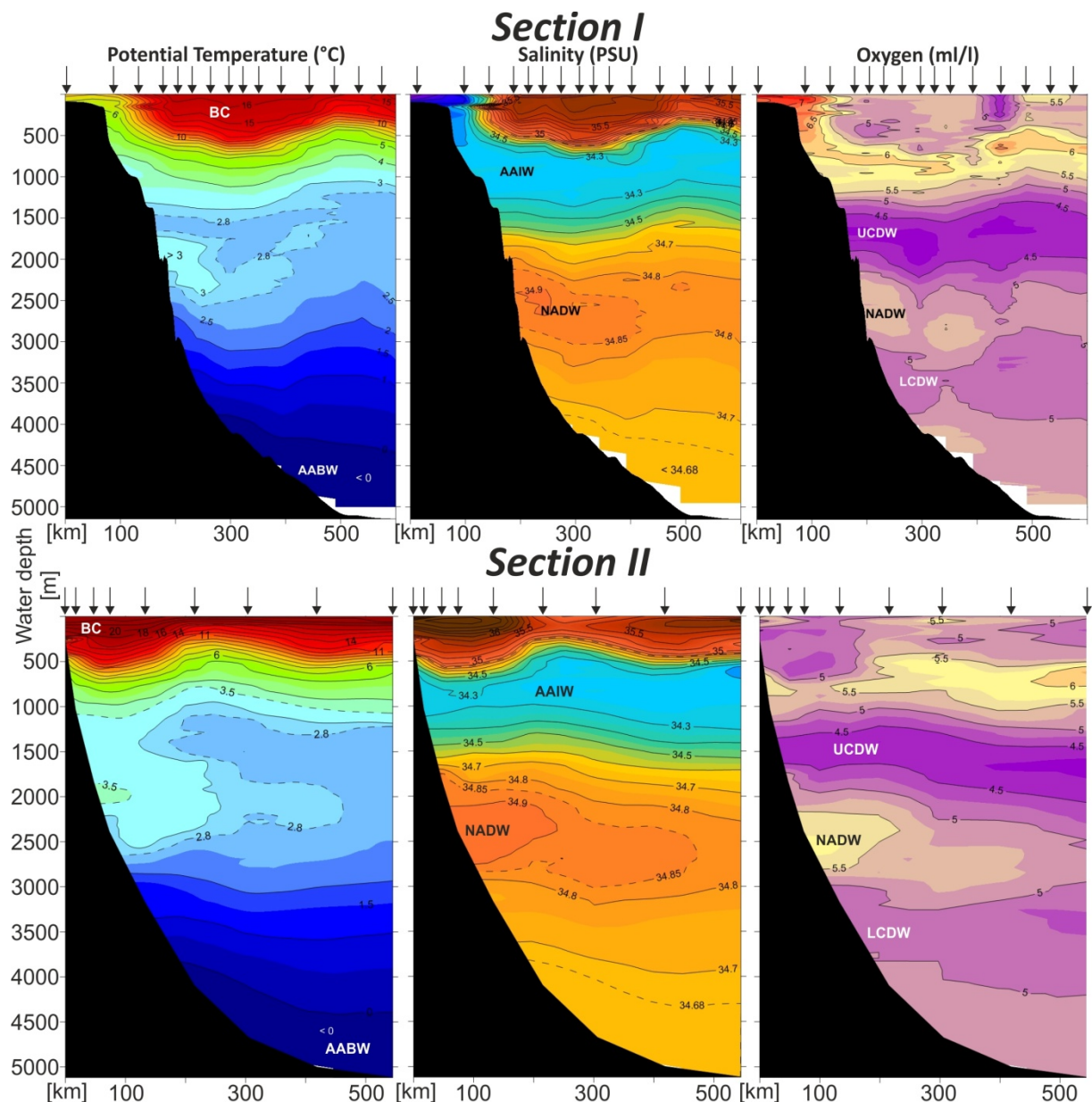


**Figure 3.9:** Hydrographic sections (location given in Fig. 3) of the study area showing lateral variations in potential temperature, salinity and oxygen from south (Section I top) to north (Section II bottom); BC – Brazil Current; AAIW – Antarctic Intermediate Water; UCDW – Upper Circumpolar Deep Water; NADW – North Atlantic Deep Water; LCDW – Lower Circumpolar Deep Water; AABW – Antarctic Bottom Water

salinity range ( $S > 34.8$ , Tab.3.1) spans the 2500-3000 m depth range. At this location LCDW ( $S < 34.8$ ,  $O_2 < 5$  ml/l) occupies the 3000-3900 m depth range. Below this layer, most of the abyssal ocean is covered by AABW ( $\theta < 0^\circ\text{C}$ ; Fig. 3.9 top).

### 3.4.3.2 Section II – North of Mar del Plata Canyon

As expected based on the general circulation patterns, further north, upstream of the detachment of the Brazil Current (BC) from the slope, we find a different structure of near-bottom water masses down the slope (Fig. 3.9 bottom). The upper layer (depths less than ~500 m) is occupied by warm ( $> 10^\circ\text{C}$ ), salty ( $S > 35$ ) South Atlantic Central Water (SACW), which flows southward associated with the Brazil Current. Also at this latitude the salinity minimum of AAIW is clearly defined in the 700-1200

m depth range (Fig. 3.9 bottom). This near-bottom AAIW core is thinner than further south, but presents similar salinity and oxygen values, suggesting it is still part of a narrow northward flowing branch in contact with the slope. At Section II the UCDW core is still present but the oxygen minimum layer, where  $O_2$  is less than 4.25 ml/l, is about 400 km east of the slope. Similarly, the  $\theta_{\min} < 2.8^\circ\text{C}$  observed in Section I close to the oxygen minimum is displaced offshore (Fig. 3.9). Consequently, in Section II the bulk of UCDW appears to have shifted offshore and occupies a thinner layer interacting with the bottom in the 1350-1650 m depth range (Fig. 3.9 bottom). The potential temperature maximum observed above the NADW maximum is not displaced vertically, but is now above  $3.5^\circ\text{C}$ , while the salinity maximum ( $S > 34.9$ ) has expanded vertically to the 2150-2800 m depth range. The region with  $S > 34.8$ , our adopted definition for NADW in the Argentine Basin, spans the 1700-2900 m depth range, thus is thicker and shallower than observed further south (Fig. 3.9 bottom). Note that because Section I is zonal and Section II runs perpendicular to the bottom topography the sections are only about 250 km apart along the 5000 m isobath. In addition, the coarser cross-slope sampling resolution in the deeper part of the slope in Section II precludes a more detailed comparison of the core properties of LCDW and AABW (Fig. 3.9).

As shown above, the vertical arrangement of deep water masses in contact with the bottom observed in Section I and II is quite distinct. In Section II the core of UCDW has shifted offshore indicating an eastward deflection of this water mass past  $38^\circ\text{S}$ . South of  $38^\circ\text{S}$  (not shown) the warm-salty and high oxygen core of NADW detaches from the slope, suggesting that the bulk of this water mass veers offshore as it flows south of that latitude.

### 3.4.3.3 Near-bottom layers

As aforementioned, we analyzed the distribution of near-bottom (within 150 m) water mass properties based on data available in the World Ocean Database 2009 in the Argentine Basin to understand the role of the circulation and water mass structure on the described morpho-sedimentary features.

AAIW is confined to the upper slope, mostly between the 200 and 1000 m isobath and its northernmost location is detected at  $34^\circ\text{S}$  (Fig. 3.10). The slope narrows northward considerably and there are no stations meeting the AAIW criteria in the narrow stripe between the 200 m and 1000 m isobaths. No near-bottom AAIW is found in the latitude range between  $34$  and  $29^\circ\text{S}$ . However, north of  $29^\circ\text{S}$  we do observe a narrow stripe of AAIW along the 1000 m isobath (Fig. 3.10). This northern core of AAIW intersects the bottom at somewhat deeper levels than the southern core (850-1100m), and flows southward below the Brazil Current. The offshore limit of near-bottom UCDW closely follows the 2000 m isobath and the bulk of this water mass extends northward to about  $35^\circ\text{S}$ . North of  $38^\circ\text{S}$  there is evidence of near-bottom NADW in the depth range 1800-3000 m (Fig. 3.10). In the western Argentine Basin LCDW occupies a narrow near-bottom stripe in the 2300-3400 m range. The interaction of LCDW with the bottom appears to extend to the southern flank of the Rio Grande Rise, and a few observations suggest isolated portions of near-bottom LCDW at depths of nearly 4000 m

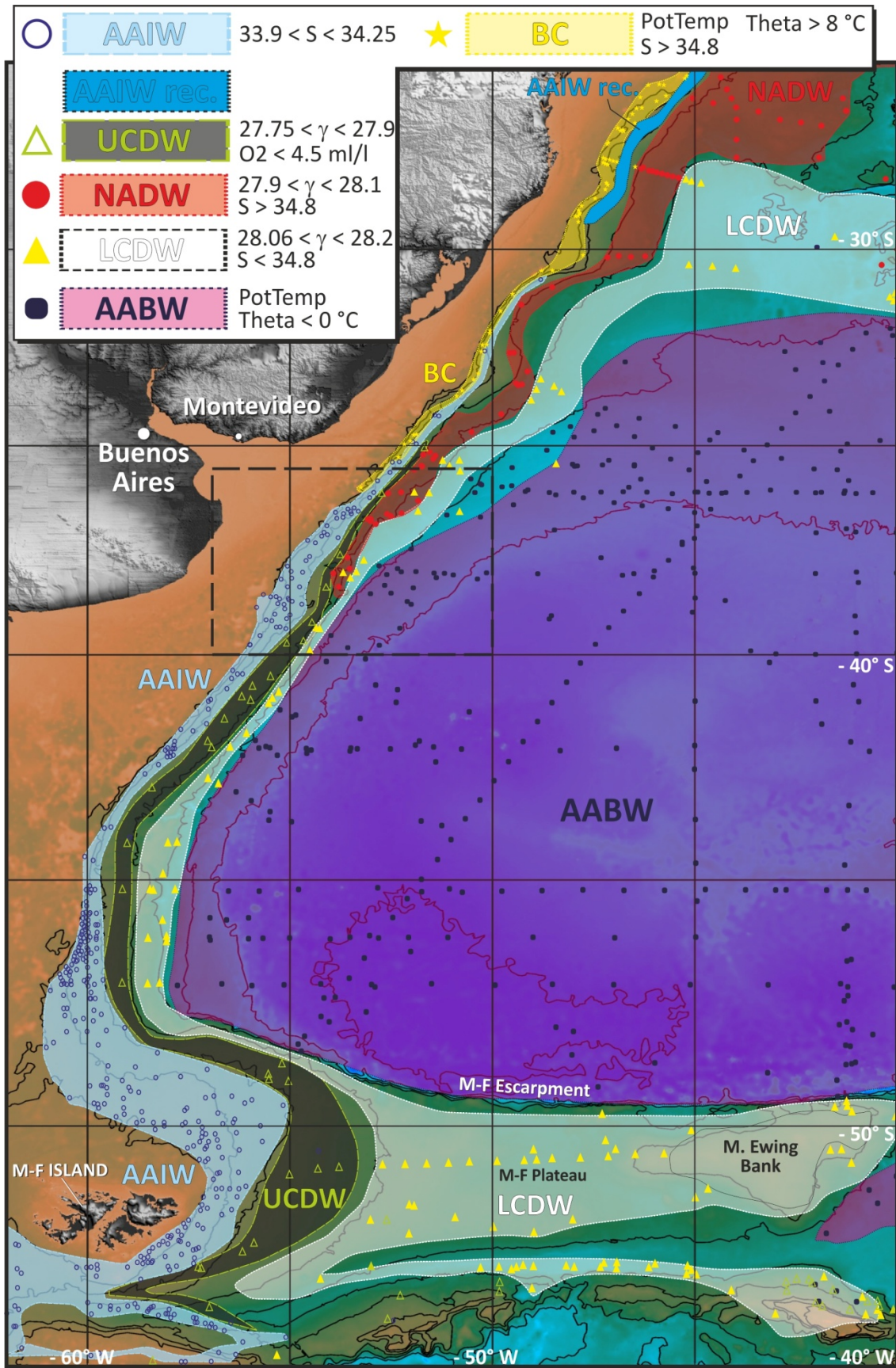


**Figure 3.10:** Map of the Argentine Basin identifying near bottom layers depending on their physical characteristics; BC – Brazil Current; AAIW- Antarctic Intermediate Water; AAIW rec. – recirculated AAIW; UCDW – Upper Circumpolar Deep Water; NADW – North Atlantic Deep Water; LCDW – Lower Circumpolar Deep Water; AABW – Antarctic Bottom Water; symbols identify sample location (WOD09) and water mass



north of 36°S. As pointed out above, most of the bottom at depths greater than 4000 m are subject to the influence of AABW (Fig. 3.10).

### **3.5 Discussion**

#### **3.5.1 Morpho-sedimentary and hydrographic features and their oceanographic and tectonic implication**

##### **3.5.1.1 Margin physiography**

The northern Argentine margin physiography is characterized by peculiar differences in slope angle north and south of the Mar del Plata Canyon (red marks in Fig. 3.4). While overall the northern part of the study area shows a margin inclination oblique to the upper slope, the slope south of the canyon dips northeastward and therefore, in an ~45° angle to its northern counterpart. This change in physiography might be related to the Salado Transfer Zone (STZ), which runs as well perpendicular to the upper slope in the center of the study area (Figs. 3.4 and 3.11). The STZ was established during the initial opening of the South Atlantic (Franke et al., 2007; Hinz et al., 1999) and is probably characterized by non-uniform cooling of adjacent margin Segments III and IV (Allen and Allen, 1990). Periods of stronger subsidence were described associated with this structure as e.g. during the Middle Miocene (Aceñolaza, 2000; Kennett, 1982; Potter and Szatmari, 2009). Consequently, the differential tilting is presumably linked to the STZ, although its effect can only be observed along the La Plata Terrace (Fig. 3.4). Further down-slope, uniform margin inclination over the study area indicates the dominance of erosive and depositional forces, which overprint the tectonic signature.

##### **3.5.1.2 Upper slope – La Plata Terrace (T1)**

The La Plata Terrace is located at the upper slope in water depths between 500-600 m deepening toward the north (Fig. 3.4 and 3.11). Its sedimentary style excludes considerable downslope transport from the shelf and points to a uniform, continuous forcing which had controlled sedimentation (Figs. 3.5 and 3.6). This kind of widespread and persistent condition can only be maintained over long time periods by ocean currents.

Analysis of the hydrographic sections (Fig. 3.9) revealed that the La Plata Terrace is located close to the interface between surface waters and the AAIW, which is in particular well defined in the BC by the steep thermocline in ~500 m water depth north of the Mar del Plata Canyon (Fig. 3.9 bottom). Such water mass interfaces, in general, represent zones dominated by turbulent, energetic current patterns driven by major vertical density gradients (Reid et al., 1977). Moreover, the high energetic environment is supported by the presence of the BC and MC, which flow not only as surface currents but as well as bottom currents along the La Plata Terrace (Fig. 3.10). Surface currents, which are in general driven by wind circulation and large lateral temperature gradients, are characterized by high flow velocities and in this way contribute to the high energetic environment dominating the uppermost 500-600 m of water depth.

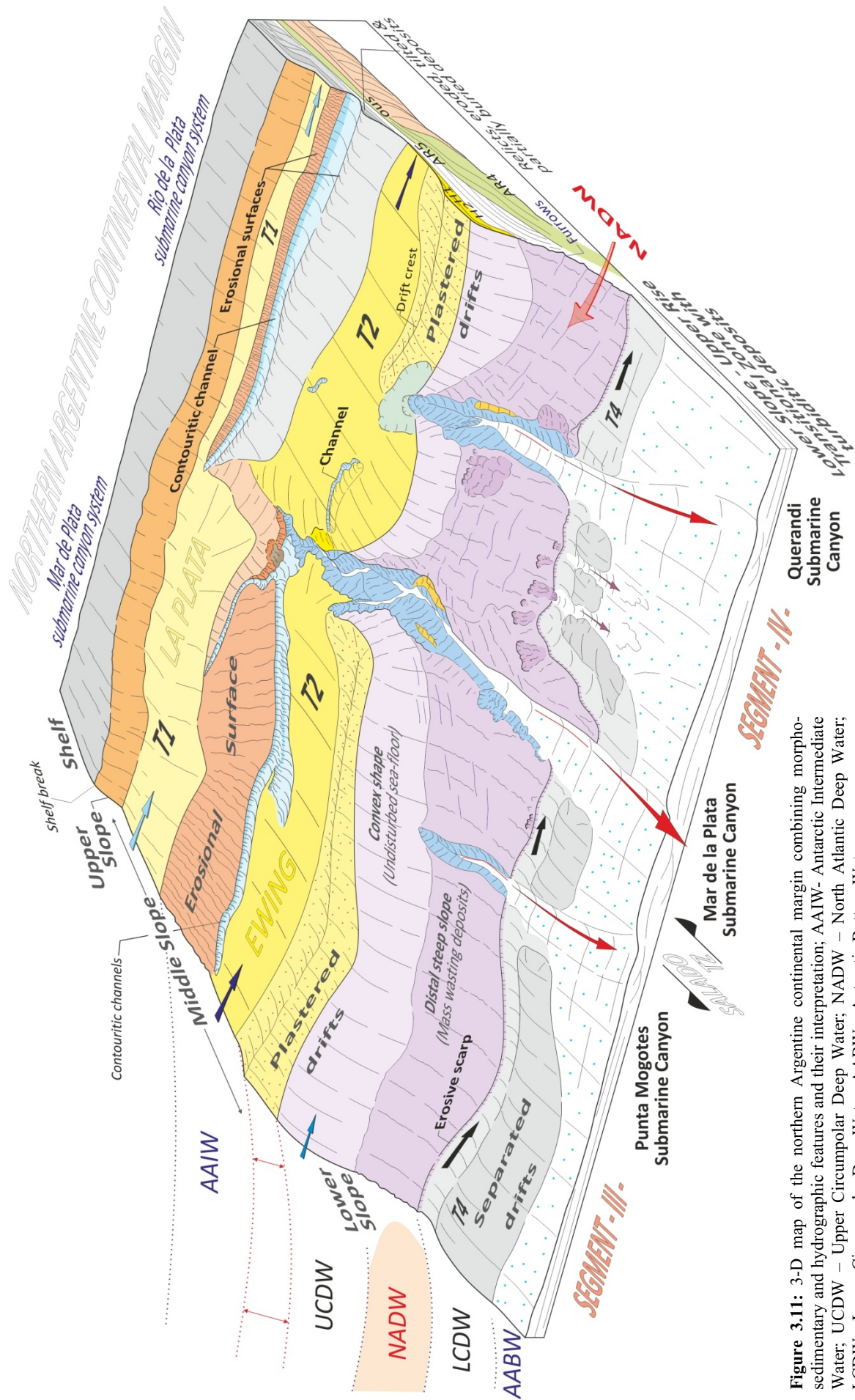


Figure 3.11: 3-D map of the northern Argentine continental margin combining morpho-sedimentary and hydrographic features and their interpretation; AAIW- Antarctic Intermediate Water; UCDW – Upper Circumpolar Deep Water; NADW – North Atlantic Deep Water; LCDW – Lower Circumpolar Deep Water; AABW – Antarctic Bottom Water

This dynamic environment is well reflected in the sedimentary style of the upper slope. Although in parts only purely imaged by means of seismo-acoustic methods, the upper slope in transition to the La Plata Terrace shows clear evidence of erosion. This remobilization of sediments is favored by the general turbulent bottom current conditions, which are locally enforced along a steep slope (McCave et al., 1982). Due to the lower slope angle, terraces are characterized by more tabular flow conditions and lower flow velocities (Hernández-Molina et al., 2008a; McCave et al., 1982). Consequently, the influence of bottom currents will result in uniform sedimentation along and across contourite terraces as was as well shown for the La Plata Terrace (Fig. 3.6). Even though current velocities are lower on top of the terrace, the dynamic current conditions are reflected in the deposited sediments, which show a silty to sandy character (Bozzano et al., 2011). Therefore, combining sedimentological and oceanographic evidence, we suggest that the upper slope including the La Plata Terrace and their associated sedimentary regime is strongly influenced by the surface water/AAIW interface (Fig. 3.11). The highest turbulent energy at this interface might be related to the presence of the BC, which due to its associated deep thermocline generates large density contrasts in 500 m water depth (Fig. 3.12). Accordingly, in particular the BC/AAIW interface might control sedimentary processes along the La Plata Terrace, although lateral bottom water distribution shows the detaching of the BC (Fig. 3.10) from the margin in the northern part of the study area. The southern area is probably controlled by BC eddies, which allow in their center isolated warm water to penetrate into the MC (Piola and Matano, 2001). In the southern area probably single eddies allow for SACW to reach this region (Piola and Matano, 2001). Finally, the La Plata terrace terminates a few kilometers south of the study area (Urien and Ewing, 1974), since the BC cannot deeply penetrate into the MC.

This mechanism becomes obvious comparing the northern and southern hydrographic/seismic intersections given in Figure 3.12. The northern section is dominated in the uppermost 500 m by waters depleted in oxygen, which represent the warm waters of the BC. In contrast, the southern section reveals high oxygen values close to the upper slope corresponding to the MC, and therefore the weaker influence of the BC (Fig. 3.12b).

### **3.5.1.3 Middle slope – Ewing Terrace (T2)**

The largest terrace in the study area, the Ewing Terrace, is located in mid-slope position in water depths of 1200-1400 m (Figs.: 3.4 and 3.11; Hernández-Molina et al., 2009; Krastel et al., 2011; Violante et al., 2010). In contrast to the La Plata Terrace, the Ewing Terrace is not a locally confined feature, but continuous along the Patagonian margin (Hernández-Molina et al., 2009), which is already indicative for a regional control of the sedimentary regime.

Comparable to the upper slope, there is clear evidence of ocean currents controlling sediment transport at the middle slope. Massive erosion of older strata (Figs. 3.5, 3.6, 3.8a and b), partly originating from Middle Miocene plastered drift deposits (Preu et al., chapter 2.), shapes the middle slope, which connects the La Plata and the Ewing Terrace (Fig. 3.11). The erosion is related to the AAIW (Figs.

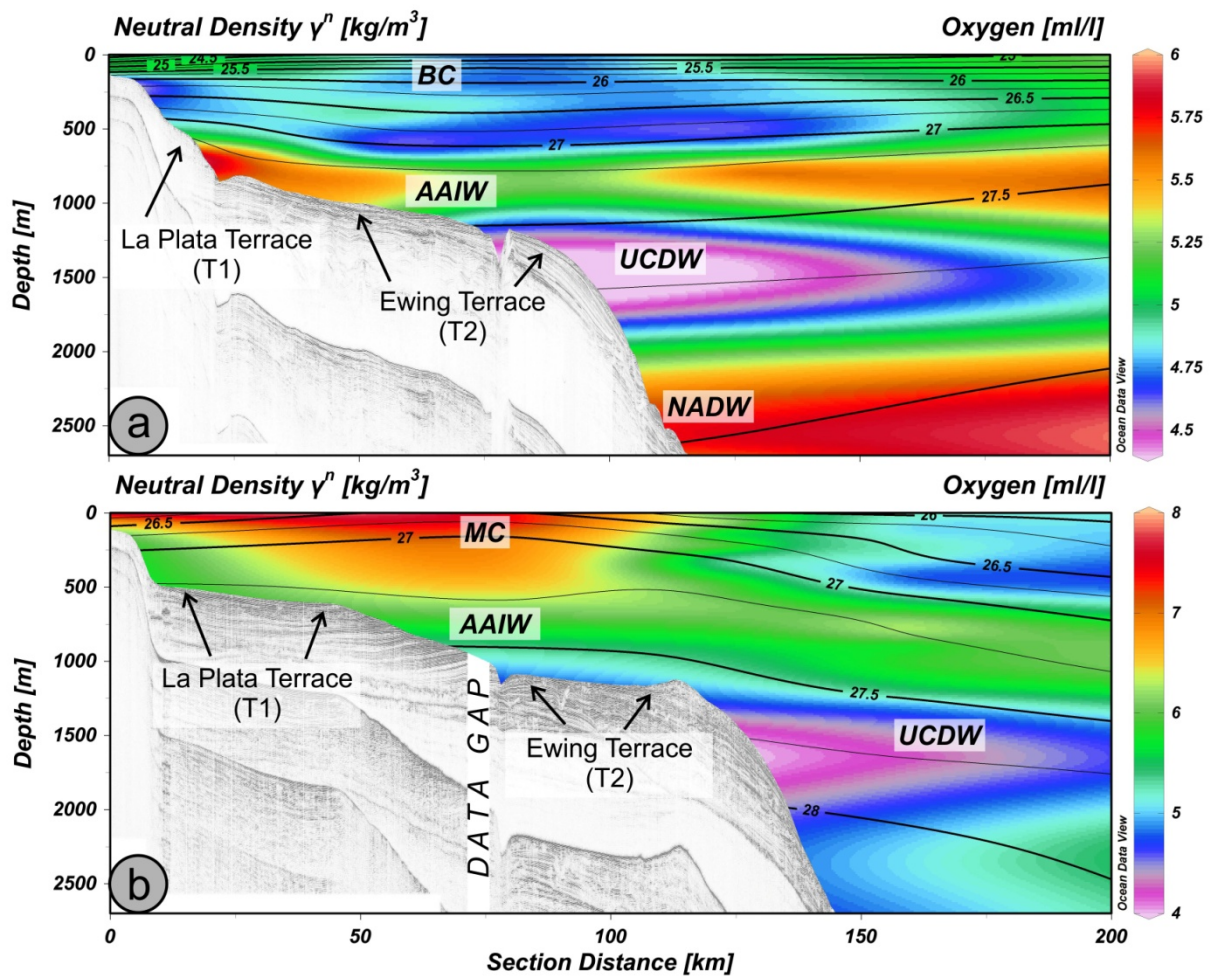


**Figure 3.12:** Seismic-hydrographic intersections from the north (a) and south (b) of the Mar del Plata Canyon; location of seismic lines and hydrographic sections is marked in Fig. 3; color code shows oxygen content in ml/l; isopycnals are indicated by black lines; BC – Brazil Current; MC -Malvinas Current; AAIW – Antarctic Intermediate Water

3.10-3.12), flowing as a fast bottom current favored by the margin morphology (McCave et al., 1982). This interpretation is strongly supported by approximated flow velocities of the OCCAM Global Ocean Model (Gwilliam et al., 1995; Gwilliam, 1996), suggesting flow velocities of ~15-20 cm/s in 1000 m water depth. Such velocities allow for fine sand to be eroded and transported (McCave, 2005; Niño et al., 2003). Moreover, associated to the dynamic current regime and the strong erosion measurements of high turbidity, which are part of the world ocean nepheloid layer composition data base assembled by the Lamont-Doherty Earth Observatory (Fig. 3.13), suggest the presence of intermediate nepheloid layers fed by the erosive margin processes within the AAIW.

At the lower boundary of the AAIW in the transition to the UCDW, which is clearly distinguished by its oxygen content (Figs. 3.9 and 3.12), the Ewing Terrace is located (Figs. 3.4 and 3.11). The turbulent processes associated to this water mass interface prohibit sediment deposition at least over a wide area of the terrace. In the transition between the middle slope and the Ewing Terrace deep contourite channels, running parallel to the margin (Figs. 3.4 and 3.11), indicate even the formation of helicoidal flow pattern. These are a result of a combination of margin morphology, Coriolis forcing and near-bottom Ekman transport.

In contrast to the proximal area of the terrace, in the distal part of the terrace a plastered drift can be

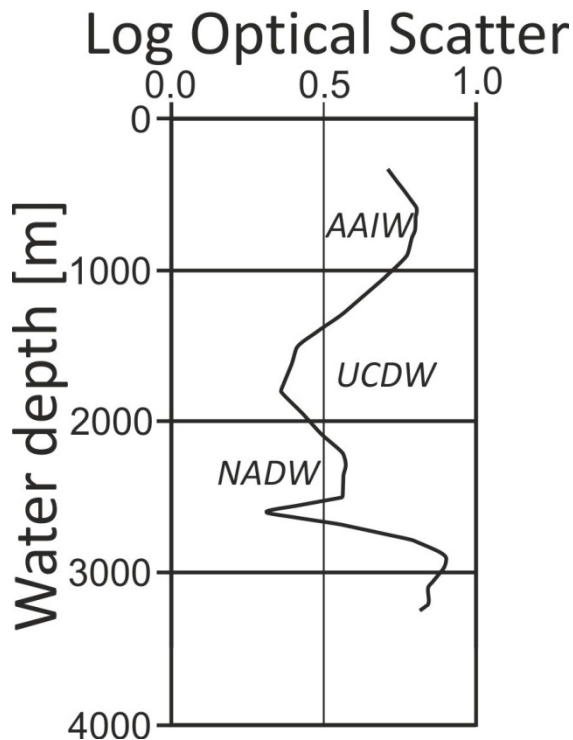


**Figure 13:** Optical scatter measurements from station RC15-83 with indicated water masses; AAIW – Antarctic Intermediate Water; UCDW – Upper Circumpolar Deep Water; NADW – North Atlantic Deep Water; station location indicated in Fig. 3.3

identified indicating sedimentation focused by along-slope processes. Since plastered drift formation are formed under slow to intermediate flow conditions (Faugères et al., 1999), this sedimentary pattern requires a continuous decrease of flow velocities with increasing distance from the steep middle slope.

This energetic regime is indicated by the lateral differences in sedimentary characteristics across the terrace. While in the transition from the upper slope erosive features are located close to the helicoidal flow pattern, the central area of the terrace is characterized by non-deposition or low sedimentation (Figs. 3.5 and 3.6). In turn, at the seaward limit of the Ewing Terrace plastered drift sequences are formed, marking the lowest current velocities. Recently published sedimentological data support this lateral change in the energetic

environment, showing a gradient from gravel rich contourite material located in the contourite channel to more silty material at the drift's crest (Bozzano et al., 2011). Additionally, this scenario as well fits to the observed turbidity values, (Fig. 3.13). Within the AAIW suspended particle load is highest, reflecting the eroded sediments along the middle slope. The amount of suspended sediments decreases drastically towards the UCDW, not only indicating the lower transport capacity of the UCDW, but as well the necessary conditions to form a plastered drift.

The described conditions at the depth of the terrace are probably significantly enhanced during glacial times, when the AAIW/UCDW interface is shifted upward (Preu et al., chapter 2) and the turbulent energy of the interface is replaced by calmer conditions characterizing the UCDW. However, the overall sedimentary configuration of the Ewing Terrace indicates that even during glacial times the steep slope allows for strong enough current velocities to prohibit sedimentation on the seaward half of the terrace.

Regionally, the morphology of the Ewing Terrace is characterized by remarkable changes. As described above and shown in Figures 3.4 and 3.11, the erosive, non-depositional and depositional patterns change their lateral distribution profoundly at the Mar del Plata Canyon.

The most prominent change in slope morphology is represented by the narrowing of the middle slope in close vicinity to the Mar del Plata Canyon (Figs. 3.4 and 3.11). One possible explanation might be offered by the BMC, which strongly influences the ocean circulation in larger depth as well (Preu et al., chapter 2). The detachment of NADW from the northern Argentine margin, which is associated

with the BMC, has a major effect on vertical water mass stratification (Carter and Cortese, 2009; Georgi, 1981; Piola and Matano, 2001; Saunders and King, 1995), and therefore on the position of water mass interfaces in the study area (cf. Figs. 3.12a and b). In addition, within the BMC, AAIW flowing northward along with the MC impinge recirculated AAIW flowing southward (Piola and Matano, 2001). The resulting high energetic mixing could be hold responsible for the stronger erosion north of the Mar del Plata Canyon and the change in margin morphology. Furthermore, this pattern would be strengthened by deep-reaching eddies traveling within the BC, which would also pass through the BMC. Such eddies are known to influence sedimentary processes even in large depth (Hollister, 1993; Hollister and McCave, 1984) and can erode large scale terraces as e.g. off SE Africa (Preu et al., 2011). At last, internal waves originating from the BC/AAIW interface might represent an enforcing factor, since these energetic patterns can result in massive sediment resuspension (Puig et al., 2004). Consequently, we propose that the lateral variations in width of the Ewing Terrace are the result of the massive forces associated to the BMC. However, partly structural control on the distinct northward narrowing of the La Plata Terrace and the middle slope cannot be excluded completely due to the presence of the Salado Transfer Zone (STZ), although satellite-derived gravimetric measurements (Smith and Sandwell, 1997) determined its position south of this major physiographic change (Franke et al., 2007).

The change in depositional style along the Ewing Terrace in the vicinity of the Mar del Plata Canyon cannot be explained by the large-scale ocean circulation. Whether the canyon or the overall change in margin physiography disturbs the sedimentary processes forming the plastered drift will be determined in future studies.

#### **3.5.1.4 Lower slope – Furrows and the Necochea Terrace (T4)**

The shape of the lower slope differs from the previously described and discussed shapes of the upper and middle slope. Figures 3.4 and 3.11 indicate the smooth and regular margin shape in water depths between 1500-2000 m, which is only disturbed by the presence of the Mar del Plata and Querandi canyons cutting into the plastered drift strata. This part of the margin is under the influence of the UCDW (Figs. 3.9-3.12), which flows with relatively low velocities along the northern Argentine margin, favoring drift deposition (Figs. 3.8c and d) as suggested by low turbidity values (Fig. 3.13).

In ~2000 m water depth not only the gradient of the lower slope changes, but also the margin morphology (Figs. 3.4 and 3.11). In contrast to the smooth surface upslope, the lower slope is characterized by a rough and hummocky surface in water depths between 2000-2900 m, which is at least in the area of the Mar del Plata Canyon and further northward incised by slope parallel incisions (Figs. 3.4 and 3.11). The hummocky surface of the lower slope indicates down-slope processes. These are probably associated to the upslope drifts building the Ewing Terrace since the Middle Miocene (Hernández-Molina et al., 2009; Preu et al., chapter 2.), which are susceptible to failure due to locally focused sedimentation (Laberg and Camerlenghi, 2008).

The minor slope parallel incisions represent furrows, which are mainly located along the scars of the former sediment failures (Figs. 3.5, and 3.8e) and suggest the influence of erosive bottom currents (Viana et al., 2008). Consequently, the abundance of furrows in water depth between 2000-3000 m points toward the NADW, flowing as erosive bottom current (Fig. 3.11). The link to the NADW as margin shaping current is strengthened by turbidity values, which increase in the corresponding water depths (Fig. 3.13). Therefore, the disappearing of the furrows south of the canyon (Figs. 3.6 and 3.8f) would be the result of the detaching of NADW from the Argentine margin, which is also indicated by the hydrographic sections. The northern Section II (Fig. 3.9 bottom) shows that the NADW water mass is thicker and shallower compared to Section I (Fig. 3.9 top). These observations suggest a more intense flow of NADW in the north than in the south. As a result, we propose that the furrows are linked to the presence of the NADW, which would be locally focused due to seafloor irregularities and minor incisions created by gravitational processes.

At the foot of the slope in water depths of ~3500m another terrace-like morphology called Necochea Terrace shapes the margin (Figs. 3.4 and 3.11). The prograding character of the deposited sediments indicates the influence of the surrounding oceanographic regime. Figure 3.9 shows clearly that the Necochea Terrace is today under the control of the LCDW and therefore, differs strongly from the La Plata Terrace and the Ewing Terrace. Comparable terraces were described for the southern Argentine margin, which are as well connected to Antarctic sourced or rather Southern Ocean sourced deep water masses (Hernández-Molina et al., 2009, 2010).

The variations in the sedimentary pattern from north to south might be linked to the variations in the NADW pattern. With the detaching of NADW from the margin the flow behavior of the LCDW probably also changes. Restrained in space by the NADW, the LCDW flows faster north of the Mar del Plata Canyon prohibiting sediment deposition. In contrast, south of the canyon the drift formation is possible due to lower current activity. However, this concept of long-term behavior is in conflict with the recent hydrographic data (Figs. 3.9 and 3.10), which suggest no significant changes in the LCDW and AABW cores within the study area.

An exception from the depositional pattern marks the area directly north of the canyon exit in the centre of the study area. There, in the current lee side exceptionally high sediment accumulation occurs supporting the hypothesis that the controlling water mass flows northward (Figs. 3.4 and 3.11). Consequently, the depositional style of the Necochea Terrace strongly depends on the NADW flow pattern, which in turn is influenced by the dynamics of the BMC.

### **3.5.2 Genesis of Contourite Terraces**

#### **3.5.2.1 General Concept**

Contourite terraces are formed by the interplay between margin physiography and the local current regime (Fig. 3.14). Water mass interfaces and their associated turbulent energy pattern might result in erosion along regular shaped margins (Fig. 3.14a). This energetic pattern might be enforced by

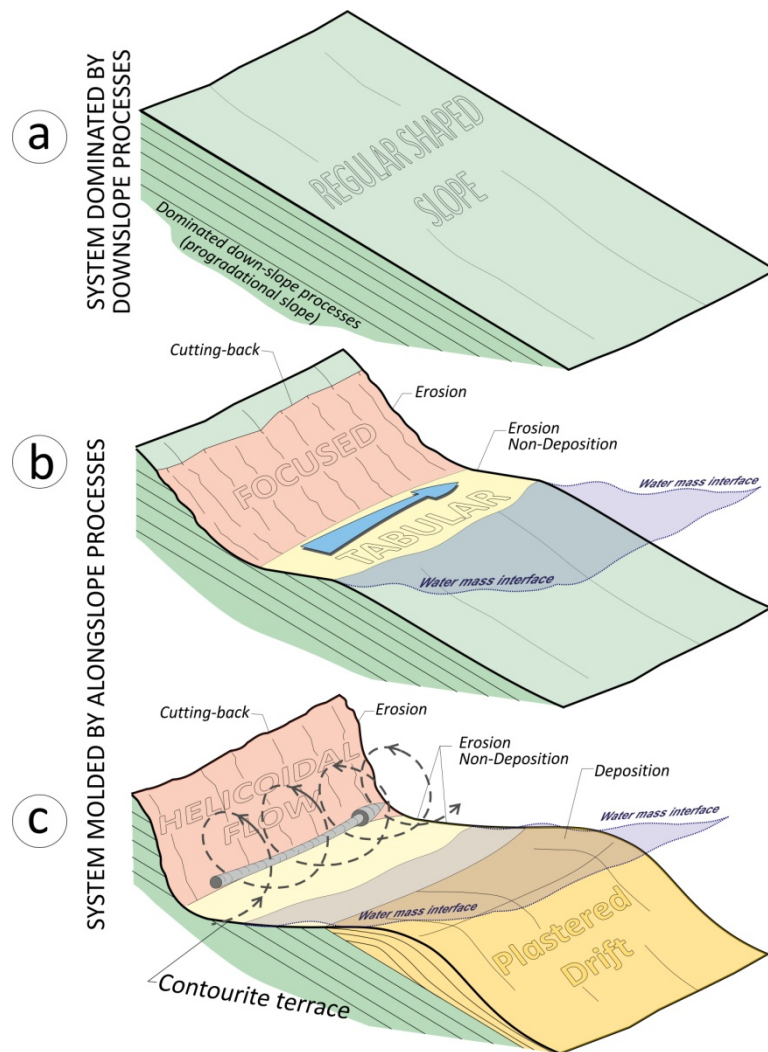


**Figure 3.14:** Schematic model explaining contourite terrace formation considering the erosive processes associated to water mass boundaries

and in consequence favor erosive processes. In contrast, terrace-like morphologies would result in calmer and more tabular flow conditions. Accordingly, a terrace would be characterized by a uniform depositional style or as the case may be laterally slow, from non-deposition to drift formation, varying depositional character on extensive terraces. While this depositional pattern would preserve the overall terrace shape, the upslope connected slope would be continuously eroded due to locally increased current velocities. On geological times the combination of both processes will lead to a cutting-back of the slope and a widening of the terrace (Fig. 3.14b).

Depending on the overall flow velocities and sediment properties, the locally confined velocity maximum might lead to enhanced erosion forming a contour channel in the transition between the steep slope and the terrace (Fig. 3.14c). Therefore, a helicoidal flow pattern can evolve, which in turn continuously deepens the channel due to enforced erosive processes. The additional resuspended material provided by this processes is transported along the terrace, where at the seaward limit drift formation is possible (Fig. 3.14c).

This model considers no structural control on the terrace formation. Since terraces, of course, might be as well predetermined by tectonic processes, for application of the model a structural control has to be

internal tides and internal waves, which have a tremendous effect on sediment dynamics and result in erosion and resuspension (Bonnin et al., 2002; Cacchione et al., 2002; Dickson and McCave, 1986; Hosegood and van Haren, 2003; van Raaphorst et al., 2001). Once the regular margin shape has been altered, upslope the slope steepens, while a smaller terrace-like feature developed along the water mass interface (Fig. 3.14b).

The terrace due to its shape will strongly influence the local flow pattern. As aforementioned, McCave et al. (1982) described the relation between slope gradient and potential flow velocities in a case study at the Bermuda Rise

suggesting that steeper slopes allow for higher current velocities



ruled out. However, once the terrace was formed, sedimentary processes will be similar to the above described (Figs. 3.14b and c).

### 3.5.2.2 Contourite terraces along the northern Argentine margin

Since structural control on terrace formation can be excluded for the northern Argentine margin based on deep reaching multichannel seismic data (Hinz et al., 1999), the evolution of contourite terraces are probably related to oceanographic processes.

Considering the above described deep thermocline associated to the BC/AAIW interface (Figs. 3.9 and 10), the origin of the La Plata Terrace can be linked to water mass interface related processes (Fig. 3.11). Since changes in temperature go along with changes in density, the BC/UCDW interface is particular susceptible for internal wave generation and propagation, which are as described above capable to initiate or enforce erosive processes (Fig. 3.12a).

These high energetic patterns might not only influence the La Plata Terrace but as well the Ewing Terrace. Since the Ewing Terrace correlates with the AAIW/UCDW interface (Fig. 3.10), which represents a convenient surface to reflect and focus internal wave energy, the evolution of the Ewing Terrace might as well be related to processes in shallower water. Additionally, several studies suggested that the Ewing Terrace is controlled by the AAIW/UCDW interface since the Middle

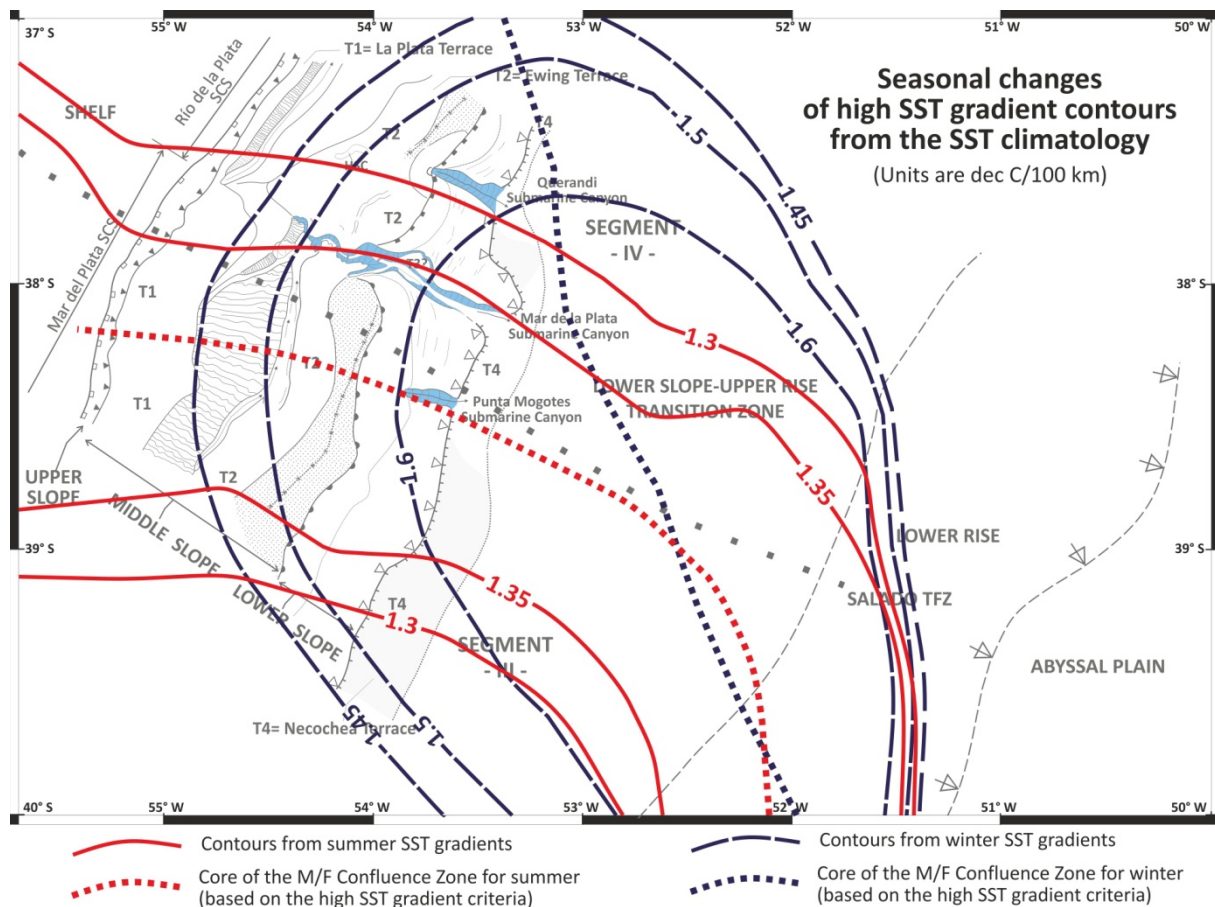


**Figure 3.15:** Seasonal variability of the Brazil-Malvinas Confluence derived from high resolution satellite climatology (Casey and Cornillon, 1999)

Miocene (Hernández-Molina et al., 2009; Violante et al., 2010; Preu et al., chapter 2.). These studies not only suggest a cutting of the terrace into former strata but a widening of the Ewing Terrace due to drift deposition at the seaward boundary of the terrace, as well (compare Fig. 3.14c, Preu et al., chapter 2).

Since the Necochea Terrace is located within the LCDW, its position along the slope seems to exclude the water mass interface model (Fig. 3.9). However, this is not completely true considering that terrace formation is a process progressing on geological times. During glacial times the overall influence of Antarctic water masses onto the southern hemisphere increases (Duplessy et al., 1988; Mulitza et al., 2007). This incorporates probably an increase in AABW production (Ninnemann and Charles, 2002; Piotrowski et al., 2008), which is still under debate (e.g.: Curry and Lohmann, 1982; Krueger et al., in press.; Weber et al., 1994). An overall strengthened influence of southern sourced water will lead to a thickening of the AABW layer at the Argentine margin. In contrast, NADW production is strongly reduced during cold periods (Knutz, 2008; McCave et al., 1995; Oppo and Fairbanks, 1987; Rasmussen et al., 1996; Venz et al., 1999), which leads to a thinning of the NADW layer along the northern Argentine margin (Kennett, 1982, Preu et al., chapter 2). While the thickening of the AABW pushes the LCDW/AABW-interface upward, there is no counterforce given by the NADW, which influence is significantly reduced. This scenario would place LCDW/AABW interface close to the Necochea Terrace during glacial times and therefore suggest that the terrace formation processes are mainly active during cold periods in this part of the margin. Consequently, the forcing responsible for the development of the Necochea Terrace would be very variable on geological timescales, which is reflected by its small-scale appearance on the margin.

### **3.5.3 Implications on geological time scales**

Linking of lateral variations in terrace morphology and the associated erosive features to the regional oceanography (Fig. 3.11 and 3.12) allow to infer not only on terrace formation processes, but as well on the history of the controlling oceanic regime. This is in particular valid for the dynamics of the BMC, which marks the southernmost penetration of the BC and the NADW along the Argentine margin.

As shown above, the lateral continuity and shape of the La Plata Terrace is strongly bound to variations in the BC flow pattern favoring internal wave generation and propagation. Since the La Plata terrace terminates a few kilometers south of the study area (Urien and Ewing, 1974), this scenario would suggest that the modern situation of the BMC would be close to its southernmost position on geological time scales. This might be at least valid for Quaternary times, when climate is dominated by glacial/interglacial cycles. While the modern position of the BMC would mark the location during interglacials, due to a stronger influence of southern sourced waters during glacials (Duplessy et al., 1988; Mulitza et al., 2007), the BMC was probably shifted northward (Preu et al., chapter 2). Approximately, this northward migration of the BMC can be shown by its seasonal

variation. Seasonal variability of the BMC (Fig. 3.15) derived from satellite observations (Saraceno et al., 2004) show a northward migration from southern hemisphere summer to winter. This interpretation is in agreement with the location of the seasonal frontal probability maxima, which was derived from very high resolution radiometer data (Saraceno et al., 2004). Following this concept, the position of the BMC would be located further northward during cold periods. Consequently, we suggest based on the La Plata terrace shape that the modern position of the BMC is probably close to its southernmost position at least during Quaternary times.

This interpretation is in agreement with the appearance of furrows at the lower slope mainly in the northern part of the study area (Figs. 3.4, 3.5, 3.8f and 3.11). As mentioned before, these features are probably produced by the interaction of NADW with the hummocky seafloor topography, which is the result from mass wasting processes. The southern limit of the NADW is marked by the location of the BMC, as well, where it is deflected and loses its margin constraint (Piola and Matano, 2001). Therefore, the abrupt disappearing of these slope parallel incisions in the southern part of the study area indicates the southernmost influence of the NADW and in turn of the BMC on geological timescales.

### **3.4 Conclusion**

Morpho-sedimentary analysis of the northern Argentine margin based on seismo-acoustic and hydro-acoustic data were used to describe erosive and depositional features including mass transport deposits and their lateral variability. Three major terraces were identified located in 500-600 m (La Plata Terrace), 1100-1300 m (Ewing Terrace) and 3500 m (Necochea Terrace) water depth, respectively. At least the two shallowest are connected upslope to particularly steep erosional slopes. In 2000-2900 m water depth the influence of downslope processes can be identified based on their hummocky surface and their chaotic seismic expression.

The margin shape including erosive and depositional features changes distinctly in the center of the study area close to the Mar del Plata Submarine Canyon. While the La Plata Terrace narrows from south to north, the Ewing Terrace widens. Seaward, gravitational deposits in the northern part of the study area show slope parallel incisions identified as current induced furrows.

Correlation of the morpho-sedimentary features with the surrounding oceanographic regime revealed a major relation between the terraces and the water masses. The location and evolution of terraces along the Argentine margin can be related to distinct water mass interfaces. While the La Plata Terrace correlates to the Brazil Current (BC)/Antarctic Intermediate Water (AAIW) interface, the Ewing Terrace is located at the AAIW/Upper Circumpolar Deep Water (UCDW) transition. The Necochea Terrace is probably located at the LCDW/Antarctic Bottom Water (AABW) interface during glacial times.

The presence of these terraces along water mass interfaces suggests turbulent energy associated to these zones as initial mechanism for terrace formation. These erosive processes might be enhanced due

to processes related to internal wave generation. Once the first smaller incision is carved into the margin, locally the currents will be enforced along the stepper segments of the slope. In contrast, calmer, tabular conditions will dominate along the terraces. The combination of both flow patterns results in a cutting-back of the margin and therefore in a widening of the terrace over time. Through time the terrace may reach a size, when the seaward boundary of the terrace is distal to the high velocity pattern focused along the steeper parts of the slope. This will result in the formation of contourite drifts.

Lateral variability of erosive features depends strongly on the surrounding oceanographic regime. Consequently, lateral variability in the shape of the northern Argentine margin indicates that the Brazil-Malvinas Confluence was located in its modern position or further northward during Quaternary times.

### **Acknowledgements**

The study was funded through DFG-Research Center / Cluster of Excellence „The Ocean in the Earth System“ and was supported by the Bremen International Graduate School for Marine Sciences (GLOMAR) that is funded by the German Research Foundation (DFG) within the frame of the Excellence Initiative by the German federal and state governments to promote science and research at German universities.

The study is related to the CONTOURIBER project (CTM 2008-06399-C04/MAR). Additional support was given by the Inter-American Institute for Global Change Research (IAI) CRN 2076 which is supported by the US National Science Foundation (Grant GEO-0452325).

The presented seismic data was interpreted and visualized using the commercial software package ‘The Kingdom Software’ (SMT).

We like to thank Captain Kull, Captain Baschek and the crew of R/V Meteor cruises M49/2 and M78/3 for their excellent work and support.

## **4. Interaction of alongslope and downslope processes: The Mar del Plata Canyon and its effects on contourite deposition**

Benedict Preu<sup>(1)</sup>, Tilmann Schwenk<sup>(1)</sup>, F. Javier Hernández-Molina<sup>(2)</sup>, Ines Voigt<sup>(1)</sup>, Roberto Violante<sup>(3)</sup>, Michael Strasser<sup>(4)</sup>, Sebastian Krastel<sup>(5)</sup>, Volkhard Spieß<sup>(1)</sup>

(1) MARUM – Center for Marine Environmental Sciences and Faculty of Geosciences, University of Bremen, Bremen, Germany

(2) Facultad de Ciencias del Mar, Universidad de Vigo, Vigo, Spain

(3) Servicio de Hidrografía Naval (SHN), Buenos Aires, Argentina

(4) Geological Institute, ETH Zurich, Zurich, Switzerland

(5) GEOMAR | Helmholtz Centre for Ocean Research Kiel, Germany

To be submitted to ‚Journal of Geophysical Research – Earth Surface‘

## **Abstract**

Sedimentary sequences of the northern Argentine contourite depositional system were studied to decipher the interaction of alongslope and downslope sediment transport processes. Based on the analysis of the sedimentary deposits in space and time by means of high-resolution multichannel seismic data, the influence of the oceanographic regime and the Mar del Plata Canyon on the slope architecture were determined.

In agreement with earlier studies, we show that bottom currents influence sedimentary processes since the Eocene/Oligocene over the middle slope, coeval with the opening of the Drake Passage. While in the Early Miocene the study area is characterized by unfocused, lateral uniform sedimentation, an elongated depocenter representing plastered drift sequences was formed in the Middle Miocene with sedimentation rates close to  $\sim 10$  cm/kyr due to the onset of the Northern Sourced Deep Water (NSDW). Afterwards, the successive closing of the Central American Seaway led to a strengthening of NSDW resulting in an upslope shift of the depocenter. Since the Late Pliocene associated with the final closure of the Central American Seaway, another plastered drift with an elongated depocenter is formed by the recent oceanographic setting.

Besides the upslope depocenter shift from the Middle to the Late Miocene, as well a lateral change in the sediment distribution is observed. The lack of sediments on the northern Mar del Plata Canyon flank since the Late Miocene suggests that this major topographic irregularity has profoundly disturbed the bottom flow pattern and therefore along-slope transport processes. We propose that the Mar del Plata Canyon is mainly fed by along-slope processes since Early Miocene times due to a decrease of flow velocity and sediment transport capacity of the Antarctic Intermediate Water, flowing as bottom current over the canyon. The origin of the canyon is probably related to non-uniform subsidence occurring along the Salado Transfer Zone during the Middle Miocene and local failure of drift sediments

## **4.1 Introduction**

Today, two different categories of sediment transport processes are known which control sediment dispersal within the deep-sea environment and which are distinguished by their initial driving force and main transport direction: downslope processes mainly driven by gravity and alongslope processes forced by bottom currents, which in turn are driven by the thermohaline circulation (Rebesco and Camerlenghi, 2008; Shanmugam, 2003, 2008). Both processes can be recognized by the appearance of associated sediment deposits in relation to margin physiography, their characteristic morphological features, which shape continental margins, and, of course, the sedimentological and acoustic characteristics of their deposits (Faugères and Stow, 1993; Faugères and Stow, 2008; Shanmugam, 2003, 2008).

Gravity-driven downslope processes dominate sediment transport in proximal areas of large terrigenous sediment sources as e.g. rivers, which form the most important transport system into the

marine realm (Milliman and Meade, 1983). There, in connection to such highly active sediment delivery systems, continental margins are often shaped by across-slope conduits of different dimensions reaching from small gullies to large canyon structures, which channelize downslope oriented sediment transport. Being unchanneled, gravitational processes can lead to creeping, extensive slides, slumps, debris and turbidity flows. These features may occur decoupled from the main sediment sources and are mostly the consequence of to locally higher sediment loads, oversteepening of slopes and excess hydrostatic pressure (Shanmugam, 2003, 2008).

In addition to downslope transport processes, along-slope sediment transport adds an important element to globally relevant sediment dispersal mechanisms which can have large impact on the shape and architecture of continental margins (e.g.: Heezen, 1959; Heezen and Hollister, 1964; Hernández-Molina et al., 2008a, 2008b; Stow et al., 2009). Along-slope sediment transport is mainly driven by bottom (contour) currents, which flow along continental margins as part of the major geostrophic and thermohaline circulation patterns interacting with the general seafloor morphology and eroding, resuspending and transporting sediments over large distances (Rebesco and Camerlenghi, 2008). Sedimentary deposits resulting from persistent bottom current activity are called contourites (Faugères and Mulder, 2011; Rebesco, 2005; Rebesco and Camerlenghi, 2008). Besides the temporal aspect the depositional characteristics of contourites strongly depend on the interplay between bottom current variability, sediment supply, and topographic framework (Faugères et al., 1993, 1999). Associated with these depositional features, areas of erosion are common in close proximity to contourites. In combination, zones of erosion and deposition reflect the dynamics of the bottom current regime and

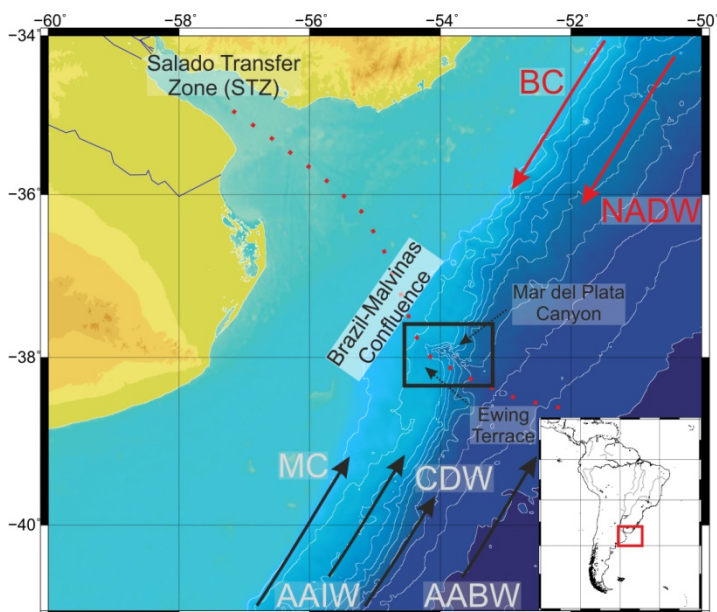


**Figure 4.1:** Map of the boundary region between Uruguay and Argentina indicating besides the main physiographic features, as well the regional oceanographic regime and the Salado Transfer Zone; BC – Brazil Current; MC – Malvinas Current; AAIW – Antarctic Intermediate Water; CDW – Circumpolar Deep Water; NADW – North Atlantic Deep Water; AABW – Antarctic Bottom Water; black box indicates the study area

are referred to as contourite depositional system (CDS) (Hernández-Molina et al., 2008a).

While several studies dealt with the identification and description of either gravitational or bottom current induced sediment transport including their importance for slope architecture (e. g.: Antobreh and Krastel, 2007; Krastel et al., 2001; Llave et al., 2001; Nowell et al., 1985; Pratson and Coakley, 1996; Preu et al., 2011), only few studies focused on sedimentary systems controlled by both, downslope and alongslope processes (e.g.: Marchès, 2008; Marchès et al., 2010; Mulder et al., 2006; Shanmugam, 2003) and

therefore, possible interactions are poorly studied and understood.

A suitable region to study the interaction between alongslope and downslope processes is located at the northern Argentine continental margin. Off the Rio de la Plata River the extensive Mar del Plata Submarine Canyon is located directly within a major CDS (Fig. 4.1), controlled by Antarctic water masses and their interaction with northern sourced waters (Hernández-Molina et al., 2009; Violante et al., 2010); Preu et al., chapters 2 and 3). In this study we describe the characteristics of both the gravity controlled and bottom current induced sedimentary structures located off northern Argentina and their spatial and temporal variability. Moreover, we will discuss the influence of both processes and their possible interaction. At last, we will propose a conceptual model, which might explain the evolution of the northern Argentine CDS from the interplay with the Mar del Plata Submarine Canyon with the ambient oceanographic regime .

## **4.2 Study site**

### **4.2.1 Oceanographic setting**

To study the interaction of highly active oceanographic processes with the seafloor, the northern Argentine margins represents a well suited study area being in one of the most dynamic basins of the world's oceans (Chelton et al., 1990). The oceanographic setting in this area is mainly known for the Brazil/Malvinas Confluence (BMC) located at  $\sim 38^{\circ}\text{S}$  (Fig. 4.1), a major convergence of two surface currents: the southward flowing Brazil Current (BC) and the northward flowing Malvinas Current (MC; Bisbal, 1995; Piola and Matano, 2001). Conditioned by the strong horizontal and vertical mixing associated with the BMC, its dynamics strongly controls sediment dynamics and margin morphology (Ewing and Lonardi, 1971; Piola and Rivas, 1997; Preu et al, chapter 3). Comparable to surface water conditions, the intermediate and deep ocean circulation encompasses as well strong mixing dominated by the encounter and interaction of Antarctic water masses (Antarctic Intermediate Water [AAIW], Circumpolar Deep Water [CDW] and Antarctic Bottom Water [AABW]) with the North Atlantic Deep Water (NADW), originating from the northern hemisphere (Fig. 4.1; Carter and Cortese, 2009; Georgi, 1981; Piola and Matano, 2001; Reid et al., 1977; Saunders and King, 1995). South of the BMC, the intermediate ocean circulation is conditioned by the northward flowing AAIW, located in 500-1200 m water depth (Figs. 4.1 and 4.2), and CDW, which flows in two fractions: the Upper-CDW (UCDW) and the Lower-CDW (LCDW; Arhan et al., 2002; Arhan et al., 2003; Piola, 2006; Reid et al., 1977). Within and north of the BMC, NADW, which flows southward in 2000-3000 m water depth (Figs. 4.1 and 4.2), separates vertically the two CDW fractions. This intercalation of water masses results in large vertical density gradients at their interfaces, which as a consequence are vertically displaced by eddies (Arhan et al., 2002, 2003; Piola and Matano, 2001). In water depths greater than 3500 to 4000 m the ocean regime is dominated by the presence of AABW, which circulates in an up to 2000 m thick basinwide cyclonic gyre (Arhan et al., 2002, 2003; Carter and Cortese, 2009; Hernández-Molina et al., 2009; Piola and Matano, 2001).



The overall circulation pattern of the northern Argentine margin may play a significant role in sedimentary processes within the Argentine basin and in particular within our study area (Arhan et al., 2002, 2003; Flood and Shor, 1988; Hernández-Molina et al., 2009).

#### **4.2.2 Physiographic and geological context**

With a continental slope of ~1500 km length and 50-300 km width the Argentine continental margin represents one of the world's most extended margins (Ewing and Lonardi, 1971). As part of the passive volcanic rifted continental margin of South America, it was formed during the opening of the South Atlantic (Ramos, 1999). Off Argentina, the margin is subdivided into four major segments each separated by a major transfer zone (Franke et al., 2007; Hinz et al., 1999). The study area is located in the transition between Segment III and IV, which is marked by the Salado Transfer Zone (STZ; Fig. 4.1).

Next to studies dealing with deeply located tectonic structures, the Argentine margin was in the focus of several local and regional studies revealing possible links between post-Cretaceous slope architecture and the oceanographic regime (e.g.: Bozzano et al., 2011; Gruetzner et al., 2011; Henkel et al., 2011; Hernández-Molina et al., 2009, 2010; Krastel et al., 2011; Violante et al., 2010; Preu et al. chapters 2 and 3). Latest since the Late Pliocene/Early Miocene the Argentine margin is under the influence of strong bottom currents. While the southern portion is mainly controlled by alongslope sediment transport processes, northward the influence of gravity-driven particle transport increases (Hernández-Molina et al., 2009; Violante et al., 2010).

A major contourite depositional system (CDS) shapes the continental slope in the study area located off the Rio de la Plata (Fig. 4.1). Typical for this kind of system is that it encompasses a variety of physiographic features, which are the result of both erosional and depositional processes. As shown by Preu et al. (chapter 3), slope morphology in the study area predominantly reveals current controlled features, in particular three major contourite terraces: The La Plata Terrace (T1, 500-600 m), the Ewing Terrace (T2, 1100-1400 m), and the Necochea Terrace (T4, 3500 m; Hernández-Molina et al., submitted; Preu et al., chapter 3). These terraces are located close to the interfaces of the water masses, which are part of the complex oceanographic setting described above (Hernández-Molina et al., 2009) Preu et al., chapters 2 and 3). A fourth terrace, the so-called T3, located between the Ewing Terrace and the Necochea Terrace in water depths of ~2900m, was briefly described by (Hernández-Molina et al., submitted). However, its margin wide appearance and link to the NADW/LCDW interface has not yet been confirmed.

Sediment deposition in the study area is restricted to the terraces. Due to their influence on bottom current conditions, they result in a tabular flow pattern necessary to allow for sedimentation in this highly dynamic oceanographic setting. Especially, along the Ewing Terrace in ~1200 m water depth large-scale plastered drift sequences were identified (Figs. 4.1 and 4.2; Preu et al, chapters 2 and 3). They form with their convex-up shape an elongated crest as part of the sedimentary deposit, oriented

towards the northeast, which distinguishes from the normal terrace shape by their positive relief (Bozzano et al., 2011; Violante et al., 2010; Preu et al., chapters 2 and 3). These are associated with a contour parallel channel running along the middle slope/terrace transition (Preu et al., chapter 3), likely linked to helical flow patterns.

Located within the CDS three submarine canyon structures are incised deeply into the continental slope (from north to south): the Querandi Canyon, the Mar del Plata Canyon and the Punta Mogotes Canyon (Krastel et al., 2011; Preu et al., chapter 3). While both the Querandi and the Punta Mogotes canyon are small-scale features and quite narrow, the Mar del Plata canyon with its 130 km length and ~15 km width forms a major physiographic irregularity within the CDS (Krastel et al., 2011). Located ~15 km northeast of the STZ (Fig. 4.1), the Mar del Plata Canyon marks a major change in the overall slope morphology due to a distinct widening of the Ewing Terrace and narrowing of the middle slope in the northern part of the study area. The canyon head is located in water depths close to 1000 m and the canyon exits in ~4000 m water depth (Fig. 4.2). Overall, the thalweg is characterized by a low sinuosity. Based on high-resolution multichannel seismic data, a connection of the Mar del Plata canyon to the Argentine shelf and therefore, a relationship to a river-derived sediment flux from the Rio de la Plata can be excluded (Fig. 4.2; Krastel et al., 2011).

### **4.3 Methods**

A variety of seismic and acoustic data sets were collected during R/V Meteor Cruises M49/2 (2001) and M78/3 (2009) with a main focus on the acquisition of high resolution multichannel seismic (MCS) data (Fig. 4.2). In 2001 the data were recorded using the GeoB high resolution MCS system, which includes a 96-channel 600 m long analog streamer. In contrast, during R/V Meteor Cruise M78/3 seismic data were acquired using the high-resolution MCS system of the IFM-GEOMAR including a digital streamer of 200 m, which incorporates 128 channels. As seismic sources served several GI-guns of various chamber volumes, which cover a frequency range of 100-800 Hz. Overall, more than 1500 km of MCS data were collected during both cruises. The high-resolution MCS data were processed with the software package 'VISTA Seismic Processing' (GEDCO) following standard procedures including common midpoint binning and sorting, stacking, bandpass filtering, correction of residual statics and time migration.

Seismostratigraphic interpretation in this study is based on previous work published by Ewing and Lonardi (1971), Hernández-Molina et al. (2010; 2009), Violante et al. (2010) and Gruetzner et al. (2011). The stratigraphic information was lately summarized as well and applied to the sedimentary sequences of the northern Argentine margin by Preu et al. (chapter 2).

Isopach maps are given in meters based on a time-to-depth conversion of the MCS data using a constant velocity of 1500 m/s.

Next to the acquisition of MCS swath bathymetry data were collected during both R/V Meteor cruises. In an integrated approach, MCS and multibeam data were interpreted jointly using the software package 'The Kingdom Software 8.6' (SMT).

#### 4.4 Slope architecture and its lateral variability

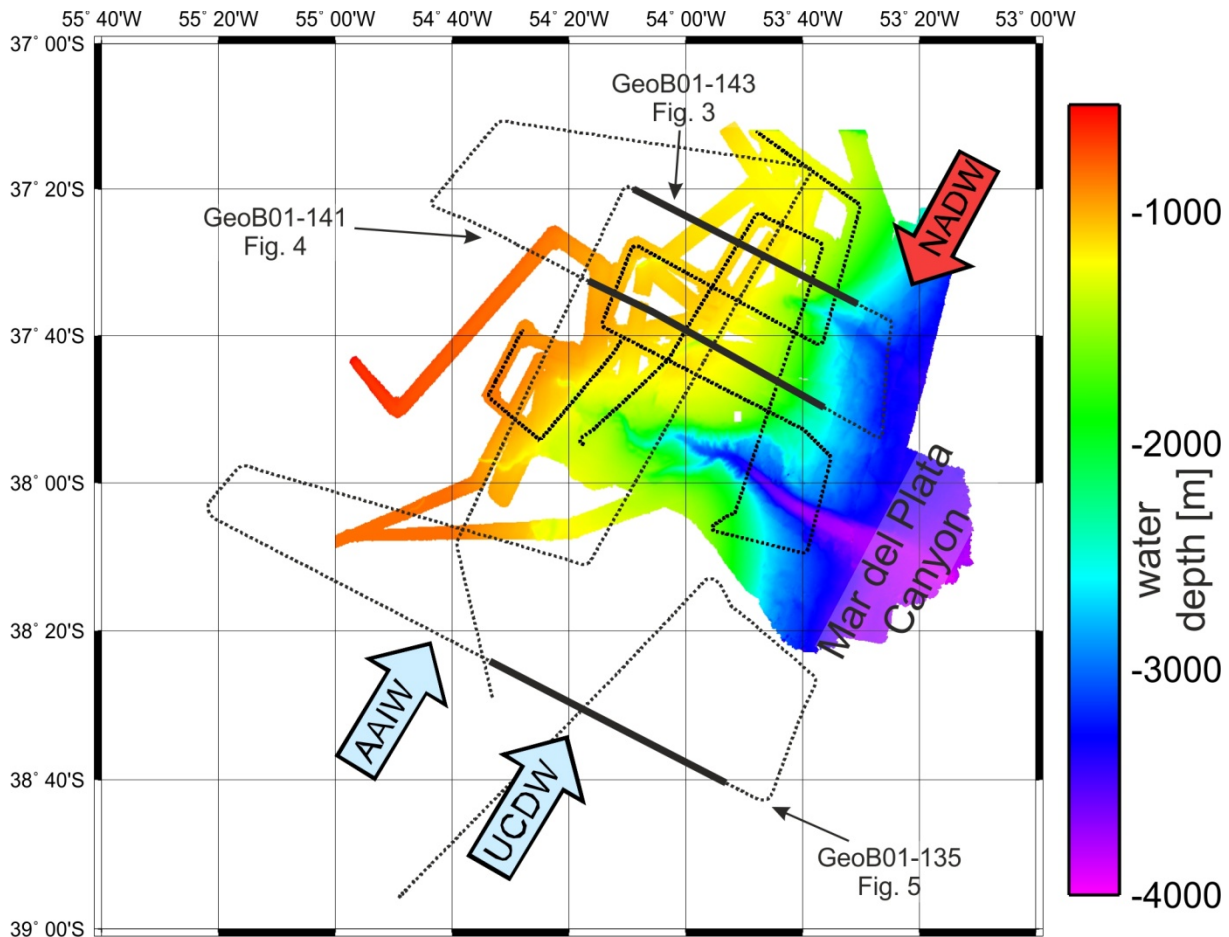


**Figure 4.2:** Bathymetric map of the Mar del Plata Canyon and the surrounding contourite depositional system based on multi-beam data recorded during R/V Meteor Cruise M78/3; arrows indicate the regional current regime; AAIW – Antarctic Intermediate Water; UCDW – Upper Circumpolar Deep Water; NADW – North Atlantic Deep Water; dotted lines indicate location of multichannel seismic data recorded during R/V Meteor Cruises M49/2 and M78/3; black lines indicate seismic sections shown in Figs. 4.3-4.5; position of study area marked in Fig. 4.1

Seismostratigraphic analysis of the subsurface of the Ewing terrace revealed four major seismic units. Based on previous interpretation of seismo-acoustic data sets presented by Preu et al. (chapter 2) the seismic units have been named the Oblique Unit, the Complex Unit, the Sigmoidal Unit and the Aggradational Unit (Figs. 4.3-4.5). These seismic units are bounded by major regional structural discontinuities within the sedimentary sequence of the Ewing terrace. From bottom to top they are named AR4, OUS, AR5 and H2.

At the landward termination of the Ewing terrace the 300 ms TWT thick Oblique Unit is located ~1000 ms TWT beneath the terrace. Clearly to identify by the onlap of seismic reflections, the lower boundary of the Oblique Unit is represented by the AR4 horizon (purple line in Figs. 4.3-4.5), marking the Eocene/Oligocene boundary. The upper termination of the Oblique Unit is given by the sigmoidal

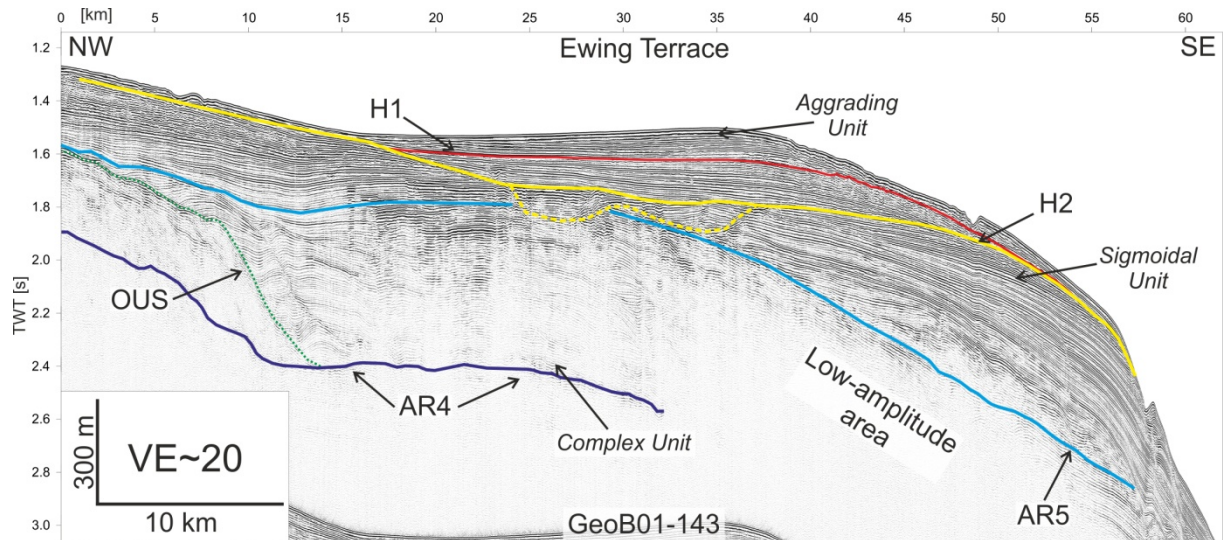


**Figure 4.3:** Section of multichannel seismic Line GeoB01-143; location of profile indicated in Fig. 4.2; VE ~20

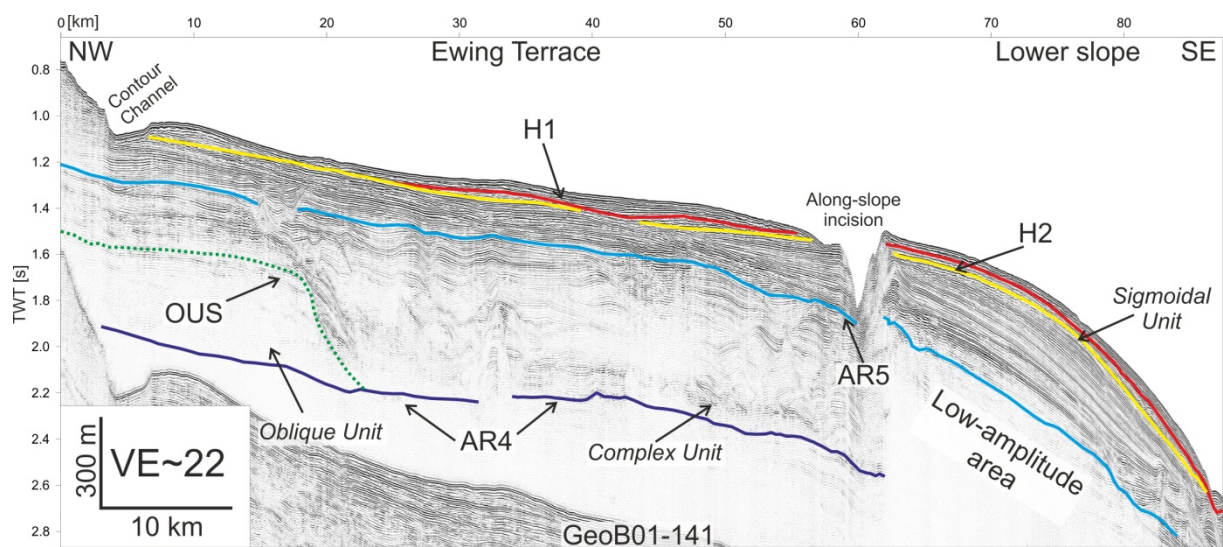


**Figure 4.4:** Section of multichannel seismic Line GeoB01-141; location of profile indicated in Fig. 4.2; VE ~22

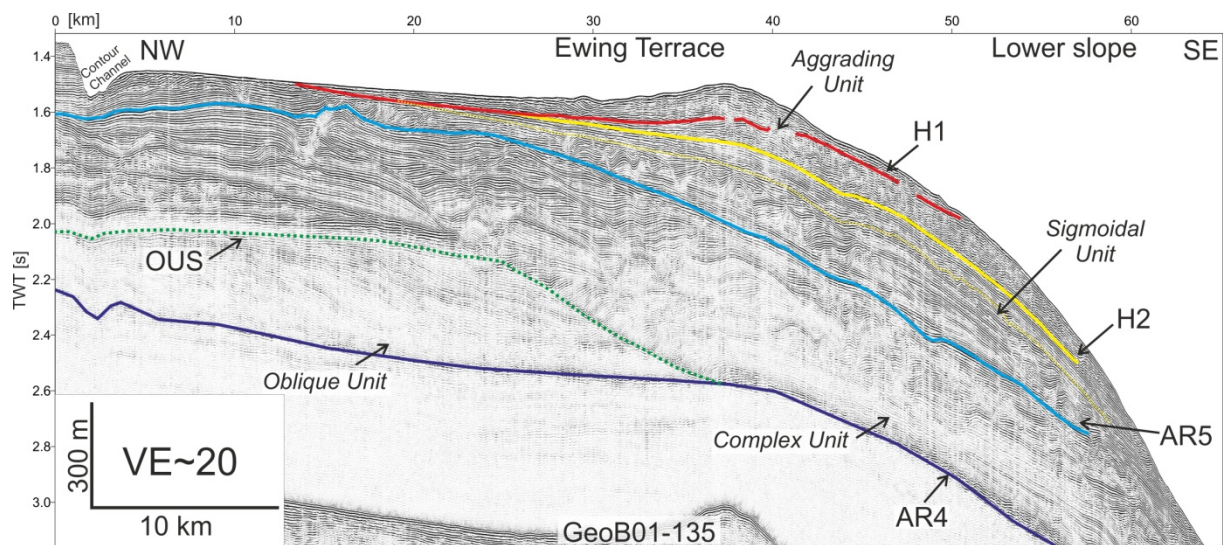


**Figure 4.5:** Section of multichannel seismic Line GeoB01-135; location of profile indicated in Fig. 4.2; VE ~20

OUS horizon (green line in Figs. 4.3- 4.5), which was suggested to be of late Oligocene age by Preu et al. (chapter 2). Seismic facies of the Oblique Unit shows an oblique-sigmoidal reflection stacking pattern forming clinofolds, which results in the bank-like morphology.

The Complex Unit (Figs. 4.3 and 4.5), which has an average thickness of ~600 ms TWT, is located ~1000 ms TWT beneath the modern seafloor of the Ewing terrace seaward of the Oblique Unit. The unit is bounded at the base by the regional horizons AR4 and OUS (Figs. 4.3-4.5) being either of Eocene/Oligocene boundary (AR4) or of Late Oligocene (OUS) age. The AR5 horizon (blue line in Figs. 4.3-4.5) marks the upper boundary, probably of Middle Miocene age (~16 Ma). The overall change from a parallel, layered reflection pattern to a wavy layered seismic facies at the base of the Complex Unit allows a clear identification of the AR4 horizon in most parts of the study area. In contrast, at the seaward and landward termination of the Ewing terrace this structural change in the seismic facies associated to the AR4 horizon cannot be clearly determined due to enhanced signal attenuation (Fig. 4.4). Overall, the Complex Unit is characterized by low amplitude reflections forming a complex wavy stacking pattern.

Combined, both units, the Oblique and the Aggradational Unit, reveal a more or less uniform sediment thickness over the total study area (Fig. 4.6a). While the Oblique Unit is only located on the landward boundary of the Ewing Terrace, the Aggradational Unit shows a distinct depocenter seaward balancing the morphological high of the Oblique Unit (Figs. 4.3-4.5).

The transition from the Complex Unit to the Sigmoidal Unit is given by the regional AR5 discontinuity, marking the middle Miocene and representing an onlap surface for reflections of the Sigmoidal Unit. The H2 horizon (yellow line in Figs. 4.3-4.5), which is of Late Miocene age, terminates the Sigmoidal Unit on its upper boundary, truncating reflections seaward.

Associated with the Sigmoidal Unit, which shows a maximum thickness of 600 ms TWT, a major change in the sedimentary stacking pattern occurs (Fig. 4.3-4.5). The small-scale wavy and low-amplitude reflections of the Complex Unit are followed by a large-scale sigmoidal convex-up shaped reflection pattern with a high amplitude seismo-acoustic facies, typical for plastered drift sequences. Through time the sigmoidal reflection character becomes more pronounced, while the average slope angle of reflections decreases (Fig. 4.5).

Besides the change in seismic facies, the Sigmoidal Unit differs from previous sedimentation by the formation of a distinct depocenter at its seaward boundary (Fig. 4.6b). This northeastward oriented elongated depocenter shows an almost four times higher sediment thickness than deposits beneath the modern center of the Ewing Terrace leading to a widening of the terrace-like shape defined by AR5 (Figs. 4.3 and 4.6b).

On top of the H2 horizon, which truncates the uppermost reflections of the Sigmoidal Unit, the Aggradational Unit is located, bounded above by the seafloor (Fig. 4.3-4.5). The Aggradational Unit with its 300 ms TWT thickness marks another significant change in the sedimentary pattern from a partly prograding to an aggradational reflection stacking pattern showing similar high amplitudes as

the Sigmoidal Unit (Figs. 4.3 and 4.5). The depositional character of the Aggradational Unit slightly changes in its center at the H1 horizon (red line in Figs. 4.3-4.5), which marks the Late Pliocene. On top of the H1 horizon a positive relief is formed at the seaward limit of the Ewing terrace as a result of a convex-up stacking pattern, representing the crest of the plastered drift sequences deposited within the Aggradational Unit. The crest has a height between 50-100 ms TWT above the surrounding terrace (Figs. 4.3 and 4.5)

In general, in transition to the Aggradational Unit the depocenter center is shifted upslope compared to the Sigmoidal Unit (compare Figs. 4.6b-d). While beneath the H2 horizon the aggradational character of the seismic unit can be clearly identified by locally increased sedimentation (Fig. 4.6c), a new elongated depocenter is formed since the Late Pliocene, which represents the modern drift crest (Fig. 4.6d). However, besides the upslope shift of the depocenter, as well alongslope changes occurred in the sedimentary pattern. From the Eocene/Oligocene boundary, marked by the AR4 horizon, to the Middle/Late Miocene transition, represented by the H2 reflection, the sediment accumulation reached until the modern axis of the Mar del Plata Canyon (Figs. 4.6a and b). Since the Late Miocene the area directly north of the canyon represents an area close to non-deposition (Figs. 4.6c and d).

#### **4.5 Oceanographic implications**

Marking the opening of the Drake Passage and its associated global cooling (Lagabrielle et al., 2009; Zachos et al., 2001), the AR4 horizon represents the change in the South Atlantic from a sluggish surface and deep water circulation to a highly dynamic oceanographic regime. This setting is dominated not only by fast flowing surface currents, but as well by bottom currents shaping the morphology of the Argentine continental margin (Gruetzner et al., 2011; Hernández-Molina et al., 2009, 2010; Preu et al., chapter 2). While the Oblique Unit with its clinoform-like structures (Figs. 4.3-4.5) was probably formed under shallow water conditions, the Complex Unit was influenced by intermediate water as indicated by the small scale wavy seismic facies. The difference between both major seismic units is therefore more controlled by margin subsidence and sea-level variations than by changes within the global oceanographic regime (Preu et al.; chapter 2). This is indeed indicated by the more or less uniform thickness of sediments deposited from the Early Oligocene until the Middle Miocene, which includes both the Oblique Unit and the Complex Unit (Fig. 4.6a). The sedimentary style suggests over the study area a uniform flow pattern of the Southern Sourced Intermediate Water (SSIW), in recent times known as AAIW, which was the shaping bottom current in this part of the margin during the Early Miocene (Preu et al., chapter 2).

During the middle Miocene with the formation of the Sigmoidal Unit a distinct NE elongated depocenter was formed (Fig. 4.6b). With estimated accumulation rates of ~10 cm/kyr in the depocenter, it clearly differs from the sedimentary pattern imaged further upslope showing ~5 times smaller values. The elongated depocenter, typical for contourites (Faugères et al., 1999; Faugères and Stow, 2008), was formed during the middle Miocene beneath the upslope migrating interface between

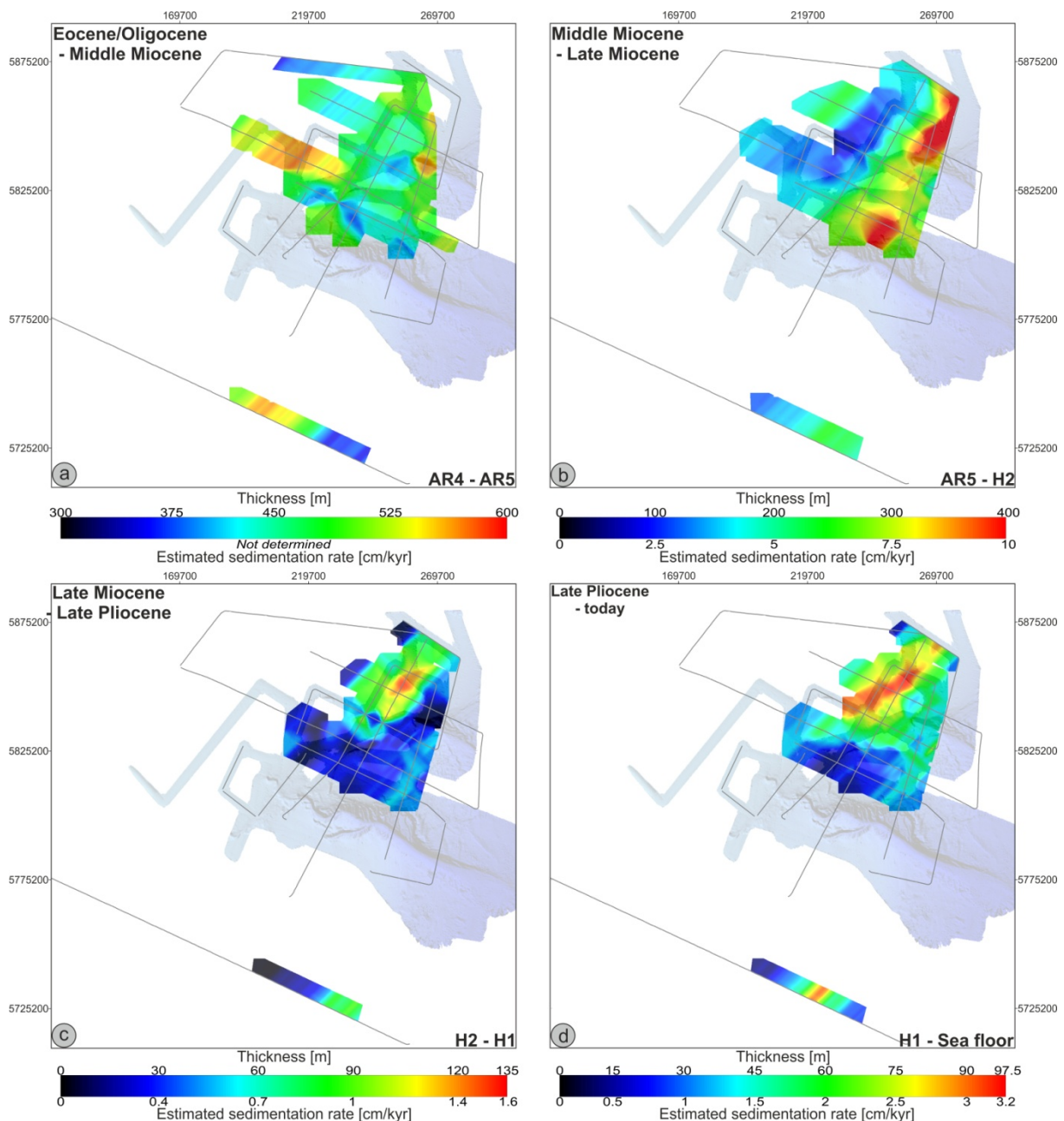


**Figure 4.6:** Isopach map of seismic units of northern Argentina; only seismic lines crossing the Ewing Terrace are considered; time-depth conversion was calculated based on a constant sound velocity of 1500 m/s; a) sediment thickness between the AR4 and AR5 horizon (Eocene/Oligocene boundary – Middle Miocene); b) sediment thickness between the AR5 and H2 horizon (Middle Miocene – Late Miocene); c) sediment thickness between the H2 and H1 horizon (Late Miocene – Late Pliocene); d) sediment thickness between the H1 horizon and the seafloor (Late Pliocene – today)

the SSIW and the Upper Southern Sourced Deep Water (USSDW), which is in modern times represented by the UCDW (Preu et al, chapter 2).

The upslope shift of the SSIW/USSDW interface and the depocenter during the Middle Miocene is linked to a major reorganization of the oceanographic regime triggered by the onset of massive deep water production in the North Atlantic. Although the overall onset of northern sourced deep water is heavily discussed at the moment, the submergence of the Faeroe-Iceland-Greenland ridge clearly has increased deep water production in the North Atlantic (Knutz, 2008; Vogt, 1972). This had a major impact on the ocean stratification in the South Atlantic as well (Kennett, 1982). Corresponding to the

vertical shift of Antarctic Water mass boundaries during this time, the depocenter shifted upslope, as well, following the low energetic flow conditions of the USSDW (Preu et al., chapter 2).

As the estimated sedimentation rates of  $\sim 1\text{-}1.6$  cm/kyr and the position of the local depocenter suggest (Fig. 4.6c), during the Late Miocene the depositional environment was limited due to high energetic current conditions and only depressions, which were the result of the sigmoidal stacking pattern of the underlying unit, were leveled by locally increased deposition. Major sediment deposition was prohibited by the SSIW/USSDW interface, which slowly shifted upward since the Late Miocene due to the successive closure of the Central American Seaway (Hermann, 1990; Newkirk and Martin, 2009; Preu et al., chapter 3).

After northern sourced deep water production was fully established with the final closure of the Central American Seaway (Burton et al., 1997; Nisancioglu et al., 2003), a new elongated depocenter was formed oriented to the NE showing sedimentation rates of  $\sim 3$  cm/kyr in its center (Fig. 4.6d). Since then, sedimentation in the study area is mainly controlled by variations in ocean stratification associated with glacial/interglacial cycles, leading to an upslope shift of the SSIW/USSDW interface during cold periods (Preu et al., chapter 2).

#### **4.6 Implications of material transport influenced by the Mar del Plata Canyon**

The Mar del Plata canyon has no modern connection to the Rio de la Plata River. The existence of a former, older connection to this major river system can be excluded, as well, based on high-resolution seismic data (Krastel et al., 2011). The additional absence of smaller gullies and channels, in which material could be transported in larger amounts off the shelf, excludes the Rio de la Plata and the northern Argentine shelf as a major sediment source for the Mar del Plata canyon and the margin segment as a whole (Krastel et al., 2011; Preu et al., chapter 3).

Two different processes, the upslope-erosion and the downslope-erosion model (Pratson et al., 1994; Twichell and Roberts, 1982), were discussed during the last decades explaining the presence of canyons detached from major river systems. While the upslope model assumes local slope failures as possible trigger, which successively cut back the canyon head, the downslope-erosion model requires buried, pre-existing erosional channels, which are episodically re-eroded by downslope sediment transport.

Both evolution schemes describe a pure feeding of the canyon by downslope processes and sediment supply sourced upslope from the shelf. However, slope parallel processes controlling drift deposition may present another possible sediment source for the Mar del Plata Canyon, which represents a natural obstacle for topography-guided contour currents (Zenk, 2008). The cyclic vertical migration of the SSIW/USSDW interface (Preu et al., chapter 2) and the low to moderate tabular current conditions enforced by the Ewing terrace morphology (McCave et al., 1982; Preu et al., chapter 3) should provide an areawide uniform forcing which controls plastered drift formation. Instead, the lack of sedimentation (Figs. 4.6c and d) and the missing drift crest north of the Mar del Plata Canyon (Fig.



4.4) indicate a major disturbance in the sedimentary regime.

This sedimentary pattern can be explained by assuming that northward flowing bottom currents, transporting sediments along the Ewing Terrace, are disturbed by the presence of the canyon. Once the bottom current reaches the canyon, it loses its topographic constraint within the ~1.5 km deep and 20 km wide Mar del Plata Canyon, which results in a drop of flow velocity and transport capacity. Consequently, the suspended sediment load associated with the AAIW (Preu et al.; chapter 2) would be released into the canyon and would not be available for plastered drift formation directly north of the canyon. The presence of another plastered drift further north (Fig. 4.3 and 4.6d) at some distance from the canyon indicates a reestablishment of the bottom current conditions.

This interpretation is in agreement with previous work regarding the interaction of alongslope and downslope processes, which indeed documented that bottom currents are significantly influenced by large topographic incisions (e.g.:Faugeres et al., 1999; Marchès, 2008; Marchès et al., 2010; Mulder et al., 2006, 2008; Salles et al., 2010; Zenk, 2008). Especially, in the northern Gulf of Cadíz detailed studies were conducted in close proximity to the Portimao Canyon. This system is characterized by trapping of the bottom current within the structure, which flows thereafter along the canyon axis (Marchès, 2008; Mulder et al., 2008). Furthermore, this down-welling leads to erosion on the downstream flank of the canyon and results in a slow migration of the canyon (Marchès, 2008).

Both mechanisms cannot be identified at the Mar del Plata Canyon due to massive differences in spatial dimensions. Since the Mar del Plata Canyon is ~10 times wider and ~15 times deeper than its northern hemisphere counterpart (c.f. Mulder et al., 2008), the decrease in flow velocity and loss of transported material are more pronounced across the canyon axis resulting in lower erosive forces at the down-stream located flank and therefore, no thalweg migration. Furthermore, the AAIW, which forms the bottom current, cannot be deeply down-welled into the canyon due to the local water mass stratification. However, the loss of topographic constraint above the canyon probably leads to minor downwelling phenomena along the AAIW/UCDW interface, which further decreases flow velocities and increases the amount of dropped material.

The above described difference in spatial dimensions is as well reflected in the sedimentary pattern of both systems. While sedimentation downstream of the Portimao Canyon in the Gulf of Cadíz is only depleted in coarse material (Marchès, 2008; Mulder et al., 2008), more or less no sediment is deposited north of the Mar del Plata Canyon (Figs.4.4 and 4.6d). Accordingly, we propose that the Mar del Plata Canyon is mainly fed by alongslope processes, which control the surrounding CDS. The canyon pirates material transported within the above flowing bottom currents, which are disrupted by the major change in physiography. In turn, this leads to a major lack in sedimentation down-stream within the CDS.

#### **4.7 Genesis and evolution of the Mar del Plata canyon**

Since the Late Miocene sedimentation on the northern flank of the Mar del Plata canyon significantly weakens compared to earlier times (Figs. 4.6c and d), where this area does not distinguish from the surrounding sedimentary pattern (Figs. 4.6a and b). Progressing through time, this part of the margin is characterized by close to non-depositional conditions, while major depocenters were formed northward in the same water depth with accumulation rates of  $\sim 3$  cm/kyr (Figs. 4.3, 4.6c and d). Due to the above described impact of the Mar del Plata Canyon on sedimentary processes in recent times, the absence of sediments on the northern canyon flank may reveal the origin of the canyon. We can conclude that since Late Miocene times the Mar del Plata Canyon likely dominates locally the sedimentary regime.

The Mar del Plata Canyon is located directly north of the Salado Transfer Zone (STZ) separating two major South American tectonic segments: III and IV (Fig. 4.1; Franke et al., 2007; Hinz et al., 1999). Associated to the STZ and the general South American tectonic regime, a period of strongly enhanced subsidence was described for the Middle Miocene (Aceñolaza, 2000; Kennett, 1982; Potter and Szatmari, 2009). The impact of this tectonically active time on sedimentary structures in particular in the northern study area is reflected by a varying inclination of reflections within the Sigmoidal Unit through time and has been described in detail by Preu et al. (chapter 2).

During this time period the Mar del Plata formed under the influence along the STZ, which defines the border between margin segments of different subsidence history. This hypothesis is supported by the presence of gas indicated by strong acoustic signal attenuation beneath the Sigmoidal Unit north of the canyon (Fig. 4.4). Since this signal anomaly can only be observed close to the Mar del Plata Canyon, gas from deeper sources probably migrates along minor fault zones upward until it reaches the plastered drift sequences of the Sigmoidal Unit.

A slow subsidence would, of course, not directly result in the genesis of a canyon, but may have created weak zones within the sedimentary column. The sediments may have started to fail as a result of the additional loading due to horizontally uneven sedimentation and non-uniform pore pressure distribution within the plastered drift, which was deposited during the Middle Miocene in the study area (Laberg and Camerlenghi, 2008). Afterwards, due to upslope erosion, the canyon head migrated landward due to successive back-cutting triggered by episodic sediment failures. While during the Middle Miocene the canyon did probably not reach a width to control the sedimentary pattern in the study area (Figs. 4.6a and b), latest since the Late Miocene the local current regime is disturbed (Figs. 4.6c and d).

Therefore, based on the sedimentary pattern we propose that the genesis of the Mar del Plata Canyon is associated to the Salado Transfer Zone and evolved during the Middle Miocene as a consequence of tectonic activity followed by continuous sediment failure. Since then the Mar del Plata canyon disturbs the local flow pattern, decreases the bottom water sediment transport capacity and catches the

sediments drop out of the water column, leading to a deficit of sediment supply north of the canyon since Late Miocene times.

#### **4.8 Conclusions**

Analysis of sedimentary sequences in time and space revealed major vertical and lateral depocenter shifts along the northern Argentine margin. Based on established regional stratigraphy vertical changes in the sediment distribution were linked to different stages in the development of the oceanographic regime. Coeval with the opening of the Drake Passage, unfocused and areawide uniform sedimentation marks the onset of the Malvinas Current and its associated northward flowing water masses during the Oligocene and the Early Miocene as a result of global cooling. Indicated by the formation of plastered drift sequences and the related elongated depocenter in the Middle Miocene, Northern Sourced Deep Water (NSDW) production had started or had at least significantly increased. Due to strengthening of NSDW as a result of the successive closure of the Central American Seaway an upslope depocenter shift occurred in the early Miocene. Since the final closure of this major ocean gateway the recent oceanographic regime was established and a new elongated depocenter representing a plastered drift is formed.

This particular modern depocenter is missing on the northern flank of the Mar del Plata Canyon, which is the result of a decrease in flow velocity and sediment transport capacity of bottom currents across the Mar del Plata Canyon. As the Mar del Plata Canyon disturbs the regional current pattern and pirates sediments from alongslope processes controlling the surrounding contourite depositional system. Tracing this distinct signature within the sedimentary deposits through time indicates that the Mar del Plata Canyon interacts with the current regime at least since the Late Miocene and was probably created during the Middle Miocene as a result of non-uniform subsidence and local sediment failure.

#### **Acknowledgements**

The study was funded through through DFG-Research Center / Cluster of Excellence „The Ocean in the Earth System“ and was supported by the Bremen International Graduate School for Marine Sciences (GLOMAR) that is funded by the German Research Foundation (DFG) within the frame of the Excellence Initiative by the German federal and state governments to promote science and research at German universities. The study is related to the CONTOURIBER project (CTM 2008-06399-C04/MAR).

The presented seismic data was interpreted and visualized using the commercial software package ‘The Kingdom Software’ (SMT).

We like to thank Captain Kull, Captain Baschek and the crew of R/V Meteor cruises M49/2 and M78/3 for their excellent work and support.

## **5. The impact of lee eddies on sediment dynamics: Acoustic imaging of Nepheloid Layers within the Agulhas Current**

Benedict Preu<sup>(1)</sup>, Volkhard Spieß<sup>(1)</sup>, Tilmann Schwenk<sup>(1)</sup>, Lars Max<sup>(2)</sup>, Ralph Schneider<sup>(3)</sup>

(1) MARUM – Center for Marine Environmental Sciences and Faculty of Geosciences,  
University of Bremen, Bremen, Germany

(2) Alfred Wegener Institute for Polar and Marine Research, Bremerhaven, Germany

(3) Institute for Geosciences, Christian-Albrecht University, Kiel, Germany

To be submitted to ‚Nature Geoscience‘

Bottom currents controlling sediment transport over longer distances and time periods were for the first time described in detail in the early 60's, when (Heezen and Hollister, 1964; Heezen et al., 1966) had revealed the impact of contour currents on sediment accumulation patterns by taking photographs of sediment traction structures in the deep sea. This observation has initiated during the 80's the High Energy Benthic Boundary Layer Experiment (HEBBLE; Hollister and McCave, 1984; McCave and Hollister, 1985; Richardson et al., 1981), which demonstrated the impact of eddies on sedimentary patterns by transporting material at the seafloor and in the water column. Following these findings several studies determined the existence and the characteristics of bottom nepheloid layers (BNLs) and intermediate nepheloid layers (INLs; Anderson et al., 1983; Bacon and Rutgers van der Loeff, 1989; McCave, 1986).

Principally, these layers are the result of material remobilized by and transported within the eroding water mass away from continental slopes (McCave et al., 2009). Visualization and mapping of BNLs and INLs were carried out using predominantly the Lamont nephelometer (Thorndike, 1975) and still today, investigations are more or less restricted to optical measurements (McCave et al., 2009).

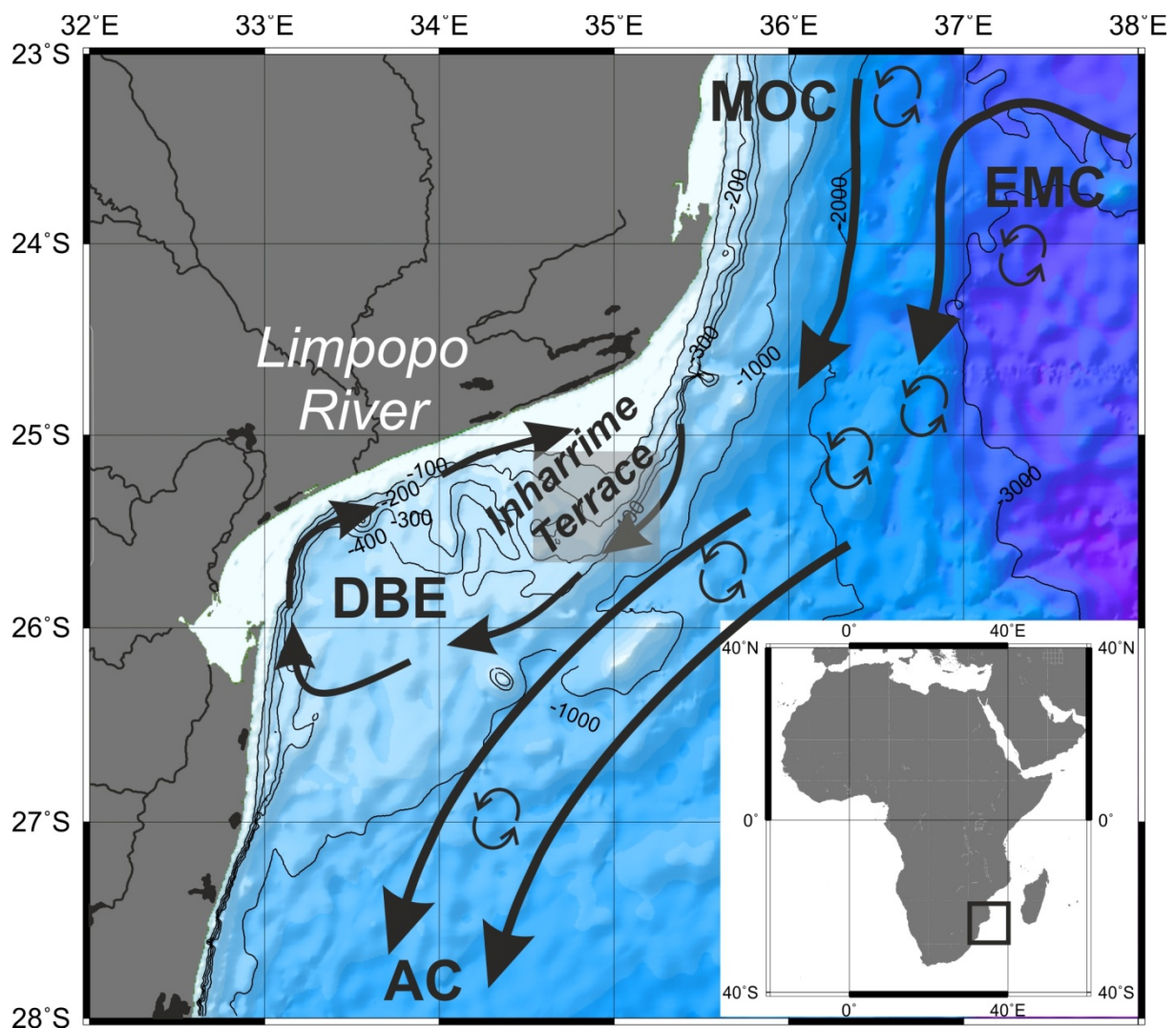


**Figure 5.1:** Map of SE Africa in the boundary region between South Africa and Mozambique; black arrows indicate main surface current directions highlighting the Mozambique Current (MOC), the East Madagascar Current (EMC), the Agulhas Current (AC) and the semi-permanent Delagoa Bight Eddy (DBE); grey box marks the study area, presented in detail in Fig. 2

Acoustic mapping of suspended particles so far was concentrated on shallow water and ultra high frequencies within the range of megahertz (e. g.: Shi et al., 1999; Thorne et al., 1993; Thorne et al., 1991), by analyzing signal attenuation and energy scattering by particles in the water column. Here we present a new approach combining Acoustic Doppler Current Profiler (ADCP) and single beam echosounder backscatter data sets (18 kHz parametric echosounder) to document active sediment transport and its mechanisms in a water depth of 0-700 m along the SE African slope (Fig. 5.1).

This area is well suited to study the highly dynamic processes of BNLs and INLs as it is located in the confluence of the Mozambique Current (MOC) and the East Madagascar Current (EMC), which merge into the Agulhas Current (AC), the second largest surface current of the modern ocean (Fig. 5.1). The AC is mainly characterized by large-scale anti-cyclonic eddies which originate in the source region of the MOC and the EMC (Lutjeharms, 2006). In addition to eddies inside the AC, at 25°S a major lee eddy system exists in front of the Limpopo River, known as the Delagoa Bight Eddy (DBE), as a result of the southward flowing currents (Lutjeharms and Da Silva, 1988). This lee eddy drives a coast parallel counter current, which transports sediment eastward along the coast (Flemming, 1981; Preu et al., 2011).

The presented Acoustic Doppler Current Profiler (ADCP) and backscatter data sets (18 kHz parametric echosounder) were acquired during R/V Meteor Cruise M75/3. For acoustic imaging of the

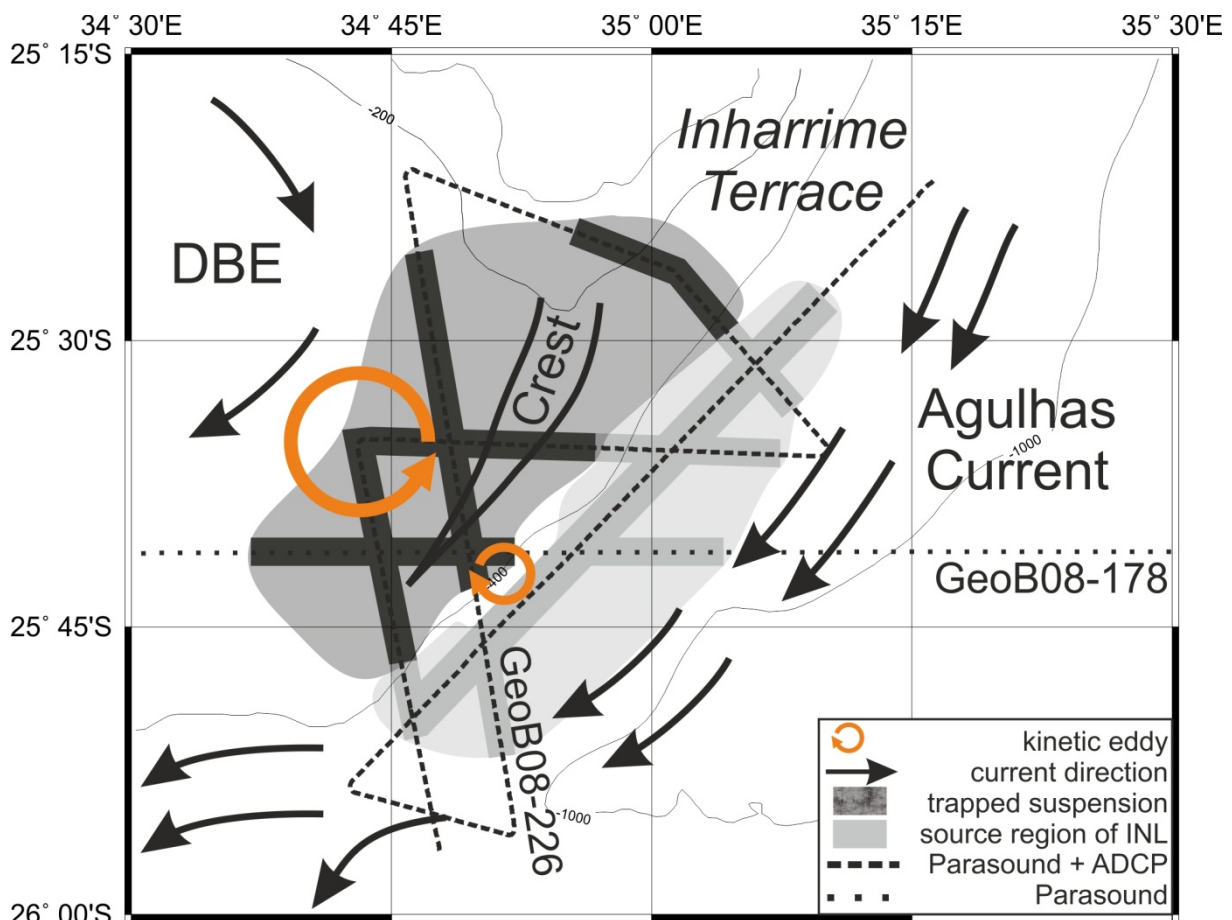


**Figure 5.2:** Close-up map of the study area; black lines mark locations of hydro-acoustic profiles; black arrows indicate the regional oceanographic regime dominated by the Agulhas Current and the Delagoa Bight Eddy (DBE); orange circles represent two eddy features including their rotation direction based on ADCP data

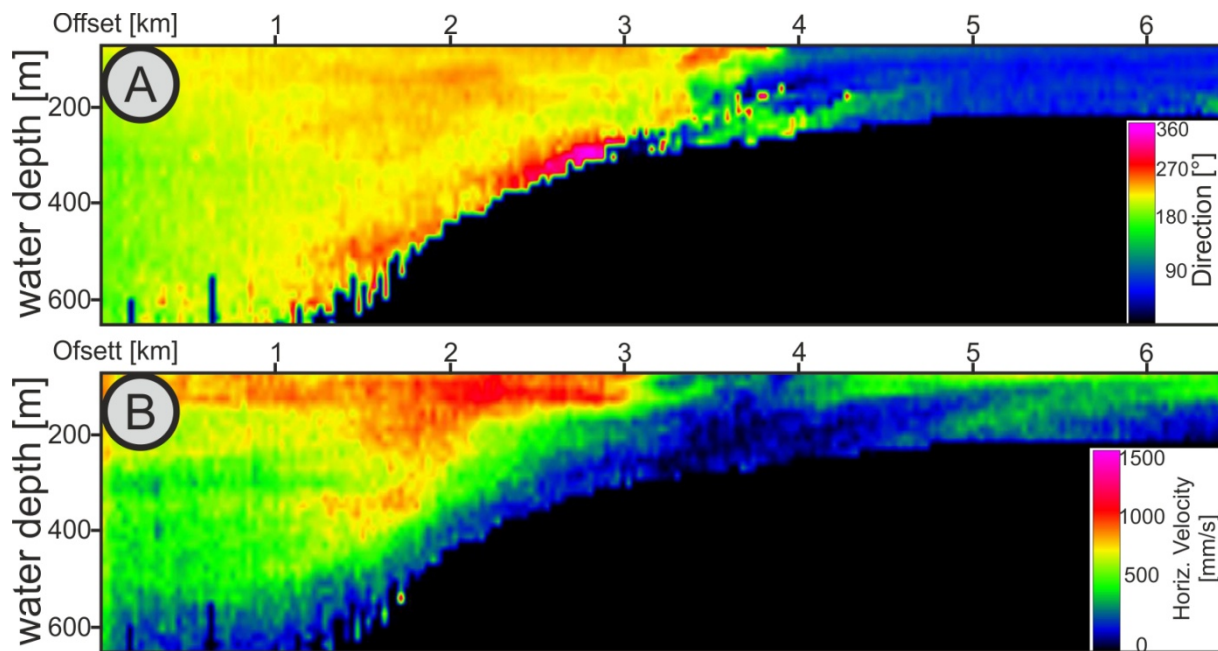


**Figure 5.3:** Collected ADCP data along profile GeoB08-226; A) estimated current direction; B) estimated horizontal current velocities; location of profile is indicated in Fig. 2

water column, the parametric echosounder ‘Parasound P70’ (Grant and Schreiber, 1990; Medwin et al., 1999) was used. Signal generation is based on the parametric effect, which occurs when very high (finite) amplitude sound waves are generated (Medwin and Clay, 1997; Spiess, 1992). In case of the the Parasound System, the Primary High Frequency (PHF) is fixed to 18 kHz, which distributes energy within a beam of  $\sim 4.5^\circ$  for a transducer of  $\sim 1$  m length. The (variable) second primary frequency was set to 22 kHz, resulting in a Secondary Low Frequency (SLF) at 4 kHz being generated and travelling within a narrow  $4.5^\circ$  beam. The PHF was used to record signals in the full water column whereas SLF data provides information about the subsurface sediment.

The Acoustic Doppler Current Profiler (ADCP, RD Instruments) was operated with a main frequency of 75 kHz, allowing measurements of current velocity and current direction versus water depth. The data were recorded with a vertical bin size set to 16 m and during the final processing the data set was averaged over 300 s, which corresponds to 750 m by a mean ship speed of 5kn.

ADCP and Parasound data were used for surveying and spatial mapping on the Inharrime Terrace (Fig. 5.2), which is a crest-like feature formed under the influence of strong bottom current forcing (Martin, 1981) as part of major contourite drift sequences (Preu et al., 2011).

As seen in Fig. 5.3B the main current direction east of the Inharrime Terrace points towards SSW in contrast to the eastward directed current in the center of the Inharrime Terrace. Spatial analysis within the transition between the flow patterns of opposite direction ADCP data revealed two small scale eddy features of  $\sim 5.5$  km diameter seaward and of  $\sim 10.5$  km landward of the crest, located within the large-scale circulation pattern of the DBE (Fig. 5.2). Fig. 5.3A indicates the current direction variability induced by the smaller eddy as a change of current direction of  $\sim 180^\circ$  between 3 and 4 km offset. Comparing current direction measurements to the horizontal current velocity (Fig. 5.3), the lowest approximated velocities are present landward of the eddy centre. Velocities significantly

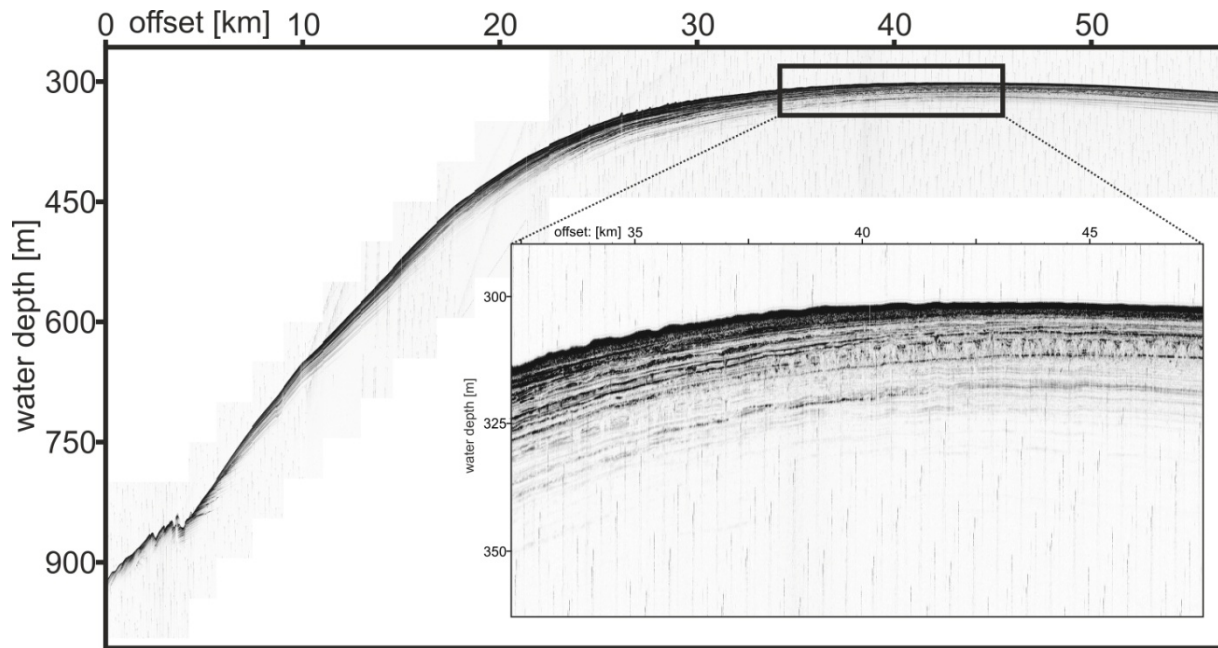


**Figure 5.4:** 4 kHz parametric echosounder data showing truncated reflections at the seafloor, in particular on the Inharrime Terrace; location of profile is indicated in Fig. 2

increase further offshore from 0.1 m/s to 1.3 m/s. From the crest towards the centre of the Inharrime Terrace, velocities increase to 0.5 m/s.

The smaller eddy on the seaward side of the crest is likely a result of the interplay between the crest morphology and the southward flowing AC (Fig. 5.2), reaching in its center 1.3 m/s. On the opposite side of the crest, the larger feature probably originates from interaction of terrace morphology and the large-scale south-eastward circulation at the Inharrime Terrace as part of the large scale DBE system. Parasound data (Figs. 5.4 and 5.5A) reveal distinct water column high backscatter anomalies and indications for surface erosion in sections, which are characterized by either low or high current velocities (Fig 5.3B). The most prominent one appears on the Inharrime Terrace directly on the landward side of the crest directly above the seafloor in conjunction with truncated reflections in the subsurface (Figs. 5.4 and 5.5).

Considering the erosion processes in this area as suggested by the SLF data (Fig. 5.4), these backscatter signals might be related to reworked fine grained material within the water column. However, it is unclear at this stage, how a suspension cloud causes higher backscatter, as the particle size/signal wavelength ratio seems insufficient, and individual particles are not expected to be imaged by the 18 kHz Parasound signal. Dense particle accumulations forming nepheloid layers, on the other hand, are likely to interact with the acoustic signal not as single particles, but rather generate volume scattering of the acoustic energy, whose spatial variation indicates changes not only in particle size but as well in particle concentration. Consequently, these backscatter signals (PHF) recorded in close proximity to both eddies suggest an interaction between eddy related kinetic energy and the particulate matter in the water column and at the seafloor, which had been documented by previous studies (e.g.: Richardson et al., 1993). Accordingly, we assume that higher backscatter areas in our data indeed



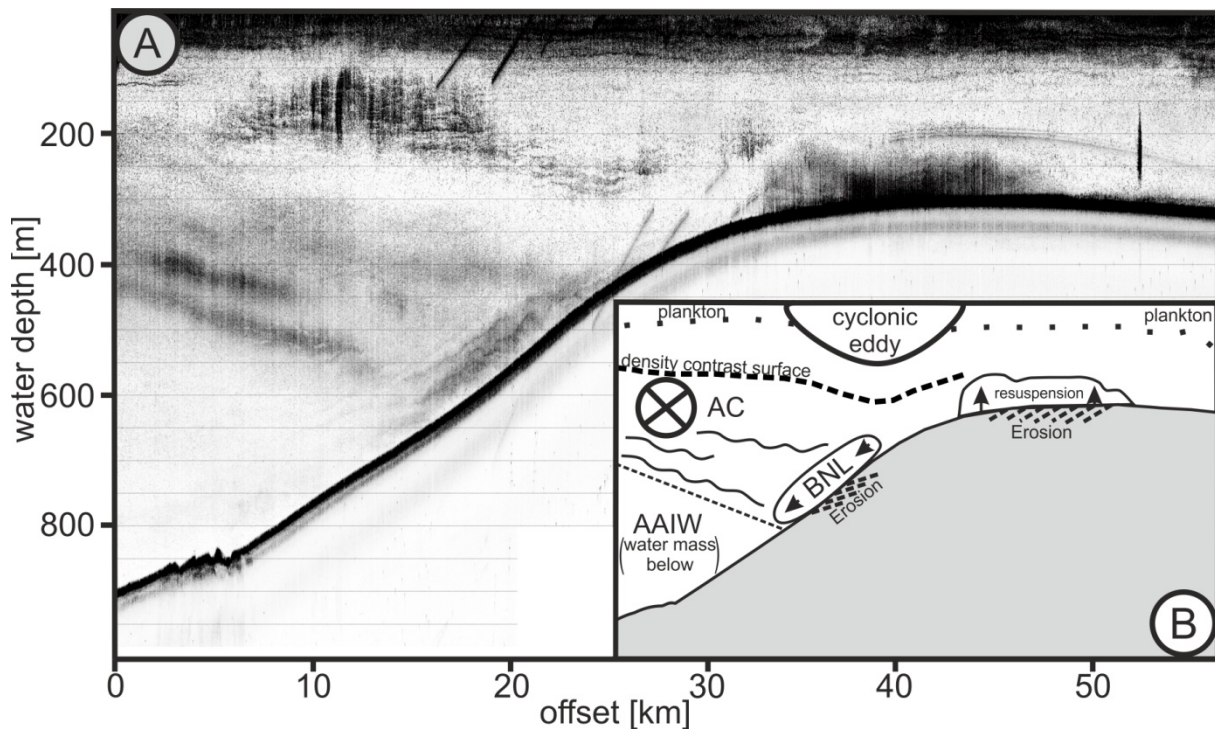


**Figure 5.5:** **A)** 18 kHz parametric echosounder data indicating backscatter anomalies within the water column; profile location is indicated in Fig. 2; **B)** Interpretation of 18 kHz profile marking schematically areas of sediment resuspension and transport in intermediate nepheloid layers (INLs) and benthic nepheloid layers (BNLs); interpretation of plankton layer in the uppermost 50 meters is based on (Medwin and Clay, 1997); location of profile indicated in Fig. 2

point to higher particle concentration in the water column, which is likely related to sediment resuspension or winnowing and active particle transport processes in this area (Fig. 5.5B).

This interpretation is also supported by the apparent current velocity field measured by ADCP, which reach velocities as low as 0.2 cm/s (Fig. 5.3B). In case of exceptionally high particle concentration, as we expect in the vicinity of the Inharrime Terrace, current velocity approximations using an 75 kHz ADCP are no longer trustworthy, since the Doppler Shift effect depends on single particles, but the suspension cloud appears as a uniform nepheloid layer without apparent movement. As a consequence, very low current velocities are measured. However, the generally high horizontal velocities on the Inharrime Terrace (0.3-0.5 m/s) measured further landward in some distance from the high energetic eddies (Fig. 5.3B) are still sufficient to transport even sandy particles (McCave, 2005). Consequently, the northwestern eddy (Fig. 5.2) concentrates winnowed and reworked material in a very small patch along the crest, which by its morphology forms a natural barrier for the E-W sediment transport. This morphology and the associated current controlled particle trap leads to a high concentration of particulate matter in the BNL, which can be imaged using ADCP and 18 kHz Parasound (Figs. 5.3 and 5.5).

A similar feature of lower magnitude (Fig. 5.5) could be identified downslope of the smaller eddy (Fig. 5.2), which suggests smaller particle sizes and/or lower particle concentrations in the water column compared to the situation on the Inharrime Terrace. The backscatter signal in this case is not restricted to the BNL, but in fact can be traced away from the slope, where schlieren-like features emerge into the water column (Fig. 5.5A). The layer appearance of the backscatter anomaly strongly

indicates the presence of INLs, which are maintained within the AC. Once in suspension, the AC, which is deflected westward by the Coriolis Force, detaches the material from the slope and keeps the matter in suspension due to its high internal velocities (Fig. 5.3). The backscatter distribution (Fig. 5.5) is the result of variations in particle density and size, since particles are forced to align along the isopycnal, determined by changes in temperature and salinity (McCave et al., 2009). The base of the INL is probably defined by the transition from the equatorial surface waters transported within the AC and the underlying subantarctic AAIW (Martin et al., 1982). The major density gradient at the interface of these water masses forms a physical barrier for sinking particles (c.f.: McCave, 1986). Along this interface even larger particles accumulate, which therefore reveal the highest backscatter amplitudes (Fig. 5.5). The water mass interface might as well be the trigger for the BNL by generating internal waves. Due to their erosive force, these energetic patterns can generate both, BNLs and INLs (Puig et al., 2004).

Beyond these observations, the INLs are not the only signals present in the water column within the AC. Directly on the crest layered acoustic backscatter anomalies indicate a strong vertical stratification within the uppermost 200 m of the Agulhas Current. While the stratification is probably related to the deep thermocline within the AC (Lutjeharms, 2006), the acoustic backscatter is likely produced by particles captured on top of this large density gradient.

The vertical stratification is lost in the center area of the smaller eddy, where the acoustic backscatter anomaly is sloping down to 280 m water depth (at 20-30 km offset in Fig. 5.5A). This spatial variation is the result of the smaller cyclonic eddy itself producing upwelling in its center. Due to the associated turbulence water mass stratification weakens and isopycnals spacing widens, which explains the deepening and weakening of the backscatter signal. These findings are in agreement with earlier studies, which have shown the impact of the AC- and DBE-induced upwelling on the sedimentary composition (Du Toit and Leith, 1974; Lutjeharms and Da Silva, 1988). However, the downward bending of the signal might be as well explained by down-welling, acting as counterforce to the upwelling in the eddy center. Whether either upwelling or downwelling prevails, might strongly depend on the seasonal or even short period variability of the system, which has been already shown in several studies using satellite and current measurements (Lutjeharms, 2006; Lutjeharms and Da Silva, 1988; Saetre and Da Silva, 1984)

In summary, our results reflect the highly dynamic oceanographic and sedimentary regime associated with the AC and DBE. Based on the integration of 18 kHz Parasound and 75 kHz ADCP data, INLs and BNLs were identified within the AC. Thereby, for the first time sediment resuspension and transport under the influence of high kinetic energy eddies could be visualized in situ using 18 kHz Parasound signals, whose amplitudes likely represent volume backscatter. Spatial variations in backscatter strength and current parameters were not only used to describe the sedimentary regime in the transition to the Inharrime Terrace but also to characterize the regional oceanographic setting, in particular two minor lee eddies. Our most significant conclusion is that massive sediment

resuspension, erosion and transport indeed occur due to the interaction of a high energetic flow pattern and the topographic framework. This might be in particular apply to the interplay between the two lee eddies located at the eastern boundary of the Inharrime Terrace and the sedimentary crest.

### **Acknowledgements**

This study is funded through 'Deutsche Forschungsgemeinschaft (DFG)'. Additionally this study is funded through DFG-Research Center / Cluster of Excellenz "The Ocean in the Earth System" at the University of Bremen and supported by the Bremen International Graduate School for Marine Sciences (GLOMAR) that is funded by the DFG within the frame of the Excellence Initiative by the German federal and state governments to promote science and research at German universities.

We would furthermore like to thank Ian Nicholas McCave for his conceptual support in this study.

## 6. Conclusions and future perspectives

This thesis presents for the first time a detailed and integrated approach to differentiate between the impact of alongslope and downslope sedimentary transport processes on slope architecture and to assess their interaction within the dynamic, high energetic oceanographic setting off northern Argentina. The research in this study followed a comprehensive approach: (1) reconstructing the oceanographic setting on geological timescales; (2) assessing the impact of the margin topography on alongslope sediment transport processes and vice versa; (3) determining the influence of a large seafloor irregularity like the Mar del Plata Canyon on alongslope sedimentary processes; (4) identifying sediment transport processes within the water column and at the seafloor.

First of all, seismic facies analysis of high-resolution multichannel seismic data revealed the presence of major drift sequences along the northern Argentine margin as part of a contourite depositional system (CDS). Based on established regional seismostratigraphy these contouritic deposits are the result of the current regime developing since Late Eocene times, which is dominated by the presence of the Brazil-Malvinas Confluence (BMC) and the associated convergence of northern and southern sourced water masses. While until the Early Miocene sedimentary processes were dominated by Antarctic water masses, the data analysis revealed that the Middle Miocene is marked by the increasing influence of Northern Sourced Deep Water (NSDW), which controls the spatial sediment distribution by vertically altering water mass stratification.

Second, based on the excellent seismic and hydroacoustic data coverage from R/V Meteor Cruises M49/2 (2001) and M78/3 (2009), which was further complemented by conventional seismic and single-beam echosounder data from Argentine and Uruguayan authorities, recent morpho-sedimentary features of the CDS were mapped in great detail. Correlation of erosive and depositional features to local hydrographic data sets allowed for the first time to link sedimentary structures to the regional ocean current regime. In particular, the existence of contourite terraces can be explained by the interplay between margin physiography and turbulent flow patterns associated with water mass interfaces and alongslope high velocity bottom currents.

Third, tracing the above described erosive and depositional signatures related to the CDS through time and space, a major lack of sedimentation was identified in a confined area north of the Mar del Plata Canyon, which is located in the center of the study area. This area of non-deposition is the result of a decrease in bottom current velocity and transport capacity across the Mar del Plata Canyon related to the loss in topographic constraint. This interaction of alongslope and downslope sediment transport processes occurs at least since Late Miocene times, which allows to allocate at least an approximate age to the time, when the canyon structure start to influence local depositional patterns.

At last, to determine the capability of bottom currents to transport the massive amounts of sediments, 18 kHz water column backscatter data were analyzed in conjunction with Acoustic Doppler Current Profiler (ADCP) measurements within the Agulhas Current, SE Africa. This novel approach revealed the impact of fast flowing bottom currents, in this case induced by small-scale lee eddies, on sediment

dynamics by eroding and resuspending off particles and the formation of nepheloid layers. This study confirmed that high energetic bottom currents in interaction with the topographic framework are indeed capable to transport the massive amounts of sediments required for the above described interplay of the Argentine CDS and the Mar del Plata Canyon.

This study provides a representative regional example for the interaction of along-slope and down-slope oriented sediment transport processes and its margin shaping character. Within the framework of a highly dynamic oceanographic setting the impact of the regional topographic framework on bottom current flow patterns is emphasized. This interplay may represent a major sediment feeding mechanism for submarine canyons, in particular for those which are not connected to rivers or shelf edges at all. While on short timescales the morphology dictates the dynamics of bottom currents, on longer timescales these dynamic flow patterns shape the ocean margin. Consequently, the existence of morphological features like terraces might represent paleoceanographic archives by itself, and the dynamics of former and recent circulation patterns can be inferred, in this case of the BMC. Overall, to study the interplay between ocean currents and the topography in greater detail a new method has been introduced using an integrated approach of 18 kHz parametric echosounder and ADCP data.

An important task for future research will be to compare the results of this thesis to continental margins, which are located in different oceanographic settings but offer a comparable physiographic configuration including contourite terraces and large incisions into the seafloor. Analysis of these systems would reveal, based on similarities and differences, the dependence of the above described interaction of alongslope and downslope processes on water mass stratification and bottom current velocity. Additionally, it would allow validating the suggested model for the evolution of contourite terraces along water mass interfaces.

Moreover, detailed mapping of small-scale structures and depocenter shifts within the sedimentary stacking pattern off the northern Argentine CDS is needed based on sediment echosounder data to study the response of this particular system during short-term climate variations. This analysis would provide new insight into the lateral migration of the BMC on glacial/interglacial cycles and would allow in particular reconstructing the associated varying impact of NSDW on along-slope sedimentary processes.

Further work is also required to improve water column imaging using an 18 kHz parametric echosounder. Linking the measured backscatter signals to particle sizes measured in situ and concentrations determined by particle camera images, optical backscatters measurements and in-situ pump samples would allow establishing quantitative analysis of the acoustic signal. This would not only offer remarkable new insight into the dynamics of large-scale marine sediment dispersal systems, but as well allow to infer plankton concentrations and their migration in the water column, which would enhance the understanding of the biological pump.

## References

- Aceñolaza, F.G., 2000. La Formación Paraná (Mioceno medio): estratigrafía, distribución regional y unidades equivalentes. In: Aceñolaza, F.G., Herbst, R. (Eds.), *El Neógeno de Argentina*. INSUGEO, Tucumán, pp. 9-27
- Allen, P., Allen, J., 1990. *Basin Analysis*. Blackwell Publishing, Malden.
- Anderson, R.F., Bacon, M.P., Brewer, P.G., 1983. Removal of <sup>230</sup>Th and <sup>231</sup>Pa at ocean margins. *Earth and Planetary Science Letters* 66, 73-90
- Antobreh, A., Krastel, S., 2007. Mauritania Slide Complex: morphology, seismic characterisation and processes of formation. *International Journal of Earth Sciences* 96 (3), 451-472. doi:10.1007/s00531-006-0112-8
- Arhan, M., Carton, X., Piola, A., Zenk, W., 2002. Deep lenses of circumpolar water in the Argentine Basin. *J. Geophys. Res.* 107 (C1), 3007. doi:10.1029/2001jc000963
- Arhan, M., Mercier, H., Park, Y.-H., 2003. On the deep water circulation of the eastern South Atlantic Ocean. *Deep Sea Research Part I: Oceanographic Research Papers* 50 (7), 889-916
- Bacon, M.P., Rutgers van der Loeff, M.M., 1989. Removal of thorium-234 by scavenging in the bottom nepheloid layer of the ocean. *Earth and Planetary Science Letters* 92 (2), 157-164
- Barker, P.A., 2001. Scotia Sea regional tectonic evolution: implications for mantle flow and palaeocirculation. *Earth-Science Reviews* 55 (1-2), 1-39. doi:10.1016/s0012-8252(01)00055-1
- Barker, P.A., Thomas, E., 2006. Potential of Scotia Sea Region for Determining the Onset and Development of the Antarctic Circumpolar Current. In: Fütterer, D.K., Damaske, D., Kleinschmidt, G., Miller, G.H., Tessensohn, F. (Eds.), *Antarctica: Contributions to global earth sciences*. Springer-Verlag, Berlin, pp. 433-440
- Barker, P.F., Filippelli, G.M., Florindo, F., Martin, E.E., Scher, H.D., 2007. Onset and role of the Antarctic Circumpolar Current. *Deep Sea Research Part II: Topical Studies in Oceanography* 54 (21-22), 2388-2398. doi:10.1016/j.dsr2.2007.07.028
- Ben-Avraham, Z., Niemi, T.M., Hartnady, C.J.H., 1994. Mid-Tertiary changes in deep ocean circulation patterns in the Natal Valley and Transkei basin, Southwest Indian Ocean. *Earth and Planetary Science Letters* 121 (3-4), 639-646
- Bisbal, G.A., 1995. The Southeast South American shelf large marine ecosystem: Evolution and components. *Marine Policy* 19 (1), 21-38. doi:10.1016/0308-597x(95)92570-w
- Bonnin, J., van Raaphorst, W., Brummer, G., van Haren, H., Malschaert, H., 2002. Intense mid-slope resuspension of particulate matter in the Faeroe–Shetland Channel: short-term deployment of near-bottom sediment traps. *Deep Sea Research Part I: Oceanographic Research Papers* 49 (8), 1485-1505. doi:10.1016/s0967-0637(02)00030-4
- Bozzano, G., Violante, R., Ceredo, M.E., 2011. Middle slope contourite deposits and associated sedimentary facies off NE Argentina. *Geo-Marine Letters* 31 (5-6), 495-507. doi:10.1007/s00367-011-0239-x
- Brackenridge, R., Stow, D.A.V., Hernández-Molina, F.J., 2011. Contourites within a deep-water sequence stratigraphic framework. *Geo-Marine Letters* 31 (5-6), 343-360. doi:10.1007/s00367-011-0256-9
- Broecker, W.S., Andree, M., Wolfli, W., Oeschger, H., Bonani, G., Kennett, J., Peteet, D., 1988. The chronology of the last Deglaciation: Implications to the cause of the Younger Dryas Event. *Paleoceanography* 3 (1), 1-19
- Broecker, W.S., Clark, E., Hajdas, I., Bonani, G., 2004. Glacial ventilation rates for the deep Pacific Ocean. *Paleoceanography* 19 (2), PA2002. doi:10.1029/2003pa000974
- Burton, K.W., Ling, H.-F., O'Nions, R.K., 1997. Closure of the Central American Isthmus and its effect on deep-water formation in the North Atlantic. *Nature* 386 (6623), 382-385
- Cacchione, D.A., Pratson, L.F., Ogston, A.S., 2002. The Shaping of Continental Slopes by Internal Tides. *Science* 296 (5568), 724-727. doi:10.1126/science.1069803
- Camp, D., Haines, W., Huber, B., 1985. *Marathon Leg 7 R/V Thomas Washington CTD/Hydrographic Data. Preliminary Report*. Lamont-Doherty Geological Observatory
- Carter, L., Cortese, G., 2009. Change in the Southern Ocean: responding to Antarctica. In: Brigham-Grette, J., Powell, R., Newman, L., Kiefer, T. (Eds.), *PAGES News: change at the Poles, a paleoscience perspective*. PAGES International Project Office, pp. 30-32

- Casey, K.S., Cornillon, P., 1999. A Comparison of Satellite and In Situ–Based Sea Surface Temperature Climatologies. *Journal of Climate* 12 (6), 1848-1863. doi:10.1175/1520-0442(1999)012<1848:acosai>2.0.co;2
- Cavallotto, J.L., Violante, R., Hernández-Molina, F.J., 2011. Geological aspects and evolution of the Patagonian continental margin. *Biological Journal of Linnean Society* 103, 346-362
- Chelton, D.B., Schlax, M.G., Witter, D.L., Richman, J.G., 1990. Geosat Altimeter Observations of the Surface Circulation of the Southern Ocean. *J. Geophys. Res.* 95(C10), 17877-17903
- Chiessi, C.M., Ulrich, S., Mulitza, S., Pätzold, J., Wefer, G., 2007. Signature of the Brazil-Malvinas Confluence (Argentine Basin) in the isotopic composition of planktonic foraminifera from surface sediments. *Marine Micropaleontology* 64 (1-2), 52-66. doi:10.1016/j.marmicro.2007.02.002
- Curry, W.B., Lohmann, G.P., 1982. Carbon isotopic changes in benthic foraminifera from the western South Atlantic: Reconstruction of glacial abyssal circulation patterns. *Quaternary Research* 18 (2), 218-235. doi:10.1016/0033-5894(82)90071-0
- de Souza, R.B., Mata, M.M., Garcia, C.A.E., Kampel, M., Oliveira, E.N., Lorenzetti, J.A., 2006. Multi-sensor satellite and in situ measurements of a warm core ocean eddy south of the Brazil–Malvinas Confluence region. *Remote Sensing of Environment* 100 (1), 52-66. doi:10.1016/j.rse.2005.09.018
- Dickson, R.R., McCave, I.N., 1986. Nepheloid layers on the continental slope west of Porcupine Bank. *Deep Sea Research Part A. Oceanographic Research Papers* 33 (6), 791-818. doi:10.1016/0198-0149(86)90089-0
- Duplessy, J.C., Shackleton, N.J., Fairbanks, R.G., Labeyrie, L., Oppo, D., Kallel, N., 1988. Deepwater source variations during the last climatic cycle and their impact on the global deepwater circulation. *Paleoceanography* 3 (3), 343-360
- Du Toit, S.R., Leith, M.J., 1974. The J(c)-1 borehole on the continental shelf near Stangar. Natal. *Trans. Geol. Soc. S. Afr.* 77, 247-252
- Dzulynski, S., Walton, E.K., 1965. *Sedimentary features of Flysch and Greywackes*. Elsevier Publishing Company, Amsterdam
- Ewing, M., Lonardi, A.G., 1971. Sediment transport and distribution in the Argentine Basin. 5. Sedimentary structure of the Argentine margin, basin, and related provinces. *Physics and Chemistry of The Earth* 8, 123-251
- Faugères, J.C., Mézerais, M.L., Stow, D.A.V., 1993. Contourite drift types and their distribution in the North and South Atlantic Ocean basins. *Sedimentary Geology* 82 (1-4), 189-203
- Faugères, J.C., Mulder, T., 2011. Contour Currents and Contourite Drifts. In: Huneke, H., Mulder, T. (Eds.), *Developments in Sedimentology*. Elsevier, Amsterdam, pp. 149-214
- Faugères, J.-C., Stow, D.A.V., 1993. Bottom-current-controlled sedimentation: a synthesis of the contourite problem. *Sedimentary Geology* 82 (1-4), 287-297
- Faugères, J.C., Stow, D.A.V., 2008. Contourite Drifts: Nature, Evolution and Controls. In: Rebesco, M., Camerlenghi, A. (Eds.), *Developments in Sedimentology*. Elsevier, pp. 257, 259-288.
- Faugeres, J.-C., Stow, D.A.V., Imbert, P., Viana, A., 1999. Seismic features diagnostic of contourite drifts. *Marine Geology* 162 (1), 1-38
- Flemming, B.W., 1981. Factors controlling shelf sediment dispersal along the southeast African continental margin. *Marine Geology* 42 (1-4), 259-277
- Flood, R.D., Shor, A.N., 1988. Mud waves in the Argentine Basin and their relationship to regional bottom circulation patterns. *Deep Sea Research Part A. Oceanographic Research Papers* 35 (6), 943-971. doi:10.1016/0198-0149(88)90070-2
- Franke, D., Neben, S., Ladage, S., Schreckenberger, B., Hinz, K., 2007. Margin segmentation and volcano-tectonic architecture along the volcanic margin off Argentina/Uruguay, South Atlantic. *Marine Geology* 244 (1-4), 46-67. doi:10.1016/j.margeo.2007.06.009
- Gao, Z.Z., Eriksson, K.A., He, Y., Luo, S.S., Guo, J.H., 1998. Deep-water traction current deposits: a study of internal tides, internal waves, contour currents and their deposits. *Science Press ; VSP, Beijing ; New York : Utrecht*
- García, M., Hernández-Molina, F.J., Llave, E., Stow, D.A.V., León, R., Fernández-Puga, M.C., Diaz del Río, V., Somoza, L., 2009. Contourite erosive features caused by the Mediterranean Outflow Water in the Gulf of Cadiz: Quaternary tectonic and oceanographic implications. *Marine Geology* 257 (1-4), 24-40. doi:10.1016/j.margeo.2008.10.009

- Georgi, D.T., 1981. On the relationship between large-scale property variations and finestructure in the Circumpolar Deep Water. *Journal of Geophysical Research* 86, 6556-6566
- Giberto, D.A., Bremec, C.S., Acha, E.M., Mianzan, H., 2004. Large-scale spatial patterns of benthic assemblages in the SW Atlantic: the Río de la Plata estuary and adjacent shelf waters. *Estuarine, Coastal and Shelf Science* 61 (1), 1-13. doi:10.1016/j.ecss.2004.03.015
- Gill, A.E., 1968. A linear model of the Antarctic circumpolar current. *Journal of Fluid Mechanics* 32 (03), 465-488. doi:10.1017/S0022112068000868
- Gonthier, E., Faugères, J.C., Stow, D.A.V., 1984. Contourite facies of the Faro Drift, Gulf of Cadiz. In: Stow, D.A.V., Piper, D.J.W. (Eds.), *Fine-grained sediments, deep-water processes and facies*. Geol Soc Spec Publ, London, pp. 275-292
- Gordon, A.L., Greengrove, C.L., 1986. Geostrophic circulation of the Brazil-Falkland confluence. *Deep Sea Research Part A. Oceanographic Research Papers* 33 (5), 573-585. doi:10.1016/0198-0149(86)90054-3
- Grant, J.A., Schreiber, R., 1990. Modern swathe sounding and sub-bottom profiling technology for research applications: The Atlas Hydrosweep and Parasound Systems. *Marine Geophysical Research* 12 (1), 9-19. doi:10.1007/bf00310559
- Gruetznner, J., Uenzelmann-Neben, G., Franke, D., 2011. Variations in bottom water activity at the southern Argentine margin: indications from a seismic analysis of a continental slope terrace. *Geo-Marine Letters* 31 (5-6), 405-417. doi:10.1007/s00367-011-0252-0
- Gwilliam, C.S., Coward, A.C., de Cuevas, B.A., Webb, D.J., Rourke, E., Thompson, S.R., Döös, K., 1995. The OCCAM Global Model. 2nd UNAM-Cray Supercomputing Conference on Numerical Simulations in the Environmental and Earth Sciences
- Gwilliam, C.S., 1996. Modelling the global ocean circulation on the T3D. In: Ecer, A., Periaux, J., Satdfuka, N., S. TaylorA2 - A. Ecer, J.P.N.S., Taylor, S. (Eds.), *Parallel Computational Fluid Dynamics 1995*. North-Holland, Amsterdam, pp. 33-40
- Habgood, E.L., Kenyon, N.H., Masson, D.G., Akhmetzhanov, A., Weaver, P.P.E., Gardner, J., Mulder, T., 2003. Deep-water sediment wave fields, bottom current sand channels and gravity flow channel-lobe systems: Gulf of Cadiz, NE Atlantic. *Sedimentology* 50 (3), 483-510. doi:10.1046/j.1365-3091.2003.00561.x
- Hanebuth, T.J.J., Henrich, R., 2009. Recurrent decadal-scale dust events over Holocene western Africa and their control on canyon turbidite activity (Mauritania). *Quaternary Science Reviews* 28 (3-4), 261-270. doi:10.1016/j.quascirev.2008.09.024
- Haq, B.U., Hardenbol, J., Vail, P.R., 1987. Chronology of Fluctuating Sea Levels Since the Triassic. *Science* 235 (4793), 1156-1167. doi:10.1126/science.235.4793.1156
- Heezen, B.C., 1959. Dynamic Processes of Abyssal Sedimentation: Erosion, Transportation, and Redeposition on the Deep-sea floor. *Geophysical Journal of the Royal Astronomical Society* 2 (2), 142-172. doi:10.1111/j.1365-246X.1959.tb05790.x
- Heezen, B.C., Ewing, M., Ericson, D.B., 1955. Reconnaissance survey of the abyssal plain south of Newfoundland. *Deep Sea Research (1953)* 2 (2), 122-133. doi:10.1016/0146-6313(55)90014-9
- Heezen, B.C., Hollister, C., 1964. Deep-sea current evidence from abyssal sediments. *Marine Geology* 1 (2), 141-174. doi:10.1016/0025-3227(64)90012-X
- Heezen, B.C., Hollister, C.D., Ruddiman, W.F., 1966. Shaping of the Continental Rise by Deep Geostrophic Contour Currents. *Science* 152 (3721), 502-508. doi:10.1126/science.152.3721.502
- Henkel, S., Strasser, M., Schwenk, T., Hanebuth, T.J.J., Hüsener, J., Arnold, G.L., Winkelmann, D., Formolo, M., Tomasini, J., Krastel, S., Kasten, S., 2011. An interdisciplinary investigation of a recent submarine mass transport deposit at the continental margin off Uruguay. *Geochem. Geophys. Geosyst.* 12 (8), Q08009. doi:10.1029/2011gc003669
- Henrich, R., Cherubini, Y., Meggers, H., in rev. Climate and sea level induced turbiditic activity in a canyon system offshore the hyperarid Western Sahara: the Timiris Canyon. *Marine Geology*
- Henrich, R., Hanebuth, T.J.J., Cherubini, Y., Krastel, S., Pierau, R., Zühlsdorff, C., 2009. Climate induced turbidity current activity in NW-African canyon systems. In: Mosher, D.C., Shipp, R.C., Moscardelli, L., Chaytor, J., Baxter, C., Lee, H., Urgeles, R. (Eds.), *Submarine mass movements and their consequences*. Symposium, November 8-11., 2009, Austin, Texas. Springer, pp. 447-459



- Hermann, D.-C., 1990. Neogene stratigraphy, paleoceanography and paleobiogeography in northwest South America and the evolution of the Panama seaway. *Palaeogeography, Palaeoclimatology, Palaeoecology* 77 (3-4), 203-234. doi:10.1016/0031-0182(90)90178-a
- Hernández-Molina, F.J., Llave, E., Somoza, L., Fernández-Puga, M.C., Maestro, A., León, R., Medialdea, T., Barnolas, A., García, M., del Río, V.D., Fernández-Salas, L.M., Vázquez, J.T., Lobo, F., Dias, J.M.A., Rodero, J., Gardner, J., 2003. Looking for clues to paleoceanographic imprints: A diagnosis of the Gulf of Cadiz contourite depositional systems. *Geology* 31 (1), 19-22. doi:10.1130/0091-7613(2003)031<0019:lfctpi>2.0.co;2
- Hernández-Molina, F.J., Llave, E., Stow, D.A.V., 2008a. Continental Slope Contourites. *Developments in Sedimentology*. Elsevier, pp. 379-408
- Hernández-Molina, F.J., Llave, E., Stow, D.A.V., García, M., Somoza, L., Vázquez, J.T., Lobo, F.J., Maestro, A., Díaz del Río, V., León, R., Medialdea, T., Gardner, J., 2006. The contourite depositional system of the Gulf of Cádiz: A sedimentary model related to the bottom current activity of the Mediterranean outflow water and its interaction with the continental margin. *Deep Sea Research Part II: Topical Studies in Oceanography* 53 (11-13), 1420-1463. doi:10.1016/j.dsr2.2006.04.016
- Hernández-Molina, F.J., Maldonado, A., Stow, D.A.V., Rebesco, M., Camerlenghi, A., 2008b. Abyssal Plain Contourites. *Developments in Sedimentology*. Elsevier, pp. 345, 347-378.
- Hernández-Molina, F.J., Paterlini, M., Somoza, L., Violante, R., Arecco, M.A., de Isasi, M., Rebesco, M., Uenzelmann-Neben, G., Neben, S., Marshall, P., 2010. Giant mounded drifts in the Argentine Continental Margin: Origins, and global implications for the history of thermohaline circulation. *Marine and Petroleum Geology* 27 (7), 1508-1530. doi:10.1016/j.marpetgeo.2010.04.003
- Hernández-Molina, F.J., Paterlini, M., Violante, R., Marshall, P., de Isasi, M., Somoza, L., Rebesco, M., 2009. Contourite depositional system on the Argentine Slope: An exceptional record of the influence of Antarctic water masses. *Geology* 37 (6), 507-510. doi:10.1130/g25578a.1
- Hernández-Molina, F.J., Preu, B., Violante, R., Piola, A., Paterlini, C.M., submitted. Las terrazas contorníticas en el Margen Continental Argentino: implicaciones morfosedimentarias y oceanográficas. GEOGACETA – Sociedad Geologica de España
- Hernández-Molina, F.J., Somoza, L., Vazquez, J.T., Lobo, F., Fernández-Puga, M.C., Llave, E., Díaz-del Río, V., 2002. Quaternary stratigraphic stacking patterns on the continental shelves of the southern Iberian Peninsula: their relationship with global climate and palaeoceanographic changes. *Quaternary International* 92 (1), 5-23. doi:10.1016/s1040-6182(01)00111-2
- Hinz, K., Neben, S., Schreckenberger, B., Roeser, H.A., Block, M., Souza, K.G.d., Meyer, H., 1999. The Argentine continental margin north of 48°S: sedimentary successions, volcanic activity during breakup. *Marine and Petroleum Geology* 16 (1), 1-25
- Hollister, C.D., 1993. The concept of deep-sea contourites. *Sedimentary Geology* 82 (1-4), 5-11
- Hollister, C.D., McCave, I.N., 1984. Sedimentation under deep-sea storms. *Nature* 309 (5965), 220-225. doi:10.1038/309220a0
- Hosegood, P., van Haren, H., 2003. Ekman-induced turbulence over the continental slope in the Faeroe–Shetland Channel as inferred from spikes in current meter observations. *Deep Sea Research Part I: Oceanographic Research Papers* 50 (5), 657-680. doi:10.1016/s0967-0637(03)00038-4
- Howe, J.A., Stoker, M.S., Stow, D.A.V., 1994. Late Cenozoic Sediment Drift Complex, Northeast Rockall Trough, North Atlantic. *Paleoceanography* 9 (6), 989-999. doi:10.1029/94pa01440
- Hunter, S., Wilkinson, D., Louarn, E., Nick McCave, I., Rohling, E., Stow, D.A.V., Bacon, S., 2007. Deep western boundary current dynamics and associated sedimentation on the Eirik Drift, Southern Greenland Margin. *Deep Sea Research Part I: Oceanographic Research Papers* 54 (12), 2036-2066
- Katz, M.E., Cramer, B.S., Toggweiler, J.R., Esmay, G., Liu, C., Miller, K.G., Rosenthal, Y., Wade, B.S., Wright, J.D., 2011. Impact of Antarctic Circumpolar Current Development on Late Paleogene Ocean Structure. *Science* 332 (6033), 1076-1079. doi:10.1126/science.1202122
- Keeley, M.L., Light, M.P.R., 1993. Basin Evolution and Prospectivity of the Argentine Continental Margin. *Journal of Petroleum Geology* 16 (4), 451-464. doi:10.1111/j.1747-5457.1993.tb00352.x
- Kennett, J., 1982. *Marine Geology*. Prentice Hall, New Jersey

- Klaus, A., Ledbetter, M.T., 1988. Deep-sea sedimentary processes in the Argentine Basin revealed by high-resolution seismic records (3.5 kHz echograms). *Deep Sea Research Part A. Oceanographic Research Papers* 35 (6), 899-917. doi:10.1016/0198-0149(88)90067-2
- Knutz, P.C., 2008. Palaeoceanographic Significance of Contourite Drifts. In: Rebesco, M., Camerlenghi, A. (Eds.), *Developments in Sedimentology*. Elsevier, Oxford, pp. 511-535
- Krastel, S., Schmincke, H.-U., Jacobs, G.L., Rihm, R., Le Bas, T.P., Alibés, B., 2001. Submarine landslides around the Canary Islands. *J. Geophys. Res.* 106 (B3), 3977-3997. doi:10.1029/2000jb900413
- Krastel, S., Wefer, G., Hanebuth, T., Antobreh, A., Freudenthal, T., Preu, B., Schwenk, T., Strasser, M., Violante, R., Winkelmann, D., party, M.s.s., 2011. Sediment dynamics and geohazards off Uruguay and the de la Plata River region (northern Argentina and Uruguay). *Geo-Marine Letters* 31 (4), 271-283. doi:10.1007/s00367-011-0232-4
- Krueger, S., Leuschner, D.C., Ehrmann, W., Schmiedl, G., Mackensen, A., in press. North Atlantic Deep Water and Antarctic Bottom Water variability during the last 200 ka recorded in an abyssal sediment core off South Africa. *Global and Planetary Change* (0). doi:10.1016/j.gloplacha.2011.10.001
- Laberg, J.S., Camerlenghi, A., 2008. The Significance of Contourites for Submarine Slope Stability. *Developments in Sedimentology*. Elsevier, pp. 537-556
- Laberg, J.S., Stoker, M.S., Dahlgren, K.I.T., Haas, H.d., Hafliðason, H., Hjelstuen, B.O., Nielsen, T., Shannon, P.M., Vorren, T.O., van Weering, T.C.E., Ceramicola, S., 2005. Cenozoic alongslope processes and sedimentation on the NW European Atlantic margin. *Marine and Petroleum Geology* 22 (9-10), 1069-1088. doi:10.1016/j.marpetgeo.2005.01.008
- Laberg, J.S., Vorren, T.O., 2004. Weichselian and Holocene growth of the northern high-latitude Lofoten Contourite Drift on the continental slope of Norway. *Sedimentary Geology* 164 (1-2), 1-17. doi:10.1016/j.sedgeo.2003.07.004
- Lagabrielle, Y., Goddérís, Y., Donnadiou, Y., Malavieille, J., Suarez, M., 2009. The tectonic history of Drake Passage and its possible impacts on global climate. *Earth and Planetary Science Letters* 279 (3-4), 197-211. doi:10.1016/j.epsl.2008.12.037
- Lastras, G., Acosta, J., Munoz, A., Canals, M., 2011. Submarine canyon formation and evolution in the Argentine Continental Margin between 44°30'S and 48°S. *Geomorphology* 128, 116-136
- Lawver, L.A., Gahagan, L.M., 2003. Evolution of Cenozoic seaways in the circum-Antarctic region. *Palaeogeography, Palaeoclimatology, Palaeoecology* 198 (1-2), 11-37. doi:10.1016/s0031-0182(03)00392-4
- Le Pichon, X., Eittréim, S.L., Ludwig, W.J., 1971. Sediment transport and distribution in the Argentine Basin. 1. Antarctic Bottom Current passage through the Falkland fracture zone. *Physics and Chemistry of The Earth* 8 (0), 1-28. doi:10.1016/0079-1946(71)90013-9
- Legeckis, R., Gordon, A.L., 1982. Satellite observations of the Brazil and Falkland currents— 1975 1976 and 1978. *Deep Sea Research Part A. Oceanographic Research Papers* 29 (3), 375-401. doi:10.1016/0198-0149(82)90101-7
- Light, M.P.R., Keeley, M.L., Maslanyj, M.R., Urien, C.M., 1993. The Tectono-Stratigraphic Development of Patagonia, and its Relevance to Hydrocarbon Exploration. *Journal of Petroleum Geology* 16 (4), 465-482. doi:10.1111/j.1747-5457.1993.tb00353.x
- Lisiecki, L.E., Raymo, M.E., 2007. Plio-Pleistocene climate evolution: trends and transitions in glacial cycle dynamics. *Quaternary Science Reviews* 26 (1-2), 56-69. doi:10.1016/j.quascirev.2006.09.005
- Livermore, R., McAdoo, D., Marks, K., 1994. Scotia Sea tectonics from high-resolution satellite gravity. *Earth and Planetary Science Letters* 123 (1-3), 255-268. doi:10.1016/0012-821x(94)90272-0
- Llave, E., Hernández-Molina, F.J., Somoza, L., Díaz-del-Río, V., Stow, D.A.V., Maestro, A., Alveirinho Dias, J.M., 2001. Seismic stacking pattern of the Faro-Albufeira contourite system (Gulf of Cadiz): a Quaternary record of paleoceanographic and tectonic influences. *Marine Geophysical Researches* 22 (5), 487-508
- Llave, E., Hernández-Molina, F.J., Somoza, L., Stow, D.A.V., Díaz Del Río, V., 2007. Quaternary evolution of the contourite depositional system in the Gulf of Cadiz. *Geological Society, London, Special Publications* 276 (1), 49-79. doi:10.1144/gsl.sp.2007.276.01.03

- Lonardi, A.G., Ewing, M., 1971. Sediment transport and distribution in the Argentine Basin. 4. Bathymetry of the continental margin, Argentine Basin and other related provinces. Canyons and sources of sediments. *Physics and Chemistry of The Earth* 8, 79-121
- Lonardi, A.G., Ewing, M., 1971. Sediment transport and distribution in the Argentine basin. 6. Exploration and study of the Argentine basin. *Physics and Chemistry of The Earth* 8, 253-263
- Lovell, J.P.B., Stow, D.A.V., 1981. Identification of ancient sandy contourites. *Geology* 9 (8), 347-349. doi:10.1130/0091-7613(1981)9<347:ioasc>2.0.co;2
- Lutjeharms, J.R.E., 2006. *The Agulhas Current*. Springer, Berlin.
- Lutjeharms, J.R.E., Da Silva, A.J., 1988. The Delagoa Bight eddy. *Deep Sea Research Part A. Oceanographic Research Papers* 35 (4), 619-634
- Marchès, E., 2008. Le système contouritique de la marge de l'Algarve: processus sédimentaires et enregistrement au cours du Quaternaire, L'Université Bordeaux I, Bordeaux.
- Marchès, E., Mulder, T., Gonthier, E., Cremer, M., Hanquiez, V., Garlan, T., Lecroart, P., 2010. Perched lobe formation in the Gulf of Cadiz: Interactions between gravity processes and contour currents (Algarve Margin, Southern Portugal). *Sedimentary Geology* 229 (3), 81-94. doi:10.1016/j.sedgeo.2009.03.008
- Martin, A.K., 1981. The influence of the Agulhas Current on the physiographic development of the northernmost Natal Valley (S.W. Indian Ocean). *Marine Geology* 39 (3-4), 259-276
- Martin, A.K., Goodlad, S.W., Salmon, D.A., 1982. Sedimentary basin in-fill in the northernmost Natal Valley, hiatus development and Agulhas Current palaeo-oceanography. *Journal of the Geological Society* 139 (2), 183-201. doi:10.1144/gsjgs.139.2.0183
- Matano, R.P., Palma, E.D., Piola, A.R., 2010. The influence of the Brazil and Malvinas Currents on the Southwestern Atlantic Shelf circulation. *Ocean Sci.* 6 (4), 983-995. doi:10.5194/os-6-983-2010
- McCave, I.N., 1986. Local and global aspects of the bottom nepheloid layers in the world ocean. *Netherlands Journal of Sea Research* 20 (2-3), 167-181
- McCave, I.N., 2005. Deposition from suspension. In: Selley, R.C., Cocks, L.R.M., Malone, M.J. (Eds.), *Encyclopedia of Geology*. Elsevier, Oxford, pp. 8-17
- McCave, I.N., Hollister, C.D., 1985. Sedimentation under deep-sea current systems: Pre-HEBBLE ideas. *Marine Geology* 66 (1-4), 13-24
- McCave, I.N., Hollister, C.D., Laine, E.P., Lonsdale, P.F., Richardson, M.J., 1982. Erosion and deposition on the eastern margin of the Bermuda Rise in the late Quaternary. *Deep Sea Research Part A. Oceanographic Research Papers* 29 (5), 535-561. doi:10.1016/0198-0149(82)90075-9
- McCave, I.N., John, H.S., Karl, K.T., Steve, A.T., 2009. Nepheloid Layers. *Encyclopedia of Ocean Sciences*. Academic Press, Oxford, pp. 8-18
- McCave, I.N., Manighetti, B., Beveridge, N.A.S., 1995. Circulation in the glacial North Atlantic inferred from grain-size measurements. *Nature* 374 (6518), 149-152
- McCave, I.N., Tucholke, B.E., 1986. Deep current controlled sedimentation in the western Atlantic. In: Vogt, P.R., Tucholke, B.E. (Eds.), *The geology of North America*. Geological Society of America, pp. 451-468
- Medwin, H., Clay, C.S., 1997. *Fundamentals of Acoustical Oceanography (Applications of Modern Acoustics)*. Academic Press, Hannover
- Medwin, H., Clay, C.S., Stanton, T.K., 1999. *Fundamentals of Acoustical Oceanography*. *The Journal of the Acoustical Society of America* 105 (4), 2065-2066
- Mézeris, M.L., Faugères, J.C., Figueiredo Jr, A.G., Massé, L., 1993. Contour current accumulation off the Vema Channel mouth, southern Brazil Basin: pattern of a "contourite fan". *Sedimentary Geology* 82 (1-4), 173-187
- Milliman, J.D., Meade, R.H., 1983. World-Wide Delivery of River Sediment to the Oceans. *The Journal of Geology* 91 (1), 1-21. doi:10.1086/628741
- Mudelsee, M., Schulz, M., 1997. The Mid-Pleistocene climate transition: onset of 100 ka cycle lags ice volume build-up by 280 ka. *Earth and Planetary Science Letters* 151 (1-2), 117-123. doi:10.1016/S0012-821X(97)00114-3
- Mulder, T., Faugères, J.C., Gonthier, E., 2008. Mixed Turbidite–Contourite Systems. In: Rebesco, M., Camerlenghi, A. (Eds.), *Developments in Sedimentology*. Elsevier, pp. 435-456.

- Mulder, T., Lecroart, P., Hanquiez, V., Marches, E., Gonthier, E., Guedes, J.C., Thiébot, E., Jaaidi, B., Kenyon, N., Voisset, M., Perez, C., Sayago, M., Fuchey, Y., Bujan, S., 2006. The western part of the Gulf of Cadiz: contour currents and turbidity currents interactions. *Geo-Marine Letters* 26 (1), 31-41. doi:10.1007/s00367-005-0013-z
- Mulder, T., Voisset, M., Lecroart, P., Le Drezen, E., Gonthier, E., Hanquiez, V., Faugères, J.C., Habgood, E., Hernandez-Molina, F.J., Estrada, F., Llave-Barranco, E., Poirier, D., Gorini, C., Fuchey, Y., Voelker, A., Freitas, P., Sanchez, F.L., Fernandez, L.M., Kenyon, N.H., Morel, J., 2003. The Gulf of Cadiz: an unstable giant contouritic levee. *Geo-Marine Letters* 23 (1), 7-18. doi:10.1007/s00367-003-0119-0
- Mulitza, S., Paul, A., Wefer, G., Scott, A.E., 2007. Late Pleistocene South Atlantic. *Encyclopedia of Quaternary Science*. Elsevier, Oxford, pp. 1816-1831
- Munk, W.H., 1950. On the wind-driven ocean circulation. *Journal of Meteorology* 7 (2), 79-93
- Nelson, C.H., Baraza, J., Maldonado, A., 1993. Mediterranean undercurrent sandy contourites, Gulf of Cadiz, Spain. *Sedimentary Geology* 82 (1-4), 103-131. doi:10.1016/0037-0738(93)90116-m
- Nelson, C.H., Baraza, J., Maldonado, A., Rodero, J., Escutia, C., Barber Jr, J.H., 1999. Influence of the Atlantic inflow and Mediterranean outflow currents on Late Quaternary sedimentary facies of the Gulf of Cadiz continental margin. *Marine Geology* 155 (1-2), 99-129. doi:10.1016/s0025-3227(98)00143-1
- Newkirk, D.R., Martin, E.E., 2009. Circulation through the Central American Seaway during the Miocene carbonate crash. *Geology* 37 (1), 87-90. doi:10.1130/g25193a.1
- Ninnemann, U.S., Charles, C.D., 2002. Changes in the mode of Southern Ocean circulation over the last glacial cycle revealed by foraminiferal stable isotopic variability. *Earth and Planetary Science Letters* 201 (2), 383-396. doi:10.1016/s0012-821x(02)00708-2
- Niño, Y., Lopez, F., Garcia, M., 2003. Threshold for particle entrainment into suspension. *Sedimentology* 50 (2), 247-263. doi:10.1046/j.1365-3091.2003.00551.x
- Nisancioglu, K.H., Raymo, M.E., Stone, P.H., 2003. Reorganization of Miocene deep water circulation in response to the shoaling of the Central American Seaway. *Paleoceanography* 18 (1), 1006. doi:10.1029/2002pa000767
- Nowell, A.R.M., McCave, I.N., Hollister, C.D., 1985. Contributions of HEBBLE to understanding marine sedimentation. *Marine Geology* 66 (1-4), 397-409
- Okada, H., Ohta, S., 1993. Photographic evidence of variable bottom-current activity in the Suruga and Sagami Bays, central Japan. *Sedimentary Geology* 82 (1-4), 221-237
- Olson, D.B., Podestá, G.P., Evans, R.H., Brown, O.B., 1988. Temporal variations in the separation of Brazil and Malvinas Currents. *Deep Sea Research Part A. Oceanographic Research Papers* 35 (12), 1971-1990. doi:10.1016/0198-0149(88)90120-3
- Oppo, D., Fairbanks, R.G., 1987. Variability in the deep and intermediate water circulation of the Atlantic Ocean during the past 25,000 years: Northern Hemisphere modulation of the Southern Ocean. *Earth Planet. Sci. Lett.* 86, 1-15
- Palamenghi, L., Schwenk, T., Spiess, V., Kudrass, H.R., 2011. Seismostratigraphic analysis with centennial to decadal time resolution of the sediment sink in the Ganges–Brahmaputra subaqueous delta. *Continental Shelf Research* 31 (6), 712-730. doi:10.1016/j.csr.2011.01.008
- Parker, G., Paterlini, C.M., Violante, R., 1997. El fondo marino. In: Boschi, E. (Ed.), *El Mar Argentino y sus Recursos Marinos, Mar del Plata*, pp. 65-87
- Parker, G., Violante, R., Paterlini, C.M., 1996. Fisiografía de la Plataforma Continental. In: Ramos, V., Turic, M.A. (Eds.), *Geología y Recursos Naturales de la Plataforma Continental Argentina, Buenos Aires*, pp. 1-16
- Parker, G., Violante, R., Paterlini, C.M., Marcolini, S., Costa, I.P., Cavallotto, J.L., 2008. Las secuencias sismoestratigráficas del Plioceno-Cuaternario en la Plataforma Submarina adyacente al litoral del este bonaerense. *Latin American journal of sedimentology and basin analysis* 15 (2), 105-124
- Peterson, R.G., 1992. The boundary currents in the western Argentine Basin. *Deep Sea Research Part A. Oceanographic Research Papers* 39 (3-4), 623-644. doi:10.1016/0198-0149(92)90092-8
- Pettijohn, F.J., Potter, P.E., 1964. Atlas and glossary of primary sedimentary structures / by F. J. Pettijohn and Paul Edwin Potter. Translations into Spanish, French, and German by Juan Carlos Riggi, Marie-Helene Sachet, and Hans-Ulrich Schmincke. Springer-Verlag, Berlin.

- Pickering, K.T., Hiscott, R.N., Hein, F.J., 1989. Deep Marine Environments: Clastic Sedimentation and Tectonics. Springer
- Piola, A., 2006. Antarctic Intermediate Water. In: Riffenburgh, B. (Ed.), Encyclopedia of the Antarctic, New York, pp. 62-66
- Piola, A., Rivas, A.L., 1997. Corrientes en la plataforma continental. In: Boschi, E. (Ed.), El mar argentino y sus recursos pesqueros, Mar del Plata, pp. 119-132
- Piola, A.R., Gordon, A.L., 1989. Intermediate waters in the southwest South Atlantic. Deep Sea Research Part A. Oceanographic Research Papers 36 (1), 1-16. doi:10.1016/0198-0149(89)90015-0
- Piola, A.R., Matano, R.P., 2001. Brazil and Falklands (Malvinas) currents. Academic Press, London.
- Piotrowski, A.M., Goldstein, S.L., Hemming, S.R., Fairbanks, R.G., Zylberberg, D.R., 2008. Oscillating glacial northern and southern deep water formation from combined neodymium and carbon isotopes. Earth and Planetary Science Letters 272 (1-2), 394-405. doi:10.1016/j.epsl.2008.05.011
- Potter, P.E., Szatmari, P., 2009. Global Miocene tectonics and the modern world. Earth-Science Reviews 96 (4), 279-295. doi:10.1016/j.earscirev.2009.07.003
- Pratson, L.F., Coakley, B.J., 1996. A model for the headward erosion of submarine canyons induced by downslope-eroding sediment flows. Geological Society of America Bulletin 108 (2), 225-234. doi:10.1130/0016-7606(1996)108<0225:amfthe>2.3.co;2
- Pratson, L.F., Ryan, W.B.F., Mountain, G.S., Twichell, D.C., 1994. Submarine canyon initiation by downslope-eroding sediment flows: Evidence in late Cenozoic strata on the New Jersey continental slope. Geological Society of America Bulletin 106 (3), 395-412. doi:10.1130/0016-7606(1994)106<0395:scibde>2.3.co;2
- Prell, W.L., 1984. Covariance Patterns of Foraminiferal  $\delta^{18}O$ : An Evaluation of Pliocene Ice Volume Changes Near 3.2 Million Years Ago. Science 226 (4675), 692-694. doi:10.1126/science.226.4675.692
- Preu, B., Spieß, V., Schwenk, T., Schneider, R., 2011. Evidence for current-controlled sedimentation along the southern Mozambique continental margin since Early Miocene times. Geo-Marine Letters 31 (5-6), 427-435. doi:10.1007/s00367-011-0238-y
- Pudsey, C.J., 2002. The Weddel Sea: contourites and hemipelagites at the northern margin of the Weddell Gyre. In: Stow, D.A.V., Pudsey, C.J., Howe, J.A., Faugères, J.C., Viana, A.R. (Eds.), Deep-water contourite systems: modern drifts and ancient series, seismic and sedimentary characteristics. Geological Society, London
- Puig, P., Palanques, A., Guillén, J., El Khatab, M., 2004. Role of internal waves in the generation of nepheloid layers on the northwestern Alboran slope: Implications for continental margin shaping. J. Geophys. Res. 109 (C9), C09011. doi:10.1029/2004jc002394
- Ramos, V., 1999. Rasgos Estructurales del Territorio Argentino. Evolución Tectónica de la Argentina. In: Caminos, R. (Ed.), Geología Argentina. SEGEMAR, Buenos Aires, pp. 715-784.
- Rasmussen, T.L., van Weering, T.C.E., Labeyrie, L., 1996. High resolution stratigraphy of the Faeroe-Shetland Channel and its relation to North Atlantic paleoceanography: the last 87 kyr. Marine Geology 131 (1-2), 75-88. doi:10.1016/0025-3227(95)00145-x
- Ravelo, A.C., 2006. Walker circulation and global warming - lessons from the past. Oceanography 19 (4), 114-122
- Ravelo, A.C., Fairbanks, R.G., Philander, S.G.H., 1990. Reconstructing tropical Atlantic hydrography using planktonic foraminifera and an ocean model. Paleoceanography 5 (3), 409-431
- Raymo, M.E., Oppo, D.W., Curry, W., 1997. The Mid-Pleistocene Climate Transition: A Deep Sea Carbon Isotopic Perspective. Paleoceanography 12 (4), 546-559. doi:10.1029/97pa01019
- Rebesco, M., 2005. Contourites. In: Selley, R., Cocks, L.R.M., Plimer, I., R. (Eds.), Encyclopedia of Geology. Elsevier, Oxford, pp. 513-527
- Rebesco, M., Camerlenghi, A., 2008. Contourites. Elsevier
- Rebesco, M., Pudsey, C.J., Canals, M., Camerlenghi, A., Barker, P.F., Estrada, F., Giorgetti, A., 2002. Sediment drifts and deep-sea channel systems, Antarctic Peninsula Pacific Margin. Geological Society, London, Memoirs 22 (1), 353-371. doi:10.1144/gsl.mem.2002.022.01.25
- Reid, J.L., 1989. On the total geostrophic circulation of the Indian Ocean: flow patterns, tracers, and transports. Progress In Oceanography 23 (1), 149-244. doi:10.1016/s0079-6611(02)00141-6

- Reid, J.L., Nowlin, W.D., Patzert, W.C., 1977. On the Characteristics and Circulation of the Southwestern Atlantic Ocean. *Journal of Physical Oceanography* 7 (1), 62-91. doi:10.1175/1520-0485(1977)007<0062:otcaco>2.0.co;2
- Richards, P.C., Ritchie, J.D., Thomson, A.R., 1987. Evolution of deep-water climbing dunes in the Rockall Trough — Implications for overflow currents across the Wyville-Thomson Ridge in the late Miocene. *Marine Geology* 76 (0), 177-183. doi:10.1016/0025-3227(87)90027-2
- Richardson, M.J., Weatherly, G.L., Gardner, W.D., 1993. Benthic storms in the Argentine Basin. *Deep Sea Research Part II: Topical Studies in Oceanography* 40 (4-5), 975-987
- Richardson, M.J., Wimbush, M., Mayer, L., 1981. Exceptionally Strong Near-Bottom Flows on the Continental Rise of Nova Scotia. *Science* 213 (4510), 887-888
- Ruddiman, W.F., 2001. *Earth's Climate - Past and Future*. W.H. Freeman and Company, New York.
- Ryan, W.B.F., Carbotte, S.M., Coplan, J.O., O'Hara, S., Melkonian, A., Arko, R., Weissel, R.A., Ferrini, V., Goodwillie, A., Nitsche, F., Bonczkowski, J., Zemsky, R., 2009. Global Multi-Resolution Topography synthesis. *Geochem. Geophys. Geosyst.* 10 (3), Q03014. doi:10.1029/2008gc002332
- Saetre, R., Da Silva, A.J., 1984. The circulation of the Mozambique channel. *Deep Sea Research Part A. Oceanographic Research Papers* 31 (5), 485-508
- Salles, T., Marchès, E., Dyt, C., Griffiths, C., Hanquiez, V., Mulder, T., 2010. Simulation of the interactions between gravity processes and contour currents on the Algarve Margin (South Portugal) using the stratigraphic forward model SedSim. *Sedimentary Geology* 229 (3), 95-109. doi:10.1016/j.sedgeo.2009.05.007
- Saraceno, M., Provost, C., Piola, A.R., Bava, J., Gagliardini, A., 2004. Brazil Malvinas Frontal System as seen from 9 years of advanced very high resolution radiometer data. *J. Geophys. Res.* 109 (C5), C05027. doi:10.1029/2003jc002127
- Saunders, P.M., King, B.A., 1995. Oceanic Fluxes on the WOCE A11 Section. *Journal of Physical Oceanography* 25 (9), 1942-1958. doi:10.1175/1520-0485(1995)025<1942:ofotwa>2.0.co;2
- Schlitzer, R., 2011. *Ocean Data View 4.0*. <http://odv.awi.de>
- Seibold, E., Berger, W.H., 1993. *The sea floor: An introduction to marine geology*. Springer, Berlin.
- Shanmugam, G., 2003. Deep-marine tidal bottom currents and their reworked sands in modern and ancient submarine canyons. *Marine and Petroleum Geology* 20 (5), 471-491. doi:10.1016/s0264-8172(03)00063-1
- Shanmugam, G., 2007. *Deep-water processes and facies models: implications for sandstone petroleum reservoirs*. Elsevier, Amsterdam
- Shanmugam, G., 2008. Deep-water Bottom Currents and their Deposits. In: Rebesco, M., Camerlenghi, A. (Eds.), *Developments in Sedimentology*. Elsevier, pp. 59-81.
- Shanmugam, G., Spalding, T.D., Rofheart, D.H., 1995. Deep-marine bottom-current reworked sand (Pliocene and Pleistocene), Ewing Bank 826 Field, Gulf of Mexico. *SEPM Core Workshop* 20, 25-54
- Shi, Z., Ren, L., Hamilton, L., 1999. Acoustic profiling of fine suspension concentration in the Changjiang estuary. *Estuaries and Coasts* 22 (3), 648-656
- Smith, W.H.F., Sandwell, D.T., 1997. Global Sea Floor Topography from Satellite Altimetry and Ship Depth Soundings. *Science* 277 (5334), 1956-1962. doi:10.1126/science.277.5334.1956
- Spiess, V., 1992. *Digitale Sedimentechographie - Neue Wege zu einer hochauflösenden Akustostratigraphie*, University of Bremen, Bremen
- Stoakes, F.A., Campbell, R., Cass, R., Ucha, N., 1991. Seismic stratigraphic analysis of the Punta del Este Basin, Offshore Uruguay. *Routh America. Bull* 75 (2), 219-240
- Stoker, M., 1995. The influence of glacial sedimentation on slope-apron development on the continental margin off northwest Britain. In: Scrutton, R.A. (Ed.), *The tectonics, sedimentation and palaeoceanography of the North Atlantic region*. Geological Society of London, London
- Stow, D.A.V., 1982. Bottom current and contourites in the North Atlantic. *Bulletin - Institut de Geologie du Bassin d'Aquitaine* 31-32, 151-166
- Stow, D.A.V., Faugères, J.C., 2008. Contourite Facies and the Facies Model. In: Rebesco, M., Camerlenghi, A. (Eds.), *Developments in Sedimentology*. Elsevier, pp. 223-256.

- Stow, D.A.V., Faugeres, J.-C., Gonthier, E., Cremer, M., Llave, E., Hernandez-Molina, F.J., Somoza, L., Diaz-Del-Rio, V., 2002. Faro-Albufeira drift complex, northern Gulf of Cadiz. *Geological Society, London, Memoirs* 22 (1), 137-154. doi:10.1144/gsl.mem.2002.022.01.11
- Stow, D.A.V., Hernández-Molina, F.J., Llave, E., Sayago-Gil, M., Díaz del Río, V., Branson, A., 2009. Bedform-velocity matrix: The estimation of bottom current velocity from bedform observations. *Geology* 37 (4), 327-330. doi:10.1130/g25259a.1
- Stow, D.A.V., Hunter, S., Wilkinson, D., Hernández-Molina, F.J., Rebesco, M., Camerlenghi, A., 2008. The Nature of Contourite Deposition. *Developments in Sedimentology*. Elsevier, pp. 143-156
- Stow, D.A.V., Lovell, J.P.B., 1979. Contourites: Their recognition in modern and ancient sediments. *Earth-Science Reviews* 14 (3), 251-291
- Stow, D.A.V., Mayall, M., 2000. Deep-water sedimentary systems: New models for the 21st century. *Marine and Petroleum Geology* 17 (2), 125-135
- Stow, D.A.V., Pudsey, C.J., Howe, J.A., Faugères, J.C., Viana, A.R., 2002. Deep-Water Contourite Systems: Modern Drifts and Ancient Series, Seismic and Sedimentary Characteristics. Geological Society, London
- Stramma, L., 1989. The Brazil current transport south of 23°S. *Deep Sea Research Part A. Oceanographic Research Papers* 36 (4), 639-646. doi:10.1016/0198-0149(89)90012-5
- Tavella, G.F., Wright, C.G., 1996. Cuenca del Salado. In: Ramos, V., Turic, M.A. (Eds.), *Geología y Recursos Naturales de la Plataforma Continental Argentina*. Asociación Geológica Argentina-Instituto Argentino del Petróleo, Buenos Aires, pp. 95-116
- Thorndike, E.M., 1975. A deep sea, photographic nephelometer. *Ocean Engineering* 3 (1), 1-15
- Thorne, P.D., Hardcastle, P.J., Soulsby, R.L., 1993. Analysis of Acoustic Measurements of Suspended Sediments. *J. Geophys. Res.* 98 (C1), 899-910. doi:10.1029/92jc01855
- Thorne, P.D., Vincent, C.E., Hardcastle, P.J., Rehman, S., Pearson, N., 1991. Measuring suspended sediment concentrations using acoustic backscatter devices. *Marine Geology* 98 (1), 7-16
- Tiedemann, R., Sarnthein, M., Shackleton, N.J., 1994. Astronomic Timescale for the Pliocene Atlantic & #948;18O and Dust Flux Records of Ocean Drilling Program Site 659. *Paleoceanography* 9 (4), 619-638. doi:10.1029/94pa00208
- Tomczak, M., Godfrey, J.S., 2001. *Regional Oceanography - An Introduction*. Butler & Tanner Ltd., London
- Twichell, D.C., Roberts, D.G., 1982. Morphology, distribution, and development of submarine canyons on the United States Atlantic continental slope between Hudson and Baltimore Canyons. *Geology* 10 (8), 408-412. doi:10.1130/0091-7613(1982)10<408:mdados>2.0.co;2
- Urien, C.M., Ewing, M., 1974. Recent Sediments and Environments of Southern Brazil, Uruguay, Buenos Aires and Rio Negro Continental Shelf. In: Burk, C.A. (Ed.), *The Geology of Continental Margins*. Springer, Berlin, p. 1009
- Urien, C.M., Zambrano, J.J., 1996. Estructura del Margen Continental. In: Ramos, V., Turic, M.A. (Eds.), *Geología y Recursos Naturales de la Plataforma Continental Argentina*. Asociación Geológica Argentina-Instituto Argentino del Petróleo, Buenos Aires, pp. 29-65
- Vail, P.R., Mitchum Jr., R.M., Thompson III, S., 1977. Seismic Stratigraphy and Global Changes of Sea Level: Part 3. Relative Changes of Sea Level from Coastal Onlap: Section 2. Application of Seismic Reflection Configuration to Stratigraphic Interpretation Memoir 26, 63-81
- van Raaphorst, W., Malschaert, H., van Haren, H., Boer, W., Brummer, G., 2001. Cross-slope zonation of erosion and deposition in the Faeroe-Shetland Channel, North Atlantic Ocean. *Deep Sea Research Part I: Oceanographic Research Papers* 48 (2), 567-591. doi:10.1016/s0967-0637(00)00052-2
- Van Rooij, D., Iglesias, J., Hernández-Molina, F.J., Ercilla, G., Gomez-Ballesteros, M., Casas, D., Llave, E., De Hauwere, A., Garcia-Gil, S., Acosta, J., Henriot, J.P., 2010. The Le Danois Contourite Depositional System: Interactions between the Mediterranean Outflow Water and the upper Cantabrian slope (North Iberian margin). *Marine Geology* 274 (1-4), 1-20. doi:10.1016/j.margeo.2010.03.001
- Venz, K.A., Hodell, D.A., Stanton, C., Warnke, D.A., 1999. A 1.0 Myr Record of Glacial North Atlantic Intermediate Water Variability from ODP Site 982 in the Northeast Atlantic. *Paleoceanography* 14 (1), 42-52. doi:10.1029/1998pa900013

- Viana, A.R., Almeida, W., Nunes, M.C.V., Bulhões, E.M., 2007. The economic importance of contourites. Geological Society, London, Special Publications 276 (1), 1-23.  
doi:10.1144/gsl.sp.2007.276.01.01
- Viana, A.R., Almeida, W.J., Almeida, C.W., 2002a. Upper slope sands: Late Quaternary shallow-water sandy contourites of Campos Basin, SW Atlantic margin. In: Stow, D.A.V., Pudsey, C.J., Howe, J.A., Faugères, J.C., Viana, A.R. (Eds.), Deep-water contourite systems: modern drifts and ancient series, seismic and sedimentary characteristics. Geol Soc Lond Mem, London, pp. 261-270
- Viana, A.R., Faugères, J.-C., 1998. Upper slope sand deposits: the example of Campos Basin, a latest Pleistocene-Holocene record of the interaction between alongslope and downslope currents. Geological Society, London, Special Publications 129 (1), 287-316.  
doi:10.1144/gsl.sp.1998.129.01.18
- Viana, A.R., Hercos, C.M., Almeida, W.J., Magalhaes, J.L.C., Andrade, S.B., 2002b. Evidence of bottom current influence on the Neogene to Quaternary sedimentation along the Northern Campos Slope, SW Atlantic Margin. In: Stow, D.A.V., Pudsey, C.J., Howe, J.A., Faugères, J.C., Viana, A.R. (Eds.), Deep-water contourite systems: modern drifts and ancient series, seismic and sedimentary characteristics. Geol Soc Lond Mem, London, pp. 249-259
- Viana, A.R., Rebesco, M., Camerlenghi, A., 2008. Economic Relevance of Contourites. *Developments in Sedimentology*. Elsevier, pp. 491, 493-510
- Violante, R.A., Paterlini, C.M., Costa, I.P., Hernández-Molina, F.J., Segovia, L.M., Cavallotto, J.L., Marcolini, S., Bozzano, G., Laprida, C., García Chaporí, N., Bickert, T., Spieß, V., 2010. Sismoestratigrafía y evolución geomorfológica del talud continental adyacente al litoral del este bonaerense, Argentina. *Latin American journal of sedimentology and basin analysis* 17, 33-62
- Violante, R.A., Paterlini, C.M., Costa, I.P., Hernández-Molina, F.J., Segovia, L.M., Cavallotto, J.L., Marcolini, S., Bozzano, G., Laprida, C., García Chaporí, N., Bickert, T., Spieß, V., 2010. Sismoestratigrafía y evolución geomorfológica del talud continental adyacente al litoral del este bonaerense, Argentina. *Latin American journal of sedimentology and basin analysis* 17, 33-62
- Vogt, P.R., 1972. The Faeroe-Iceland-Greenland Aseismic Ridge and the Western Boundary Undercurrent. *Nature* 239 (5367), 79-81
- von Lom-Keil, H., Spieß, V., Hopf, V., 2002. Fine-grained sediment waves on the western flank of the Zapiola Drift, Argentine Basin: evidence for variations in Late Quaternary bottom flow activity. *Marine Geology* 192 (1-3), 239-258
- Weber, M.E., Bonani, G., Fütterer, K.D., 1994. Sedimentation Processes within Channel-Ridge Systems, Southeastern Weddell Sea, Antarctica. *Paleoceanography* 9 (6), 1027-1048.  
doi:10.1029/94pa01443
- Wolinsky, M.A., Pratson, L.F., 2005. Constraints on landscape evolution from slope histograms. *Geology* 33 (6), 477-480. doi:10.1130/g21296.1
- Wüst, G., 1936. Schichtung und Zirkulation des Atlantischen Ozeans. Das Bodenwasser und die Stratosphäre. *Wiss. Erg. Dtsch. Atlant. "Meteor"* 6, 1-288
- Wüst, G., 1955. Stromgeschwindigkeiten im Tiefen und Bodenwasser des Atlantischen Ozeans auf Grund dynamischer Berechnung der Meter-Profile der Deutschen Atlantischen Expedition 1925-1927. *Papers in Marine Biology and Oceanography Supplement to Deep Sea Research* 3, 373-393
- Wüst, G., 1958. Die Stromgeschwindigkeiten und Stromengen in der Atlantischen Tiefsee. *Geol. Rundsch.* 47, 187-195
- Yilmaz, Ö., 1987. *Seismic Data Processing*. Society of Exploration Geophysicists, Tulsa.
- Yrigoyen, M.R., 1975. Geología del subsuelo y Plataforma Continental. *Relatorio: Geología de la Prov. de Buenos Aires, VI Congreso Geológico Argentino, Bahía Blanca*, pp. 139-168.
- Zachos, J., Pagani, M., Sloan, L., Thomas, E., Billups, K., 2001. Trends, Rhythms, and Aberrations in Global Climate 65 Ma to Present. *Science* 292 (5517), 686-693. doi:10.1126/science.1059412
- Zachos, J.C., Stott, L.D., Lohmann, K.C., 1994. Evolution of Early Cenozoic Marine Temperatures. *Paleoceanography* 9 (2), 353-387. doi:10.1029/93pa03266
- Zenk, W., 2008. Abyssal and Contour Currents. In: Rebesco, M., Camerlenghi, A. (Eds.), *Developments in Sedimentology*. Elsevier, pp. 35, 37-57



- Zühlsdorff, C., Hanebuth, T., Henrich, R., 2008. Persistent quasi-periodic turbidite activity off Saharan Africa and its comparability to orbital and climate cyclicities. *Geo-Marine Letters* 28 (2), 87-95

**Abbreviations**

AABW	Antarctic Bottom Water
AAIW	Antarctic Intermediate Water
AC	Agulhas Current
ACC	Antarctic Circumpolar Current
BC	Brazil Current
BMC/BMCZ	Brazil-Malvinas Confluence (Zone)
CAS	Central American Seaway
CDS	Contourite Depositional System
CDW	Circumpolar Deep Water
DBE	Delagoa Bight Eddy
EMC	East Madagascar Current
LCDW	Lower Circumpolar Deep Water
MC	Malvinas Current
MCS	Multichannel seismic
MOC	Mozambique Current
NADW	North Atlantic Deep Water
PHF	Primary High Frequency
SACW	South Atlantic Central Water
SLF	Secondary Low Frequency
SSDW	Southern Sourced Deep Water
SSIW	Southern Sourced Intermediate Water
TW	Tropical Water
UCDW	Upper Circumpolar Deep Water
USSDW	Upper Southern Sourced Deep Water

## **Appendix 1: Evidence for current-controlled sedimentation along the southern Mozambique continental margin since Early Miocene times**

Benedict Preu<sup>(1)</sup>, Volkhard Spieß<sup>(1)</sup>, Tilmann Schwenk<sup>(1)</sup>, Ralph Schneider<sup>(2)</sup>

(1) MARUM – Center for Marine Environmental Sciences and Faculty of Geosciences, University of Bremen, Bremen, Germany

(2) Institute for Geosciences, Christian-Albrecht University, Kiel, Germany

Printed in ,Geo-Marine Letters' 2011  
Reprinted with permission from Springer

Geo-Mar Lett (2011) 31:427–435  
DOI 10.1007/s00367-011-0238-y

ORIGINAL

## Evidence for current-controlled sedimentation along the southern Mozambique continental margin since Early Miocene times

Benedict Preu · Volkhard Spieß · Tilmann Schwenk · Ralph Schneider

Received: 4 January 2011 / Accepted: 19 May 2011 / Published online: 11 June 2011  
© Springer-Verlag 2011

**Abstract** Major plastered drift sequences were imaged using high-resolution multichannel seismics during R/V Meteor cruises M63/1 and M75/3 south of the Mozambique Channel along the continental margin of Mozambique off the Limpopo River. Detailed seismic-stratigraphic analyses enabled the reconstruction of the onset and development of the modern, discontinuous, eddy-dominated Mozambique Current. Major drift sequences can first be identified during the Early Miocene. Consistent with earlier findings, a progressive northward shift of the depocenter indicates that, on a geological timescale, a steady but variable Mozambique Current existed from this time onward. It can furthermore be shown that, during the Early/Middle Miocene, a coast-parallel current was established off the Limpopo River as part of a lee eddy system driven by the Mozambique Current. Modern sedimentation is controlled by the interplay between slope morphology and the lee eddy system, resulting in upwelling of Antarctic Intermediate Water. Drift accumulations at larger depths are related to the reworking of sediment by deep-reaching eddies that migrate southward, forming the Mozambique Current and eventually merging with the Agulhas Current.

Responsible guest editor: D.A.V. Stow

B. Preu (✉) · V. Spieß · T. Schwenk  
MARUM—Center for Marine Environmental Sciences,  
University of Bremen,  
28359 Bremen, Germany  
e-mail: bpreu@uni-bremen.de

V. Spieß · T. Schwenk  
Faculty of Geosciences, University of Bremen,  
28359 Bremen, Germany

R. Schneider  
Department of Geosciences, Christian-Albrecht University Kiel,  
24118 Kiel, Germany

### Introduction

The southwestern Indian Ocean and its western boundary currents (Fig. 1) play a key role in the global redistribution of mass, heat and freshwater (DiMarco et al. 2002). Especially the Agulhas Current (AC), one of the strongest geostrophic currents of the modern oceans (Tomczak and Godfrey 2001), forms a major inter-ocean exchange system by transporting waters from the Indian into the South Atlantic oceans (Gordon 1985). Due to the large amount of heat that the AC collects at low latitudes and carries to higher latitudes, it also plays a significant role in the global vertical heat flux, and thus the linkage between oceans and the atmosphere (Lutjeharms 2006).

To gain a better understanding of AC dynamics and related sedimentary processes, several geoscientific datasets were acquired during R/V Meteor cruises M63/1 (2005) and M75/3 (2008) along the South African and Mozambican coast. These include high-resolution multichannel seismic surveys southeast of the Limpopo River, enabling evaluation of sedimentary deposits under control of the Agulhas Current and its main sources, the Mozambique Current (MC) and the East Madagascar Current (EMC). In particular, the internal geometry of the Inharrime Terrace and the middle slope to the east, located in water depths between 150 and 1,500 m (Fig. 2), were investigated to reconstruct the evolution of depositional patterns through time. From this it was hoped to gain insights into the evolution and circulation pattern of the MC, which today acts as a contour current along the Inharrime Terrace.

The principal role of bottom currents as a major process shaping continental margins became evident in the mid-1960s when deep-sea photographs revealed distinct current-induced ripple marks on the continental rise off the eastern United States (Heezen and Hollister 1964; Heezen et al. 1966).

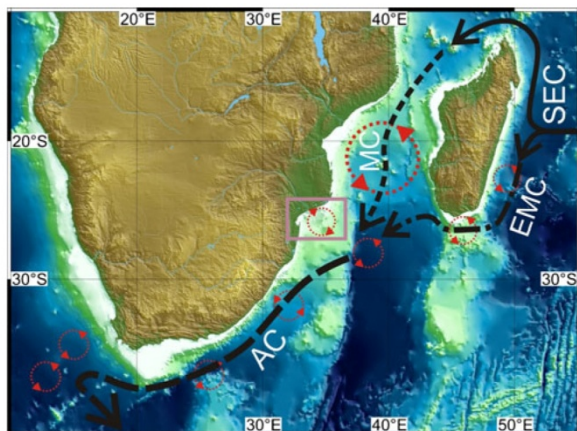


**Fig. 1** Map of southern Africa (GEBCO, 2005, <http://www.gebco.net/>) showing the study area (purple box); black arrows mark the flow paths of the main surface currents: SEC South Equatorial Current, EMC East Madagascar Current, MC Mozambique Current, AC Agulhas Current; red circles presence or travel pathway of large-scale eddies, and their direction of rotation

Thereafter, many sedimentary deposits were identified as originating from bottom current action, ranging in water depths from oceanic abyssal plains to shallow lacustrine environments (e.g., Hernández-Molina et al. 2008a, b; Verdicchio et al. 2008). Today, detailed analyses of large-scale geometries and internal seismo-acoustic and sedimentary facies have enabled the classification of contourite drift sequences in terms of complex controlling processes (Stow et al. 2008). These processes result from the interplay between bathymetry, morphological evolution, current velocity and its variability, amount and type of sediment available, and duration of current action (e.g., Faugères et al. 1999; Hernández-Molina et al. 2009; Stow et al. 2009). Using seismo-acoustic methods to determine paleo-morphology and to identify major depositor shifts, paleo-current regimes and their evolution in time and space can be reconstructed.

East of the Limpopo River mouth, the MC and the EMC merge into the AC (Fig. 2; Lutjeharms 2006). Due to the fact that the discontinuous MC as well as the EMC deliver high kinetic energy in form of eddies to this region (Lutjeharms et al. 1981; Sætre and Da Silva 1984), sedimentation under the influence of strong bottom currents and contourite drift deposition appear likely. Supporting this hypothesis, Hollister and McCave (1984) already speculated that the region between the Natal Valley and the Mozambique Basin may be under the influence of strong bottom currents. Indeed, earlier work had described thick sediment accumulations southeast of the Limpopo River mouth as being current-controlled (Martin 1981a; Martin et al. 1982).

In this context, the primary goal of this study is the identification, classification, and detailed mapping of con-

tourite drifts from data newly acquired in 2005 and 2008. Furthermore, as their spatial and temporal evolution would reveal the formation mechanisms involved, it was anticipated that the data would enable the reconstruction of the evolving Mozambique Current over geological timescales.

### Physical setting

Today, the highest amount of terrigenous sediment released into the southwestern Indian Ocean is discharged by large rivers (Flemming 1981). Likewise, the main terrigenous sediment source for the Natal Valley is, or was in the past, via numerous river systems along the Natal coast.

The Natal Valley itself is a north-south-trending, sediment-filled basin between the SE African coast and the Mozambique Ridge (Dingle et al. 1978). Toward the south the Natal Valley merges with the Transkei Basin, while its northern border is marked by the low-lying coastal plain of southeastern Mozambique. Since the early Mesozoic, the development of this basin has been controlled by deep-seated tectonic structures formed during the breakup of Gondwanaland (Dingle and Scrutton 1974).

River systems are, and have been, the main sediment source and have therefore been actively involved in the formation of the continental margin, which, in this region, is generally narrow, irregular and approximately parallel to the coastline. In particular, the large sedimentary feature fronting the Limpopo River reaches into deeper water, shifting the shelf break further offshore and, accordingly,

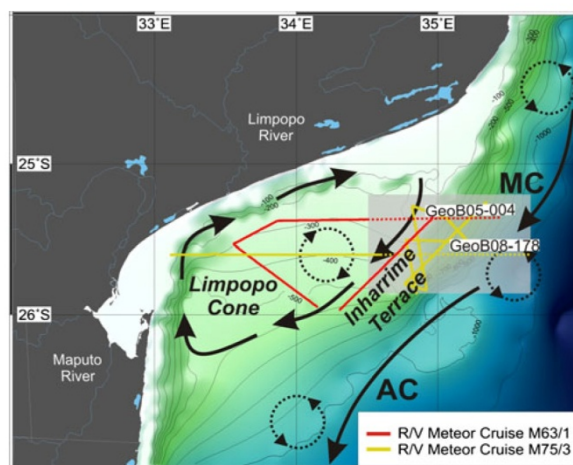


**Fig. 2** Map of the study area at the border between Mozambique and South Africa (cf. Fig. 1, purple box); black arrows main current pathways, including floating and coastal lee eddy features; colored lines seismic line grid (red spring 2005, yellow spring 2008); dotted lines portions of seismic lines GeoB08-178 and GeoB05-004 shown in Figs. 3 and 4

the upper slope seaward. Compared to the large sediment loads carried by other regional river systems such as the Tugela River, the contribution of the Limpopo River is quite moderate (Dingle et al. 1978).

The physiographic characteristics of the seafloor offshore of the Limpopo River have previously been described by Dingle et al. (1978), Martin (1981a), and Martin et al. (1982) on the basis of seismo-acoustic data. They subdivided the region into two major physiographic provinces: the Limpopo Cone, and the Inharrime Terrace (Fig. 2).

The Limpopo Cone, which extends 300 km south from the Limpopo River mouth (Martin 1981a), has a smooth surface displaying a prominent terrace between 400 and 600 m of water depth (Dingle et al. 1978). The western termination is formed by the continental slope off Maputo Bay. In the east, the Limpopo Cone fades into the Inharrime Terrace, which is a smooth, convex, curvilinear sedimentary feature extending 140 km southwest of Ponta Zavora. While its eastern slope descends toward the Mozambique Ridge, the western boundary bends toward Maputo. In combination, the Limpopo Cone and the Inharrime Terrace form a large triangular-shaped sedimentary body in the northwestern Natal Valley (Martin 1981a).

The eastern slope of the morphological terrace coincides with the main surficial water flow path in this region, which is oriented toward the southeast. This flow pattern is the result of two major interacting ocean currents that form the AC further to the south: the Mozambique Current, and the East Madagascar Current. The EMC is directly fed by the South Equatorial Current (SEC), which continuously transports water westward from Indonesia (e.g., Tomczak and Godfrey 2001). As shown in Fig. 2, the SEC impinges on the eastern margin of Madagascar (Lutjeharms 1976) before it splits into a northern branch, which is the continuation of the SEC, and a southern branch, the EMC, which transports 41 Sv southward at current velocities of 1–1.5 m/s (e.g., Lutjeharms et al. 1981; DiMarco et al. 2002). This narrow and intense current closely follows the bathymetric contours. At the southern tip of Madagascar, the EMC is retroflected eastward (Lutjeharms and van Ballegooyen 1988). Also, offshore cyclonic eddies can develop westward at this point (Fig. 2), linking the EMC with the AC (Quartly et al. 2006). The drifting eddies can follow two passageways. Thus, eddies can drift northward into the Mozambique Channel close to the Madagascan coastline, where they start to move westward. The other pathway leads directly westward until the EMC eventually merges with the MC (Lutjeharms et al. 1981), thereby contributing to the AC.

While drifter and model data enable rough estimations about the importance of the EMC for the Agulhas Current (Lutjeharms 2006), the contribution of the MC is still unclear. After the bifurcation of the SEC off the east coast of Madagascar (Fig. 1), the northern branch follows the

coastline northward until it divides into the north-setting Zanzibar Current and its continuation into the North Equatorial Counter Current, and a southern branch that enters the Mozambique Basin (Tomczak and Godfrey 2001). Controversies in published studies exist about how much water enters the Mozambique Basin, and about whether the current continues into the Mozambique Channel and, if yes, how much water is effectively transported through the Mozambique Channel (e.g., Sætre and Da Silva 1984; Lutjeharms et al. 2000; DiMarco et al. 2002; Ridderinkhof and de Ruijter 2003). Hydrographic measurements and modeling results suggest a strong dependence of the amount of water entering the Mozambique Channel on the African monsoon system (DiMarco et al. 2002). According to Lutjeharms (2006), the MC transports ~19.2 Sv southward with an average velocity of 1–2 m/s. However, this transport is discontinuous on short timescales and is mainly driven by anti-cyclonic eddies (Fig. 2), as shown by current measurements that support this concept and indicate the regular creation of eddies in the northern Mozambique Channel (e.g., de Ruijter et al. 2002; Schouten et al. 2003; Penven et al. 2006). These eddies transport huge amounts of water southward (~15 Sv), their speed and energy load increasing toward the southern limit of the Mozambique Channel. They can reach about 1,500 m water depth, trapping both surface water and intermediate water (Lutjeharms 2006). These eddies merge with the EMC in close proximity to the Inharrime Terrace, to form the AC (Fig. 2). Circulation patterns in the Mozambique Channel are further complicated by the fact that this is a macrotidal region (e.g., Flemming 2005). Tidal ranges exceed 6 m along the Mozambican coast, and the tides rotate around Madagascar in an anti-cyclonic mode that would reinforce any south-setting oceanic current in the western parts of the Mozambique Channel. Today, geological evidence of a frequent and, over long time periods, persistent southward flow in the Mozambique Current includes the existence of large-scale current-induced bedforms off the Zambezi River. There, a wide dune field with 5-m-high crests was described by Beiersdorf et al. (1980), which supports the concept of a strong and, at least on longer timescales, constant southward flow.

Eddies formed in the northern part of the Mozambique Channel, and which float southward as part of the MC, are not the only ones associated with the MC. Others occur in the form of trapped, coastal lee eddies such as the cyclonic eddy system east of Maputo called the Delagoa Bight eddy, which is of special interest to this study (Fig. 2). This type of eddy is the result of channelized and focused currents that lose their bathymetric constraint and form local recirculation cells in the lee of the main current pathway.

The cyclonic Delagoa Bight eddy is driven by the rapid southward flow of water through the Mozambique Channel

as a result of the southward migration of anti-cyclonic eddies (Lamont et al. 2010), which detach from the slope east of the Inharrime Terrace. The Delagoa Bight eddy can reach a diameter of 100 km, and locally transports  $\sim 18$  Sv (Lutjeharms 2006). Temperature and salinity measurements carried out by Lutjeharms and Da Silva (1988) show clear evidence for upwelling from depths of at least 900 m in the center of the eddy. Due to the presence of the cyclonic lee eddy, a strong coast-parallel counter current is formed on the shelf off northern Natal and in Maputo Bay (Gründlingh 1977). This counter current is strong enough to generate large subaqueous dunes transporting sediment northward along the shelf (Flemming 1981; Fig. 2). Although part of this sediment may be lost to the Limpopo Cone (Green 2009), a substantial portion is considered to be transported past the Limpopo River mouth toward the northeastern shelf break (Flemming 1981), where it would be flushed southward by the MC.

Modern sedimentation on the Limpopo Cone and the Inharrime Terrace is hence mainly controlled by the regional current regime. According to Martin (1981b), the eastern slope of the Inharrime Terrace is under the influence of the southward-flowing MC, or rather the newly formed AC, and associated upwelling, which is strongest in the shallowest part of the Inharrime Terrace. In contrast, the western part of the Inharrime Terrace and the Limpopo Cone is mainly controlled by the coast-parallel counter current. The sediment delivered by the Limpopo and Maputo rivers is swept northeastward along the shore, resulting in low sedimentation rates at the central Limpopo Cone (Martin 1981a, b).

Due to the capacity of the regional currents to transport sediment over 1,000 s of kilometers, even distant rivers may potentially contribute to the overall sediment flux. For example, the Zambezi River, which discharges into the western central Mozambique Channel, is the largest river system in southern Africa (Moore et al. 2007). It supplies  $\sim 20$  Gt of sediment per year (Milliman and Meade 1983). Reconstructions of the temporal evolution of the related delta system

have revealed that the Zambezi River input has constantly increased since Oligocene times (Walford et al. 2005).

## Methods

During R/V Meteor cruises M63/1 in spring 2005 and M75/3 in spring 2008, a variety of seismic and acoustic measurements were carried out, including multichannel seismics with the GeoB high-resolution multichannel seismic system developed by the Department of Geoscience, Bremen, which includes GI-guns and a 96-channel 600-m-long analogue streamer, a Parasound acoustic profiler, and a multibeam system. In an integrated approach, small-scale sedimentary structures and closely spaced layers can be imaged and jointly interpreted.

Standard seismic processing was applied to the data, including band-pass filtering, stacking, and time migration. In total, over 940 km of seismic profiles were processed and analyzed for this study. The seismo-stratigraphy is based on the correlation of borehole and seismic data published by Dingle et al. (1978) and Martin (1981a). Isopach maps are given in meters after time-to-depth conversion using a constant velocity of 1,500 m/s.

Parasound and Hydrosweep are registered trademarks of Atlas Hydrographic GmbH. Acoustic data were processed using Vista 2D/3D Seismic Processing, which is a registered trademark of GEDCO. Seismic interpretation and isopach images were undertaken using Seismic Micro-Technology KINGDOM Advanced™.

## Results

Bathymetric data (Figs. 1 and 2) as well as lines GeoB08-178 (Fig. 3) and GeoB05-004 (Fig. 4) show a smooth morphology on the Inharrime Terrace, with a moderate slope on its western and a steep slope on its eastern flank. Four major seismic units were identified on the basis of major structural

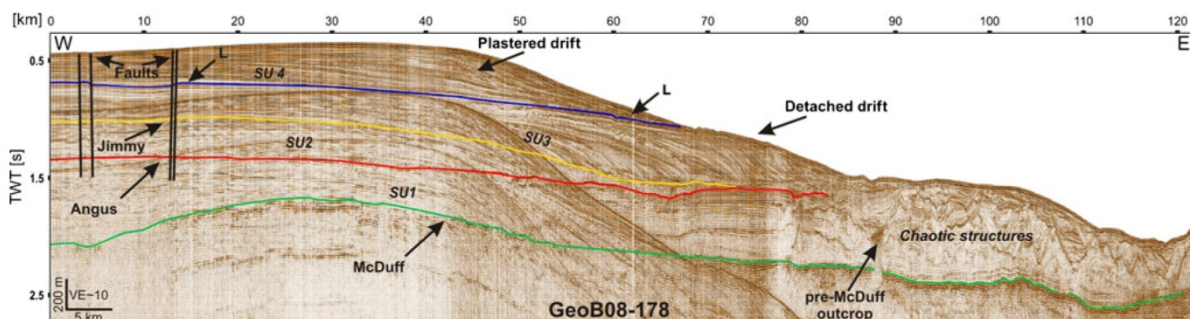


**Fig. 3** Multichannel seismic line GeoB08-178 (cf. location in Fig. 2); SU 1 to 4 refer to seismic units 1–4 described in the text; reflectors McDuff, Angus, Jimmy and L are based on the seismic stratigraphy provided by Dingle et al. (1978) and Martin (1981a). *VE* Vertical exaggeration

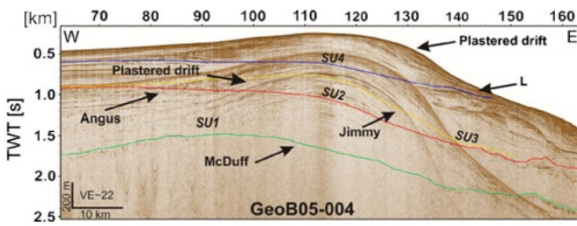


**Fig. 4** Multichannel seismic line GeoB08-178 (cf. location in Fig. 2); SU 1 to 4 refer to seismic units 1–4 described in the text; reflectors McDuff, Angus, Jimmy and L are based on the seismic stratigraphy provided by Dingle et al. (1978) and Martin (1981a). VE Vertical exaggeration

base of this unit is marked by discontinuous, closely spaced high-amplitude reflections. This reflection pattern correlates with the McDuff horizon (green line in Figs. 3 and 4) defined by Dingle et al. (1978) as the Cenomanian–Turonian boundary by cross-correlation to a sedimentary hiatus in the JC-1 borehole (Du Toit and Leith 1974). Beneath the Inharrime Terrace, seismic unit 1 shows an aggradational stacking pattern with horizontally layered reflections.

discontinuities within the sedimentary sequences of the Inharrime Terrace. Seismic unit 1 (Fig. 3), which has a thickness of ~500 ms TWT (two-way travel time), is located ~1,000 ms TWT below the crest of the terrace. The

The transition from seismic unit 1 to seismic unit 2 is indicated by a strongly reflecting structural discontinuity named Angus (red line in Fig. 3). Dingle et al. (1978) and Martin (1981a) linked this change to a hiatus of either Late Oligocene or Early Miocene age (Figs. 3 and 4). Seismic unit 1 reveals relatively uniform sediment accumulation across the Inharrime Terrace, with a sediment thickness minimum in its central part. In the northeast, the thickness increases toward the Limpopo River mouth (Fig. 5a).

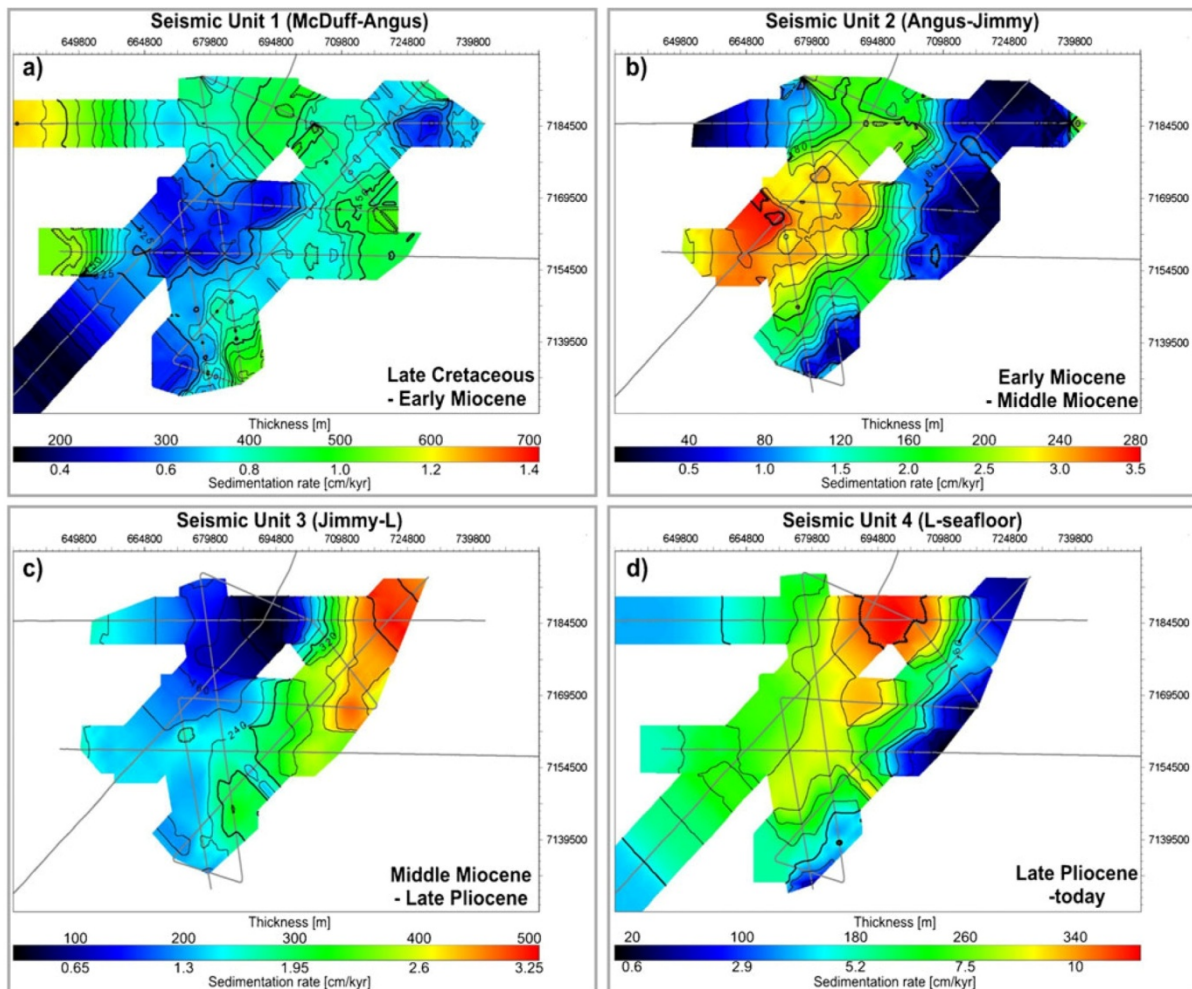


**Fig. 5** Temporal development of the Inharrime Terrace since the Late Cretaceous, based on isopach charts of seismic units 1–4



On top of seismic unit 1, three major drift sequences can be identified. The deepest one (seismic unit 2, Figs. 2 and 3) has a mounded morphology with a maximum thickness of ~350 ms TWT, forming a plastered drift on top of the Angus reflector and having an age between Late Oligocene/Early Miocene and Middle Miocene. The top of this unit is represented by the Jimmy reflector (Figs. 3 and 4, yellow line). Due to strong seismic multiples, only the flanks of the unit could be adequately analyzed, whereas the inner core of the drift sequence remains poorly imaged. The faint reflections indicate a downslope prograding stacking pattern forming a convex-up geometry. Figure 5b shows the spatial pattern of sediment accumulation for this time period, which was focused on the central part of the Inharrime Terrace. Overall, the depocenter forms a NE-SW-oriented, elongate sediment body.

The transition between seismic unit 2 and seismic unit 3 (Fig. 2) marks a major shift in depocenter (Fig. 5b, c) toward the northeast, forming a detached drift of ~500 ms TWT thickness above the Jimmy reflector. Most of this unit has accumulated along the mid-slope and has a sigmoidal shape, similar to clinoforms with downslope progradation oriented perpendicular to the modern crest axis. The seismic facies of unit 3 is characterized by sequences of high-amplitude reflections into which acoustically transparent or seismically chaotic sequences are intercalated. This reflection pattern is partly disturbed by V-shaped, partly wavy incisions cutting into the transparent zones. These irregular surfaces are leveled by locally higher accumulations in depressions containing the same sediment as the transparent units above (Fig. 3, between kilometers 50 and 70 at depths of 1–1.2 s TWT).

On top of horizon L (blue line in Figs. 3 and 4), seismic unit 4, which has a maximum thickness of ~500 ms TWT, defines the modern seafloor morphology with a NE-SW-striking crest aligned with the central part of the Inharrime Terrace (Fig. 2). Discontinuity L was already described by Martin (1981a), but no borehole correlation and age assignments are thus far available. The geometric shape of seismic unit 4 is comparable to that of seismic unit 2. It shows a mounded and convex-up morphology as a result of the downslope prograding stacking pattern. The seismo-acoustic facies is expressed by several depositional sequences showing variations in reflection character, from strong, clear and continuous to acoustically transparent or weak. Shape and seismo-acoustic facies characteristics suggest a plastered drift.

In the western part of line GeoB08-178 (Fig. 3), northwest of the Inharrime Terrace, the seismic units are vertically offset. These offsets can be traced downward into deeper units, being largest at the acoustic basement and decreasing toward the seafloor. Along line GeoB05-004 the largest offsets reach 50 ms TWT (Fig. 4), decreasing upward to 4 ms TWT at the seafloor.

Further downslope and to the east, these stacking patterns change where a wide terrace appears at a water depth of ~1,100 m. This terrace is built by a complex and partly chaotic sedimentary unit, including several deep V-shaped incisions with a complex fill pattern. The major seismic units identified beneath the Inharrime Terrace cannot be recognized along this part of the margin. Only the McDuff reflector can be clearly seen where the acoustic basement forms a structural high (Fig. 3, at ~90 km and a depth of 2 s TWT).

## Discussion

Close to the Cenomanian–Turonian boundary, the McDuff reflector marks a change from an euxinic to an open marine sedimentation regime as a result of the opening of several oceanic gateways including the Mozambique Channel (Martin et al. 1982). Whether tectonic movement, the onset of ocean current influence such as the MC in that region, or a combination of both resulted in this hiatus remains unclear. While the structural high produced by normal faulting at depths of ~0.3–0.4 s TWT (Fig. 3; Martin 1981a) would indicate tectonic activity, the shape of the margin and the overall aggradational stacking pattern on top of the McDuff reflector suggest the formation of a wide and regular terrace in the early Neogene that was characterized by spatially uniform sedimentation. Such terraces can form as a result of either uniform pelagic sedimentation or a fast tabular current, which can today be shown to create comparable morphological features off southern Argentina (Hernández-Molina et al. 2009).

Based on the seismic stratigraphy, it is possible to roughly estimate the sedimentation rates. Sediment accumulation showed intermediate values of 0.5–0.9 cm/1,000 years from Late Cretaceous times to the Late Oligocene/Early Miocene (seismic unit 1). The lowest sediment accumulation during that period occurred in the central area of the Inharrime Terrace, where its modern crest is located (Fig. 5a). The sedimentation rate appears to have been highest in the northwestern part of the terrace, which points toward the Limpopo River as the main sediment source. Uniformly low sedimentation rates on the Inharrime Terrace with an increasing trend toward the river system indicate a period of low current activity and a general absence of current-controlled lateral sediment transport.

The shape and internal stacking pattern of seismic units 2 to 4 clearly indicate that all three units were deposited under current-dominated conditions, a conclusion already reached by Martin (1981b) and Martin et al. (1982). In seismic unit 2, which represents the Early to Middle Miocene period, a depocenter shift suggests a change in the dominant current regime (Fig. 5b). In the process, a plastered drift was formed on top of the Angus reflector at

the center of the Inharrime Terrace (Figs. 2 and 3). Here, between 160 and 260 m of sediment has accumulated at sedimentation rates of  $\sim 1.8$  cm/1,000 years. Much lower sedimentation rates existed in the northwestern part of the study area and at the eastern foot of the Inharrime Terrace.

Compared to seismic unit 1, the sediment distribution of seismic unit 2 shows a strong local focusing of material in the central area of the Inharrime Terrace, resulting in pronounced lateral sedimentation gradients. Especially the lack of sedimentation in the northwestern study area indicates an increase in sediment transport distance from the river mouth toward the east. This sediment transport can be explained by the onset of the Delagoa Bight lee eddy system, which is still active in modern times (e.g., Lutjeharms and Da Silva 1988; Lutjeharms 2006; Lamont et al. 2010). This eddy system causes a coast-parallel counter current off northern KwaZulu-Natal and Maputo Bay (Martin 1981b), transporting sediment along the coast (Flemming 1981; Green 2009) toward the north and east past the Limpopo River mouth. Due to the fact that the Angus horizon developed in Oligocene to Early Miocene times, it is concluded that the onset of this current regime occurred in the Early Miocene, i.e., in the course of the rising sea level during the major Oligocene–Miocene regression/transgression cycle recorded around southern Africa (Siesser and Dingle 1981; Dingle et al. 1983).

Because the Delagoa Bight lee eddy is directly linked to the presence of a strong southward flow within the Mozambique Channel, a possible reason for the initiation is the onset of the MC itself during the Early/Middle Miocene. The newly formed, southward-flowing MC would have been able to generate the current regime necessary to form the north-south-aligned plastered drift represented by seismic unit 3. This interpretation is consistent with Zambezi delta reconstructions that suggest an onset of the MC at least  $\sim 16$  Ma ago (Walford et al. 2005). A possible forcing mechanism for this scenario would assume an increased southward flow of the SEC due to the closure of the Tethys at the eastern portal of the Mediterranean Sea, which took place in the same time period. The closure of this northern gateway severely interrupted equatorial circulation, and had a major impact on the global thermohaline circulation and especially on the Indian Ocean current regime (Hsü and Bernoulli 1978). Overall, the current conditions during the Early to Middle Miocene had to be moderate because plastered drifts as seen in seismic unit 3 are mainly formed under low to intermediate current velocities (Faugères et al. 1999).

Not only the large shift in the depocenter (Fig. 5c), but also the change in the shape of the depositional system indicate that the Jimmy horizon (Figs. 3 and 4) reflects a substantial change in the local hydrodynamic regime. The major focus on mid-slope sedimentation with its sigmoidal,

downslope prograding stacking pattern is probably a result of strong coast-parallel sediment transport as described by Flemming (1981) and Green (2009). The large contrast to the sediments deposited seaward of the Inharrime Terrace indicates that during this time the eastward sediment transport was much more efficient than during the Early Miocene, the sediment having been more or less swept off the terrace to form clinof orm-like structures. Where the current weakened along the margin due to the loss of bathymetric forcing, the sediments formed a detached drift and the sedimentation rate locally increased up to 4.5 cm/1,000 years. For this reason, the main depocenter is located in the northeast where the coast-parallel current overshoots the terrace, and from there it extends southwestward due to transport by the MC (Figs. 2 and 5c). The flat morphology during deposition of seismic unit 3 above the Jimmy horizon may point toward strong, unfocused currents on the central terrace. The paucity of deposition to the west of the drift (Fig. 5c) further hints at locally increased current velocity, possibly marking the central position of the lee eddy system during this time interval.

For hydrodynamic reasons, the strengthening of the coast-parallel current must be directly linked to its driving force, the Mozambique Current. Martin et al. (1982) linked the reflector Jimmy, the base of seismic unit 3, to changes in the extent of the Antarctic ice sheet and the build-up of Arctic ice in the transition from the Late Miocene to the Pliocene. Since that time, the flow path of the global circulation system has remained stable (Schnitker 1980) and the MC probably reached its full strength.

A fault system identified northwest of the Inharrime Terrace crest must have been active at least since the Middle Miocene (Figs. 3 and 4). These faults are probably related to the uplift and denudation history of southern Africa. A smaller uplift pulse may have occurred in the Early/Middle Miocene (Partridge 1998), and thereby initiated the fault activity. As initial uplift occurred during the Early Cretaceous, Gallagher and Brown (1999) suggested that older structures had been reactivated during the denudation of southern Africa. It is thus very likely that the faults reach much deeper than seen on the seismic images, and are of pre-Jimmy age.

Modern drift accumulation building seismic unit 4 reflects the conditions after the modern MC system had been established. Upwelling induced by the semi-stationary Delagoa Bight lee eddy, in interplay with the regional bathymetric framework, forces Antarctic Intermediate Water from depths greater than 900 m toward the upper slope and the modern sedimentary crest (Martin 1981a; Lutjeharms and Da Silva 1988). The glauconite- and organic-rich sediments that dominate modern deposition are a response to the position and strength

of the nutrient-rich upwelling cell in post-horizon L times (Martin et al. 1982). The modern position of the depocenter, and therefore the crest, is further to the west compared to pre-horizon L times (Fig. 5d). This may be an indication that the forcing induced by the lee eddy system weakened since the formation of horizon L, and that a similar current regime exists today as was the case in the Early/Middle Miocene to again form a plastered drift. As mentioned above, it has not yet been possible to determine the age of reflector L. However, a possible scenario explaining the change in the depositional pattern may be related to the narrowing of the Indonesian through-flow passage at the transition from the Miocene to the Pliocene (Karas et al. 2009). This would have weakened the SEC and, in turn, would have reduced the strength of the MC and EMC, and of the associated Delagoa Bight eddy system. Assuming this age for the formation of reflector L, the sedimentation rates in seismic unit 1 would be 9.5 cm/1,000 years. The apparent increase in accumulation may well be attributed to increased sedimentation induced by the upwelling enforced by the lee eddy system.

To explain the presence of the terrace at 1,100 m water depth east of the Inharrime Terrace (lower part of Fig. 3) is more complex than for the build-up of the terrace itself. Although the chaotic sedimentary structures (lower part of Fig. 3) along the eastern foot of the Inharrime Terrace have prevented a stratigraphic assignment, the generally high-energy current conditions have probably been responsible for the depositional style. It should be noted, however, that the proximity to basement outcrops may also have been responsible for such a complex and potentially three-dimensional pattern. Furthermore, the upper portion may be stratigraphically attributed to the time period between the McDuff and Angus horizons (lower part of Fig. 3). In general, it can be concluded that since Late Cretaceous times only 450 m of sediment has accumulated on this terrace, yielding a sedimentation rate of 0.8 cm/1,000 years. This relatively low Neogene sedimentation rate, in comparison to that of the Inharrime Terrace, may be an indication that sediment draping the basement outcrops and their surroundings was removed by subsequent erosion and/or winnowing due to strong bottom currents. As the mid-Cretaceous sedimentary basin was substantially reduced in size and the water circulation restricted (Davies et al. 1975), erosion by strong currents can be excluded during the Cretaceous.

If the MC was initiated in the Early/Middle Miocene, however, then this could also mark the beginning of the erosional and depositional processes controlling sedimentation on the eastern slope of the Inharrime Terrace. Hence, eddies migrating through the Mozambique Channel are a result of the position of Madagascar relative to Africa, and the location of the South Equatorial Current (Lutjeharms 2006). Such eddies have occurred since the initiation of the MC as a

dominant force comparable to the modern situation, and have subsequently controlled the local current regime. Reaching 1,500 m water depth (Lutjeharms 2006), these eddies may be responsible for erosional and depositional features similar to those observed in long-term studies off Nova Scotia (Hollister and McCave 1984; Hollister 1993).

## Conclusions

Whereas during the Late Cretaceous the northern Natal Basin was dominated by weak current conditions resulting in uniform sediment distribution, sedimentation has been controlled and focused by current action since the Early Miocene, thereby forming major contourite drift sequences. The formation of a plastered drift and the low sedimentation rates offshore of the Limpopo River, in contrast to the drift crest, suggest that the existence of the Mozambique Current was persistent on geological timescales, and that the directly connected Delagoa Bight lee eddy was active since that time. A large-scale shift in depocenter toward the eastern slope of the Inharrime Terrace during the Middle Miocene points toward an intensification of the Mozambique Current as well as the lee eddy, resulting in a strong coast-parallel current. Another plastered drift, comparable to the one formed during the Early Miocene, has developed on the Inharrime Terrace since the Late Pliocene. Modern sedimentation is probably strongly enhanced by upwelling of Antarctic Intermediate Water induced by the lee eddy located in the Delagoa Bight.

**Acknowledgements** R/V Meteor cruises M63/1 and M75/3 were funded by the Deutsche Forschungsgemeinschaft (DFG), and were associated with the *Safari* IODP proposal. The authors would like to thank especially Prof. Rainer Zahn and Prof. Ian Hall. Useful comments by B.W. Flemming, an anonymous referee, and the editor significantly improved the quality of this manuscript.

## References

- Beiersdorf H, Kudrass H-R, von Stackelberg U (1980) Placer deposits of ilmenite and zircon on the Zambezi Shelf. *Geol Jahrbuch Reihe* 36:5–85
- Davies TA, Weser OE, Luyendyk BP, Kidd RB (1975) Unconformities in the sediments of the Indian Ocean. *Nature* 253:15–19. doi:10.1038/253015a0
- de Ruijter WPM, Ridderinkhof H, Lutjeharms JRE, Schouten MW, Veth C (2002) Observations of the flow in the Mozambique Channel. *Geophys Res Lett* 29(10):1502. doi:10.1029/2001GL013714
- DiMarco SF, Chapman P, Nowlin WD, Hacker P, Donohue K, Luther M, Johnson GC, Toole J (2002) Volume transport and property distributions of the Mozambique Channel. *Deep Sea Res II* 49:1481–1511. doi:10.1016/s0967-0645(01)00159-x
- Dingle RV, Scrutton RA (1974) Continental breakup and the development of post-Paleozoic sedimentary basins around southern Africa. *Geol Soc Am Bull* 85:1467–1474. doi:10.1130/0016-7606(1974)85<1467:CBATDO>2.0.CO;2

- Dingle RV, Goodlad SW, Martin AK (1978) Bathymetry and stratigraphy of the northern Natal Valley (SW Indian Ocean): a preliminary account. *Mar Geol* 28:89–106. doi:10.1016/0025-3227(78)90099-3
- Dingle RV, Siesser WG, Newton AR (1983) Mesozoic and tertiary geology of southern Africa. AA Balkema, Rotterdam
- Du Toit SR, Leith MJ (1974) The J(c)-1 borehole on the continental shelf near Stanger, Natal. *Trans Geol Soc S Afr* 77:247–252
- Faugères J-C, Stow DAV, Imbert P, Viana A (1999) Seismic features diagnostic of contourite drifts. *Mar Geol* 162:1–38. doi:10.1016/S0025-3227(99)00068-7
- Flemming BW (1981) Factors controlling shelf sediment dispersal along the southeast African continental margin. *Mar Geol* 42:259–277. doi:10.1016/0025-3227(81)90166-3
- Flemming BW (2005) Tidal environments. In: Schwartz ML (ed) *Encyclopedia of coastal science*. Springer, Dordrecht, pp 954–958
- Gallagher K, Brown R (1999) The Mesozoic denudation history of the Atlantic margins of southern Africa and southeast Brazil and the relationship to offshore sedimentation. *Geol Soc Lond Spec Publ* 153:41–53. doi:10.1144/gsl.sp.1999.153.01.03
- Gordon AL (1985) Indian-Atlantic transfer of thermocline water at the Agulhas Retroflection. *Science* 227:1030–1033. doi:10.1126/science.227.4690.1030
- Green A (2009) Sediment dynamics on the narrow, canyon-incised and current-swept shelf of the northern KwaZulu-Natal continental shelf, South Africa. *Geo Mar Lett* 29(4):201–219. doi:10.1007/s00367-009-0135-9
- Gründlingh ML (1977) Drift observations from Nimbus VI satellite-tracked buoys in the southwestern Indian ocean. *Deep Sea Res* 24:903–910. doi:10.1016/0146-6291(77)90559-8
- Heezen BC, Hollister C (1964) Deep-sea current evidence from abyssal sediments. *Mar Geol* 1:141–174. doi:10.1016/0025-3227(64)90012-X
- Heezen BC, Hollister CD, Ruddiman WF (1966) Shaping of the continental rise by deep geostrophic contour currents. *Science* 152:502–508. doi:10.1126/science.152.3721.502
- Hernández-Molina FJ, Llave E, Stow DAV (2008a) Continental slope contourites. In: Rebesco M, Camerlenghi A (eds) *Contourites. Developments in sedimentology*, vol 60. Elsevier, Amsterdam, pp 379–408
- Hernández-Molina FJ, Maldonado A, Stow DAV, Rebesco M, Camerlenghi A (2008b) Abyssal plain contourites. In: Rebesco M, Camerlenghi A (eds) *Contourites. Developments in sedimentology*, vol 60. Elsevier, Amsterdam, pp 347–378
- Hernández-Molina FJ, Paterlini M, Violante R, Marshall P, de Isasi M, Somoza L, Rebesco M (2009) Contourite depositional system on the Argentine Slope: an exceptional record of the influence of Antarctic water masses. *Geology* 37:507–510. doi:10.1130/g25578a.1
- Hollister CD (1993) The concept of deep-sea contourites. *Sediment Geol* 82:5–11. doi:10.1016/0037-0738(93)90109-1
- Hollister CD, McCave IN (1984) Sedimentation under deep-sea storms. *Nature* 309:220–225. doi:10.1038/309220a0
- Hsü KJ, Bernoulli D (1978) Genesis of the Tethys and the Mediterranean. *Initial Reports of the Deep Sea Drilling Project* 42:943–949. doi:10.2973/dsdp.proc.42-1.149.1978
- Karas C, Numberg D, Gupta AK, Tiedemann R, Mohan K, Bickert T (2009) Mid-Pliocene climate change amplified by a switch in Indonesian subsurface throughflow. *Nat Geosci* 2:434–438. doi:10.1038/ngeo520
- Lamont T, Roberts MJ, Barlow RG, Morris T, van den Berg MA (2010) Circulation patterns in the Delagoa Bight, Mozambique, and the influence of deep ocean eddies. *Afr J Mar Sci* 32:553–562. doi:10.2989/1814232X.2010.538147
- Lutjeharms JRE (1976) The Agulhas Current system during the northeast monsoon season. *J Phys Oceanogr* 6:665–670. doi:10.1175/1520-0485(1976)006<0665:TACSDT>2.0.CO;2
- Lutjeharms JRE (2006) *The Agulhas Current*. Springer, Berlin
- Lutjeharms JRE, Da Silva AJ (1988) The Delagoa Bight eddy. *Deep Sea Res A* 35:619–634. doi:10.1016/0198-0149(88)90134-3
- Lutjeharms JRE, van Ballegooyen RC (1988) Anomalous upstream retroflection in the Agulhas Current. *Science* 240:1770. doi:10.1126/science.240.4860.1770
- Lutjeharms JRE, Bang ND, Duncan CP (1981) Characteristics of the currents east and south of Madagascar. *Deep Sea Res A* 28:879–899. doi:10.1016/0198-0149(81)90008-x
- Lutjeharms JRE, Cooper J, Roberts M (2000) Upwelling at the inshore edge of the Agulhas Current. *Continent Shelf Res* 20:737–761. doi:10.1016/S0278-4343(99)00092-8
- Martin AK (1981a) The influence of the Agulhas Current on the physiographic development of the northernmost Natal Valley (S.W. Indian Ocean). *Mar Geol* 39:259–276. doi:10.1016/0025-3227(81)90075-x
- Martin AK (1981b) Evolution of the Agulhas Current and its paleo-ecological implications. *S Afr J Sci* 77:547–554
- Martin AK, Goodlad SW, Salmon DA (1982) Sedimentary basin in-fill in the northernmost Natal Valley, hiatus development and Agulhas Current palaeo-oceanography. *J Geol Soc* 139:183–201. doi:10.1144/gsjgs.139.2.0183
- Milliman JD, Meade RH (1983) World-wide delivery of river sediment to the oceans. *J Geol* 91:1–21. doi:10.1086/628741
- Moore AE, Cotterill FPD, Main MPL, Williams HB (2007) *The Zambezi River*. Wiley, Chichester
- Partridge TC (1998) Of diamonds, dinosaurs and diastrophism; 150 million years of landscape evolution in southern Africa. *S Afr J Geol* 101:167–184
- Penven P, Lutjeharms JRE, Florenchie P (2006) Madagascar: a pacemaker for the Agulhas Current? *Geophys Res Lett* 29(10):1502. doi:10.1029/2001GL013714
- Quartly GD, Buck JH, Srokosz MA, Coward AC (2006) Eddies around Madagascar—the retroflection re-considered. *J Mar Syst* 63:115–129. doi:10.1016/j.jmarsys.2006.06.001
- Ridderinkhof H, de Ruijter WPM (2003) Moored current observations in the Mozambique Channel. *Deep Sea Res II* 50:1933–1955. doi:10.1016/S0967-0645(03)00041-9
- Sætre R, Da Silva AJ (1984) The circulation of the Mozambique channel. *Deep Sea Res A* 31:485–508. doi:10.1016/0198-0149(84)90098-0
- Schnitker D (1980) North Atlantic oceanography as possible cause of Antarctic glaciation and eutrophication. *Nature* 284:615–616. doi:10.1038/284615a0
- Schouten MW, de Ruijter WPM, van Leeuwen PJ, Ridderinkhof H (2003) Eddies and variability in the Mozambique Channel. *Deep Sea Res II* 50:1987–2003. doi:10.1016/S0967-0645(03)00042-0
- Siesser WG, Dingle RV (1981) Tertiary sea-level movements around southern Africa. *J Geol* 89:83–96
- Stow DAV, Hunter S, Wilkinson D, Hernández-Molina FJ, Rebesco M, Camerlenghi A (2008) The nature of contourite deposition. In: Rebesco M, Camerlenghi A (eds) *Contourites. Developments in Sedimentology*, vol 60. Elsevier, Amsterdam, pp 143–156
- Stow DAV, Hernández-Molina FJ, Llave E, Sayago-Gil M, Díaz del Río V, Branson A (2009) Bedform-velocity matrix: the estimation of bottom current velocity from bedform observations. *Geology* 37:327–330. doi:10.1130/G25259A.1
- Tomczak M, Godfrey JS (2001) *Regional oceanography—an introduction*. Butler & Tanner, London
- Verdicchio G, Trincardi F, Rebesco M, Camerlenghi A (2008) Shallow-water contourites. In: Rebesco M, Camerlenghi A (eds) *Contourites. Developments in Sedimentology*, vol 60. Elsevier, Amsterdam, pp 409–433
- Walford HL, White NJ, Sydow JC (2005) Solid sediment load history of the Zambezi Delta. *Earth Planet Sci Lett* 238:49–63. doi:10.1016/j.epsl.2005.07.014

## **Appendix 1: Sediment dynamics and geohazards off Uruguay and the la Plata River region (northern Argentina and Uruguay)**

Sebastian Krastel, Gerold Wefer, Till J.J. Hanebuth, Andrew A. Antobreh, Tim Freudenthal, Benedict Preu<sup>(1)</sup>, Tilmann Schwenk<sup>(1)</sup>, Michael Strasser, Roberto Violante, Daniel Winkelmann and M78/3 shipboard party

(1) Leibniz Institute of Marine Sciences (IFM-GEOMAR), Kiel, Germany

(2) MARUM – Center for Marine Environmental Sciences and Faculty of Geosciences, University of Bremen, Bremen, Germany

(3) Exploro Geoservices AS, Sandvika, Norway

(4) Department of Oceanography, Division of Marine Geology and Geophysics, Argentina Hydrographic Survey, Buenos Aires, Argentina

Printed in ‚Geo-Marine Letters’ 2011

First page reprinted with permission from Springer

Geo-Mar Lett (2011) 31:271–283  
DOI 10.1007/s00367-011-0232-4

ORIGINAL

## Sediment dynamics and geohazards off Uruguay and the de la Plata River region (northern Argentina and Uruguay)

Sebastian Krastel · Gerold Wefer · Till J. J. Hanebuth · Andrew A. Antobreh · Tim Freudenthal · Benedict Preu · Tilmann Schwenk · Michael Strasser · Roberto Violante · Daniel Winkelmann · M78/3 shipboard scientific party

Received: 7 September 2010 / Accepted: 24 March 2011 / Published online: 27 April 2011  
© Springer-Verlag 2011

**Abstract** The continental margin off Uruguay and northern Argentina is characterized by high fluvial input by the de la Plata River and a complex oceanographic regime. Here we present first results from RV Meteor Cruise M78/3 of May–July 2009, which overall aimed at investigating sediment transport processes from the coast to the deep sea by means of hydroacoustic and seismic mapping, as well as coring using conventional tools and the new MARUM seafloor drill rig (MeBo). Various mechanisms of sediment instabilities were identified based on geophysical and core data, documenting particularly the continental slope offshore

Uruguay to be locus of submarine landsliding. Individual landslides are relatively small with volumes  $<2\text{km}^3$ . Gravitational downslope sediment transport also occurs through the prominent Mar del Plata Canyon and several smaller canyons. The canyons originate at a midslope position, and the absence of buried upslope continuations strongly suggests upslope erosion as main process for canyon evolution. Many other morphological features (e.g., slope-parallel scarps with scour geometries) and abundant contourites in a 35-m-long MeBo core reveal that sediment transport and erosion are controlled predominantly by strong contour currents. Despite numerous landslide events, their geohazard potential is considered to be relatively small, because of their small volumes and their occurrence at relatively deep water depths of more than 1,500 m.

S. Krastel (✉) · D. Winkelmann  
Cluster of Excellence: The Future Ocean,  
Christian-Albrechts-Universität zu Kiel,  
Leibniz Institute of Marine Sciences (IFM-GEOMAR),  
Wischhofstr. 1-3,  
24148 Kiel, Germany  
e-mail: skrastel@ifm-geomar.de

G. Wefer · T. J. J. Hanebuth · T. Freudenthal · B. Preu ·  
T. Schwenk · M. Strasser  
MARUM—Center for Marine Environmental Sciences,  
and Faculty of Geosciences, University of Bremen,  
Klagenfurter Strasse,  
28359 Bremen, Germany

A. A. Antobreh  
Exploro Geoservices AS,  
Kjørbokollen 30,  
1337 Sandvika, Norway

R. Violante  
Department of Oceanography, Division of Marine Geology and  
Geophysics, Argentina Hydrographic Survey,  
Av. Montes de Oca 2124,  
C1271ABV, Buenos Aires, Argentina

### Introduction

As much as 90% of the sediments generated by weathering and erosion on continents is eventually deposited at the ocean margins (McCave 2002). The transport of sediments from their terrigenous sources to marine sinks is one of the most important processes shaping the surface morphology of the Earth. The processes distributing the sediments on land are relatively well understood, but there is an urgent need for more detailed investigations of submarine transport and sedimentation processes. The modes of sediment transport at continental margins are manifold, and involve turbidity currents as well as landslides (e.g., Stow and Mayall 2000; Canals and De Mol 2009). The term landslide is used in a very broad sense in this article, and includes all mass-wasting features irrespective of the processes in-

## Acknowledgements

First of all, I would like to thank Volkhard Spieß for his great support, the fruitful discussions and all the advice. Thank you for the trust and all the given opportunities. The same applies to Tilmann Schwenk, who with almost endless patience advised me and endured all my moods. I really want to say 'Thank you' to both of you for a fantastic time in Bremen, on conferences and on Board.

I also wish to thank Dierk Hebbeln, who even under shortest notice and under a lot of pressure from his own work agreed to evaluate this thesis.

'Mil gracias' to Javier Hernández-Molina for all the scientific discussions, advice, encouragement, affecting me with the 'alongslope transport thickness' and the time in Argentina, Spain and Bremen. I really enjoyed the thesis committee meeting on the Islas Cies. Talking about thesis committee meetings: I wish to thank as well the other members of my thesis committee: Till Hanebuth, Michael Strasser and Ian Nicholas McCave. The exchange of ideas, the extensive discussions, which mostly continued afterwards via email, and the always present good mood made you to a showcase thesis committee, in my opinion.

Furthermore, I wish to thank my South American colleagues from South to North: Thank you, Roberto Violante, Alberto Piola, and Marcelo Paterlini not only for the good cooperation, but also for the great time we had in Bremen during the SW Atlantic workshop and, of course, in Buenos Aires. Special thanks I owe to Juan Tomasini for having me not only one week in Montevideo working in ANCAP, but as well as a guest in his home. Coming to Brazil, I want to thank Christiano Chiessi for helpful comments and fruitful discussions.

But there are still so many people to thank: Thank you to Ines Voigt, Sebastian Razik and Hendrik Lantzsich for the nice cooperation. I also wish to thank all members of R/V Meteor Cruise M78/3a+b for the nice stay and good collaboration on board. In the course of that, special thanks to Sebastian Krastel. Moreover, I want to thank Natascha Riedinger and Susann Henkel for standing me for both legs. I thank all members of the Marine Technologies /Environmental Research working group for the comprehensive help. Whether computer problems, processing glitches, the necessity of a three minutes break or the desire for beer after work – you are the right guys. Thanks as well to our student assistants Julia Haberkern, Fenna Bergmann and Lena Steinmann. The study was funded through through DFG-Research Center / Cluster of Excellence „The Ocean in the Earth System“ and was supported by the Bremen International Graduate School for Marine Sciences (GLOMAR) that is funded by the German Research Foundation (DFG) within the frame of the Excellence Initiative by the German federal and state governments to promote science and research at German universities.

At last, special thanks go to the people in my non-academic life: my friends, my flat mates, my family and my dear Tamara for their ongoing, never ending support and encouragement.